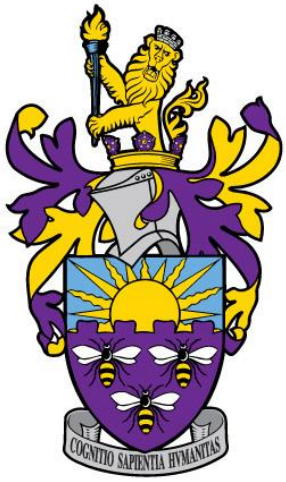

Optimisation of Interlaminar Stitching for Textile Composites

A thesis submitted to the University of Manchester for the degree of Doctor of Philosophy in the Faculty of Science and Engineering

2022

Chloe A McDonnell

School of Natural Sciences

Department of Materials

The University of Manchester

BLANK PAGE

Contents

Word Count: 55,251

List of Figures

List of Tables

List of Abbreviations

ANOVA	Analysis of Variance
BVID	Barely Visible Impact Damage
CAI	Compression after Impact
DCS	Double-thread Chain-stitch
FRP	Fibre Reinforced Polymer
ISO	International Standards Organisation
MLS	Modified Lock-stitch
NCF	Non-Crimp Fibre
OSS	One Sided Stitching
PBO	Polyphenylenbenzobisozasol
PEEK	Polyetheretherketon
PES	Polyester
PP	Polypropylene
PVC	Polyvinyl Chloride
S_D	Stitch Density
S_p	Stitch Pitch
S_s	Stitch Space
TT	Through-thickness
VARIM	Vacuum Assisted Resin Infusion Moulding
X-ray	X-radiation
µCT	Micro-computed Tomography
2D	Two-Dimensional
3D	Three Dimensional

Abstract

Fibre reinforced polymer composites are frequently replacing metals and alloys in structural applications for the aerospace, automotive and marine industries due to their high specific strength and stiffness and excellent corrosion resistance. However, a key limitation of composite laminates is their low resistance to out-of-plane loading and susceptibility to delamination. Improving the out-of-plane resistance to delamination in composites is achievable through the insertion of a z-direction reinforcement. There are several available techniques to achieve this, of which, through-thickness stitching is considered an effective, low cost option. Despite its popularity, limitations to the current stitch geometries employed for composites often result in significant geometrical defects and degradation of the in-plane properties.

The aim of this research was to optimise the stitching geometry in order to effectively improve the impact resistance of textile composites without causing excessive damage to the in-plane tensile properties. This research details the employment and optimisation of a novel stitch type for the composite industry, the ISO-401 double-thread chain-stitch. Although this stitch type is used regularly throughout the textile industry, no research to date considers its suitability to composite reinforcement.

Adjustment of the junction positon of the upper and lower stitching ISO-401 threads demonstrated that defects such as resin pocket size and fibre waviness can be reduced through optimisation. Thus, at high density stitching, which is reported as beneficial to improving the out-of-plane properties, the tensile properties are not significantly affected and therefore maintained. Under low velocity impact, stitching was found to significantly reduce the damage area through an arrest and bridging technique. This resulted in improved compressive strength after impact in stitched composites due to the smaller initiated damage size and further bridging effects of the stitches under loading. Considering the importance of the ISO-401 junction location, a final case study also revealed that the preform fabric characteristics can significantly affect the junction position under the same stitching conditions. Therefore, careful consideration of the sewing conditions and parameters must be taken to achieve the desired geometry.

The work completed for this thesis demonstrates that ISO-401 shows good compatibility for the through-thickness reinforcement of textile composites and that it can address some of the limitations of other popular stitch types.

Declaration

No portion of the work referred to in the thesis has been submitted in support of an application for another degree or qualification of this or any other university or other institute of learning.

Copyright Statement

i. The author of this thesis (including any appendices and/or schedules to this thesis) owns certain copyright or related rights in it (the "Copyright") and s/he has given the University of Manchester certain rights to use such Copyright, including for administrative purposes.

ii. Copies of this thesis, either in full or in extracts and whether in hard or electronic copy, may be made **only** in accordance with the Copyright, Designs and Patents Act 1988 (as amended) and regulations issued under it or, where appropriate, in accordance with licensing agreements which the University has from time to time. This page must form part of any such copies made.

iii. The ownership of certain Copyright, patents, designs, trademarks and other intellectual property (the "Intellectual Property") and any reproductions of copyright works in the thesis, for example graphs and tables ("Reproductions"), which may be described in this thesis, may not be owned by the author and may be owned by third parties. Such Intellectual Property and Reproductions cannot and must not be made available for use without the prior written permission of the owner(s) of the relevant Intellectual Property and/or Reproductions.

iv. Further information on the conditions under which disclosure, publication and commercialisation of this thesis, the Copyright and any Intellectual Property and/or Reproductions described in it may take place is available in the University IP Policy (see http://documents.manchester.ac.uk/DocuInfo.aspx?DocID=2442 0), in any relevant Thesis restriction declarations deposited in the University Library, the University Library's regulations (see http://www.library.manchester.ac.uk/about/regulations/) and in the University's policy on Presentation of Theses.

Acknowledgements

I would like to start by thanking my PhD supervisors; Dr. Steven Hayes and Prof. Prasad Potluri for their guidance and support throughout my doctoral studies at The University of Manchester.

I would also like to give thanks to the academics and members of the technical support team at the North West Composites Centre and Department of Materials for their support with material preparation and mechanical testing, their input has been invaluable and I am very grateful for their help.

Thanks must also be made to the EPSRC for their funding of my doctoral studies.

I wish to also thank my friends and colleagues, new and old, who have supported and joined me on this journey.

Special thanks must go to my family; Mum, Dad, Jodie, Grandad, Julie, Summer and Saylor, for your unconditional love and support.

Last but not least thank you, River, for your love and patience, for always believing in me and most of all for making me laugh every day.

Chapter 1

Introduction

1.1 Background

Over the past three decades, interest in utilising advanced fibre reinforced polymer (FRP) composites has grown considerably for structural applications in industries such as aerospace, automotive, marine and civil engineering [1–3]. FRP composites are now used extensively throughout the aerospace industry, increasingly in the manufacture of primary structural parts, due to their high specific strength and stiffness, low density and good corrosion and fatigue performance, compared with their metallic counterparts [4–8]. The principal need of the aerospace industry is to produce faster, stronger and lighter structures and FRP composite materials can excellently address these demands due to their anisotropic nature. An example of their success can be seen in the Boeing 787 Dreamliner, which made history in 2011 as the world's first major commercial airliner to utilise FRP composite materials in its primary structure, by volume it is 80% composite, with the remaining 20% made up from metals such as titanium, aluminium and steel. To date, it remains to be Boeing's most fuel efficient aircraft [9].

Laminated FRP composites have excellent in-plane properties but a critical limitation is their low resistance to out-of-plane loading and susceptibility to delamination, which are situations that may arise from geometrical defects, manufacturing defects, or low-velocity impact [10–12]. This typical characteristic of multi-layer composites is due to a lack of z-direction fibre reinforcement and can lead to extreme reductions in the structural integrity by reducing residual strength and lead to catastrophic failure [4,11,13,14]. The low damage tolerance of laminated composites has also resulted in their commercial use being restricted to strain levels far below their potential [15]. Delamination is of particular concern for the aerospace industry as it can present as barely visible at the composite surface, yet at the same time can have catastrophic effects on the stiffness and strength of the composite structure [16]. Therefore, improving the low out-of-plane damage tolerance and delamination resistance of FRP laminates is a critically important measure when designing and developing composites [4].

It is well-known that the introduction of a through-thickness (TT) reinforcement can significantly enhance the delamination resistance of FRP composites [1,13]. To date, an extensive amount of research has been published on a variety of suitable TT reinforcement methods, including stitching [4,17–31], tufting [5,32–34], pinning [2,35–37], 3D weaving [2,8,14,38–41]. Of these methods, z-direction stitching is considered to be a very promising, low cost option technique to improve the interlaminar fracture toughness (IFT) and impact resistance of composites [2,4,24,29,42,43]. There continues to be a growing interest in TT stitching as it has been found to cause less in-plane damage compared to z-pinning and to degrade, or less commonly, improve, the tensile properties by up to 20% which is comparable to the properties of 3D woven structures [2,17]. Moreover, stitching is an attractive option for the reinforcement of structural composites because existing textile technologies and techniques can be used.

1.2 Problem Definition

Despite TT stitching being proven as a suitable reinforcement technique, still of major concern is the effect it has on the composite in-plane tensile properties. It is frequently the case that TT stitching causes an undesirable reduction in tensile properties [4,17,20,22,31,44]. This is because the stitching process causes microstructural defects including in-plane fibre distortions, fibre breakages, and resin pockets, which negatively affect the tensile properties [4,13,17,19,45,46]. Under loading conditions, resin pockets act as structural weak points due to the reduction of fibre reinforcement in these regions and cracks propagate from these areas as a result of stress concentration [17,47]. Due to their anisotropic nature, FRP composites exhibit highly complex damage mechanisms resulting from the interaction of multiple micro-scale failure modes [48,49]. Furthermore, researchers have reported new and different dominating damage mechanisms in stitched composite tensile specimens compared with unstitched counterparts [31,46]. The variation in damage modes are associated with the microstructural changes and damage imparted by the stitching process to the final composite geometry.

Of particular interest to this research is the optimisation of stitching for TT reinforcement of composites. Much of the subject literature considers the effects of TT stitching with a common geometry for the textile industry, the ISO-301 lock-stitch. For composite applications, the ISO-301 is frequently modified from the original geometry to ensure that the upper and lower threads are interlaced at the composite surface and not inter-ply [17,24,50,51], see figure 1.1. This results in reduced distortion of the in-plane fibres and associated stress concentrations in the final

composite structure [2,13,21]. However, there are still some key issues associated with the modified ISO-301. For example, the rotary hook mechanism can create a tortuous and damaging path for brittle advanced fibres [51], and the small capacity of the bobbin thread limits the seam length causing disruption to the manufacturing process as repeated pausing is required to replace the bobbin. For stitched composites to prove their worth, it is certain that they must dramatically improve the out of plane properties whilst not causing excessive reduction to the in-plane properties or damage to the reinforcement fibres. Importantly, stitching technology and machinery originates from the textile industry and it is clear that much of the knowledge of stitch formation and available geometries remains in the textile industry. It is the basis of this research that there are opportunities to optimise the stitching geometry that have not yet been explored for composites.

The work in this thesis supports the use of a novel stitch type for the composite industry, the ISO-401 double-thread chain-stitch, which to date has not been critically evaluated for use as an interlaminar composite reinforcement but it is the basis of this research that is has the potential to be suitable. The ISO-401 is commonly used throughout the textile industry and the geometry such that the interlooping junction between two threads naturally occurs at the preform surface (see figure 1.1), a beneficial factor in applications where in-plane fibre alignment is critical. Interestingly, the stitch junction can be repositioned across the surface, offering the opportunity for specific tailoring to the composite preform type and expected loading conditions. The ISO-401 also has the potential to address some of the shortcomings associated with ISO-301 stitched composites. For example, ISO-401 stitching operates under much lower thread tensions compared with ISO-301, which is likely to be less destructive to advanced fibre threads. Additionally, both the needle and looper threads are supplied on industrial sized creels for ISO-401 stitching which sufficiently increases the seam length capability during manufacture, compared with ISO-301.

(a) (b)

Figure 1.1 Schematic of stitch geometries; (a) modified lock-stitch based on ISO-301; and (b) ISO-401 double-thread chain-stitch.

1.3 Research Methods

To achieve the primary aim and objectives of this research, a combination of both quantitative and qualitative research methods were employed. Quantitative data was collected through experimental work, including the manufacturing and mechanical property testing of stitched FRP composites. Qualitative observations of damage mechanisms and composite structures were made through the visual assessment of optical micrographs of composite samples.

1.4 Research Aim and Objectives

The overall aim of this research is to find a form of through-thickness stitch-type reinforcement for FRP composites which effectively improves their damage tolerance without causing excessive damage to the in-plane reinforcement fibres and resultant tensile properties.

This aim has been fulfilled by completion of the following primary objectives:

- Review and analyse the existing stitch geometries for composite TT reinforcement, identifying their advantages and limitations in order to establish a benchmark for an alternative stitch geometry;

- Optimise the novel ISO-401 geometry for TT reinforcement of composites through selection and modification of the stitching parameters;

- Experimentally compare the in-plane tensile properties of composites stitched with the novel ISO-401 geometry and the commonly used ISO-301 geometry;

- Determine the impact and damage tolerance, of textile composites reinforced with the alternative stitch geometry;

- In-depth case study investigating the effect of the preform fabric characteristics on the ISO-401 stitch formation process.

1.5 Project Summary

The thesis chapters that follow this introductory chapter will cover a review of the literature, the research methods, results and discussion of the experimental work and conclusions and recommendations for future work.

Chapter 2 Review of Stitching and the Properties of Stitched Composites

The work in the literature review chapter consists of an in-depth review of the principle of stitch formation, the microstructural defects that stitching can cause in FRP composites and the various stitch geometries currently used in TT composite stitching. This is followed by a detailed discussion of a potential new stitch type for composites, the ISO-401 double-thread chain-stitch. The geometry and formation of the ISO-401 is discussed and comparisons are made with the common stitch type for composites, ISO-301 modified lock-stitch. Following this, the latest research on the mechanical properties of stitched composites is discussed. Particular attention is paid to the influence of stitching on the impact, damage tolerance and in-plane tensile properties.

Chapter 3 General Composite Manufacture

Chapter 3 covers a general overview of the composite manufacturing process. Details about the preform preparation, stitching machinery, stitching processes and parameters are given. Following this, the composite consolidation process is detailed, including the resin infusion method followed and the specimen preparation methods.

Chapter 4 Effect of the Junction Position and Stitch Density on the Tensile Properties of FRP composites

Chapter 4 is the first of three results chapters in this thesis. This chapter reports on the effects of varying the ISO-401 stitch junction position and stitch density on the composite tensile properties, compared with equivalent unstitched composites. Analysis of this experimental data enables an optimum stitch junction position to be proposed for FRP composites. Secondly, to provide a benchmark against a commonly used composite stitch type, the tensile properties FRP composites stitched the optimised ISO-401 stitching geometry are compared with ISO-301 stitched composites.

Chapter 5 Tensile Properties and Damage Tolerance of ISO-401 Stitched Composites

The work presented in Chapter 5 builds on the findings from the previous chapter to introduce the optimised ISO-401 TT stitching into the composite structure using advanced glass-fibre thread. In order to achieve this, adjustments to the sewing machine from its factory settings had to be made and these are detailed within this chapter. Comparisons of tensile properties are made between glass fibre-stitched, polyester-stitched and unstitched composites. Following this, the impact and damage tolerance of glass fibre-stitched and unstitched composites are reported in detail. The effect of ISO-401 stitching on the in-plane and out of plane properties are discussed in-depth.

Chapter 6 Effect of the Preform Fabric on the Stitch Junction Position and Tensile Properties

The final results chapter considers how the ISO-401 stitch formation process is affected by the preform fabric characteristics and the effect this has on the tensile properties of the final composite. The parameters of two different preforming fabrics are determined through experimental investigation. The results from this investigation are used to examine how the fabric characteristics affect the stitch formation process and resulting junction position. Lastly, the effect of TT stitching on the tensile properties of both type of composites are reported and discussed.

Chapter 7 Conclusions and Future Work

The final chapter of the thesis provides a summary of the findings from each chapter with an overall focus of demonstrating the contributions made to the field of research. The main achievements and limitations are discussed and recommendations are made for future work.

Chapter 2

Literature Review

2.1 Introduction

This chapter aims to summarise the method of stitching and the geometries used for the reinforcement of advanced fibre preforms, such as for those found in the aerospace and automotive industries. Traditionally, two-dimensional (2D) fibre reinforced polymer (FRP) composite laminates have been constructed through the lay-up, infusion and curing of woven advanced fibre tows or of pre-impregnated (pre-preg) fibre plies. Both of these methods are designed to enable improved handling during the preforming stage by limiting the movement of in-plane fibres. Weaving is a fabric manufacturing technique that originated in the textile industry and is the process of interlacing reinforcement yarns at 0° and 90°, known as warp and weft respectively. In the case of pre-preg, the reinforcement fabric has already been impregnated with high viscosity resin matrix, prior to lay-up and partially cured to enable handling of the fabric plies. The resulting multilayer FRP composites have excellent in-plane properties. Composites are used extensively throughout the aerospace industry, particularly in the manufacture of structural parts for civil aircraft, due to their high specific strength and stiffness, good corrosion and fatigue performances [4,7,12]. However, a critical limitation of FRP composite laminates is their susceptibility to delamination and fibre debonding when loaded out-of-plane. This is a direct result of the laminate geometry, where individual plies in the through thickness (TT) direction are bonded by the matrix only and not by z-axis fibres [1,47]. Therefore, out-of-plane stresses are borne only by the matrix system which leads to reliance on the boundary condition between the reinforcement fibres and matrix. This typical characteristic of multi-layer composites can lead to extreme reductions in the structural integrity by reducing residual strength and even in some cases catastrophic failure [4,10,11].

Improving the resistance of FRP composite laminates to out-of-plane loading can be successfully achieved by introducing a z-direction reinforcement, creating a three-dimensional (3D) architecture. Popular techniques of TT reinforcement include: stitching, 3D weaving, tufting and pinning. An extensive body of research [11,13,21,29,42,43,52–55], published since the mid-

1990's, has reported stitching to be a low-cost and effective TT reinforcement technique. Furthermore, stitching is an attractive technique because existing and mature stitching technology can be implemented. Discussed below are the basics of stitching technology and its application to composite laminates. Particular attention is paid to the available stitching geometries and their application in composites in order to identify a gap for a novel stitch type for composite application. Then, this chapter goes on to discuss in detail the damage mechanisms and mechanical properties of stitched composites as reported by other researchers.

2.2 Fibre Reinforced Polymer Composites

Composite materials in general are materials which consist of two or more components with distinctly different chemical properties and boundaries. The combination of such materials produces a composite with superior properties than the individual constituents. FRP (fibre reinforced polymer) composite laminates are the most common type of composite used for various types of industrial applications including aerospace, wind energy and in the automotive industry. The main advantages of such composites is that they have high specific strength and stiffness and excellent fatigue and corrosion resistance [37]. At the most basic level, FRP composites consist of long continuous fibres characterised by a high aspect ratio and high strength and stiffness [4,56,57]. The fibres are usually connected together through some form of textile processing, such as weaving, knitting, braiding, stitching and non-woven techniques, to produce a reinforcement fabric. High performance fibres such as glass and carbon are often used and thus FRP composites are widely referred to as advanced composites [58].

To manufacture the composite laminate, layers of advanced fibre plies are stacked together to produce the preform and are bound by a polymer matrix which usually accounts for less than 50% of the total volume, see Figure 2.1. The role of the matrix is to protect the fibres and maintain the composite geometry but also, importantly, to efficiently transfer load to the fibres during service. Thus, the laminate properties are highly dependent upon the fibre properties, it is common for the volume fraction of fibres to be from 50 % up to 70 %. Of critical importance to the mechanical properties is the bonding strength at the polymer-matrix interface. Damage to this interface or weak bonding can significantly affect the composite properties and in-service life [48]. As Figure 2.2 demonstrates, the reinforcement fibres can be orientated in different directions and thus the in-plane properties can be tailored for specific applications [56,57]. The anisotropic nature of FRP composites means that they will always have superior properties in the direction of the fibres [59].

The main benefit here is that strength and Young's modulus can be engineered in the load-bearing directions. However, the heterogeneous nature of composite laminates also presents some challenges.

A critical limitation of composite laminate structures is their low resistance to out-of-plane stress or loading and susceptibility to delamination, which are situations that may arise from geometrical defects, manufacturing defects, or low-velocity impact [10–12,56,60]. This typical characteristic of multi-layer composites can lead to extreme reductions in the structural integrity by reducing residual strength and even in some cases catastrophic failure [4,11,13,17]. The reason for poor interlaminar toughness is a result of the laminate geometry, where individual plies in the through thickness (TT) direction are bonded by the matrix only and not by z-axis tows or fibres [42,47]. The low damage tolerance of laminated composites has also resulted in their commercial use being restricted to strain levels far below their potential in the past [14,15]. Thus, improving the out-of-plane properties of composite laminates through introducing z-direction reinforcement fibres has been the subject of a lot of research papers in the past 20-30 years [13,14,31,61,62].

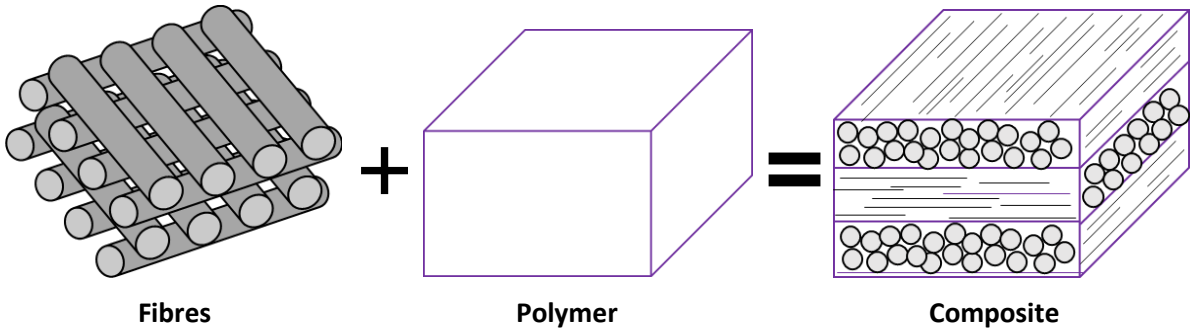

Figure 2.1 Schematic showing the fibre and matrix components and how are combined to form a composite laminate structure.

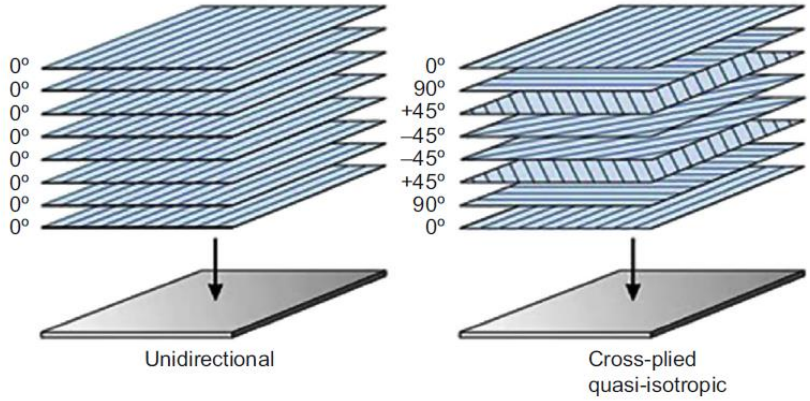

Figure 2.2 Schematic of FRP laminated composites showing different lay-ups [56].

2.3 Composite Interlaminar Reinforcement

There are a range of techniques available, aside from TT stitching, to produce FRP composites with a z-binder reinforcement in order to improve out-of-plane properties. New methods that are becoming more popular include 3D knitting, 3D weaving and 3D braiding. These techniques use processes that are based on traditional textile manufacturing techniques and machinery of 2D weaving, knitting and braiding [1]. A major benefit to these geometries is that near-net shape preforming can be achieved through a limited amount of automated steps in the manufacturing and production process.

2.3.1 3D Weaving

Out of the above mentioned techniques, TT stitching is often benchmarked against 3D weaving because this technique can be used to produce a similar composite geometry, a flat laminate plate with z-direction fibres. Figure 2.3 presents a schematic of the orthogonal 3D woven architecture, a common 3D woven architecture employed for FRP composite manufacture. Other 3D woven structures include 3D angle-interlock and 3D cellular. Reviewing the mechanical properties of these composites in-depth is beyond the scope of this thesis but it should be noted that they have been shown to offer both excellent resistance to impact and interlaminar properties as well as high in-plane strength and stiffness [13,14]. However, there are some limitations associated with the architecture of 3D woven composites. For example, the pressure of z-direction binder yarns causes undulations (crimping) of the in-plane fibres, which has been shown to be detrimental to the in-

plane tensile properties [2,63]. Also, the displacement of in-plane fibres around the binder yarns can cause reduced in-plane properties due to high reductions in fibre volume fraction [63]. Damage to the TT binder yarns can also be caused during the weaving process due to abrasion against weaving machinery and other yarns, resulting in reduction of yarn strength [64,65]. Additionally, a key drawback to the manufacturing process is that it can be a challenging process to insert z-direction yarns on existing 2D weaving machines and doing so requires an intimate knowledge of the weaving process. There are some examples of small specialised looms that have been developed for specific projects. However, these are mostly lab-scale, producing highly specialised products and are not suitable for wider industrial application. For example, NASA recently developed a loom to weave 3D thermal protection heatshield material used for shuttle entry into extreme environments [66,67]. Thus, to date, the commercial viability of 3D weaving for composite preform structures remains limited.

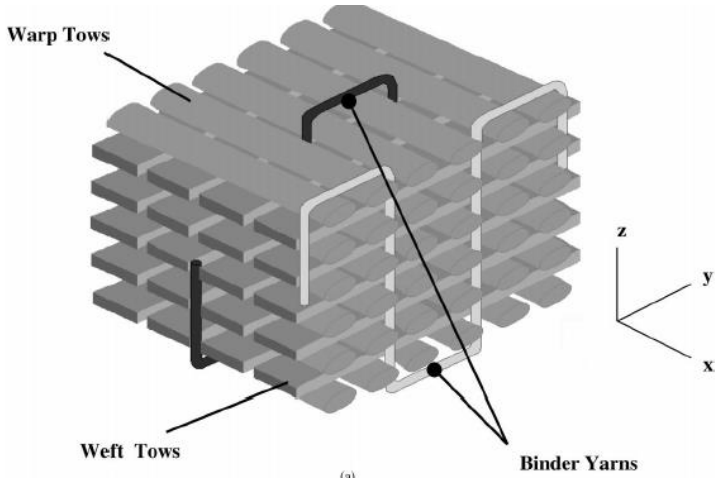

Figure 2.3 Orthogonal woven architecture commonly used in 3D woven composites from [14].

2.3.2 Z-Pinning

Z-pinning is a technique that uses very small pins, with a diameter of 02-1.0 mm, to reinforce FRP composites through the thickness. High strength, high stiffness materials are used for the z-pins, including carbon fibre composite, or metals such as titanium alloy and steel. The major advantage here is that it is one of the only techniques capable of reinforcing pre-preg laminates without causing excessive damage to the reinforcement fibres [36]. Other techniques such as stitching and tufting are mostly suited to the reinforcement dry fibre preforms as they can cause excess damage

when processing tacky pre-preg materials due to resin building up on the needle and the repeated penetrating action of the needle. A considerable amount of research has proven z-pinning to be an effective technique at improving the impact resistance [37,68] and the interlaminar fracture toughness [69–72] by having excellent crack bridging abilities, see Figure 2.4. However the in-plane tensile properties of z-pinned composites are less well understood. From the research that has been conducted, it is common for z-pinning to consistently cause a reduction in the in-plane properties [36], whereas for stitching, using optimised parameters can sometimes improve or even maintain the tensile properties [17].

Figure 2.4 Schematic demonstrating the bridging effect of z-pins during steady state crack propagation [69].

2.3.3 Tufting

The process of tufting originated as a technique for carpet manufacturing but has been specifically modified for composite TT reinforcement [73]. Similar to the stitching process, tufting threads or yarns are inserted into the preform using a needle. The difference here is that only one yarn is required, there is not a second yarn or looper that secures the needle thread, as in stitching, as in Figure 2.5. This makes tufting a much simpler manufacturing process than stitching as only access to one side of the preform is required, it is therefore classed as a one side stitching (OSS) technique. As the needle thread loop is left unsecured at the bottom surface, it relies upon the friction between the preform material and itself to remain in place [33,74]. Inter-ply slippage can be an issue in tufted composites due to the lack of an additional holding yarn, though this effect can be addressed by increasing tufting density [34]. The needle inserts the TT thread by penetrating the preform thickness either fully to the underside of the preform, or partially to a specified depth. An extensive body of research has demonstrated that tufting can be used to improve the interlaminar fracture toughness, both mode I [5,75], mode II [76,77], and damage tolerance properties [78] of FRP composites.

When the thread is carried through the full thickness of the preform, a loop of thread is left on the underside surface, as can be seen in Figure 2.5. During infusion, the surface loops are pressed against the composite surface and fill with resin, which forms an undesirable external resin-rich surface layer [33]. The resin filled loops then act as areas of structural weakness in the final composite which can negatively affect the in-plane properties [79]. Whereas for stitching, the needle loop is secured by either an additional thread or the intralooping of a single thread. Researchers [80] have found that removing the surface loop or tufted composites via machining methods improved the in-plane compression and compression after impact properties of tufted carbon/epoxy composites. However, this may be an undesirable approach as it creates the need for an additional manufacturing step.

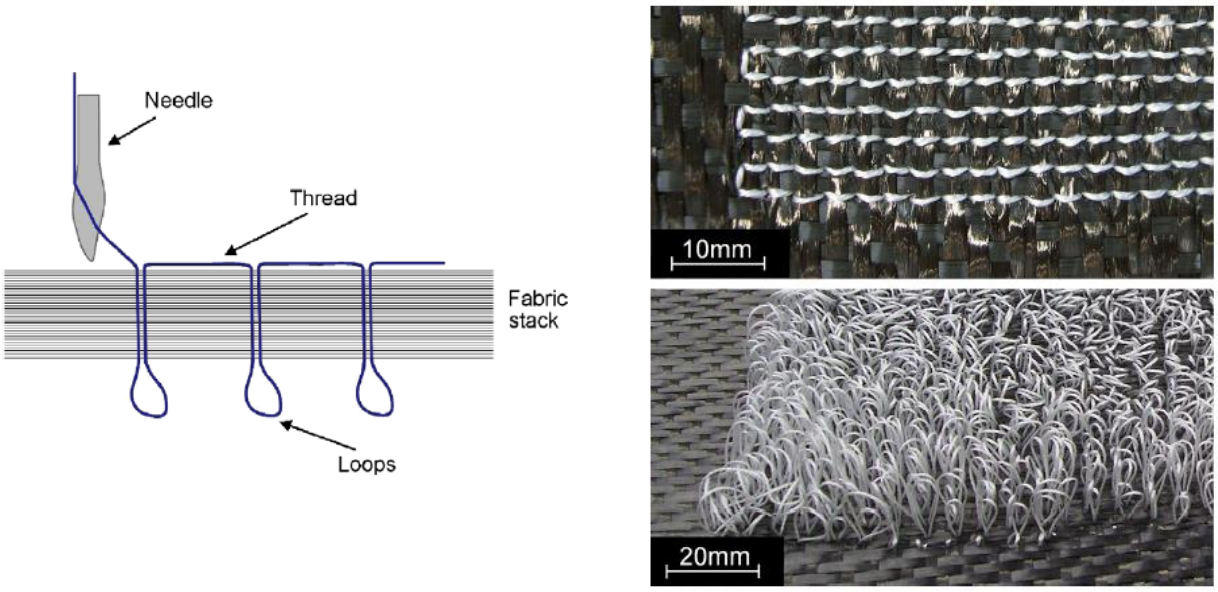

(a) (b)

Figure 2.5 (a) Schematic of thread insertion by the tufting process; (b) top and bottom sides of carbon fibre preform tufted with glass fibre thread [33].

2.4 Stitching

There is a continued interest in TT stitching as a laminate reinforcement technique as it has been found to cause less in-plane damage, including crimping, compared to z-pinning and to improve or degrade the tensile properties by up to 20% depending upon the stitch parameters used, which is comparable to the properties of 3D woven structures [2,17]. Moreover, stitching is an attractive option for the reinforcement of structural composites because existing and mature textile

technologies and techniques can be used. Due to its many benefits, some researchers consider that stitching is the most effective type of z-direction reinforcement [4,21].

In basic terms, stitching can be defined as the intra-looping, inter-looping or interlacement of stitch threads to join together two or more textile substrates. In the textile industry, stitches are grouped or defined by their formation type into six classes, from class ISO (International Standards Organisation) 100 to 600. Intra-looping is constructed from a single thread where a passing of a loop through another loop is made by the same thread, for example in ISO 101 single thread chain-stitch. In the case of inter-looping, a loop formed by one thread is passed through the loop of another thread, as in ISO 401 chain-stitch. Interlacing is the process of passing one thread over or around another thread, as in ISO 301 lock-stitch [81–85]. Furthermore, the continuous group or line of stitches produced by the sewing (joining) of textiles is commonly referred to as a seam. In the textile industry there are many variations of seam types, for example, bound, double lapped, superimposed. Seam construction or type is chosen based on the suitability to the intended purpose of the product or garment being sewn. Important considerations when choosing a seam include, aesthetic appearance, comfort, durability, strength and cost [81,86,87].

The method of joining flexible materials by hand-stitching long predates the invention of the sewing machine and even fabric construction methods such as weaving and knitting. Archaeologists have found 20,000 year old evidence that our ancestors fashioned needles from animal bones and thread from animal sinew to join animal skins for clothing. The first sewing machine was invented in the 18th century and was designed to replicate and automate the process of hand-stitching [88,89]. Since their invention, the speed, efficacy and consistency of industrial sewing machines has improved significantly [90]. In the last 30 years, industrial sewing machines and stitching geometries from textiles have found application in the advanced fibre composite industry.

Since the early 1990's, recognition for stitching as a composite reinforcement has increased as it has been demonstrated to cause less in-plane damage compared to z-pinning and have comparable effects compared to 3D woven structures [1,2,17,91]. Stitching can be applied to composite preforms for structural or non-structural applications. In the case of non-structural stitching, stitching with fine thread, usually with a non-advanced fibre, is conducted to assist with the consolidation of fibres and to minimise in-plane displacement during the lay-up process. Non-structural stitching is not intended to enhance the out-of-plane performance of composites. On the other hand, structural stitching, is applied to enhance the mechanical properties of the final composite, particularly in the out-of-plane direction. Structural stitching is usually performed with

high-performance yarns such as carbon fibre, glass fibre, Kevlar (aramid), Vectran (liquid-crystal polymer). Inevitably, the introduction of structural stitching also helps to improve the handling of the preform and reduce the risk of inter-ply movement [1,2,13,45,92]. Stitching is usually performed on dry reinforcement fibres, followed by resin infusion such as the vacuum assisted resin infusion method (VARIM). The stitching of pre-preg is feasible but more difficult and not carried out as frequently because the needle action is obstructed by the increased friction between the needle and the tacky uncured resin [1]. Undesirable levels of damage to in-plane fibres can occur during the stitching of pre-preg fabrics because the needle tip can fracture fibres as they are less able to adjust around the needle, compared with dry fibres, due to the uncured resin coating, leading to an increase in material discontinuity and areas of stress concentration in stitched pre-pregs [2,11,91].

2.5 The Principle of Stitch Formation

The basic principle of stitching, regardless of the chosen stitch geometry, is the formation of a loop on the under surface of the material being sewn. Furthermore, the consistency of the formed needle loop is critical to the stitch formation [81]. Creation of the needle thread loop is such that the needle descends into the fabric, to the underside of the fabric and to the bottom of its stroke, taking the needle thread with it and as the needle returns and retracts back through the fabric, the friction created between the fabric and the needle thread enables a loop to form at the scarf of the needle. At this point, depending on stitch geometry, the loop is picked up by a looper (as in chain-stitching) or rotary hook (as in lock-stitching). Conformation of the stitch is then completed in one of three ways; the needle thread loop is intralooped with itself (as in single-thread chain-stitching), interlaced with a bottom thread (as in lock-stitching) or interlooped with at least one bottom thread (as in double-thread chain-stitching). The needle thread loop is then cast-off from the looper or rotary hook. Finally, the process is completed by setting the newly formed stitch into the fabric, usually through tensioning [83,85].

The processing of the stitch formation relies upon a group of synchronised key elements known as; the needle, the hook, looper or shuttle, take up lever and the feed mechanism [93]. It is worth establishing that the coordinated timings and geometries of these mechanisms are essential in the process of sewing and so it is difficult for them to be discussed or considered in isolation. However, for the purpose of this work they are discussed in succession in order to establish their role within the stitch formation process.

2.5.1 Basic Function of the Needle

Central to the stitching process and a key factor affecting loop formation and eventual seam strength regardless of the chosen stitch geometry, is the needle geometry. Selecting the correct needle type for the machine, stitching thread and the fabric being stitched is critical [83,94–96]. Common issues during sewing as a result of poor loop formation, including skipped stitches and thread breakages, can be attributed to the usage of an incorrect needle type [83]. This is because the generation a consistent loop requires the optimum level of friction to occur between the needle thread and the fabric, of which needle geometry is a main contributing factor. The needle geometry, as presented in Figure 2.6, is designed to effectively deliver the needle thread to the underside of the fabric and form a loop when the needle is at the beginning of its ascent. The end of the needle consists of the needle point, the combination of the point and extreme tip of the needle is designed for suitable penetration of the fabric substrate, ideally pushing the yarns apart creating the needle path, as opposed to puncturing and breaking the fibres [95]. The needle tip can vary widely to suit different fabric types, such as ball-point for knitted fabrics, sharp point for woven fabrics and chisel-shaped for leather.

The front of the needle has a long groove where the thread is channelled before it is fed into the needle eye. During the needle descent, the long groove enables the thread to be effectively drawn down through the fabric. The back of the needle features the short groove and above it, the scarf. When the needle ascends, the short groove encourages a loop to form as the thread at the back of the needle becomes trapped and lags as it is unable to return smoothly back through the fabric as the short groove channel is not long enough. At the scarf, the needle cross-section is reduced to allow some clearance for the loop to be retrieved by either a looper, hook or shuttle [83]. The needle dimensions, such as the thickness, length of the blade and shank length must correspond with the timing of the bottom mechanism for effective loop formation and conformation [81]. For example, if the needle is too short, the looper, hook or shuttle will be unable to interact with the loop and if the needle is too long or thick, it can be damaged by coming in contact with the bottom mechanism. Therefore, every machine type has a specific set of suitable needle dimensions, these are commonly identified as the needle system.

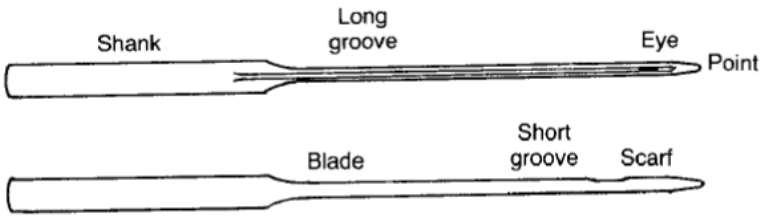

Figure 2.6

Schematic of the sewing machine needle geometry from [83].

In the stitching of composite preforms, a commonly reported stitch-induced defect is the breakage of fibres during needle penetration, thus consideration of the needle type and geometry must be taken to help minimise these effects. Furthermore, reinforcement fibre breakage during preform stitching can lead to microstructural defects and reduced mechanical properties in the final composite [2,17]. While it may be hard to avoid this completely as brittle yarns will be inherently more susceptible to fracture, selection of the appropriate needle point for the reinforcement material could potentially minimise in-plane fibre breakage. Another consideration when selecting the sewing needle for composites is the size of the needle eye. If the advanced fibre reinforcement thread is being used as the needle thread, as in this project, it is essential that the needle eye size is adequate to avoid fracture of the thread. During needle penetration, friction between the needle thread, needle hole and the fabric can be enough to fracture the thread. This is particularly relevant in the case of composites as the needle and thread are travelling through multi-layers of fabrics at a time, potentially further increasing friction on the thread.

2.5.2 The Take up Lever and Timing of the Loop Taking Mechanism

The loop taking mechanism, such as the looper, used in chain-stitching or the rotary hook or shuttle used in lock-stitching, provides one of the essential operations in the stitch formation as it is responsible for the junction of the thread or threads [97]. As such, each of the above mentioned mechanisms are designed to pick up the newly formed thread loop from the back of the needle and create the stitch thread junction through the process of interlooping or interlacement with at least one other thread or by intralooping the single needle thread. Therefore, the timing of such mechanism is critically important to the stitch conformation process as it has to catch the needle loop when the needle is at the optimum position.

The purpose of the take-up lever is to provide fundamental control of the feeding of the needle thread through the machine [98]. The needle thread is tensioned and threaded through an eye on the take-up lever before it is threaded through the needle eye. During the stitch formation process, the take-up lever repeatedly travels up and down on a vertical path applying and releasing tension to the needle thread at various points. As the needle is retracting through the fabric and the newly created stitch is being set, the take-up lever lifts to apply tension to the needle thread, picking up the slack and helping to draw the thread back out of the fabric. The lever then moves down to feed the prescribed thread length from the needle thread creel for the next stitch, this occurs simultaneously to the fabric being fed through the machine by one successive stitch length by the feed dog [98,99].

2.5.3 Machine Feeding Systems

The achievement of the formation of successive stitches relies upon the sewing machine feeding system, which is responsible for advancing the material through the machine by one prescribed stitch length at a time. There are several variations of feeding systems available which are suited to different fabric types and it is therefore essential that careful consideration of the feed type is taken for the requirements of the fabric and of the seam type. The most common feeding system is the four motion drop feed system, which consists of three main components, the presser foot, feed dog and the throat plate, as presented in Figure 2.7 [81,83,100].

The role of the throat plate is to provide a smooth flat surface for the fabric to advance over. Within the throat plate are several openings, one to allow the needle to descend to the underside of the preform and interact with the looper and one to accommodate the feed dog [81,100]. Flagging of the material being stitched can occur if the needle opening is too large for the needle size, which can lead to defects such as fibre rupture and skipped stitches. In order to avoid these issues, the needle opening should be approximately 30 % larger than the needle [83].

The feed dog is made from a serrated metal plate and operates in a circular motion in order to advance the fabric through the system by a controlled stitch length, as in Figure 2.7. For this feed type, the feed dog has four degrees of movement; it ascends up above the throat plate to make contact with the fabric, advances the fabric one stitch length towards the back of the machine, descends below the throat plate releasing contact with the fabric and travels back to its original position underneath the plate and the cycle begins again [81,83,100].

The role of the presser foot is to provide the required amount of pressure to control the fabric feeding and constrain fabric movement during the needle penetration and withdrawal steps of the sewing process. During the stitching process, it is desirable to apply the minimum amount of pressure required to the fabric via the presser foot to correctly feed the material [81]. However, achieving optimal presser foot force for every sewing situation can be difficult. For example, lowering the force is favourable to reduce damage to the fabric, however the presser foot can lose contact with the fabric intermittently at high speed resulting in a faulty seam [100,101].

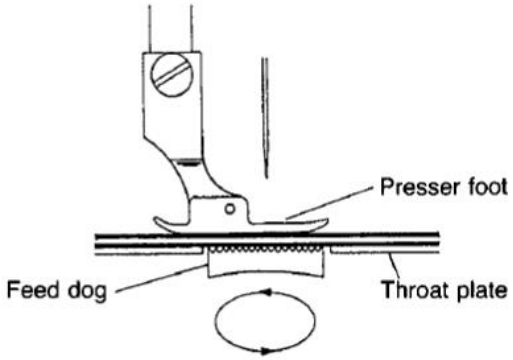

Figure 2.7 Schematic of the drop feed system [83].

2.6 Optimisation of Stitching for Composites

Stitching is considered a flexible and versatile z-direction reinforcement technique due to the fact that existing textile machinery and stitch types can be explored for composites [11]. This flexibility is a product of the wide range of stitch parameters that can be altered and implemented, these can include: stitch geometry, stitch density, needle-type, stitch thread type, thread linear density, and stitch thread tensions. Theoretically, the large range of parameters involved in the stitching process allows for the specific tailoring and optimising of the final composite structure. Researchers have well-established that the degree to which the mechanical properties of composites are affected by TT stitching is dependent upon the stitching parameters along with the manufacturing process and test conditions [4,11,13,17,45,51]. For example, it has been demonstrated that the ability of stitching to arrest and delay the delamination growth during impact is directly related to the stitching parameters [21] which consequently affect the mechanical

properties such as, delamination resistance, interlaminar toughness and tensile properties of the composite structure [17]. Furthermore, researchers have reported that the proportion of energy dissipation through stitched composite damage mechanisms is different depending on the different stitch parameters [42,102]. The large number of associated changeable stitch parameters and their varied effects on the final composite properties can make them difficult to study and the interpretation of such data is complex and can be case-dependent [92]. For the benefits of TT stitching to be realised for composites, optimisation of the process and parameters is required in order to reduce some of the negative side effects stitching can cause. Additionally, much of the practical knowledge and understanding of stitch formation and geometry remains in the textile industry, utilising this knowledge may help to gain a broader understanding of how to optimise stitched composites. Thus, it is the intention of this thesis to contribute to this area of research by investigating the stitch formation process and the effects of the stitch geometry on the mechanical properties and geometry of FRP composites.

2.6.1 Stitching Induced Defects

Despite the advantages of interlaminar stitching for improving out-of-plane properties, the process of stitching can introduce architectural irregularities into the preform and consequently lead to microstructural defects in the consolidated composite [1,45,80,91]. Common defects include in-plane fibre breakages, in-plane fibre crimping and waviness, resin rich regions and misaligned z-direction fibres [2,4,19,91,103]. Such fibre defects have been shown to act as damage initiation sites and can directly influence the mechanical properties of the final composite structure [17,45]. In particular, distortions to the reinforcement fibres have been demonstrated to have a negative effect the fibre dominated properties, such as in-plane tensile properties, which are reliant on the volume and orientation of the reinforcement fibres [17,19,104].

2.6.1.1 *Fibre Fracture*

The action of needle penetration into a multilayer composite preform is executed at high forces, therefore the fracturing of brittle advanced fibres is not unexpected [14]. During the preforming stage, broken surface fibres may be evident post-stitching. Additionally, it is important to recognise that the size of the needle stem diameter is not significantly small relative to the in-plane fibre tows, therefore displacement of in-plane fibres is inevitable.

2.6.1.2 *Fibre Waviness and Resin Pockets*

Fibre waviness in stitched preforms occurs due to the displacement of in-plane fibres around the penetrating needle action and as a result of the z-reinforcement fibre that is introduced into the structure. As the needle descends into the preform, it distorts the in-plane fibres from their original path to create a passage for the thread, this results in the in-plane fibres being permanently bent around the stitches in an ellipse (see Figure 2.8(a)). Generally, most of the fibre spreading occurs on the top and bottom surface of the preforms where the thread is entering or exiting the preform at an angle at the stitch points. It is considered that the damage to the middle plies is less severe as the needle thread is running in the z-direction without any small radius loops or angles. During resin infusion and composite consolidation, these areas of low fibre volume at the top and bottom surface are particularly susceptible to becoming filled with resin, creating resin rich zones. Figure 2.8(b) presents an optical micrographs of a stitched composite cross-section with resin pockets. In the final composite, these zones are areas of structural weakness as they contain little or no reinforcement fibres [17,19,24,27,104].

2.6.1.3 *Fibre Crimping*

The mechanical properties of FRP composites are largely dependent on the in-plane fibre volume fraction (FVF) [105], therefore changes to the FVF value due to stitching can have a significant effect on the resultant properties of the composite. There have been contradicting reports in which interlaminar stitching has been shown to either increase or decrease the FVF, however despite its importance, any changes to FVF by stitching remains a largely unreported material characteristic [17]. It is considered that defects induced by the stitching process can influence the FVF of the final composite, for example, large resin pockets can potentially cause a reduction in FVF compared to unstitched equivalent composites. On the other hand, very taut stitching may increase the volume fraction of fibres and reduce composite thickness [17]. However, this approach may increase the potential of crimped z-direction thread and thus potentially reducing their effectiveness for out-of-plane reinforcement [91]. Figure 2.8(c) presents a microscopic image taken from composites made for this study of crimped TT stitch threads. Crimping is caused mainly by a combination of the pressing of the stitch crowns (thread junction points) into the underside of the composite structure during the pressurised environment of resin infusion and the static tension of the stitch threads.

It is evident that the very nature of the stitching process will inevitably impart some undesirable damage to advanced fibre preforms, with these sites resulting in microstructural defects in the final composite. It is also clear that such defects are a direct influence on the engineering properties of composite structures [17,19,104]. Therefore, whilst some stitch related damage is unavoidable, attempting to optimise the stitching process to reduce some of the negative side effects is necessary. Key to optimising stitching for composite is adjustment of the stitching parameters. All of the defects mentioned will inevitably be a feature of stitched composites [17] but understanding stitching process may help to reduce the severity of them and optimise stitching for composites.

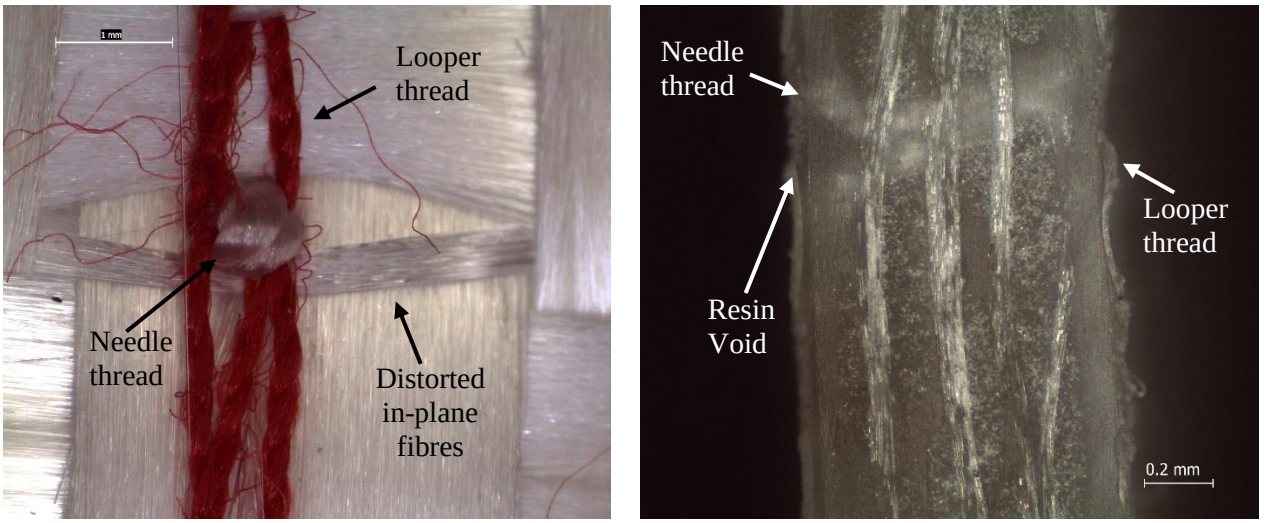

(a) (b)

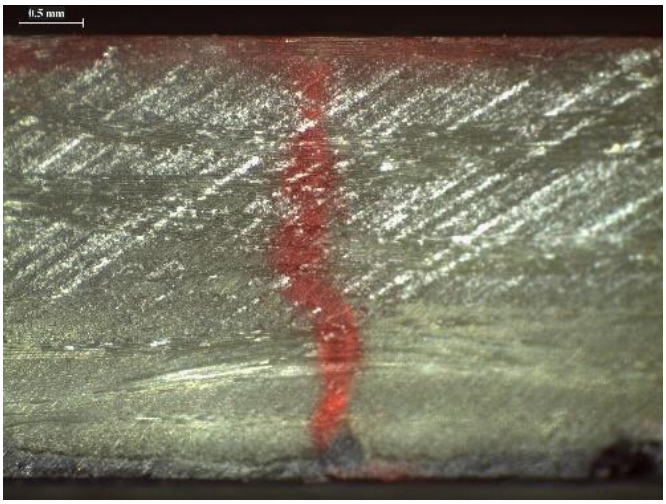

(c)

Figure 2.8 Stitch-induced defects (a) optical micrograph of the underside of an ISO-401 stitched preform showing in-plane fibre deviations around a stitch point; (b) Cross-section of an ISO-401 stitched E-glass/epoxy composite with resin void; (c) optical micrograph from this research showing crimped needle thread yarn in an E-glass/epoxy composite cross-section.

2.7 Stitch Geometries Employed for Composite Reinforcement

There are a large variety of stitch types and geometries that have been developed for use within the apparel and textile industries, for example in the manufacture of automotive airbags and parachute fabrics. Some of these stitch types from textiles have been applied to multi-layer FRP composites to successfully improve interlaminar properties, enhance resistance to delamination and improve handling, such as ISO 101, ISO 205 and ISO 301 [21,24,50,106,107]. The formation and path of the stitching thread is uniquely dependent upon the stitch geometry and so the mechanical behaviour of the final composite after impregnation of the resin matrix can differ depending upon the applied stitch geometry [24]. Despite the application of some stitch types for composites, much of the knowledge and understanding of the mechanisms of stitching and stitch formation are virtually unknown outside of the textile and garment industry. There is little in-depth research that experimentally compares different readily available stitch geometries for the purpose of reinforcing composite laminates.

It is therefore the purpose of this research to investigate the potential of an existing stitch type that has not yet been considered for composites. In particular, it is proposed that the double-thread chain-stitch (ISO-401) geometry is of interest to composite reinforcement. The main advantage here is that the inter-looping junction is not placed inter-ply and instead occurs naturally at the bottom surface of the material without requiring high tension, a positioning that is preferable when stitching composite laminates as it reduces the risk of damage to in-plane fibres. The following sub-sections discuss the application and stitch formation of the limited range of stitch geometries currently used or explored for composite reinforcement. The potential of ISO-401, the basis of this research, is then discussed with respect to the most common stitch type used for composite reinforcement, the modified lock-stitch (ISO-301).

Considering the wide choice of existing stitch geometries, many of them are considered unsuitable for composites [17,24,108], particularly classes ISO 500-600 and some ISO-400 and -300 types because they include complex multi-looping in their formation, see Figure 2.9. Additionally, some of these geometries employ multiple needles and threads (usually three to five) which are likely to cause undesirable damage to advanced fibre stitching threads and result in an inefficient final composite geometry with many surface loops.

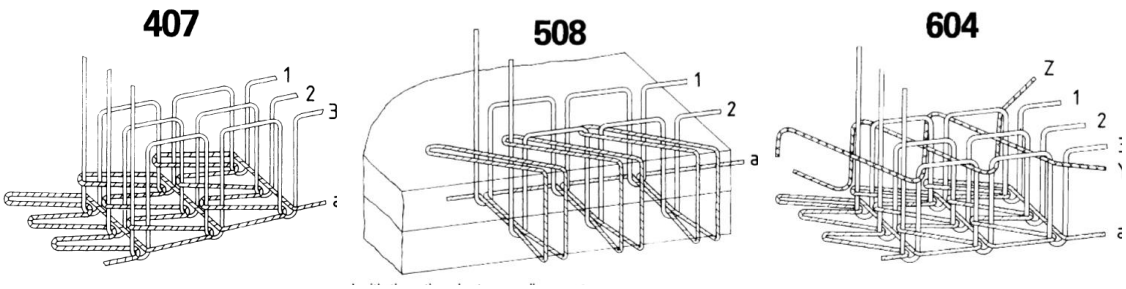

Figure 2.9 Examples of multi-looping, multi-thread stitch classes determined to be unsuitable for the TT stitching of composite laminates, from [82].

2.7.1 ISO 101 Single-thread Chain-stitch

The single-thread chain-stitch is created by the intra-looping of a single thread on the surface or around the fabric plies. The use of ISO-101 in composites is mostly restricted to non-structural applications because a high degree of thread flexibility is required to achieve the complex intra-looping configuration. During the stitch formation process, the needle ascends from the bottom of its stroke and a loop of needle thread is formed at the needle scarf. Once the needle has begun its retraction into the fabric, the looper has enough clearance to come forward and catch the loop whilst the fabric is fed through the machine at a prescribed distance according to the stitch length. The looper retracts, leaving the original bottom surface loop in the needle path. As the needle descends to the bottom its stroke, it passes a new loop through the original loop. The new loop is caught by the looper and the interlooping point at the original loop is consolidated, setting the stitch into the fabric [85]. The final geometry leaves a single discontinuous line of thread at the top surface and an accumulation of thread loops at the bottom surface which provides increase flexibility of the seam in comparison to the common lock-stitch [21,82,83,85]. The uncomplicated mechanism by which the ISO-101 is formed means that stitching can be performed at low thread tension and high manufacturing speeds can be achieved [50]. As each successive stitch is reliant on the previous loop for security, it is commonly used in the textile industry as a temporary holding stitch because of its ease of removal. When used in more permanent applications, it is crucial to secure each end to avoid unravelling [81].

To form this geometry, the thread is required to undergo small radius 360° loops which makes it an unsuitable process for advanced reinforcing fibre threads such as glass and carbon fibre due to their brittle nature [21,91]. Furthermore, when considering the potential composite reinforcement benefits of this stitch, the geometry is not as advantageous as others. At each needle insertion point there are two z-direction threads inserted, however, these are accompanied by three lots of

surface thread, one length of thread on the upper surface and two repeating loops of thread on the bottom surface, both which contribute little to the mechanical properties of the composite [50].

Despite its shortcomings, ISO-101 is still regularly used in composites, it has played a very important role in the development of revolutionary NCF multi-axial non--crimp fibre (NCF) preforms as an intra-ply holding stitch. As an alternative to weaving, in NCF preforms straight yarns are laid in multiple directions and bound together with a single-thread chain-stitch, common configurations of NCF fabrics include biaxial, triaxial and quadraxial. For example, to create biaxial NCF fabric, two straight fibre tows are aligned in the 0/90° or ± 45° and bound together with a single-thread chain-stitch to create one ply [109–111]. NCF has been shown to achieve better tensile and impact properties due to the non-crimping of in-plane fibres associated with woven structures [111].

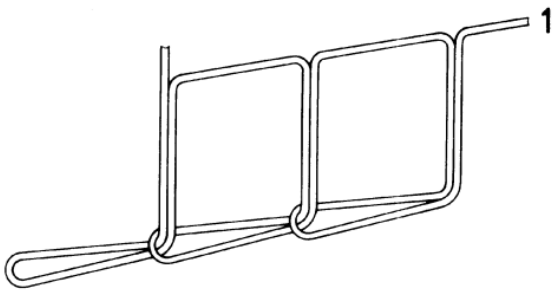

Figure 2.10 Schematic of ISO-101 single-thread chain-stitch [82]

2.7.2 ISO-301 Lock-stitch

The ISO-301 lock-stitch is the most common type of stitch geometry used in the textile and apparel industry and it is subsequently the most widely used stitch type for the structural stitching of composites. Due to its interlocking threads, the ISO-301 is a robust stitch resulting in a seam with little extensibility, in the order of ~30%. Consequently, a lot of attention has been focused on adapting lock-stitching for composite reinforcement and investigating the properties of lock-stitched composites [17,24,50,51]. The lock-stitch is generated with a top thread, supplied by the needle and a bottom thread supplied by a bobbin. The needle thread, supplied from a creel external to the machine, is fed through a pre-tensioner before it passes between two tensions discs which exerts the majority of the frictional resistance upon the thread. The thread then loops around the check spring (a coiled spring) which exerts some additional friction on the thread and aids in

controlling the thread consumption [112]. From the check spring, the thread passes through a guide, through the take-up lever, and a final guide before it is threaded through the needle eye [98,113]. The bobbin is positioned in a de-mountable case underneath the machine bed and houses the bottom thread supply. The bobbin case-spring exerts controllable friction on the thread as it is unwound from the bobbin case during stitching.

In the traditional geometry, the stitching process is such that the needle and bobbin threads are secured between the fabric plies by interlacing, see figure 2.11. To form the stitch, the needle penetrates the fabric and as it rises from the bottom of its stroke, a loop is formed at the needle scarf. The rotary hook catches the newly formed loop and rotates the needle thread around the bobbin case (360°) in a counter-clockwise direction. Consequently, the needle thread interlaces with the bobbin thread during its rotation. As the needle ascends through the fabric, tension is applied to pull the needle thread and interlacement junction with it and set it into the fabric [24,50,51]. A step by step process of the ISO-301 formation can be seen in Figure 2.11. Traditionally, the interlacement junction occurs central between the plies of fabric (inter-ply) and the resultant structure is reinforced by two threads at each needle insertion point. This is preferable in the sewing of textiles to create a secure, balanced and symmetrical seam. In the balanced ISO-301 stitch, the thread tensions of both the needle and bobbin thread are equal which creates a neat seam appearance with a single line of thread visible on both surfaces of the fabric plies. This stitch type is popular due to its many advantages, for example; it is the only stitch type to reliably stitch around 90° bends when pivoting around the needle point, different threads can be used for both components of the seam and thread consumption is very efficient [50,81].

For composite applications, the balanced lock-stitch geometry damages the in-plane fibres and leads to stress concentration at the stitch points as the interlacement is nested inter-ply, disrupting the in-plane fibres. Consequently, ISO-301 has been modified to unbalance the geometry and ensure the interlacement position between the needle and bobbin threads occur at the preform surface (top or bottom), as in Figure 2.11. Thus reducing the associated stress concentrations which is beneficial in applications where in-plane fibre directional alignment is critical [2,13,21]. To create an unbalanced ISO-301 where the bobbin thread is carried through the preform on to the upper surface where the interlacement point is set, the bobbin thread tension must be reduced and the needle thread tension increased. The bobbin thread tension is reduced by loosening the bobbin case-spring via the tensioning screw. The needle thread tension is increased by manual adjustment of the tension-disc [21,50]. The low tensioning of the bobbin thread for this configuration means it is more accommodating to the loading of brittle advanced fibres. However,

the loading associated with the combined winding and unwinding of the bobbin thread on brittle advanced fibres cannot be ignored.

Alternatively, the interlacement position can be positioned at the bottom of the preform surface by increasing the tension in the bobbin yarn and reducing the needle thread tension. An advantage of this interlacement position is that the bobbin thread is not required to travel twice through the preform thickness with each stitch and therefore the stitch length is less reliant on the small bobbin capacity [51]. Instead, the needle thread, which is supplied on a much larger thread creel, is pulled by the high tensioned bobbin thread through the thickness of the composite preform, thus providing the interlaminar reinforcement. However, the needle thread path through various tensioning devices, the check spring and widening around the bobbin case by the rotary hook all present a tortuous and damaging route for brittle advanced fibres [51]. As a result, when employing the modified ISO-301 geometry for composites, it is most commonly the case that the advanced reinforcement thread is supplied by the bobbin mechanism [17,21,50].

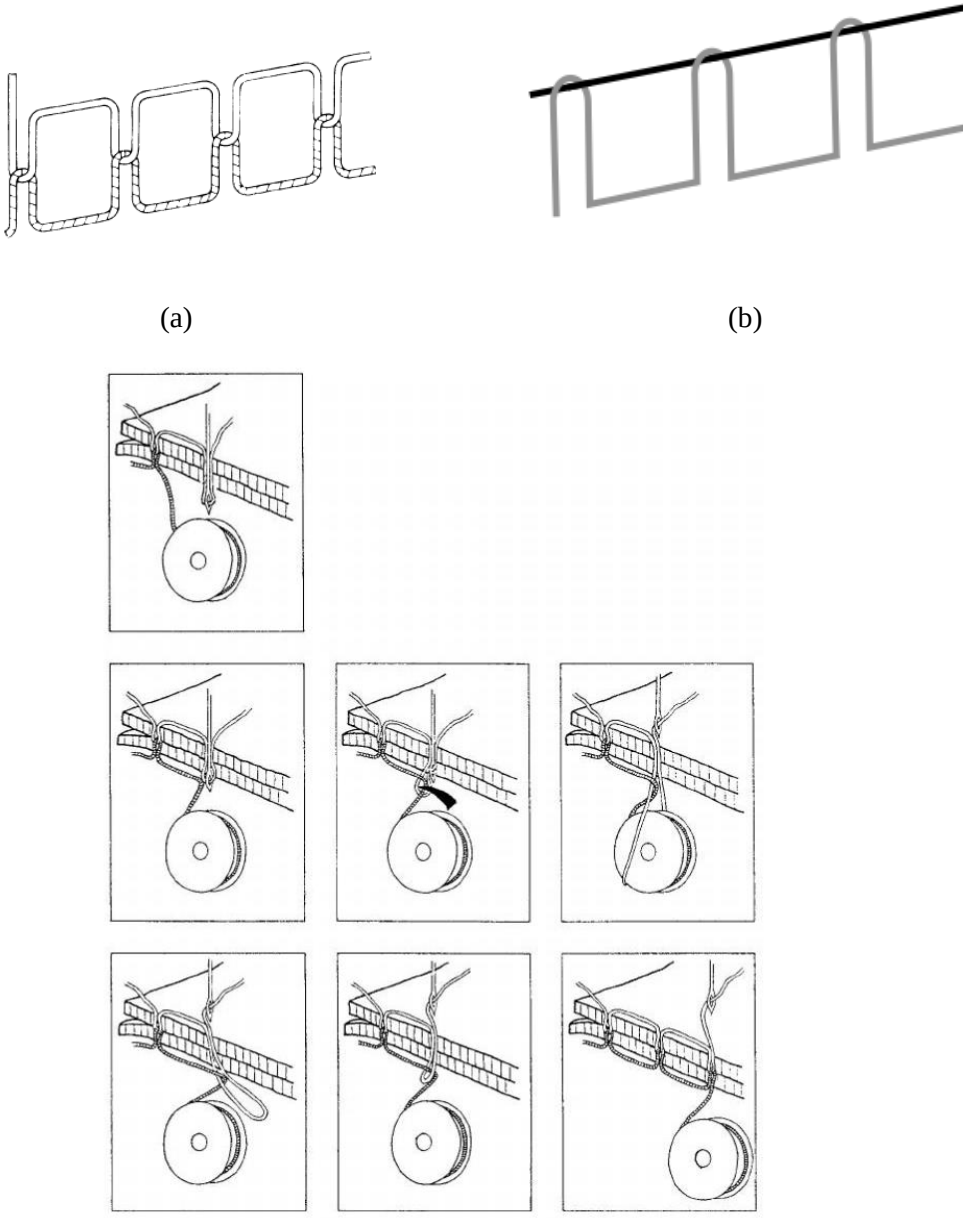

(a) (b)

(c)

Figure 2.11 (a) Schematic of the standard ISO-301 lock-stitch geometry, [82]; (b) Schematic of modified lock-stitch; (c) step by step process of ISO-301 formation [83].

2.8 ISO-205 Orthogonal Stitch

In order to overcome some of the disadvantages associated with the modified lock-stitch and single-thread geometry, recent research originating from The University of Manchester has demonstrated the potential of the orthogonal stitch. Composites stitched with orthogonal stitch have been shown to have interlaminar properties which outperform that of modified lock-stitch [21,50,114]. The geometry requires just a single thread and is structurally much simpler than ISO-301 and ISO-101. The geometry is such that the thread is inserted through to the bottom of the preform surface, one stitch length is placed on the surface before the thread is reinserted from the bottom surface and advanced one stich length on the top surface, the whole process is then repeated. This technique creates a discontinuous line of top and bottom surface threads and a single z-direction thread. The geometry is advantageous for developing stitched composites with advanced brittle fibres because the thread is not required to make any radius loops or angles above 90°. Figure 2.12 presents a schematic of the orthogonal stitch geometry.

However, a major drawback to the studies mentioned above is that the application of orthogonal stitch to composites was administered manually by hand. Besides the obvious restrictive manufacturing technique for this stitch type, the application process also means that the thread tension is not controlled to the point that it would be during machine stitching, thus potentially leading to greater tension variation [21,50]. To address these issues, a recent study at The University of Manchester [115] has focused on developing an automatic process for the TT orthogonal stitching of composite preforms with some success. A prototype robotic stitch head was developed with the capability of consistently producing orthogonal stitched composite preforms. Although the study produced promising results, further work is still required to industrialise and progress the technique, thus the use of orthogonal stitch for composite reinforcement remains very restricted.

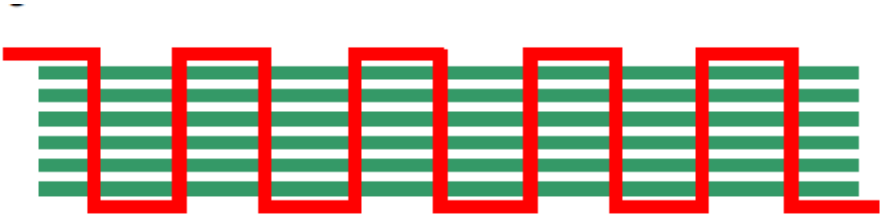

Figure 2.12 Schematic of the orthogonal stitch geometry for composites [50].

2.9 ISO 401 Double-thread Chain-stitch

In the textile industry, the study of sewing dynamics including the effects of machine settings and fabric properties of lock-stitch has been well documented, as in [90,98,100,116–119]. However, there is limited published research [118,120,121] on the sewing dynamics of the double-thread chain-stitch (ISO-401) likely due to its geometrical complexity in comparison to lock-stitch. It is the intention of this research to determine the suitability of ISO-401 to composites and add to the knowledge of the stitch formation and sewing dynamics. To date, the double-thread chain-stitch (ISO-401) stitch geometry has not been critically evaluated for use as an interlaminar composite reinforcement but it is the basis of this research that is has the potential to be suitable for composites and even address some of the shortcomings associated with modified lockstitch. Figure 2.13 presents a schematic of the ISO-401 stitch geometry. There are two aspects of its geometry that are well-suited to composites; (i) the interlooping junction naturally occurs under low tension on the bottom surface of the plies and not inter-ply, (ii) the surface location of the thread interlooping position can be altered via adjustment stitch thread tensions. Compared with the commonly used ISO-301, this stitch type utilises low thread tensions and so is less likely to suffer from puckering of thread damage. The flexible interlacement position of the geometry presents the opportunity for interlaminar stitching to be optimised or even tailored for use in composites and thus potentially reduce some of the negative impact stitching can have on the composite geometry.

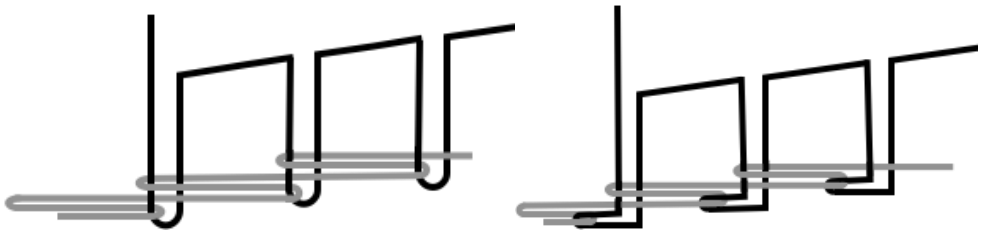

(a)


DÜRKOPP ADLER
173
STOCKS

(b)

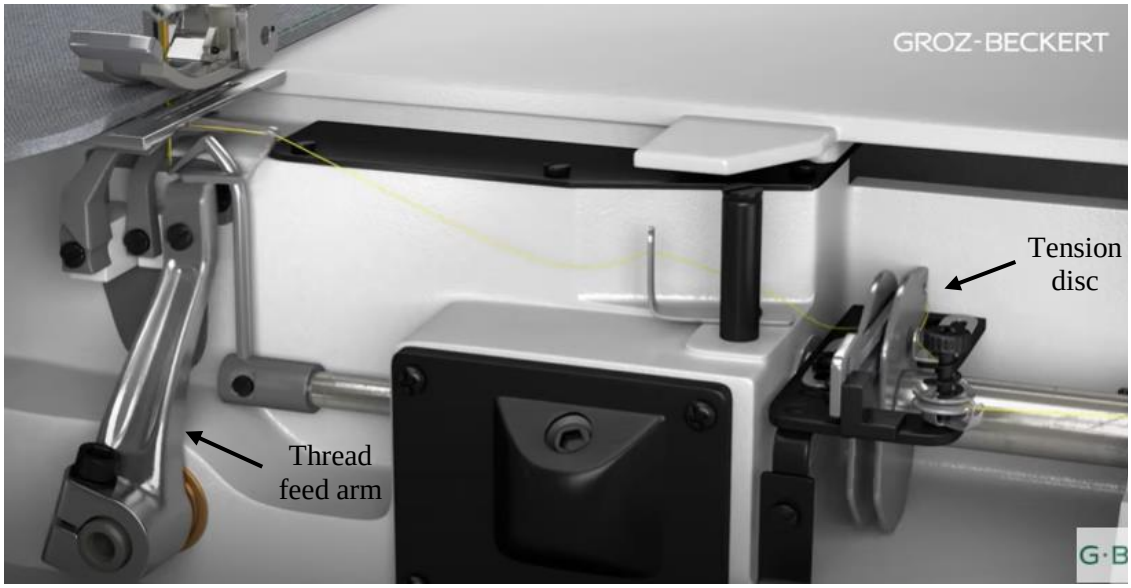
GROZ-BECKERT
Tension disc
Thread feed arm

(c)

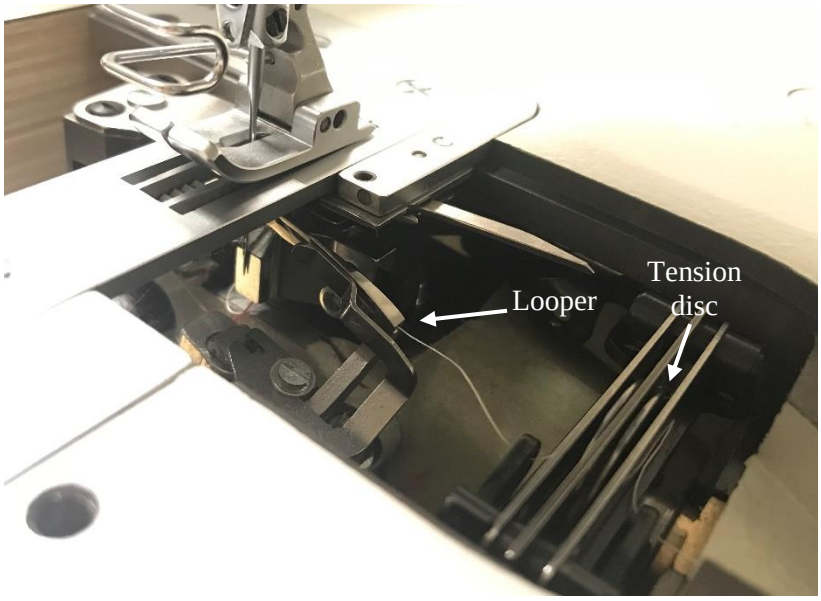

(d)

Figure 2.13 (a) Schematic of the standard ISO-401 Double-thread chain-stitch geometry and of an alternative stitch junction position; (b) needle thread path; (c) looper thread path taken from an animation by [122]; (d) looper thread travelling around the tension disc and through the looper.

The ISO-401 double-thread chain-stitch employs two threads which are inter-looped together and when formed correctly, it produces a strong yet extensible seam. It is commonly used stitch in the textile industry in applications where high strength and elasticity is required, for example it is frequently used in the joining of materials in areas where shock is applied such as for automotive airbags [123] and for parachute canopies [118]. Other apparel specific applications include the joining of knitted fabrics and in garment waistbands. The ISO-401 is formed with two threads, an upper needle thread and a lower thread supplied by a looper as opposed to a bobbin in ISO-301. Both threads are supplied external to the machine via a thread creel. The initial needle and looper paths are similar, they travel through a thread guide on the top of the machine into their corresponding tensioning devices, which are responsible for exerting the majority of the tension on the threads. The initial tensioning elements are made from a coil spring and a flat disc, the threads are guided underneath the flat disc which applies tension to the thread. The spring can be wound and unwound to increase or reduce the amount of tension on the disc and thus adjust the amount of static tension applied to the thread.

Figure 2.13 presents images of both the needle thread and the looper thread paths. From the spring tensioning device, the needle thread travels through several guides and into a hole on the take-up

lever, from there it is guided through the needle bar, through a guide at the top of the needle and into the needle hole itself. After tensioning, the looper thread travels beneath the machine, through a series of guides before it travels through a thread feeding arm, which has a similar role to the take-up lever, and then around another tensioning disc. The tensioning disc is an irregular shape and as it rotates during sewing, thus tension is applied and released on the looper thread when necessary. From there, it is guided through the entrance hole on the looper and emerges out at the top end of the looper.

To form the stitch, the needle descends through the fabric to the bottom of its stroke, as it begins to retract, a loop is formed at the scarf of the needle. At this point, the looper projects forward to the end of its stroke, carrying the looper thread through the formed needle loop (at the back of the needle). As the needle ascends, the looper remains at the end of its stroke and the 'caught' loop remains on the looper arm while the material is fed one stitch length. Then the needle descends again, this time at the back of the looper, and inside the boundary of the looper thread to the left and the old needle loop to the right. The looper then retracts before the needle reaches the bottom of its stroke, casting off the old loop and interlacing it with the looper thread. As the needle ascends, the new loop is formed and caught by the needle and the stitch formation process starts again [85]. A step-by-step schematic of this process is illustrated in Figure 2.14. The stitch formation process of the ISO-401 is more complex than that of the ISO-301 as twice as many bottom thread loops are formed compared with the top needle thread. Due its geometry, the ISO-401 stitch is commonly referred to as a 'double-locked' stitch [83].

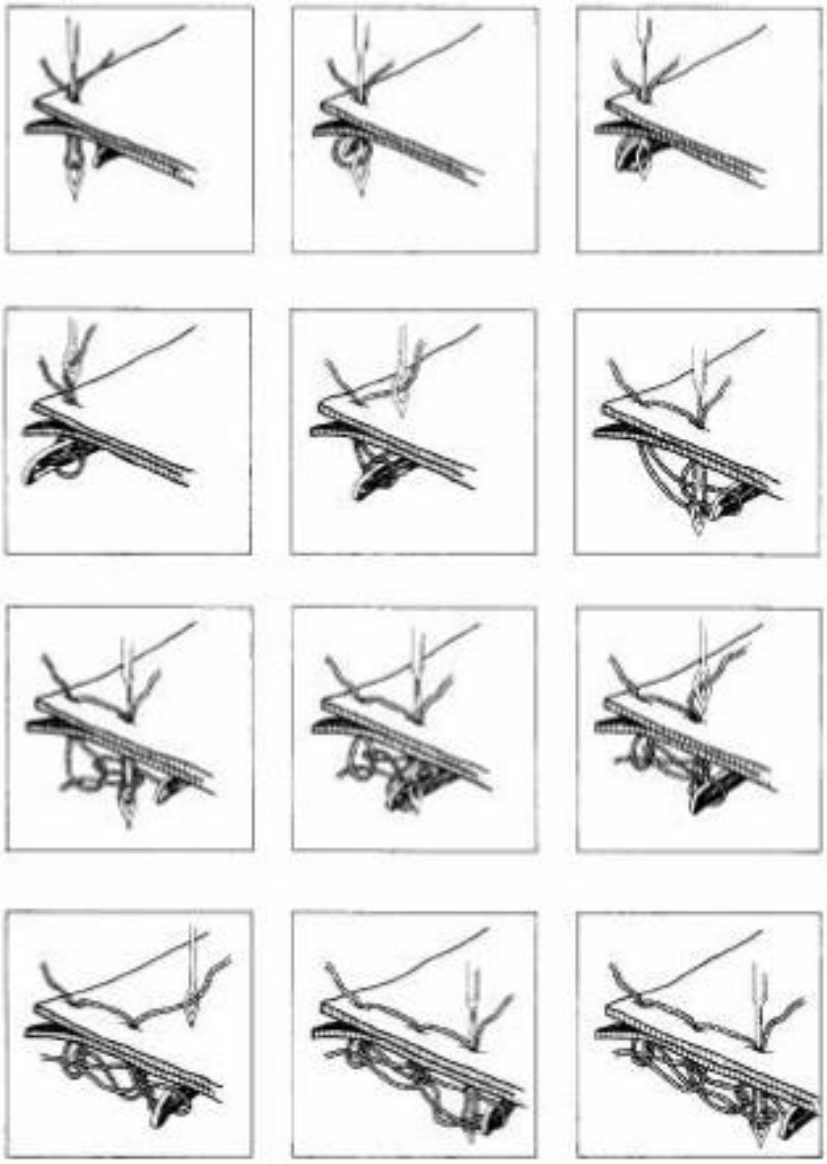

Figure 2.14 Step by step process of the ISO-401 stitch formation process [83].

2.10 Critical Summary of ISO-401 and ISO-301 for Composite Reinforcement

It is the proposal of this research that the use of ISO-401, a relatively novel stitch type for the composite industry, may be well-suited to composite reinforcement and also address some of the shortcomings associated with the production of ISO-301 stitched composites. For the purpose of this discussion, the proposed benefits have been categorised into advantages associated with the ISO-401 stitch geometry and advantages associated with the manufacturing process.

2.10.1 Potential Advantages of the ISO-401 Stitch Geometry

It has been well-reported, and also discussed earlier in this review, that stitching can induce some geometrical defects into the final composite structure, such as, resin pockets, thread crimping, fibre misalignment and in-plane fibre to breakage. Such defects can weaken the composite structure by acting as damage initiation sites under loading conditions [17,19,24,104]. Despite stitching proving its value as a composite reinforcement technique and whilst some stitch induced damage is expected with stitching [17], it is desirable to optimise the stitching geometry in order to negate some of the associated defects. Due to the stitch formation process of the ISO-301, the only modification for composite reinforcement that can be made is by moving the junction position to the surface. Whilst the important benefits that this modification brings for composites cannot be ignored, resin pockets and fibre misalignment are still prevalent in ISO-301 stitched composite structures. However, ISO-401 stitch junction can be repositioned across the surface. This may offer the opportunity for further optimisation for composite application, such as specific tailoring to the composite preform type and expected loading conditions. Also of benefit to the preform structure is the fact that ISO-401 stitching operates under much lower thread tensions compared with ISO-301. Lower tension stitching is less likely to produce faulty seam characteristics, such as puckering or skipped stitches [81]. In the context of composites, this could lead to advantages such as reduced risk of z-direction fibre crimping, which is usually caused by a combination of both taut stitching and the pressurised environment of the resin transfer process.

It is advantageous when introducing a z-direction reinforcement thread into the composite structure to use an advanced fibre such as glass or carbon thread, however these materials are brittle and the process of sewing can cause damage during insertion into the preform. Compared

with lock-stitch, it is proposed that the needle thread path for the ISO-401 would potentially cause less damage to brittle fibres as the path is not as tortuous or highly tensioned. In the case of modified lockstitch, there is flexibility to employ the TT advanced fibre could as either the bobbin or the needle thread, however both thread positions can cause potential issues for stitching with advanced fibres. Firstly, both the winding and unwinding action of the bobbin thread can be damaging to brittle fibres. Secondly, the needle thread is subjected to increased levels of tension during its 360° rotation around the bobbin case [50], which can be potentially damaging to brittle threads. For ISO-401, the needle thread path requires less repeated bending of the thread and therefore the process is predicted to be less destructive to advanced fibres.

2.10.2 Manufacturing Advantages of ISO-401

In comparison to ISO-301, there are some associated manufacturing advantages with the ISO-401 stitch geometry. A critical limitation of lock-stitching is the small capacity of the bobbin thread, which limits the seam length that can be sewn and is disruptive to the industrial-scale manufacturing process as repeated pausing is required to replace the bobbin. The capacity of the bobbin thread supply cannot be increased because the stitching process is such that the needle thread has to pass around the bobbin case to create the interlacement of treads [21,50]. On the other hand, both the needle and looper threads are supplied on industrial sized creels for ISO-401 stitching which sufficiently increases the seam length capability during manufacture. Thus, less time is dedicated to pausing manufacture and replacing the thread supply.

Higher productivity can be achieved when employing ISO-401 compared with ISO -301 due to the use of a looper mechanism as opposed to a bobbin and rotary hook. For lock-stitching, the rotary hook mechanism is required to make two revolutions per one stitch, therefore demanding the rotary hook to spin at twice the speed of the needle movement. Thus, the ultimate operational speed of the machine is restricted and is approximately half that of a chain-stitch machine [50].

2.11 Damage Tolerance of Stitched Composites

The damage tolerance of composites can be defined as the ability of a composite structure to withstand damage, usually caused by in-service abuse, and maintain sufficient residual strength and stiffness even after permanent alteration to the structure has occurred [124–126]. As the trend to incorporate FRP composites into primary aerospace structures continues to rise, understanding

the damage tolerance of composites remains of critical importance. During service, certain parts of the aircraft including the fuselage are particularly susceptible to low-velocity impact damage, which can arise from situations such as during baggage handling, dropped tooling during maintenance and large hailstones [8,124]. Thus the compression after impact (CAI) performance of composites is an important design benchmark, particularly for the aerospace industry, because impact damage to composite structures can cause catastrophic reduction in post-impact compressive strength [8,107,126–129]. Preventing the initiation of delamination and delaying the spread of delaminations are key to improving the lifetime of FRP composites [130].

2.11.1 Impact Properties of Stitched Composites

Impact loading sustained by FRP composites can be categorised as either high velocity or low velocity impact. High velocity impact usually arises from situations such as debris impact during landing. Compared with low velocity impact, the damage that occurs is much more localised as the material does not have time to respond and is usually characterised by damage such as penetrating fibre breakage that is clearly visible [60,61,131]. On the other hand, for low velocity impacts the contact time is increased, therefore the material has more time to respond. As a result, the response is more globalised causing delamination and matrix cracking to spread far from the impact site [60]. Characterising the low velocity impact response of composites is of particular interest because these events can cause barely-visible impact damage (BVID) and thus the residual load bearing capacity can be reduced without obvious surface damage [1,130].

When considering metal structures, low velocity impact damage in particular is not considered a major threat to the structure because of the ductile nature of the system. The atomic structure of metals is such that large yield strains can be absorbed by the material before the onset of strain hardening and permanent deformation. On the other hand, low velocity damage is detrimental to FRP composites because they are brittle materials and therefore can only absorb energy through elastic deformation and complex damage response mechanisms such as matrix cracking, interlaminar delamination, fibre rupture, fibre pull-out and additionally for stitched composites stitch thread fracture and pull-out [15,54,60]. This multi-mode response is further complicated when TT stitching is employed as distortions to the in-plane fibres and geometrical defects can be introduced [13,54]. Given its importance, the following discussion is focused on discussing the response and behaviour of FRP composites subjected to low-velocity impacts.

In general, interlaminar stitching has been found to be a highly effective method of suppressing the propagation of damage under low-velocity impact loading. From the subject literature, it is also clear that the stitching parameters, such as stitch density, stitch thread thickness, stitch pattern and stitch thread type can influence the damage response of stitched composites [15,54,84,130,132–134]. A study by Zhao et al. [15] found stitching works to reduce the spread of delaminations by contributing a high amount of energy absorption through stitch thread fracture during the damage propagation phase. Preforms were developed from 6 layers of E-glass and polypropylene comingled twill woven pre-preg (Twintex®) and stitched with lock-stitch. It is assumed that standard lock-stitch is used here as no reference is made to modifying the geometry for composites. A range of stitch thread types were employed, including glass fibre of various thicknesses, glass and polyphenylenbenzobisozasol (PBO), polyester (PES), carbon and polyetheretherketon (PEEK). Low velocity impact was applied using the Charpy pendulum test method. For all stitched combinations, delamination size was reduced and the impact toughness increased due to extra energy being absorbed by fracture and pull-out of the sewing threads. It was found that both stitch thread strength and surface topography influenced the impact toughness. Composites stitched with glass fibre thread were found to have higher impact toughness compared with PBO stitched specimens due to improved interfacial bonding strength. The PBO threads had a smooth surface and few fibre breakages were found post-impact indicating weak interfacial bonding. For glass fibre stitched composites, better bonding adhesion was characterised by extensive sewing fibre fracture and short-length pull out. Additionally, it was found that increased impact toughness could be achieved through increasing the strength of the glass fibre sewing thread used.

Work by Tan et al. [54] investigated the drop-weight impact response of carbon fibre/epoxy composites stitched with Vectran thread. Testing was conducted to energy levels of between 6.7 J and 60.8 J and modified lock-stitching was employed. The stitch thread linear density (denier) was varied between 200d and 400d and the stitch density was varied by employing a 3 mm or 6 mm stitch pitch and stitch space. Stitch pitch refers to the distance between two adjacent stitch holes and stitch space refers to the distance between rows of stitching. Overall, delamination growth was reduced by stitching by up to 40%, which is in-line with the work by Zhao et al. [15] and other researchers [30,61,133]. Delamination growth was found to be most effectively suppressed when stitching was employed with high density and high thread thickness. However, when considering the effect of the stitching parameters, it was found that varying of stitch thread thickness compared with stitch density had very little influence on the damage mechanisms and distribution. Furthermore, in a study by Bilisik and Yolacan [133], it was found that the

delamination growth of E-glass/polyester stitched composites was further suppressed by a combination of high stitch density and also by employing stitching in multiple directions.

There are mixed reports of stitching either reducing [84,130,133] or having no effect [28,84,133] on the peak impact force, which is a result of the wide range of tailorable stitching parameters. However, it is nearly always the case that stitching has been found to reduce the spread of delamination [15,28,30,61,133,134]. The use of micro-computed tomography (μCT) in the study by Tan et al. [54] helped to observe these damage mechanisms in detail. It was revealed that complementary mechanisms of crack bridging and crack arresting occur in stitched composites which are responsible for both improved impact damage resistance and reduced delamination by working together to significantly reduce crack growth. Figure 2.15 presents a μCT image of the crack bridging and arresting mechanisms. The mechanism of crack arresting is such that the stitching greatly impedes the driving force of the crack. In crack bridging, the stitch threads apply a closure force on the propagating cracks which works to reduce the crack opening stress experienced by the crack tip [54]. The effects of these mechanisms were more pronounced in densely stitched composites.

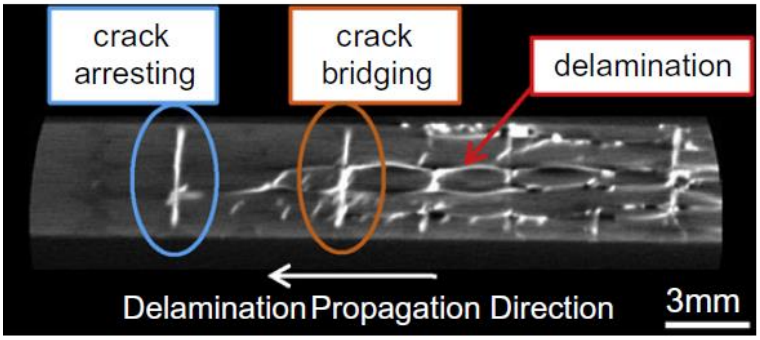

Figure 2.15 μCT image of the crack arresting and bridging mechanisms in stitched composites [54].

It has also been reported that the shape of the TT damage for stitched composites is different compared with unstitched composites. In [61], reported damage for glass fibre/epoxy composites was more localised and penetrated through the thickness of the laminate, as opposed to more lateral spreading of delaminations. Similarly in [84], it was found that specifically at higher impact energies, composites were fully penetrated through the thickness by the impactor. A comparable effect was found in [54] but was observed to be influenced specifically by the stitch density. When dense stitching was employed, the angle of delamination spread was noticeably smaller and thus

the damage was less conical and more cylindrical shaped and penetrating through the thickness, compared with moderately stitched and unstitched composites. This indicates that although stitching is effective at delaying the spread of impact delamination damage, it may also lead to undesirable through-thickness penetration of the composite under high loads or when stitched with high stitch density.

Interestingly, stitching has not been found to be successful in preventing damage initiation [16,28] and in some cases [54] damage onset has been reported to occur earlier in stitched composites. This behaviour has been attributed to the geometrical defects that stitching introduces into the composite structure. Resin pockets around the stitch insertion points and stitch joint are areas of structural weakness and as a result these areas have been found to cause additional matrix cracking upon impact loading [28,54]. This effect has been found to be more pronounced in high density stitching since there are more stitch insertion points [54], yet high density stitching is simultaneously effective at dramatically reducing delamination spread [54,132].

2.11.2 Compression After Impact Response of Stitched Composites

The compression after impact test is an important test for determining the damage tolerance of composites because impact damage to composite structures can cause catastrophic reduction in post-impact compressive strength [8,126,135]. Before discussing the CAI properties of stitched FRP composites, it is first relevant to understand the damage mechanisms present in FRP composites under compression loading without prior impact damage or TT reinforcement stitching. The tensile properties of FRP composites are dominated by the reinforcement fibre properties and therefore they have high tensile strength and strain properties due to the high aspect ratio of the fibres. However, this high length to diameter characteristic leads to compression properties being far less in comparison, approximately 40-60% less than tensile strength in most cases [136]. As a result, the compression properties of FRP composites have been studied in depth over approximately the last 50 years in order to better understand compression failure. There are numerous literatures dedicated to understanding this subject [136–143].

One of the dominant failure modes of composites under compressive loading is kink banding and there are generally three stages to the development of kink bands under compression loading: incipient kinking, transient kinking and broadening of the kink band. Following elastic behaviour, incipient kinking is the earliest form of plastic behaviour; where localised fibre buckling and plastic shearing occurs. These initial local areas of plastic deformation grow and merge to form

during the transient kinking stage to form one larger area of kink banding. Finally, the kink band broadens laterally and the orientation of the kink band is much steeper than in the earlier stages, until finally the fibres fracture [137,138,143]. The formation of kink bands are a complex phenomenon to study since they are known to develop abruptly and catastrophically [139], in less than 1.2 ms, as reported by Wang et al. [144]. Therefore, most studies investigate the kinking of post-mortem specimens rather than in-situ [142]. Despite this, kink bands have been reported to develop from regions of fibre micro-buckling, and defected areas such as crushed and fractured fibres [139]. It is therefore not unreasonable to propose that since stitching introduces some geometrical defects to the composite, these weak points could act as initiation points for kink bands to form.

In general, stitching has been found to reduce the undamaged compressive properties of composites [17,25]. In [25], the damage response was investigated using optical microscopy in an effort to reveal the failure sequence of stitched composites subjected to compressive loading. Carbon fibre/epoxy compsites were stitched with Vectran thread employing the modified lock-stitch. Compared with unstitched composites, the compressive strength of stitched specimens was reduced by up 16%. Damage such as resin cracks were initiated earlier in stitched composites and spread from the resin rich pockets at the stitch points. Kink banding was found to rapidly grow from areas of damage such as matrix cracks and fibre splitting that were situated at the sites of deviated fibres. Furthermore, a strong correlation was found between in-plane fibre waviness angle and compressive strength.

For impacted composites, the compressive damage response including delamination, matrix cracking, fibre buckling and kinking propagates from the structurally weakened impacted area. In general, stitched composites are reported to have superior CAI properties compared to unstitched equivalent of composites [107,128,145–147]. However, when reviewing the subject literature it is clear that the extent to which CAI properties are improved by stitching is dependent upon the employed stitch parameters. Earlier works tend to focus on comparing the properties of simply stitched and unstitched composites [147,148], whereas more recent works, such as [107,128], have begun to consider the effects of altering the stitch parameters, such as stitch density and stitch thread thickness, on CAI properties. It should also be noted that there appears to be little investigation of the in-situ micro-mechanical damage progression to help explain the damage response of stitched composites subjected to CAI.

Work by Aymerich and Priolo [148] investigated the CAI properties of graphite/epoxy Kevlar stitched composites. Stitching was employed in the modified lock-stitch geometry with Kevlar

stitching thread and a stitch space and stitch pitch of 5 mm. Stitching was found to reduce the delamination area of impacted specimens and stunt the growth of further delaminations under compressive loading. As the loading increased during the test, delaminations were able to propagate unrestricted in the transverse direction from the impact area for unstitched composites. As Figure 2.16 shows, for stitched composites, the bridging action of the stitches restricted delamination spread. Despite this, CAI strength remained similar or slightly worse for stitched composites. When this happens, it is likely the case that the stitch induced defects acted as areas of structural weakness and were severe enough to counteract the advantageous effects of stitching [148]. Additionally, the effect of stitch density cannot be ignored, if the stitch density is not high enough local buckling may occur between stitch lines when they are not optimally spaced [107].

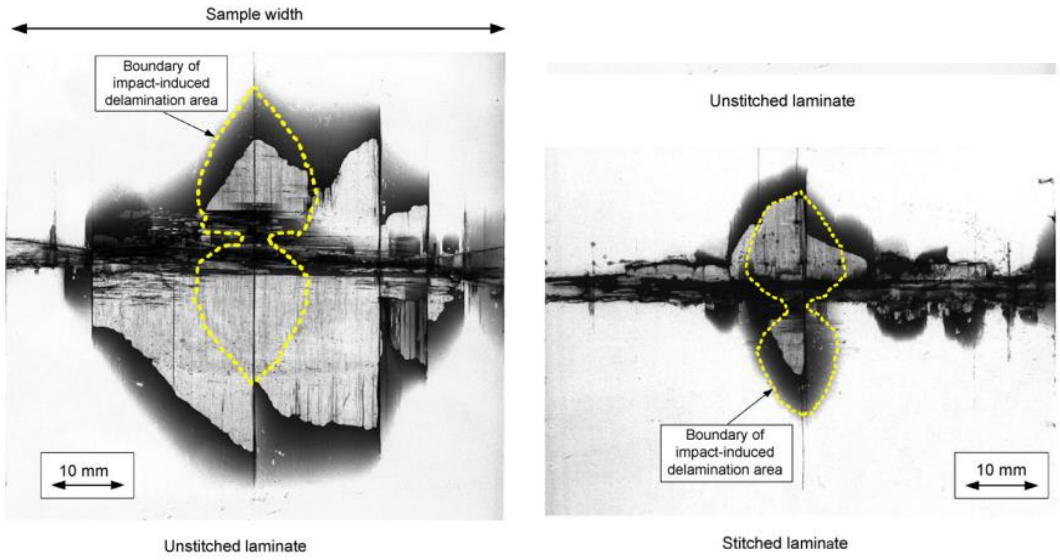

Figure 2.16 X-radiograph of CAI test specimens for stitched and unstitched FRP composites [148].

In a study by Tan et al. [107], carbon fibre/epoxy Vectran stitched composites were subjected to CAI testing. Stitching was employed in modified lock-stitch configuration, with two different stitch thread linear densities and in both moderate and high stitching densities. Overall, CAI strength of the stitched composites was improved for all stitch parameter combinations, up to 45%, due to the fact that stitching confined the impact area and also due to the bridging effect of the intact stitches during compression loading suppressing the propagation of further delaminations and matrix cracking. The effects were reported to be more prominent for densely

stitched composites where the stitch lines were closer together. X-ray radiographs of the post-mortem specimens revealed that kink banding and local buckling occurred between the stitch lines. For densely stitched composites it was evident that the stitch threads were highly effective at bridging the damage spreading as excessive stitch thread rupture was found post-mortem. However, in moderately stitched composites, where the stitch lines were spaced further apart, local buckling could occur largely unimpeded and thus the bridging effect of the stitches was less effective. Therefore, high amounts of energy were absorbed by the fracturing of stitch threads when they were spaced closer together. Furthermore, utilising thicker stitching thread also increased the stitch bridging effectiveness but only for higher impacts, for lower impacts the effect was negligible and the bridging effect was mainly attributed to stitch density.

In [128], the effect of the stitch pattern on CAI properties of E-glass/epoxy composites woven/knitted hybrid composites was investigated. Stitching was conducted with E-glass 136 tex yarn in diamond, square and circular patterns. Interestingly, this means that for each stitched composite iteration, the stitching was conducted in multiple directions, whereas for other studies [107,147,149] stitching is usually employed only in the 0° direction. It was found that for all patterns, stitching improved the CAI strength, again this is attributed to both the smaller impact damage in stitched composites and the bridging effect of the stitches restricting the damage growth from propagating at the impact site under compressive loading. No further information is provided on the compression damage mechanisms in stitched versus unstitched composites.

From the review in sections 2.11.1 and 2.11.2, it is clear that TT stitching is an effective form of interlaminar reinforcement for composites and have repeatedly been used to improve the impact [15,28,30,61,133,134] and damage tolerance [107,128,145–147] of FRP composites. A key mechanism for this is the ability of stitching to impede damage growth via a bridging effect [54,128]. It is clear that the stitching parameters employed can influence the effectiveness of the crack bridging and damage suppression, for example both impact [54,132] and CAI [107] responses were improved by employing a high stitching density. However, many of the studies discussed above do not report on the composite tensile properties, along with the out-of-plane properties, therefore it is difficult to get a full view on the effect of stitching on FRP composite behaviour. More specifically, it is not unrealistic to suspect that increasing parameters such as stitch density could cause increased stitch-induced defects to reinforcement fibres and thus have detrimental effect on the in-plane fibre dominated properties, such as Young's modulus. Therefore, whilst studies published in this area have been informative, a complete understanding of the mechanical properties of stitched composites is still lacking.

2.12 Stitched Composite Response under Tensile Loading

The tensile testing of materials is a fundamental test method to understanding the behaviour of a material under loading conditions. Specifically, conducting a tensile test can measure the properties of Young's modulus, ultimate tensile strength, ultimate tensile strain and Poisson's ratio [150]. The tensile properties of FRP composites are fibre dominated, meaning that they are mostly determined by the strength, orientation and volume of the fibres because the fibre breaking strength is much higher than that of the polymer matrix. This also means that the tensile properties of FRP composites can be highly sensitive to the presence of defects in the fibres such as cracks or voids [151].

Stitching has proven its value in improving the out-of-plane properties of composite laminates and the improved interlaminar and impact strength of z-stitched composites has been well documented, for example in, [11,42,91,102,106,147,152]. However, there are concerns and limited understanding on the effect of inter-laminar stitching on the in-plane mechanical properties of composites, despite the importance of such properties in industrial applications, such as for the aircraft industry [1,4,19,35]. It is critically important to investigate the tensile properties as tensile modulus is widely regarded as the most important elastic constant, particularly to engineering applications [4,17,19]. As the versatility of TT stitching presents a large collection of changeable stitch parameters, test data is specific to the chosen parameters and drawing generalisations can be complex and require a broad knowledge of the area [19,92]. Whilst it is difficult to report on the effects of all stitch-related parameters, the influence of stitch density [4,19,44], stitch thread thickness [4,15], stitch thread type [31,44] and stitching direction [15,19,31,44,153] on the tensile properties of composite laminates have been the focus of a growing number of studies in this area.

In 1997 and 2000, work published by Mouritz and co-workers in the form of in-depth literature reviews [13,17] found inconclusive results on the effect of various stitch parameters on the tensile properties of composites. This was mainly attributed to the fact that stitching causes changes to the composite structure, such as; fibre volume fraction and void content, though these changes were not always reported in the research papers they included in their reviews. Additionally, the stitching parameters can vary from study to study and the full list of stitch parameters are not always reported. Thus, working to reduce the negative effect that stitching can have on the tensile properties of FRP composites is important during their design and manufacture. Ultimately, for

TT stitched composites, the in-plane properties should, at the very least, be maintained whilst out-of-plane properties must be improved significantly [4]. In the subsequent years, more research has been dedicated to this area [4,19,20,22,26,46,153–156].

Generally, it is common for TT stitching to cause a reduction in composite tensile properties, this is due to the inevitable geometrical induced flaws or defects imparted during the stitching process. The presence of fibre distortion (waviness), resin rich regions, in-plane fibre breakages, porosity, and fibre volume fraction change are of particular concern and have been shown to negatively impact the in-plane composite properties [4,13,17,19,45,46,157,158]. Where stitching has been found to improve tensile properties, in most cases there is not an across the board improvement in tensile strength, strain and modulus and usually a combination of degraded, improved or maintained properties occur concurrently [4,10,15,17,47,155,156]. Thus, there is still no single conclusion on the mechanisms of how stitching controls the tensile properties but increases or decreases of up to 20% are commonly reported [13,17,159].

Of particular concern is the effect of stitching on the stiffness or tensile modulus of composites as tensile modulus is heavily dominated by in-plane fibre volume fraction and orientation., thus understanding the effect of stitching is imperative [17]. Earlier work by Yudhanto et al. [159] found that the tensile modulus of stitched composites was reduced by up to 4%. These reductions were attributed to in-plane fibre misalignment caused by stitching, as 0° tows were misaligned in-plane and out-of-plane by up to 4.68°. However, the correlation between tow waviness angle and tensile modulus was not investigated. Later work by the same authors [4] investigated the relationship between 0° tow waviness angle and tensile properties of modified lock-stitched Vectran reinforced carbon fibre/epoxy composites. The effect of stitch density and stitch thread linear density (thickness) were considered, stitch density was 3 x 3 or 6 x 6 cm (S_s x S_p) and thread thickness was either 400 or 200 denier. In all cases, the tensile moduli of the stitched composites were found to be reduced by 3.7-6.9 %, the fibre volume fraction remained unaffected by stitching. The average in-plane (*x-y* plane) fibre waviness angles reported were 0.1° for unstitched composites and increased to between 2.5-7° for stitched composites. A strong negative correlation coefficient, (R^2 of 0.8154) was found in stitched composites between misalignment angle and tensile modulus. The highest waviness angle (~*7*°) and therefore largest modulus reduction (-6.9 %) was reported for the composites stitched with the highest density (3 x 3 cm) and thickest thread (400 denier). Under uniaxial tension, composite specimens with larger in-plane waviness angles exhibited more lateral deformation, thus were less stiff in the longitudinal direction. Interestingly, the same combination of stitching parameters provided the highest CAI

improvement, as in [107]. However, in the same study as discussed above [4], the tensile strength was maintained for low density stitching or slightly increased, by up to 7 % for high density stitching, despite the tensile modulus being reduced. This was attributed to the fact that stitching can successfully impede delamination growth.

Conversely, in [19] the tensile modulus of standard lock-stitched Twaron/epoxy composites was unaffected by stitching, though no actual values are given. On the other hand, the tensile strength was significantly decreased for higher stitch densities and increased for lower stitching densities. Stitched composites were found to have similar characteristic defects such as resin pockets and fibre misalignment, as reported in [4], therefore it was suggested by the authors that as the stitching density increased, the tensile strength reduced as a result of the increasing number of defects. In this case, it is unclear why the tensile modulus was unaffected for stitched composites. It is possible that in the elastic region, the small increase in fibre volume fraction (1-2 %), due to compaction of the laminate by the stitching, counteracted the damage caused by stitching. Whereas considering ultimate tensile strength, increases in the stitching defects severely affected the load bearing properties of the in-plane fibres.

In [47], when low stitching density was employed in both single thread chain-stitch and orthogonal stitch formation, the tensile modulus and strength were both improved. This has been attributed to the fact that stitching thread can actually help towards load transfer by evening out stress distribution among the in-plane fibres [47,92]. Conversely, stitching caused increasing stress concentration as the stitch density increased, resulting in a reduction of both tensile strength and modulus. Similarly in [26], for silk fibre stitched kenaf/epoxy composites, the tensile strength and modulus were increased due to the load distribution effects of the stitching fibres. The stitch density employed is similar to that of [47] and considered to be low-moderate and the FVF was also slightly increased by 1-2%.

The tensile properties of multi-directional stitching have also been investigated [22,31,44], interest in the stitching patterns arises from the fact that uniform distribution of the TT thread can be achieved. Multi-directional stitching has been shown to be successful at improving the damage tolerance of composites [128] but little is known about its effect on the in-plane properties. Both the warp, weft and off-axis tensile properties of plain woven glass fibre/polyester composites were investigated in [31] and [44]. The composites were directionally stitched in 0°, 0° and 90°, and 0°, 90°, +/- 45° (in the bias directions) using nylon 66 and Kevlar stitching thread in modified lock-stitch configuration. When both moderate and dense stitching densities were employed in the 0° direction only it was found that the in-plane tensile strength, modulus and strain were slightly

improved, despite the introduction of stitch defects. Off-axis tensile strength was reduced but tensile modulus remained similar to that of unstitched. However, when the number of stitching directions was increased there was a progressive reduction in the tensile strength and modulus values [31,44]. The in-plane tensile strain was found to be increased when the stitching directions increased [31]. Similar results were found in [22], where orthogonal stitch (hand-stitching) with Kevlar thread was applied to glass fibre/polyester composites in a graphene pattern which required stitching in multiple directions. Both tensile strength and modulus were reduced but the tensile strain was slightly improved which increased for higher density stitching. In these cases, it is possible that the strain was improved due to the contribution of stitch thread rupture during loading.

From the subject literature, it is evident that stitching can have undesirable effects on the tensile properties, such as causing a reduction in Young's modulus. Although research in this area is limited, it has been shown that in-plane tow waviness, induced by the stitching, can be particularly detrimental to fibre dominated properties. Considering this further investigation is warranted to attempt to optimise the stitching process and geometry in order to reduce such defects.

2.13 Summary and Research Gaps

It is clear that there are many benefits to incorporating composites into aerospace and other engineering structures, such as their high specific strength and stiffness and excellent fatigue and corrosion resistance. Yet, as FRP composite laminates are anisotropic materials, they tend to have excellent in-plane properties but a critical limitation is their low resistance to out-of-plane stress or loading and susceptibility to delamination. Furthermore, their heterogeneous nature leads to them having complex and mixed-mode damage mechanisms which are still not well understood, despite their popularity. An extensive and growing body of work has reported stitching as an effective, low cost option of TT reinforcement to improve the interlaminar fracture toughness, impact resistance and damage tolerance of composites. However, inclusion of a z-binder usually causes some distortion of the in-plane fibres and it is clear that this is commonly the case for TT stitching. Distortion of the in-plane fibres can lead to reductions in FVF and consequently degradations of the in-plane properties, in particular tensile modulus and strength. Yet, there remains a continued interest in TT stitching as a laminate reinforcement technique as it has been found to cause less fibre damage compared to z-pinning and to improve or degrade the tensile properties by up to 20%, which is comparable to 3D woven structures.

For TT stitched composites to be truly worthwhile in primary structures, they must be developed to suppress any associated negative aspects whilst simultaneously improving the composite interlaminar properties significantly. As discussed, a key advantage to TT stitching is that it has many changeable parameters, which in theory allows for the opportunity to finely adapt the stitching process to composite application and produce highly tailored structures. However, in practice, it is clear that there are still uncertainties surrounding the topic as employing TT stitching into the composite structure adds further complexity to the laminate geometry and damage mechanisms, which can change vastly depending on the chosen parameters.

It is evident from conducting the review that has informed this chapter that the knowledge of available stitch geometries and stitch formation is virtually unknown outside of the textile and apparel industry. Consequently, there is a lack of in-depth research that critically appraises different readily available stitch geometries for the purpose of reinforcing composite laminates. Developing further knowledge on the effect of various stitch types and their impact on composite properties is integral to advancing the subject.

It is therefore the basis of this work to critically appraise a relatively novel stitch type to the composite industry, double-thread chain-stitch (ISO-401). The ISO-401 is a common stitch type used in the textile industry that has not yet been evaluated for composite reinforcement, despite theoretically being suited to composites and potentially addressing some of the shortcomings of the commonly used modified lock-stitch (ISO-301). A major advantage is that the inter-looping junction between the needle and looper thread can occur at various points on the composite surface between two adjacent stitch points the needle hole or externally, via adjustment of the thread tension wheels or the relative timings between the take-up mechanisms and the feed system. It is anticipated that the flexibility of the thread junction positioning would allow for the geometry to be optimised for composites to reduce in-plane fibre distortion. There are also manufacturing related advantages associated with the use ISO-401; firstly, the action of needle thread insertion is less damaging to advanced brittle fibres compared with ISO-301 stitching and secondly, both needle and looper threads are supplied on industrial size creels. Therefore, thread replacement occurs more infrequently compared with ISO-301 production. No research currently exists that investigates the double-thread chain-stitch geometry for composites, this is likely to do with the fact that it is relatively unknown outside of the textile and apparel industry.

Chapter 3

General Composite Manufacture

The purpose of this research is to investigate the suitability of ISO-401 double-thread chain-stitch, a novel geometry for the composite industry, as an interlaminar stitching type. As discussed in the previous chapter, a major advantage to the ISO-401 stitch type is that the inter-looping junction between the needle and looper thread can occur at various points on the composite surface between two adjacent stitch points, via adjustment of the thread tensions. As ISO-401 stitching has never been applied to composites before, it was a first priority to establish a benchmark for the optimum ISO-401 stitch junction position for composites. This initial work was carried out with polyester yarn because it is easy to obtain and widely applied in various textile applications. A series of tensile testing was carried out to understand the effect of ISO-401 stitching on the in-plane composite strength and Young's modulus. After the optimum junction was established, the in-plane tensile properties were compared against composites stitched with a common reinforcement stitch type, ISO-301 modified lock-stitch. Due to availability of the stitching machines, all composite structures were able to be manufactured at The University of Manchester, which allowed for maximum processing control. The results of this study are reported and discussed in Chapter 4.

For the next step, the damage tolerance and tensile properties of ISO-401 composites were examined. Glass fibre thread was used as the stitching thread here because it is used commonly for composite reinforcement. To prepare these composites, the sewing machine used for ISO-401 stitching had to be adapted from its factory settings to enable successive stitches to form properly when glass fibre stitching thread was employed. The machine adjustments, results and discussion of this study is reported in Chapter 5. Finally, in Chapter 6, the optimised ISO-401 geometry is applied to two fabric types with varying characteristics, in order to develop a deeper understanding of the relationship between the fabric properties and stitch formation. For each reinforcement fabric, a full assessment of the fabric properties is carried out and the relationship between these properties and the final thread junction position is examined. Following this, a series of tensile testing is carried out on the resultant composites to understand the effects of ISO-401 stitching on the strength and Young's modulus.

The aim of this chapter is to explain the general composite manufacturing process which consists of the following steps; preparation of the preform, TT stitching of the preform, the resin infusion process and the preparation of the composite test specimens. For this research, two categories of composite were manufactured, stitched and unstitched. Within this chapter are details of the preparation of the novel ISO-401 composites including specification of the machine acquired by The University of Manchester for this research and selected feeding system and needle type. For both categories, various subtypes were manufactured, the main changeable variables were reinforcement fabric construction type, stitch geometry, stitch density and sewing threads. Specific details of the composite subtypes, composite evaluation methods and sewing machine adjustments are discussed within the relevant chapters 4-6 and thus will not be covered here. Instead, this chapter will focus on the general composite preparation and manufacturing process.

3.1 Preform Preparation

The preforming process consists of several stages in order to prepare the reinforcement fabric for composite manufacture. These include, cutting of the reinforcement fabric, layering of the fabric plies, marking of the specimens and stitching. For this research, three different types of glass fibre fabric were employed. These fabrics were chosen because they are readily available and commonly used in the composite industry. Table 3.1 presents the fabric parameters and the chapters in which the resultant composite properties are evaluated. Each of the fabrics were supplied on a 1m roll. Individual plies with dimensions of 310mm (length) x 310mm (width) were marked onto the fabric, a rotary blade was preferred over fabric shears to avoid unnecessary distortion of the yarns. For each of the fabrics, eight plies were align-layered in the 0° (warp) direction to create the preform, at this point the stitching was performed. The stitching process is covered in detail in the next section.

Table 3.1 Composite preform specifications.

	Weave Type		
	2/2 twill	Plain	Plain
Specimen names	1-UNS, 1A, 1B, 1C	2-UNS, 2-DCS-G, 2DCS-P	3-UNS, 3-DCS-G
Supplier	Easy Composites Ltd	MB Fibreglass Ltd	MB Fibreglass Ltd
Fibre type	E-glass	E-glass	E-glass
Warp and weft density [1/cm]	8 x 7	2 x 2	1.5 x 1.5
Areal density [g/m^2]	280	600	600
Filament diameter [µm]	13	15	15
Yarn linear density [Tex]	1000	1200	1200
Stitch type	ISO-401	ISO-401, ISO-301	ISO-401
Sewing thread type	Polyester	Polyester, glass fibre	Glass fibre
Total number of composite plies	8	8	8
Composite thickness [mm] (unstitched/stitched)	1.7/1.74	3.5/3.65	3.78/3.52
Mechanical evaluation method	Tensile	Tensile, impact and compression after impact	Tensile
Appears in chapter(s)	5	5, 6	6, 7

3.2 Interlaminar Stitching Process

Once the plies had been layered to create the desired preform, the specimen dimensions and proposed stitch lines were marked onto the preforms to ensure that each stitch specimen had the same quantity and positioning of the stitch lines. The specimen dimensions were dictated by the tensile, impact and compression after impact composite evaluation test standards. The individual test methods and required specimen sizes are covered in detail in the relevant chapters 4-6. Interlaminar stitching was employed in two different geometries, double-thread chain-stitch (ISO-401) and lockstitch (ISO-301). All preform stitching was performed in-house at The University of Manchester and stitch speed and operator handling were kept consistent to ensure the stitching process was performed in a similar manner for all preform panels.

3.2.1 Needle Type

For both ISO-401 and ISO-301stitch types, the corresponding sewing machines were fitted with a ball-point needle type, as opposed to a pointed tip, as it was found during early experiments to be the most suitable needle type for the stitching of composite preforms. For ball-point needles, the tip of the needle is rounded rather than pointed which encourages the needle to push through the fabric, parting the in-plane tow fibres as it descends into the preform rather than piercing through them as a pointed tip would. Whilst in-plane fibre breakages are expected as part of the stitching process, using a ball-point needle type helped to ensure that fractures to brittle advanced fibres were minimised. Excessive damage to the in-plane fibres could lead to reduction in the composite properties and therefore every effort to minimise damage should be taken.

In the textile industry, the ball-point needle type is traditionally used for the sewing of knitted fabrics as opposed to woven fabrics, as the shape of the needle tip ensures the knitted loops are not damaged or broken during the stitching process which could cause them to unravel. For woven fabrics, it is common to use a universal pointed needle with a sharp tip to enable the needle to penetrate tightly woven yarns. However, the glass fibre woven reinforcement fabrics used for this work were less dimensionally stable compared with traditional woven textile fabrics for clothing. As a result, very careful handling is required when cutting and layering the preform plies as yarn slippage can occur easily. This also meant that they were well-suited to the use of ball-pointed needles as the in-plane yarns could easily be pushed apart to allow the needle through the preform.

3.2.2 ISO-401 Double-Thread Chain-Stitch Machine

To carry out this research an industrial Durkopp Adler 173-141621 single needle double-thread chain-stitch machine was acquired, see Figure 3.1. This machine was primarily developed by the manufacturer for industrial use in the textile industry and so consideration of the feed type was made to provide optimum conditions for TT stitching of composite preforms. It was important that the most appropriate feed system was chosen for composite preform stitching to minimise ply and tow slippage. The machine was fitted with a modified drop feed system, which includes a bottom feed and a retractable top driven puller feed, as in Figure 3.1. In the textile industry, this type of system is particularly well-suited to stitching heavy duty fabric such as tent fabric and leather upholstery. The feeding system consists of four main parts, the throat plate, feed dog, presser foot and roller. Additionally, the machine was fitted with two metal arms, positioned either side of the needle to help with guiding the fabric through the sewing process.

In a drop feed system, since the feeding of the material relies solely upon feed dog contact with the single bottom ply, in the textile industry the drop feed system is well-known to cause ply slippage when used with multi-layered fabric structures [160]. To help avoid ply slippage during the stitching process the machine was fitted with an optional roller puller feed, situated behind the needle as in Figure 3.1. The puller roller is designed to come in contact with the top fabric ply, applying downward pressure and thus helping to control the feeding of the fabric stack more efficiently through the system. Additionally, the puller roller is well-suited to ensuring stitch lines are kept completely straight, which is advantageous in this work as it helps to maintain consistency between preforms. From early experiments, it was found that the addition of the roller system was appropriate for use on the thin glass composites as produced for Chapter 4. However, it was found that for thicker preforms made from 600 g/m^2 glass fibre fabric produced for Chapters 4-6, the pulling action of the roller distorted the fabric tows and fibres from their original orientation. Thus, the puller roller feed was not used for the sewing of thicker glass fibre preforms. Removing the roller meant that the preform was fed through the system using only the bottom feed dog and so to avoid inter-ply slippage during the sewing process, the side of the preform stack were secured with tape before sewing, as in Figure 3.1.

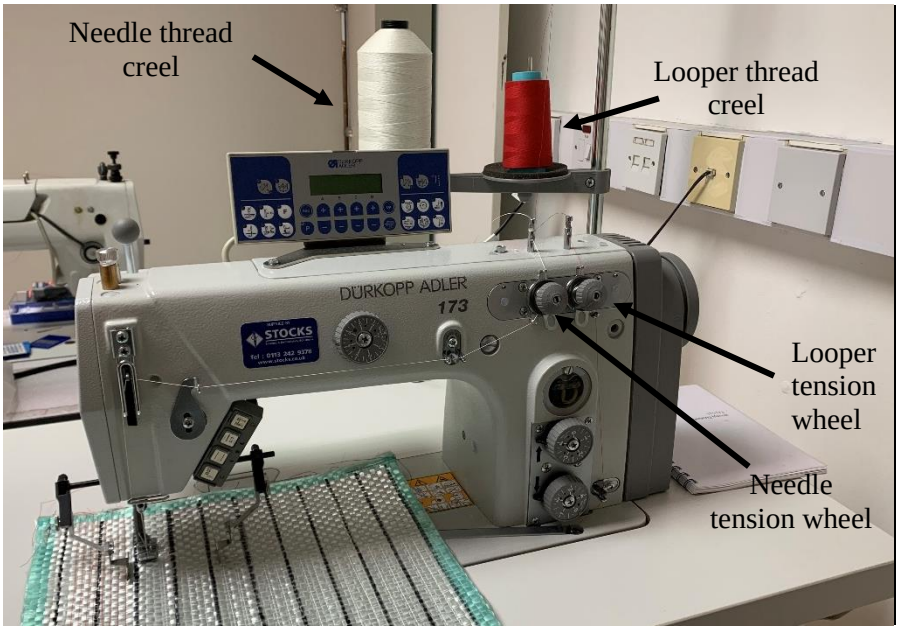
Needle thread creel
Looper thread creel
DÜRKOPP ADLER
173
STOCKS
Looper tension wheel
Needle tension wheel

(a)

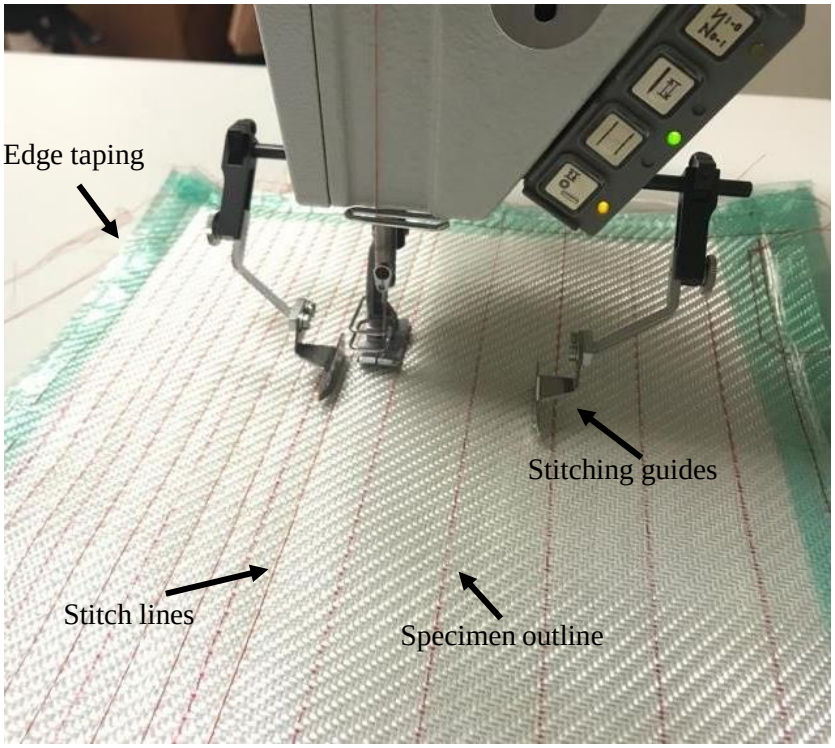
Edge taping
Stitching guides
Stitch lines
Specimen outline

(b)

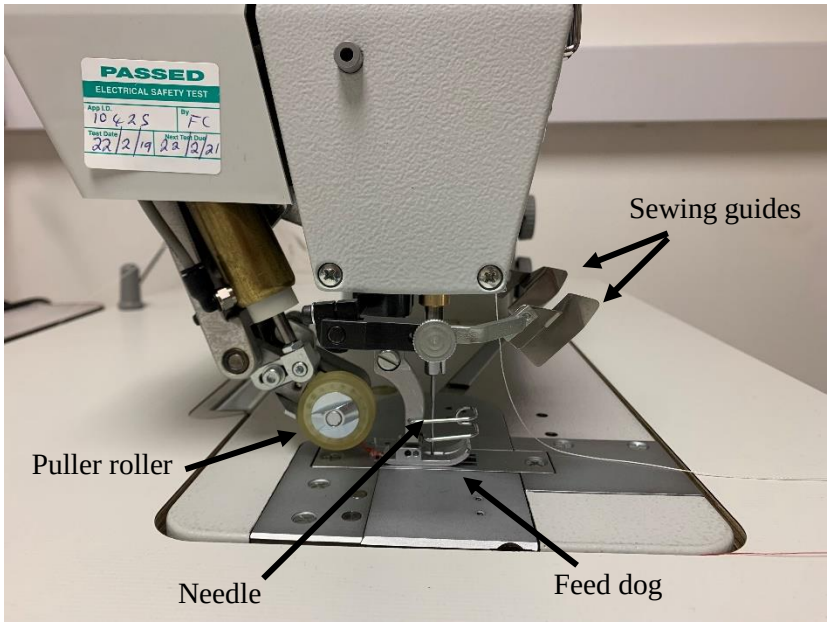

(c)

Figure 3.1 (a) ISO-401 sewing machine; (b) image of preform stitching process; (c) image of machine feeding system.

3.2.3 Measurement of Thread Tensions

For the purpose of this research, adjustment of the needle and looper thread tensions for ISO-401 stitching was conducted for two main reasons; to enable the machine to stitch thick composite preforms and to optimise the stitch junction position. Static thread tensions were altered by adjustment of the corresponding tension wheels, as in Figure 3.1. A spring device was then used to measure the thread tension in g/f of each individual thread. During early experiments it was found that small incremental increase or decrease of the tensions followed by visual inspection of the stitch lines, followed by further adjustment if needed, was the best method to achieve the intended geometry. Once the desired stitch geometry had been achieved, the averaged value of three measurements for each thread type was recorded to ensure repeatability. Figure 3.2 demonstrates the process of measuring the needle and looper thread tensions. For the needle thread, it was released from the needle eye and pulled horizontally from the needle bar. For the looper thread, it was released from the looper arm and pulled horizontally from the tensioning cog, which was positioned at the highest tensioning point.

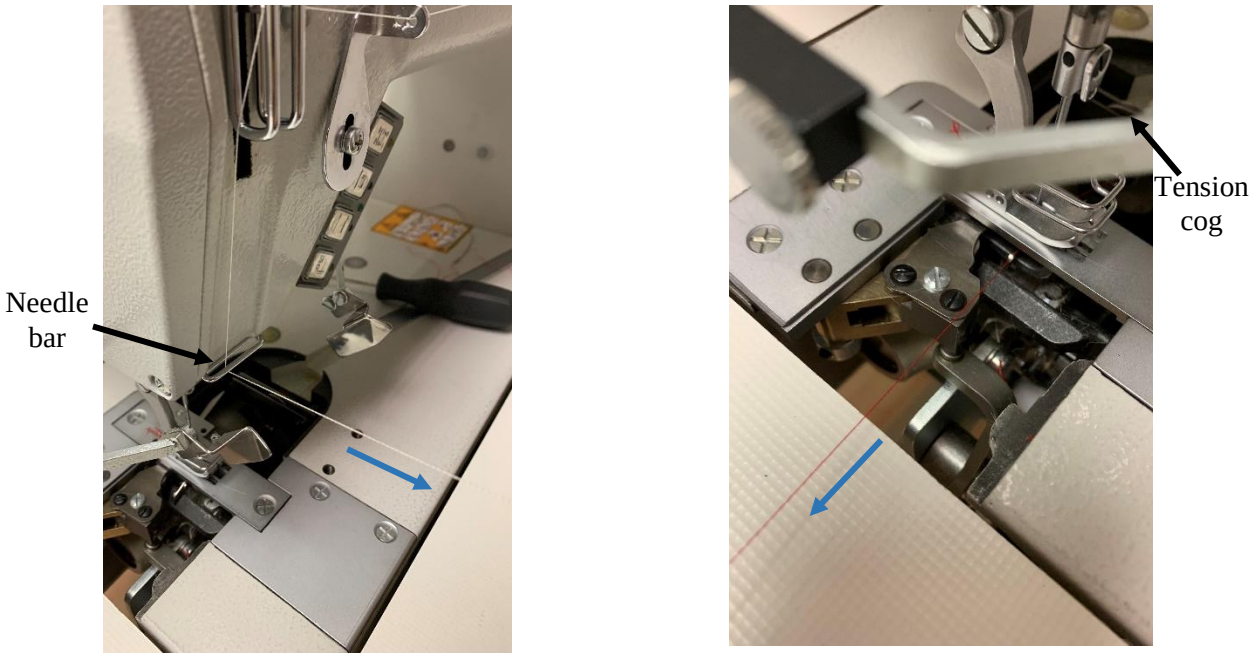

(a) (b)

Figure 3.2 Images of sewing thread positions for measuring thread tension (a) needle thread; (b) looper thread.

3.2.4 ISO-301 Modified Lock-stitch Machine

Lock-stitching was performed in-house using a Durkopp Adler N201-DA220C5300. For the purpose of TT stitching, the ISO-301 geometry was modified by the researcher to ensure that the interlacement position was placed at the surface of the composite preform and not between the plies. To achieve this, the bobbin tension was reduced by loosening the bobbin case-spring via the tensioning screw and the needle thread tension was increased by manual adjustment of the tension-disc. Careful assessment of the stitched preforms prior to resin infusion was taken to ensure that the interlacement of the threads was not penetrating the fabric preform and instead was sitting on the preform surface. The modified ISO-301 in a composite cross-section can be viewed in the image in Figure 3.3.

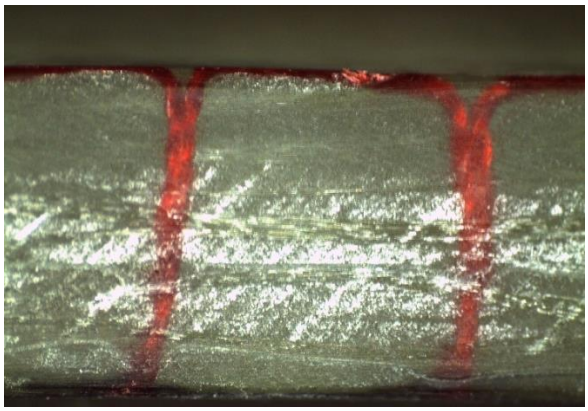

Figure 3.3 Image of modified lock-stitched composite cross-section.

3.2.5 Stitch Density

The stitch density describes the total quantity of stitching for a given area. Stitch density was calculated using the following equation, as in [132]:

$$S_D = \frac{1}{S_p \times S_s} \tag{3.1}$$

Where S_p is defined as the distance between two adjacent stitch holes and S_s is the distance between two parallel stitch rows. A schematic of the stitch arrangement can be viewed in Figure 3.4.

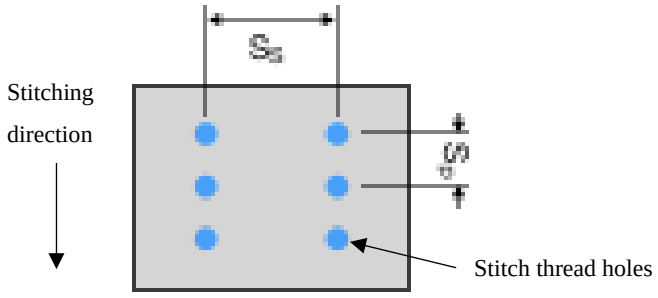

Figure 3.4 Schematic of the stitch arrangement.

3.3 Manufacturing Process for Composite Panels

In order to manufacture composite panels from the stitched and unstitched preforms, three main steps were completed; moulding and vacuum bagging, resin infusion and curing, debagging and specimen preparation.

3.3.1 Moulding and Vacuum Bagging

Once the preform manufacturing process had been completed, the preform was prepared for resin infusion by moulding the structure and applying the vacuum bagging. Figure 3.5 presents a schematic of the mould lay-up. For the mould, a flat steel plate of 500mm x 500mm was used. To prepare the mould, EasyLease™ solvent mould cleaner, supplied by Easy Composites, was applied using a cotton cloth to remove any debris and clean the surface. Post tool cleaning, four layers of EasyLease™ mould release agent (supplied by Easy Composites) were applied at five minute intervals with a clean cotton cloth. The purpose of this process was to ensure easy release of the preform panel after completion of the curing cycle.

The preform lay-up onto the mould consisted of; (i) one layer of polyester infusion mesh, (ii) one layer of nylon peel-ply, (iii) the preform stack, (iv) one layer of peel-ply, (v) one layer of infusion mesh, as presented in Figure 3.5. The fabric lay-up was secured at the corners with flash tape to prevent any movement or distortion during the process. Both the infusion mesh and peel ply fabrics were supplied on a linear metre roll from Easy Composites. The peel-ply layers were cut to dimensions of 400mm x 400mm and the infusion mesh was cut to dimensions of 290mm x 290mm. The purpose of the peel-ply and mesh layers was to aid thorough wetting of the preform fibres during the infusion process and to ensure even distribution of resin.

The inlet and outlet components were constructed from a combination of a PVC (polyvinyl chloride) clear unperforated hose and PP (polypropylene) spiral cut tubing. A 300mm length of the spiral tubing was attached to the end of a 600mm hose using flash tape. The constructed tubes were then secured to the mould at the top and bottom of the preform stack using flash tape. The purpose of the unperforated component of the inlet is to enable the flow of resin from the resin basin to the spiral cut tube. The open structure of the spiral cut tube allows for even distribution of resin flow and infusion into the preform. Polyisobutylene vacuum bagging sealant tape was applied around the perimeter of the mould tool to create a seal between the vacuum bagging and the mould surface. A vacuum was then applied by securing the outlet to the vacuum pump whilst

the inlet was sealed by a steel clamp. To ensure the seal was completely air tight around the prepared preform and there were no significant leaks in the vacuum, the air pressure was monitored over approximately 6 hours.

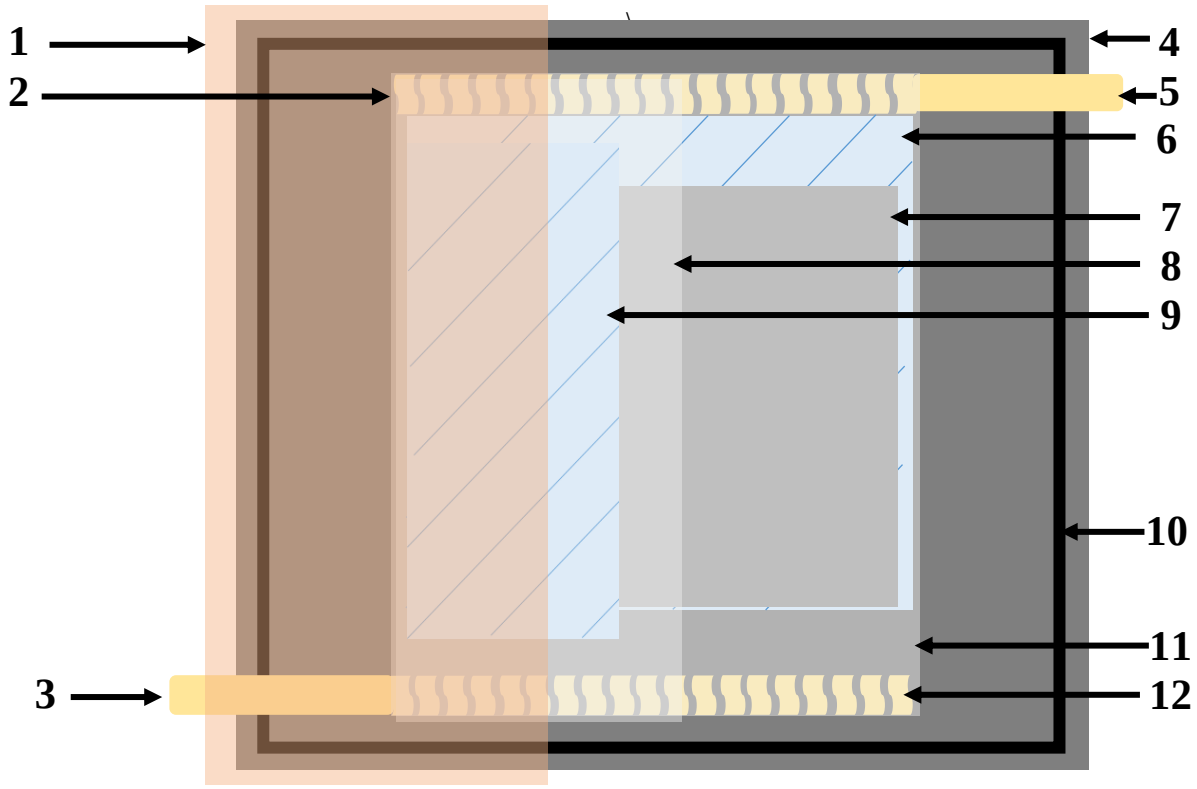

Figure 3.5 Schematic of typical flat panel composite set-up for VARIM technique. For reference to the numbers see Table 3.2 below.

Table 3.2 List of materials for the VARIM process

1	Vacuum bagging
2	Inlet spiral tube
3	Unperforated outlet tube
4	Steel mould tool
5	Unperforated inlet tube
6	Bottom mesh layer
7	E-glass composite preform
8	Top peel ply layer
9	Top mesh layer
10	Polyisobutylene vacuum bagging sealant tape
11	Bottom peel ply layer
12	Outlet Spiral tube

3.3.2 Resin Infusion and Curing Process

To infuse the resin, the vacuum assisted resin infusion moulding (VARIM) technique was followed, as in [161]. The preforms were consolidated with a Bisphenol-A type epoxy (Araldite LY1564) resin with a density of 1.2 g/cm^3 and an amine type (Aradur 2954 cycloaliphatic polyamine) hardener with a density of 0.95 g/cm^3, both supplied by Huntsman, UK Ltd. This system was used because it is commonly used in the aerospace industry for consolidating textile composite structures. The resin system was mixed homogeneously in a weight proportion of 100:34, as prescribed by the manufacturer, then the mixture was degassed with the use of a resin pump to remove excess air from the solution that was induced as a result of the mixing process.

Following preparation of the resin mixture, the inlet tube was submerged into the resin basin. The outlet was then attached to the vacuum pump which enabled resin to be drawn into the inlet tube due to suction. The resin was drawn through the unperforated hose and into the spiral tubing, which enabled resin flow into the preform structure. From there it flowed towards the outlet,

infusing and fully saturating through the preform. The infusion process was continued until the preform was fully saturated and the resin began to flow into the outlet tubing. The whole VARIM process took between 1-1.5 hours, depending upon the composite thickness. The fully infused and vacuum sealed preform panel was moved into a Thermo-Scientific Heraeus T20P Oven in order to cure (solidify) the resin. Figure 3.6 presents the curing cycle, curing conditions were as prescribed by the manufacturer. The curing cycle includes an initial 30 minute ramp period to allow the oven to reach the desired temperature of 80°C, followed by two hours at 80°C constant. During these initial two hours, the resin is undergoing gelation, a higher than necessary temperature at this stage can result in shrinkage and internal stresses within the structure. Following this, there is a second ramp time of 30 minutes to increase the temperature to 140°C, which is then maintained for 8 hours, during this stage the resin is hardening and undergoing its final cure. The final stage is the cooling stage, where oven is turned off and the composite panel cools in an uncontrolled way.

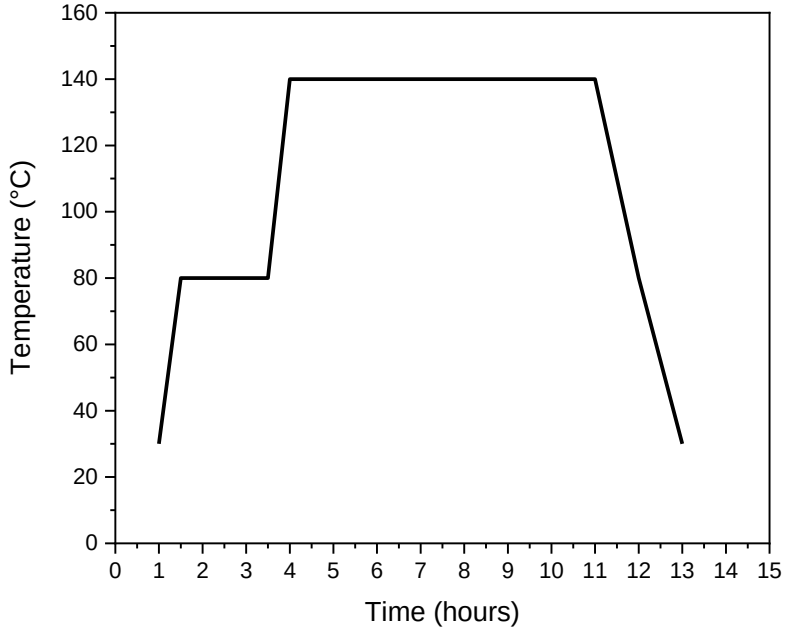

Figure 3.6 Cure cycle for composite epoxy resin (Araldite LY1564 and Aradur 2954) with cooling stage.

3.3.3 Debagging and Specimen Preparation

After curing and once cool, the composite panels were removed from the mould and vacuum bagging, ready for cutting into specimens for testing. Before cutting, the composite panels were inspected for any manufacturing defects that can occur as a result of the resin infusion process, further details of this process are included in the following section.

Composite specimens were cut using a CNC (computer numerical control) diamond saw with a blade thickness of 4mm and an accuracy of +/- 0.2 mm. A diamond saw was preferred because it grinds the material rather than fracturing it, thus reducing the risk of inducing any damage to the composite whilst cutting. First, approximately ~20mm from the perimeter of each composite panel was removed to ensure that the specimens were not cut from areas where there may be defects as a result of materials used in the manufacturing process, such as edge taping. The specimen dimensions were dictated by the relevant test standard. Full details of the specimen dimensions and any additional preparation processes, such as the addition of tabbing, are provided in the results chapters 4-6.

3.4 Quality Control Measures Taken During the VARIM Process

The resin infusion process can induce manufacturing defects into the final composite structure, the most serious being incomplete infusion of the resin. This can be caused by several factors, including a leak in the vacuum seal, too much or too little vacuum pull and exhaustion of the resin supply. It is therefore vital to the VARIM process that careful control of the infusion steps is taken in order to minimise avoidable issues. Non-destructive testing (NDT) methods were used to inspect the newly manufactured composite panels for obvious signs of poor infusion prior to specimen cutting to ensure as far as possible that test specimens were defect free. Poor resin infusion commonly leads to air bubbles in the final composite or areas of not fully wetted through fibres. Visual observations of the composite topside and underside surfaces were conducted after debagging to identify any obvious surface defects such as air bubbles. Additionally, once specimens had been cut to the required dimensions, the cross sections were observed for any internal air bubbles that may not have been obvious on the surface.

Even when the surface appears defect free, it is possible that regions of dry fibres could still exist within the composite structure that are undetectable from the surface. To investigate if this had occurred, the composite panels were subjected to ultrasonic C-scanning. The principle of the C-

scan is to use ultrasonic waves to detect a change in density which signifies internal structure voids. Defects such as void or cracks that occur in the path of the ultrasound deflect the signal and the detector identifies a reflection of the ultrasonic wave [16]. By scanning the full composite and thus collecting information on the reflected signals across the whole sample, it is possible to build a map of the defects in the sample, this is known as the C-scan image. Since defects lead to greater rebounding of the ultrasonic signal, they show up as dark areas on the scan image. More severe defects scatter the ultrasonic signal more significantly and therefore show up the darkest.

The composite panels were C-scanned using a Midas, ultrasonic C-scan system. The panels were securely clamped to the test bed and scanned using a 5MHz water jet probe. The panels were scanned to a resolution of 4 pixels per millimetre. The C-scan images were then reviewed to identify any poorly infused areas of the composite and these areas were avoided during specimen cutting. Occasionally, water droplets from the jets can interfere with the transducer which can appear on the C-scan as small dark speckles across the specimen. As air bubble defects within the composite are generally too small to be identified using the c-scan method, it is important that these fault-like speckles are not confused as voids within the system.

Chapter 4

Effect of the Stitch Junction Position and Stitch Density on the Tensile Properties of FRP Composites

4.1 Introduction

This chapter covers the comparative tensile properties of stitched and unstitched E-glass fibres composites. It is evident from the literature review in Chapter 2 that stitching is an excellent TT technique for improving the composite interlaminar properties but a major drawback is that it nearly always degrades the in-plane tensile properties. It was also discussed that there are some major challenges associated with the production of modified ISO-301 stitched composites, the most common stitch type used in the composites industry. These include, structural defects caused by the stitching threads, the stitching process being damaging to brittle advanced fibres as they are unwound from the bobbin case and the very small capacity of the bobbin supply compared to the needle thread creel. In an effort to address these shortcomings, this work investigates the potential of a new stitch type for TT composite reinforcement, the ISO-401 double thread chain-stitch.

In order to contribute to the optimisation of TT stitching for composite reinforcement, this chapter considers the effect of the novel ISO-401 on the tensile properties of E-glass fibre reinforced polymer (FRP) composites. Specifically, it considers the impact of adjusting the needle and looper thread inter-looping junction position. The effect of different stitch junction positions is also investigated in two different stitch densities. Different densities have been used here because in other research it has been found that smaller spaces between stitches (increased stitched density) are more effective in improving composite out-of-plane properties, such as impact resistance and compression after impact strength [1,84,107,162]. Finally, the optimised ISO-401 stitch is then applied to thicker glass FRP composites, which are produced by employing heavier weight glass fibre fabric. The glass fibre fabric is in a similar weight range to that used by other researchers

[21,62,163,164] in the field to develop composites which are intended for use as structural elements for aerospace applications. In order to provide an appropriate base-line for comparison, the tensile properties of these composites are compared with modified ISO-301 stitched composites. A portion of the work presented in this chapter has been published in a journal [165].

4.2 Composite Manufacturing Process

For this chapter, two different types of E-glass fibre fabric were used to make both stitched and unstitched composites. These fabrics were chosen because they are easy to obtain and widely used in the composite industry. The full manufacturing process of the composite plates and cutting of the specimens is presented in Chapter 3. The stitched and unstitched composite specifications are presented in Table 4.1. The first fabric type used for type 1A-1C composites was 2 x 2 twill woven fabric with a mass of 280 g/m^2 (supplied by Easy Composites Ltd). The filament diameter was 13 µm, the linear density was 1000 Tex and the warp and weft densities were 8 tows/cm and 7 tows/cm. The second, used for 2-UNS, 2-DCS-P and 2-MLS-P type composites, was a plain woven fabric with a mass of 600 g/m^2 (supplied by MB Fibreglass Ltd). The filament diameter was 15 µm, the linear density was 1200 Tex and the warp and weft densities were 2 tows/cm. For each composite type, eight layers of fabric were used to make the preform stack. The preforms were consolidated with a Bisphenol-A type epoxy (Araldite LY1564) resin and an amine type (Aradur 2954 cycloaliphatic polyamine) hardener (supplied by Huntsman UK Ltd). For both composite types the plate dimensions were 300 mm x 300 mm.

Table 4.1 Basic Composite Properties

Specimen	Stitch Type	Junction type	t_c [mm]	FVF [%]	S_p [mm]	S_s [mm]	S_D [1/cm^2]	S_T [cN]	
								T_n	T_l
1-UNS	-	N/A	1.70	51.9	-	-	-	-	-
1A-4	ISO-401	External	1.74	51.2	4	10	0.025	29.4	196.1
1A-3	ISO-401	External	1.74	51.1	3	10	0.033	29.4	196.1
1B-4	ISO-401	External-central	1.73	51.6	4	10	0.025	39.2	88.2
1B-3	ISO-401	External-central	1.74	51.5	3	10	0.033	39.2	88.2
1C-4	ISO-401	Internal	1.72	52.0	4	10	0.025	68.6	176.5
1C-3	ISO-401	Internal	1.72	51.8	3	10	0.033	68.6	176.5
2-UNS	-	-	3.5	58	-	-	-	-	-
2-DCS-P	ISO-401	Internal	3.65	57.6	4	10	0.025	68.6	88.2
2-MLS-P	ISO-301	-	3.63	57.5	4	10	0.025	-	-

4.3 TT Stitching Process

ISO-401 and ISO-301 stitching was performed using the same machines and protocol detailed in Chapter 3. The sewing thread used for both stitch types was polyester core-spun with a thread density of 24 tex, supplied by Coats Ltd and the needle type was a size 90 ball-point. For all stitched specimens, stitching was conducted in the 0° direction.

4.3.1 Twill Woven Stitched Composites (Type 1)

For type 1 composites there were three sub-groups, 1A, 1B, and 1C, each with a different placement of the interloping junction. Composite type 1A had an external junction position (Fig. 4.1(a)), type 1B had an external-central junction position (Fig. 4.1(b)), and type 1C had an internal junction position (Fig. 4.1(c)). Schematics of the junction positions are presented in Figure 4.1(d-f). The inter-looping position of the threads was adjusted by increasing or reducing the needle thread (T_n) and looper thread (T_l) tensions via the corresponding tension wheels, thus each of the

three junction positions had different overall stitch tension (S_T) values. The same process of measuring the corresponding thread tensions as described in Chapter 3 was followed. Incremental changes to the tensions were made until the desired positions were achieved. Then the static tensions were set and left unchanged for the production of each composite type. The stitch junction position types and corresponding tensions for type 1 composites are presented in Table 4.1. Stitching was applied in two different stitch densities (S_D) by varying the stitch pitch (S_p) at 4 mm and 3 mm, the stitch space (S_s) was maintained at 10 mm. The S_D value was calculated using equation 3.1 from Chapter 3.

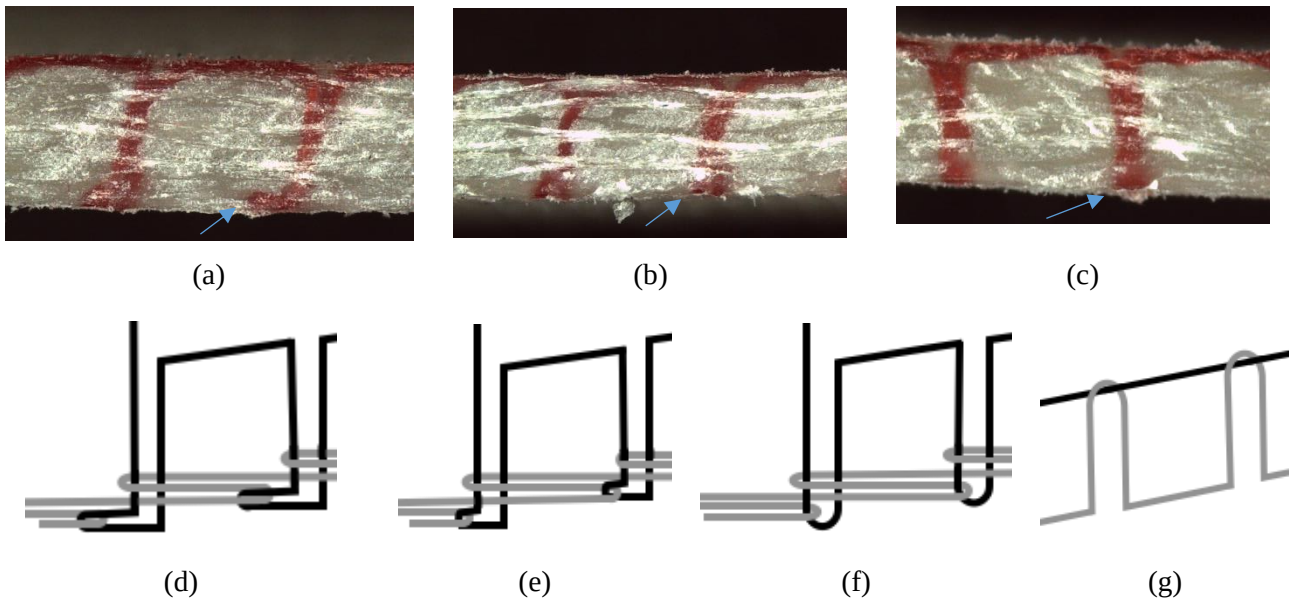

(a) (b) (c)

(d) (e) (f) (g)

Figure 4.1 Example images of the stitch junction positions in stitched composite cross-sections; (a) 1A; (b) 1B; (c) 1C. Stitching geometry schematics; (d) type 1A external junction for specimen 1A; (e) type 1B external-central; (f) type 1C and 2-DCS-P internal junction; (g) modified ISO-301 for type 2-MLS-P.

4.3.2 Plain Woven Stitched Composites (Type 2)

For type 2 composites, there were two machine-stitched iterations, type 2-DCS-P (DCS stitched, fabric 2) and type 2-MLS-P (MLS stitched, fabric 2). Composite 2-DCS-P was stitched with an optimised ISO-401 geometry (Figure 4.1(f)), based on the findings from the early experiments on type 1 composites. Type 2-MLS-P was stitched with a modified ISO-301 geometry which is a standard stitch type for the composite industry and used by other researchers in the field [13,17,21], see (Figure 4.1(g)).

The junction location of 2-DCS-P was based on the position of the junction in type 1C composites. Type 2 preforms were considerably stiffer than type 1 preforms due to the plain weave construction, significant increase in weight from 280 g/m^2 to 600 g/m^2 and approximately 100% increase in preform thickness from ~1.5 mm to 3 mm. Therefore, to replicate the junction position at the needle hole in the new preform type, slight adjustments in the thread tensions had to be made. Early attempts to stitch under the same needle (68.6 cN) and looper (176.5 cN) thread tensions resulted in thread fracture at approximately every ~20mm of stitching. The machine was unable to stitch continuously without catastrophic stitch thread breakage because the friction on the needle thread during insertion and retraction was too high when considering the increase in thickness and stiffness of the sewn fabric preform. To resolve this, the looper thread tension was carefully reduced in small increments of ~10-15 cN until stitching could be performed without any obvious thread fracture and the junction still remained in the target position at the needle insertion point. A looper thread tension of 88.2 cN was found to be optimal whilst the needle thread tension was maintained at 68.6 cN.

For type 2-MLS-P composites, the ISO-301 junction was modified to replicate the most common stitch type used for TT reinforcement of composites. To achieve this geometry recommendations suggested by other authors [21,50] as detailed in Chapter 3 were followed. The bobbin tension was reduced by loosening the bobbin case-spring via the tensioning screw and the needle thread tension was increased is increased by manual adjustment of the tension-disc. In this configuration, the bobbin thread was inserted into the TT of the preform and the needle thread was placed on the surface.

4.4 Material Characterisation

4.4.1 Measurement of Resin Pockets

Prior to tensile testing, cross sections of the undamaged stitched composites were investigated using an optical microscope to identify any resin pockets around the stitching threads. Micrographs were then loaded into ImageJ software for measurement of the resin pocket dimensions. The width and height of the voids were measured using the measuring tool. Before any measurements were taken, calibration was conducted to a known length on each image. In the early experimental work it was found that the spread of data could be quite large, this is because the fabric structure can be different at each stitch point. Depending on where the stitch junction is placed in the woven structure, the resultant resin pocket can vary in shape and size due to the

anisotropic nature of the fabric. Therefore, for each composite, a total of 20 individual resin pockets were measured in order to collect an average, this value was found to give a level of satisfactory repeatability.

4.4.2 Fibre Volume Fraction Method for Type 1 Composites

For type 1 composites, the fibre volume fraction FVF was determined using a theoretical method using the following equation, according to ASTM D3171 [166]:

$$FVF = (A_F \times N)/(\rho_f \times t_c) \quad (4.1)$$

Where N is the number of plies, A_F is the areal weight of the fabric, ρ_f is the fibre density, and t_c is the thickness of the composite laminate.

Additionally, to calculate the FVF of the stitched composites, the stitch thread consumption value was required. There are different methods for predicting thread consumption for ISO-401 recorded in the literature but a considerable limitation is that few of them consider the effect of stitch tension along with fabric thickness, stitch density and thread linear density. These parameters have been shown to affect the volume of thread consumption, therefore ignoring them from calculations leads to significant errors in predictions [167]. In [167], the authors optimised existing thread consumption formulae to include thread tension, using regression analysis. The resulting formulae reduced error percentage considerably when predicting ISO-401 thread consumption, to 4.85%, compared to 14.51% in [168]. For this work, it was important to consider the effect of stitch tension on thread consumption as the stitch tension varied for the different stitch junction positions developed. Thus, this work makes use of the formulae proposed in [167] to predict thread consumption, as they can be generally applied to many cases by inputting specific values of sewing variables associated with this study, such as stitch density, thread linear density, thread tension and fabric preform thickness. Considering this, thread consumption was defined per 10 cm stitching length for needle thread (D_n) using equation 4.2 and looper thread (D_l) using equation 4.3, as in [167]:

$$D_n = 0.25nT + 4.137c + 4.836eT - 4.154T + 61.027 \quad (4.2)$$

$$D_l = 2.312n + 2.623c + 2.53T + 351.32 \quad (4.3)$$

where, n is stitch density (stitches per cm), c is the linear density in tex of the sewing thread, T is the corresponding thread tension and e is the fabric preform thickness. For stitched composites, the total thread consumption in g/cm^2 for the applied S_D was added to the A_F value in order to determine FVF.

4.4.3 Fibre Volume Fraction Method for Type 2 Composites

To experimentally determine the FVF of type 2-UNS composites, the ASTM D3171-99 standard test method for matrix burn-off was followed [166]. The method dictates that the minimum surface area of the specimens should be 625mm^2, the specimens were cut to dimensions of 25 mm x 25 mm from each panel using the same CNC diamond saw used for general specimen cutting as described in Chapter 3. For each composite type 3 specimens were tested. After cutting, the specimens were dried in a Scientific Heraeus T20P oven for a maximum of 3 hours at 40°C or until the weight of the specimen was stable. Once dry, the specimens were placed into a desiccator and left in ambient conditions of 23 $\pm$ 2°C overnight. The density (ρ_s) and the weight (W_s) of the samples were measured using a Mettler Toledo electronic balance and density kit which uses Archimedes' principle. The samples were placed into individual ceramic crucibles and placed in a muffle furnace that had been preheated to 500°C, the samples were then heated to 600°C for 2 hours. Early experiments determined that after 2 hours at 600°C, the matrix had been sufficiently combusted. Samples were optically examined to determine that the fibres did not contain any remnants of matrix polymer and that the matrix/reinforcement block no longer existed. The specimens and crucibles were placed back into the desiccator for cooling and were left for 12 hours. The weight of the remaining fibres (W_f) was then measured and the density of the fibres was already known from the literature as 2.54 g/cm^3 for E-glass fibres. FVF was calculated using the below formula:

$$FVF = \left(W_f/\rho_f\right) \times \left(\rho_s/W_s\right) \quad (4.4)$$

It was found that using the above method for the type 2 polyester stitched composites (2-DCS-P and 2-MLS-P) was unsuitable as the polyester thread combusted as the same time as the resin, thus the stitching thread was removed from the samples. To overcome this, the total weight of the inserted needle and looper thread at the given stitch density was determined manually. To do this, preforms were stitched then specimens of dimensions 1cm x 1cm were marked onto the composite preforms. From these areas, the needle and looper (or needle and bobbin) yarn lengths were unravelled from the preform and their weights measured. For each composite iteration this process was repeated three times and an average was taken. The thread consumption value in gcm^2 was then added to the W_f value in order to determine FVF.

4.4.4 Fibre Volume Fraction Results

Comparing the FVF values of stitched composites to unstitched equivalents in Table 4.1, it can be seen that ISO-401 stitching in this case did not significantly affect the FVF value. The increase or decrease in FVF are in the range of 0.7 % and 1.4 % for all of the stitched composite types. Similar values have been reported by other researchers [19,159]. In this study, it is proposed that stitching did not have a significant effect on the FVF of the FRP composites because the stitching thread used was relatively fine, with a similar linear density to thread commonly used for NCF (non-crimp fibre) stitching. Fine thread is used for the stitching of NCF to ensure minimal disruption to the fibres but provide a non-structural holding stitch. Therefore, it is likely the case in the work for this chapter that any deviation to the in-plane fibres was minimal and any associated negative effects, such as stress concentration, were highly localised. It is therefore important to consider in the following discussions that since the tensile properties are a fibre-dominated property, when the effect on the FVF value by stitching is small, as in this study, any improvement or reduction of the tensile properties can mainly be attributed to the role of stitches. For example, optimum spaced stitching can help to transfer even load distribution to the reinforcement threads under loading but conversely, stitching can induce geometrical defects which become areas of structural weakness under loading conditions [13,47,159].

4.5 Tensile Properties of Stitched Composites

4.5.1 Protocol for Tensile Testing

Tensile testing was conducted to investigate the mechanical properties of the stitched and unstitched composites, namely tensile strength (σ_{ULT}) tensile failure strain (ε_f) and tensile modulus (E_1). The testing was carried out in-line with the industry standard ASTM D3039M on a commercial INSTRON-5569 machine in ambient conditions [169]. The tensile test was repeated 3 times for each composite type due to limited test specimens. The test parameters recommended by the standard were as follows: 50kN load cell for type 1 composites and a 100kN load cell for type 2 composites, 2 mm/min cross-head speed, using a video extensometer with 50 mm gauge length for strain measurement and specimen dimensions of 25 mm (width) x 250 mm (length) and a gauge length of 150 mm. E was defined according to the standard as the slope between $\varepsilon = 0.1$ % and $\varepsilon = 0.3$ %. Loading was applied in the 0° direction, which was the same as the stitching direction. Early tests revealed that for composites type 1, tabbing was unnecessary as all specimens failed in the gauge length of the specimen without the application of tabs. The use of hydraulic wedge grips minimised any damage in the area gripped by the machine and effectively minimised stress concentration at these areas hence the specimens did not fail at the tabbing site.

Conversely, for type 2 composites it was clear from the early experimental work that tabbing was required to minimise stress concentration at the gripped area during tensile loading. It was found that untabbed type 2 composite specimens regularly failed at or close to the grip edge and upon inspection the specimen area held within the grips was noticeably damaged after testing. With the addition of tabs, type 2 composites failed within the gauge length and thus stress concentration was reduced. The tabbing material used was a 2.4 mm thick glass fibre/epoxy composite sheet, supplied by Croylek Ltd. The tabs were cut to the required dimensions (50 mm length x 25 mm width) and secured in place with 3M™ Scotch-Weld™, a two-part structural epoxy and amine adhesive. The adhesive system was mixed homogenously at 20°C then applied to the composite panels and tabbing material, the curing process was two hours at 65°C. For each tab, a set of three bulldog clips were evenly spaced and secured around the tab to ensure contact with the panel was maintained during curing.

4.5.2 Tensile Properties of Stitched Thin E-Glass Fibre Composites

The tensile properties for all stitched and unstitched composites are presented in Table 4.2 and representative stress strain curves are presented in Figure 4.2. FVF values are reported in Table 4.1, as discussed FVF was not significantly affected by the presence of the stitching thread in the stitched composites due to the fine stitching thread. It can be seen that the loading is generally linear until tensile failure which was characterised by loud explosive sound indicative of complete breakage of the in-plane tows. During the test, damage initiation in the form of matrix cracking was audible in stitched specimens at around 40 % of ultimate tensile strength, compared to 60% for the UNS specimens. This suggests that the resin pockets in stitched composites acted as stress concentrators and crack initiation sites during tensile loading. Investigation of the composite cross-sections found that resin pockets were present in the stitched specimens around each stitch point. Figure 4.3 presents images of in-plane fibres deviating around the stitching threads in the preform and in the final composite cross-section, resulting in a resin pocket.

Example images of the front surface and cross-sectional images of the tensile failure site are presented in Figure 4.4. For UNS specimens, post-mortem investigation revealed the dissipation of energy in the form of fibre pull-out, fibre fracture, matrix fracture, and extensive delamination at tensile failure site. For stitched specimens damage mechanisms observed were stitch thread breakage, fibre pull-out, matrix cracking, and local delamination. For all iterations of A, B, and C type composites, stitching was found to visibly maintain the specimen integrity and reduce the delamination area at the tensile failure site, compared to UNS specimens.

Table 4.2 Longitudinal tensile properties of stitched and unstitched composites, standard deviation is shown in brackets.

Properties	**UNS-1**	**1A-4**	**1A-3**	**1B-4**	**1B-3**	**1C-4**	**1C-3**
$\sigma_{ULT}\ [MPa]$	348.9 (9.6)	361.6 (10.1)	310.1 (6.0)	355.3 (5.3)	281.7 (7.4)	363.4 (6.5)	352.4 (9.0)
ε_f [%]	2.32 (0.04)	2.34 (0.08)	2.21 (0.03)	2.35 (0.11)	2.19 (0.08)	2.31 (0.24)	2.35 (0.22)
$E\ [GPa]$	16.9 (0.3)	17.2 (0.2)	15.0 (0.6)	17.3 (0.4)	16.5 (0.5)	17.0 (0.4)	16.9 (0.8)

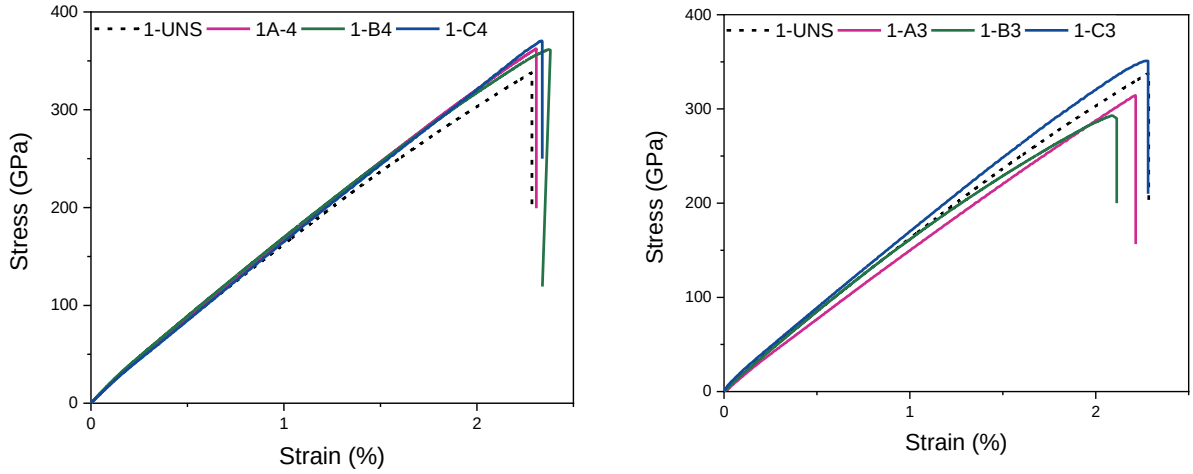

(a) (b)

Figure 4.2 Representative stress-strain curves of stitched and unstitched composites; (a) stitch pitch of 4 mm and; (b) stitch pitch of 3mm.

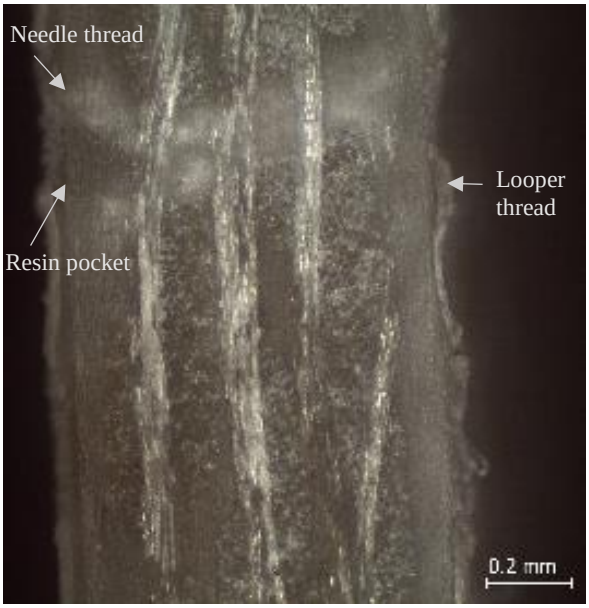

(a)

(b)

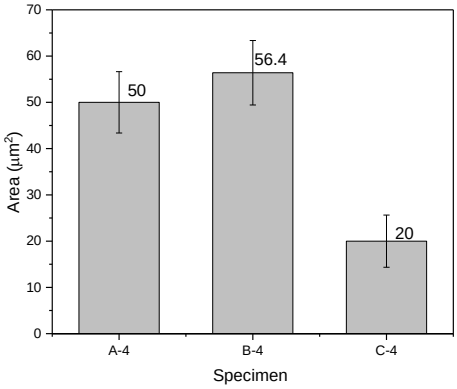

(c)

Figure 4.3 (a) Micrograph of resin pocket in ISO-401 stitched composite cross-section; (b) image of in-plane fibre deviations around stitch holes on preform surface; (c) comparison of resin pocket areas for ISO-401 stitched specimens.

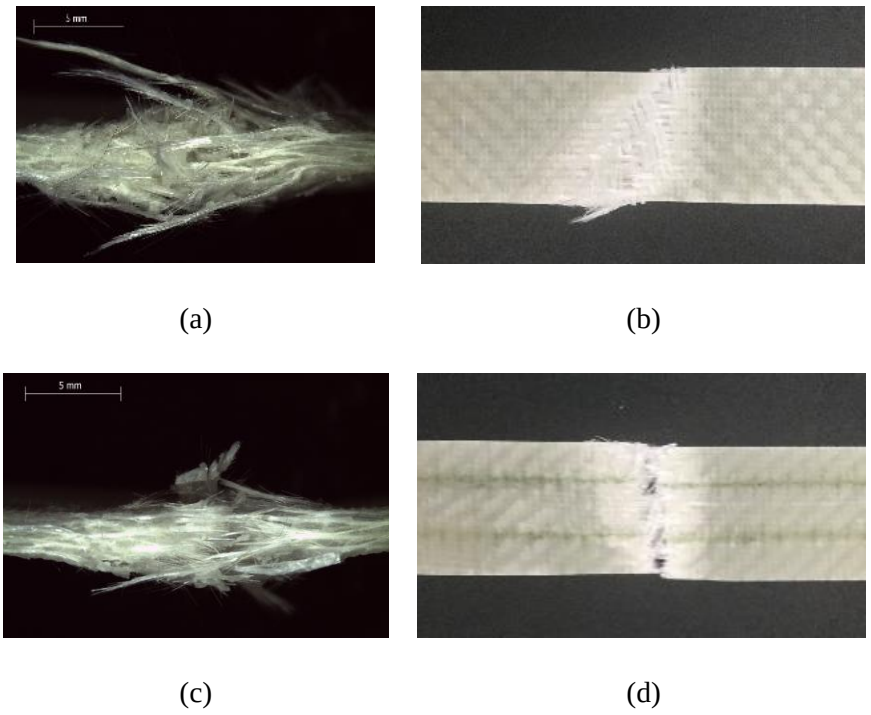

(a) (b)

(c) (d)

Figure 4.4 Tensile failure site of (a) unstitched cross sectional view; (b) unstitched front view; (c) stitched cross sectional view; (d) stitched front view.

The **tensile moduli** values for 1-UNS, 1A-4, 1B-4, 1C-4, were 16.9 GPa, 17.2 GPa, 17.3 GPa and 17 GPa, respectively. Figure 4.5 presents a comparison of tensile modulus values for stitched and unstitched specimens. The results show that unstitched and composites stitched with a moderate stitch density (S_p = 4 mm) have similar tensile modulus values in this case. Since tensile modulus is highly dependent upon the orientation of in-plane fibres, it is proposed that a combination of fine stitching thread and optimum stitch distance resulted in limited fibre deviation in the final composite and thus low stress concentration at these areas under loading conditions. This is in line with other researchers who have found optimum densities and stitch conditions to contribute to even distribution of load transfer [47]. Additionally, little or no reduction in tensile modulus is indicative of minimal fibre waviness caused by stitching [159].

When the stitch density is increased (S_p = 3 mm), the tensile modulus for 1A-3, 1B-3 and 1C-3 were 15 GPa, 16.5 GPa and 16.9 GPa respectively. In the case of 1A-3 and 1B-3 composites, the tensile modulus is reduced by 11% and 2.4%. For 1A-3 composites, the reduction in modulus reached statistical significance at a threshold of $p<0.05$. For 1C-3 the tensile modulus remained

similar to the UNS value. Investigations of the composite cross sections revealed that reductions in tensile modulus for 1A-3 and 1B-3 can be associated with both the size and frequency of resin pockets in the final structure. Resin pockets are caused by distortion of in-plane fibres in an elipse around the stitching threads, the thread type, machine parameters and fabric structure can all influence this [24,27]. In this case, the other variables were kept constant but changing the machine parameters altered the thread junction location for the stitched composites. Whilst resin pockets are expected to be found in composites stitched with two threads, attempting to minimise them and their detrimental effect was one important aspect of this work.

Figure 4.3 presents the average resin pocket sizes found in the composite cross-sections. It can be seen that when the junction occurred further from the needle hole as in type 1A and 1B composites, the resin pockets were 60-65% larger than type C composites, where the junction occurred at the needle thread insertion point. This is because the distance between the insertion needle thread and the return needle thread is wider, thus distorting in-plane fibres more significantly along its path. Once the stitch pitch was reduced to 3mm to increase the stitch density, the combination of frequency and severity of the resin pockets in the composite structure has increased the in-plane fibre waviness and thus reduced the tensile modulus. These effects were more pronounced when the stitch density was increased (1A-3 and 1B-3) because the total number of resin pockets increased. Therefore, a higher degree of fibre waviness for type 1A-3 and 1B-3 composites caused more lateral deformation to occur during loading and resulted in reduced tensile properties. Very high densities are commonly considered to cause stress concentration during tensile loading [47]. Conversely, for type 1C composites, the distortion to in-plane fibres remained minimal and therefore the tensile modulus was similar to 1-UNS composites.

The **tensile strengths** for 1-UNS, 1A-4, 1A-3, 1B-4, 1B-3, 1C-4, and 1C-3 were 349 MPa, 362 MPa, 310 MPa, 355 MPa, 282 MPa, 363 MPa and 352 MPa respectively. Comparison of tensile strength for unstitched and stitched composites is presented in Figure 4.5. The tensile strength of UNS and stitched specimens with 4 mm stitch pitch are similar and in the case of A-4 and C-4 slightly improved, though the improvement did not reach statistical significance at a threshold of $p<0.05$. The results indicate that a moderate stitching density did not affect the tensile strength, which is similar to the effect of stitching on tensile modulus for these specimen types. However, when the stitch pitch is reduced (3 mm), the tensile strength is significantly reduced in A-3 and B-3 composites by 11% and 19% respectively, compared to UNS composites. As discussed above, this can be attributed to increasing frequency of resin pockets in the composite structure,

therefore they have become substantial enough to reduce the load-bearing capacity of the in-plane fibre tows.

The values of **tensile strain** for UNS, A-4, A-3, B-4, B-3, C-4, and C-3 were 2.3 %, 2.3 %, 2.2 %, 2.4 %, 2.2 %, 2.3 %, and 2.4 % respectively. For all of the stitched specimens, the tensile strain was maintained or slightly improved when a moderate stitch density (S_p = 4 mm) was employed. The results indicate that the inclusion of stitching thread into the composite structure may have helped to effectively delay crack growth and thus slightly improve the toughness of the composites. When dense stitching was employed (S_p = 3 mm), for C-3 type composites tensile strain is unaffected but in the case of A-3 and B-3 composites, it is reduced slightly. Again, this effect can be attributed to the size and frequency of the resin pockets and associated in-plane tow distortions.

Overall, the tensile modulus, strength and strain of type 1C composites, stitched at both densities, remained similar to that of 1-UNS composites. This suggests that the specific stitch geometry employed in these composites had a minimal negative effect on the in-plane fibres hence preserving the tensile properties, even when the stitch density was increased (1C-3 composites). For this stitch geometry, the needle thread path did not extend along the surface of the composite as in junction types 1A and 1B. Restricting the needle thread path so that the inter-looping junction occurred close to the needle hole resulted in a smaller distance between the insertion thread and returning thread. This meant that fewer in-plane fibres were being pushed apart by the static thread tension and thus resin pockets in the composite structure were significantly smaller for 1C type composites.

Conversely, for type 1A and 1B composites the stitch related defects were more severe, for example, as resin pockets were found to be 60-65% larger in comparison to those measured in type 1C composites. Despite this, when the stitch density was moderate, the tensile properties were still comparable with unstitched composites. However, once the density was increased, the effects were more pronounced because the total number of resin pockets in the structure increased. Therefore, a higher degree of fibre waviness for type A-3 and B-3 composites caused more lateral deformation to occur during loading and resulted in reduced tensile properties. Overall, the tensile properties for type 1A-3 and type 1B-3 were reduced by a maximum of 19%, this is comparable with the literature where stitching with modified ISO-301 has been found to reduce tensile properties by up to 20% [2,17].

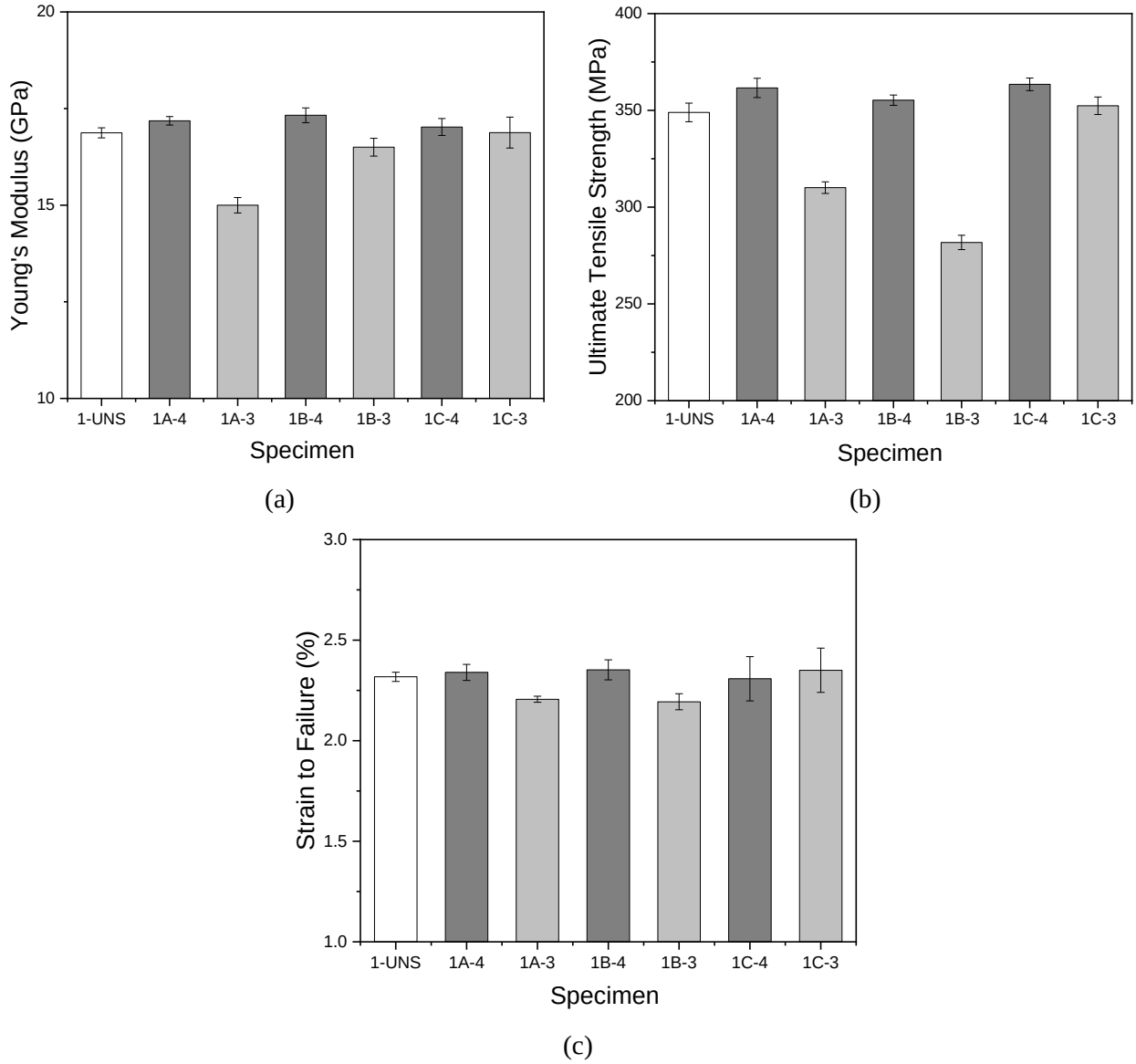

Figure 4.5 The effect of TT stitching on; (a) Young's modulus; (b) ultimate tensile strength; (c) tensile strain at failure.

4.5.3 Tensile Properties of ISO-401 and ISO-301 Stitched Thick E-Glass Fibre Composites

In this section, the optimised ISO-401 geometry that was identified from the results of the previous section was applied to thicker glass fibre composites (2-DCS-P). The thicker composites are more representative of composites produced for aerospace applications. Comparing the properties of

ISO-401 stitched composites with ISO-301 stitched composites is an important part of this work and will help to further investigate the suitability of the ISO-401 geometry as an alternative composite reinforcement technique.

Table 4.3 and Table 4.1 present the tensile properties and FVF values for all stitched and unstitched type 2 composites. The stress-strain curves are presented in Figure 4.6. Similar to the previous section, the loading is linear until final failure, which was characterised by the explosive sound of the in-plane fibre tows breaking. Investigation of the tensile failure sites revealed similar damage mechanisms as reported in the previous section. Images of the tensile failure sites are presented in Figure 4.7. Damage mechanisms included fibre pull-out, fibre fracture, matrix fracture, and extensive delamination at tensile failure site and additionally for stitched specimens stitch thread breakage stitch thread fibre pull-out, and local delamination. Figure 4.8 presents optical micrographs of the localised delamination around the stitch threads. As was found in the previous section, for stitched specimens the failure area was generally more localised and contained by the stitching, compared with unstitched specimens where delamination was extensive.

Table 4.3 Longitudinal tensile properties of stitched and unstitched composites, standard deviation is shown in brackets.

Properties	**2-UNS**	**2-DCS-P**	**2-MLS-P**
σ_{ULT} $[MPa]$	465.4 (4.5)	449.4 (16)	433.5 (16)
ε_f [%]	2.29 (0.06)	2.26 (0.05)	2.23 (0.11)
E $[GPa]$	22.9 (0.7)	22.4 (1.5)	23.5 (0.41)

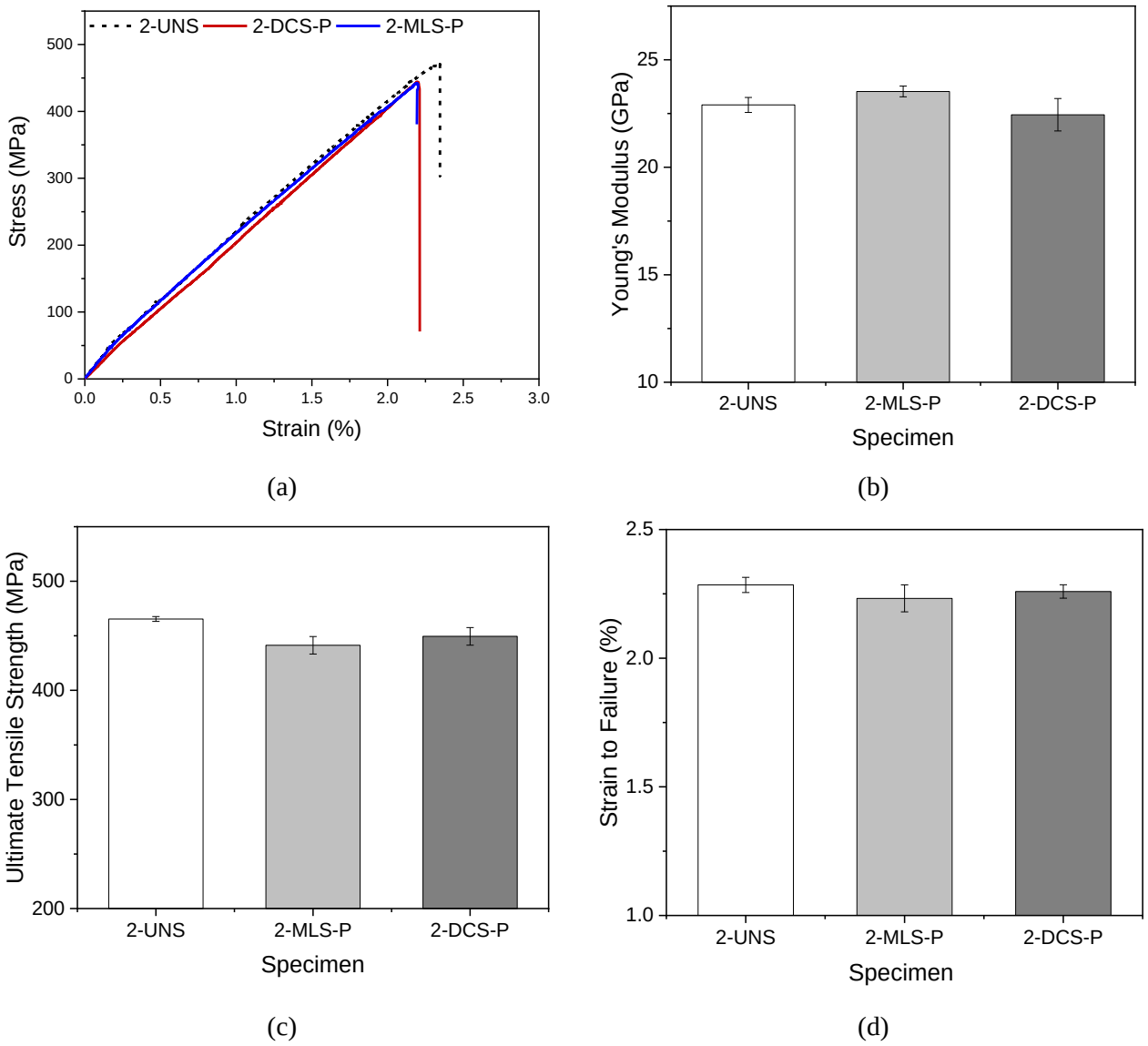

Figure 4.6 (a) Representative stress-strain curves of stitched and unstitched composites; (b) Young's modulus comparison; (c) tensile strength comparison; (d) tensile strain comparison.

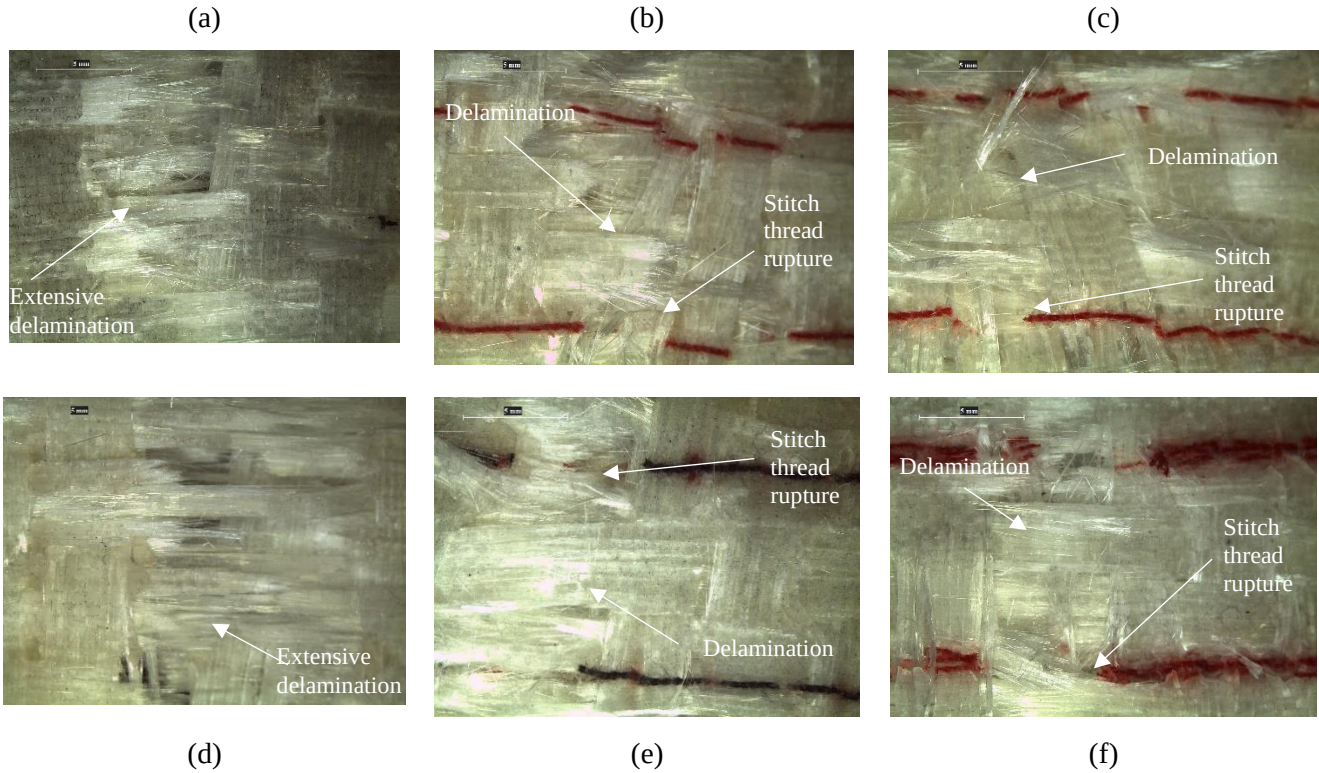

Figure 4.7 Optical micrographs of the tensile failure sites of the front surfaces; (a) 2-UNS, (b) 2-MLS-P; (c) 2-DCS-P; and of the back surfaces; (d) 2-UNS, (e) 2-MLS-P; (f) 2-DCS-P.

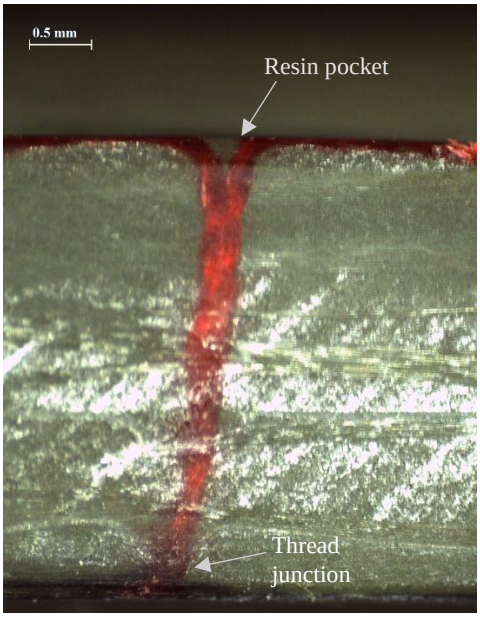

(a)

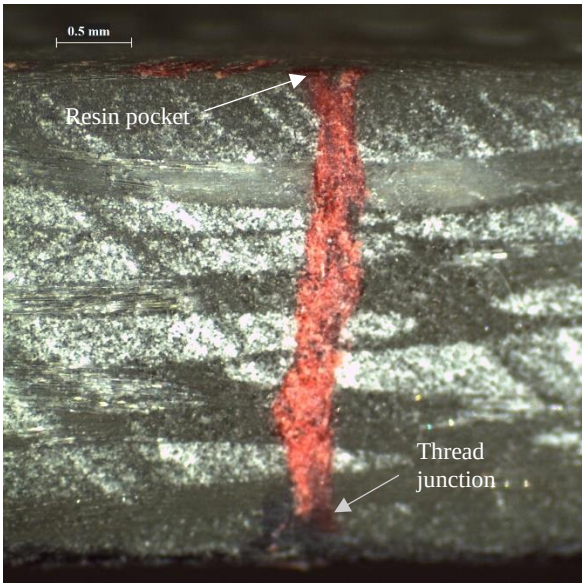

(b)

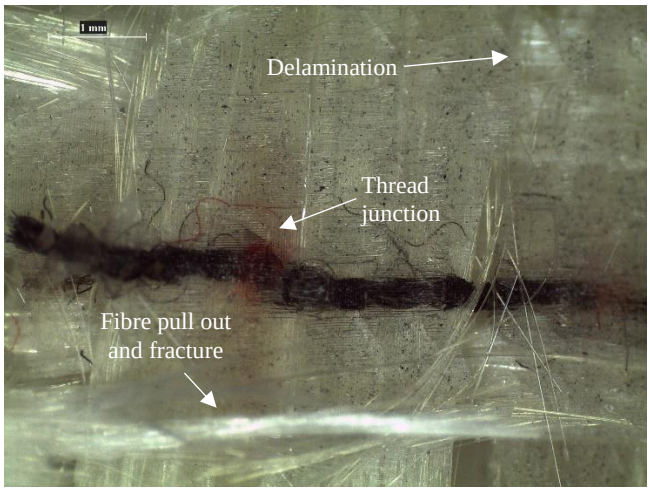

(c)

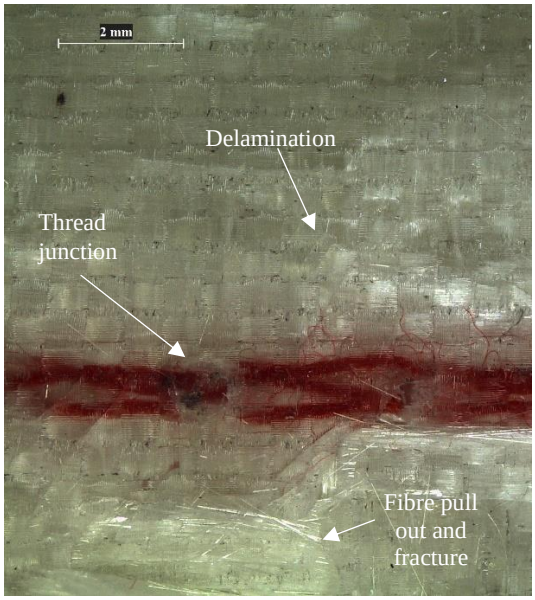

(d)

Figure 4.8 Cross-sectional optical micrographs of (a) 2-MLS-P and (b) 2-DCS-P; and bottom surface micrographs of the failed specimens showing the stitch junction sites for (c) 2-MLS-P composites; (d) 2-DCS-P composites.

Figure 4.6 presents a comparison of the **tensile moduli** values for all stitched and unstitched composites. For 2-UNS, 2-DCS-P and 2-MLS-P, the tensile moduli values were 22.9 GPa, 22.4

GPa and 23.5 GPa. For 2-DCS-P, the average reduction in modulus was 2.2%, for 2-MLS-P, the increase was 2.6%. For the 2-DCS-P composites, the junction location was optimised based on the previous study to induce the least amount of in-plane fibre misalignment as possible. It is relevant here to consider why MLS stitching slightly increased the tensile modulus and DCS stitching slightly reduced it. Comparing the resin pocket size at the needle thread insertion point for both stitching types, 2-MLS-P composites has slightly larger resin pockets on average, by approximately 15%, see Figure 4.9. Figure 4.8 presents images of the resin pockets in stitched composite cross-sections. Comparing the stitched composite cross-sections, in 2-DCS-P specimens, the looper thread is visible in the composite cross section because the junction location was positioned at the stitching site, as opposed to between two successive stitching points where it would occur at the composite surface. It is proposed that the small radius looping of the 2-DCS-P threads have also caused additional distortion the in-plane reinforcement tows. Conversely for MLS stitched composites, since the threads are interlaced, as opposed to interlooped, the thread junction is smaller therefore causing less displacement of the in-plane fibres as a result. Hence, despite MLS composites having larger resin pockets, the small reduction in modulus for the 2-DCS-P composites could be as a result of the combined effect of resin pockets and increased quantity of misaligned reinforcement fibres around the interlooping junction. However, it is important to acknowledge that the modulus reduction found in 2-DCS-P composites is considered small and reductions below 5% indicate that the in-plane fibre waviness induced by the stitching threads is still minimal [17,159]. In both cases, stitching did not have a significant effect the tensile modulus at a threshold of $p<0.05$, this is likely because the stitching thread employed was very fine and in general did not severely misalign the in-plane fibres. Therefore, the results suggest that any negative effect of these resin pockets under loading conditions were highly localised and thus the load bearing capacity of the reinforcement fibres was mostly unaffected.

The **tensile strength** values for 2-UNS, 2-DCS-P and 2-MLS-P were 465 MPa, 449 MPa and 434 MPa respectively. For 2-DCS-P, the average reduction in strength is 3.4%, which did not reach significance. For 2-MLS-P, the decrease is 6.7%, which reached statistical significance at a threshold of $p<0.05$. Reduction in tensile strength can be attributed to the breakage of in-plane fibres due to the sewing process [17]. It is proposed that in both cases, stitching caused some damage to the in-plane fibres as the standard deviation was much larger in comparison to 2-UNS, indicating more variation between the specimens as a result of the stitching process. It is suggested that for 2-MLS-P, fracture damage to the reinforcement fibres due to the stitching process could have been more severe compared with 2-DCS-P composites. Therefore, this effect, combined with the larger resin pockets caused an overall reduction in tensile strength.

The **tensile strain** values for 2-UNS, 2-DCS-P and 2-MLS-P were 2.29%, 2.26% and 2.23%. A comparison of tensile strain values for stitched and unstitched specimens is presented in Figure 4.6. In both cases, on average stitching reduced the tensile strain slightly by 1.3% for 2-DCS-P and 2.6% for 2-MLS-P, the reductions were not statistically significant. It is also evident that the standard deviation value has increased for stitched specimens, again suggesting more variation between specimens which is likely due to the stitch induced defects. Thus, the slight strain to failure reduction in stitched composites can be attributed to the stitch induced resin pockets and in-plane fibre misalignment, as documented.

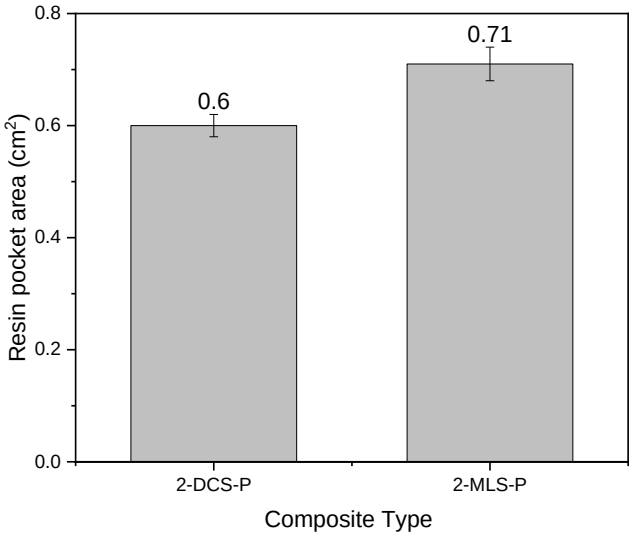

Figure 4.9 Comparison of resin pocket areas for stitched composites.

4.6 Concluding Remarks

It has been found that the ISO-401 stitching geometry can be optimised for the TT reinforcement of FRP composites. By adjusting the stitch thread junction location to occur at the needle thread insertion point, as in type 1C composites, even when the stitch density was increased, the tensile properties were generally comparable to unstitched equivalent composites. This is significant because stitching is often reported to reduce the tensile properties when high density stitching is employed [4,159]. For the other ISO-401 junction locations (type 1A and 1B), where the junction occurred between the stitch insertion points, stitching did not affect the tensile properties when

the density was moderate but when the density was increased, the tensile properties were reduced. This is because for 1A and 1B composites, the resin pocket areas were on average 60-65 % larger than in 1C composites, due to the effect of widening of the elipse around the stitch threads as a result of the junction location. Therefore, increasing the stitch density increased the amount of larger resin pockets in the structure, thus causing a reduction in tensile properties. Since the tensile properties for 1C-4 and 1C-3 were similar to unstitched equivalents, it is suggested that the stitch-induced defects were more localised and had a minimal effect on the tensile performance because the resin pockets were smaller. It is also proposed that the needle hole junction location contributed to the even distribution of load transfer under testing conditions. However, it should be considered that tensile property reductions for 1A and 1B composites never exceeded 19 % which is in-line with the subject literature where modified ISO-301 stitching has been found to reduce tensile properties by up to 20% [2,17].

As the ISO-401 geometry with a needle hole stitch junction location was found to be optimal for FRP composites, the same geometry was replicated in thicker composites which better represent those used in the aerospace industry. Additionally, the geometry was compared with modified ISO-301 as this is commonly used for TT FRP composite reinforcement and therefore provided a good benchmark for the new stitch type. To achieve optimum stitching conditions on the plain woven 600 g/m^2 fabric, the looper tension had to be reduced. This helped to reduce tension on the needle thread whilst still achieving the desired stitch geometry type.

It was found that the tensile modulus and tensile strain of 2-DCS-P and 2-MLS-P composites was similar to unstitched equivalents, any differences were small and not considered statistically significant. It is proposed that any stitch induced damage was not severe enough to effect the composite toughness. The average tensile strengths of 2-DCS-P and 2-MLS-P were found to be lower on average than 2-UNS, with the reduction in 2-MLS-P composites reaching significance. It is likely that the stitched in-plane fibre misalignment, larger resin pockets and possibly increased in-plane fractured threads were the cause of the reduction. Ultimately, the results indicate that the ISO-401 geometry can produce composites with similar in-plane tensile properties to both unstitched and ISO-301 stitched composites. This is significant because it supports the case for using ISO-401 stitch type as a TT FRP composite reinforcement and warrants further investigations.

Chapter 5

Tensile Properties and Damage Tolerance of ISO-401 Stitched Composites

5.1 Introduction

In the previous chapter, the experimental work established that the ISO-401 stitch type can be considered a suitable TT (through-thickness) composite reinforcement technique and ISO-401 composites had comparable properties to composites stitched with the commonly used modified ISO-301 stitch type. Building on this knowledge and to investigate ISO-401 stitched composites further, the work completed for this chapter involved employing glass fibre thread for the TT stitching yarn and evaluating the tensile, damage resistance and damage tolerance of ISO-401 stitched composites. Glass fibre thread was introduced here as it is an advanced fibre thread which is favoured in the literature as it is considered to provide higher damage tolerance [13,25,45]. However, early investigations found that due to the increased thickness of the glass fibre thread, some adjustments to the ISO-401 sewing machine, particularly concerning the needle and looper mechanism positions, were required to achieve reliable and repeatable stitch formation while preventing unnecessary damage or fracture of the stitching thread. Therefore, the first line of investigation was to adapt the ISO-401 machine settings to enable correct loop formation for stitching preforms with glass fibre thread. The process of these adjustments are detailed within this chapter. Following this, the tensile properties of the resultant composites are compared with those of unstitched and polyester stitched equivalent composites from the previous chapter to determine the effects of ISO-401 stitching with glass fibre thread.

Finally, it was imperative to verify the damage resistance and damage tolerance of ISO-401 glass fibre stitched composites as these properties have not yet been investigated for this stitch type. This is a common test used to evaluate the properties of 3D composites because TT reinforcement techniques, such as stitching, are known to improve the damage resistance of FRP composites [128]. The impact resistance and damage tolerance properties of glass fibre stitched composites are compared with unstitched composites. Subjecting FRP composite panels to impact testing can reveal information about the damage resistance and damage response characteristics of the material. The test method involves subjecting the composite test coupons to a range of impact energy levels and studying the resulting damage using non-destructive techniques such as, ultrasonic c-scan and optical microscopy [6,8]. Of particular interest to this work is the low impact response of stitched and unstitched composites, which is designed to replicate situations in service such as impact from a dropped work tool. Damage tolerance is defined as the ability of a material or structure to retain its load bearing capacity after being subjected to damage. The most common method for evaluating the damage tolerance of composites is the compression after impact (CAI) method, as compressive strength is known to reduce considerably after impact damage has been sustained [8,127,128].

5.2 Composite Manufacturing and Stitching Process

The experiments for this chapter were performed on unstitched and stitched composites manufactured from eight plies of E-glass plain woven fabric with an areal weight of 600 g/m^2, which is the same as was used for the work in the previous Chapter 4. The filament diameter was 15 µm, the yarn linear density was 1200 Tex and the warp and weft densities were 2 tows/cm. Two types of composite were manufactured, unstitched (2-UNS) and ISO-401 machine stitched, (2-DCS-P and 2-DCS-G). It should be noted that composite types 2-UNS and 2-DCS-P were the same composites that were manufactured for the previous Chapter 4. Composite type 2-DCS-G is a new iteration of stitched composite with different parameters that was specifically manufactured for the work in this Chapter. Specification of the three composite types are shown in Table 5.1. Stitching was performed prior to the VARIM process, the stitching process is detailed below and the VARIM process is discussed in detail in Chapter 3.

For double-thread chain-stitching, the preforms were stitched with the same machine and protocol as described in Chapter 3. Two sewing thread types were employed, polyester core-spun and glass fibre, specification of the threads can be viewed in Table 5.2. There were two sub-types of

machine stitched composites, 2-DCS-P for which the needle and looper threads were polyester and 2-DCS-G, for which the needle thread was glass fibre and the looper thread was polyester. Since glass fibre thread was to be used as the TT reinforcement, it was employed as the needle thread. Polyester thread was used as the looper thread because this acts as a holding thread for the needle thread, securing it to the composite surface, thus it does not run through the thickness or provide interlaminar reinforcement. For all stitched composites, stitching was conducted in the 0° direction. Both the stitch pitch and stitch space were kept constant at 4 mm and 10 mm respectively, resulting in a stitch density of 0.025 mm^{-2}. Equation 3.1 in Chapter 3 was used to determine the stitch density.

The sewing machine had to be adapted from its factory settings for composite stitching with the glass fibre needle thread, full details of the machine adjustments are detailed in the next section. Once adjustments to the loop forming mechanisms had been made, the thread tensions were adjusted to ensure that the stitch junction was comparable to the junctions reported in 2-DCS-P for the previous chapter, details of which are reported in Table 5.1. The same method for adjusting the thread tensions was followed from Chapter 3. During initial experiments, it was found that when the needle and looper tensions were the same as for 2-DCS-P, the junction location for 2-DCS-G was different. It was placed away from the needle insertion point and further towards the middle point between two stitching points. Increasing the static needle thread tension by ~30 cN and reducing the looper thread tension by ~10 cN was sufficient to achieve the correct junction position.

Table 5.1 Basic Composite Properties

	2-UNS	**2-DCS-G**	**2-DCS-P**
Reinforcement fibre type	E-glass	E-glass	E-glass
Needle stitching fibre	-	Glass fibre 2-ply twisted	Polyester corespun
Looper stitching fibre	-	Polyester corespun	Polyester corespun
Needle/looper tension [cN]	-	98.0/78.5	68.6/88.2
Fabric weight [gsm]	600	600	600
Composite thickness [mm]	3.5	3.65	3.52
Fibre volume fraction [%]	58 (1.34)	55 (0.35)	57.6

Table 5.2 Properties of the Stitching Threads and Corresponding Needle Size

	E-glass	**Polyester**
Construction	2-ply twisted	Corespun
Thread diameter [mm]	0.34 (0.03)	0.24 (0.03)
Needle Size	110	90

5.3 ISO-401 Machine Adjustments for Stitching with Glass Fibre Thread

The needle thread was changed from polyester to glass fibre in order to prepare type 2-DCS-G composites. Early experiments revealed that since the linear density and handling and properties of the glass fibre thread were different to the previous stitch thread, stitches could not be formed properly, which necessitated some adjustments to the sewing machine. There were two main issues that prevented adequate stitch formation and successive stitching; (i) the combined properties of the glass fibre stitching thread and glass fibre preform fabric, and: (i) the increased needle size and its relationship to the looper mechanism.

5.3.1 Needle Adjustments

The initial set of adjustments were made to the sewing machine needle. In particular, employing glass fibre stitching thread with a larger diameter, compared to the previously used corespun PES thread, required the needle size to be significantly increased. Needle sizes were increased incrementally and trialled on the preforms to determine their suitability. The stitched preforms were then visually inspected to identify any damage or obvious fracture to the stitching threads. It was determined that sizes 90 and 100 were incompatible as they caused excessive fracture to the stitching thread due to increased friction between the glass fibre thread and the needle eye, and fabric plies, therefore causing needle thread rupture during its retraction through the preform plies. The most suitable needle size was found to be size 110 which enabled consistent needle

deployment into the preform fabric at high operational speed without obvious or catastrophic fracturing of the needle thread.

As discussed in Chapter 2, a key element of correct loop formation is the requirement of adequate friction between the needle thread, needle, and the fabric upon needle retraction. However, in this case once the correct needle size had been determined, insufficient friction between the stitch thread and preform fabric resulted in only a shallow loop being formed during needle retraction, likely caused by multiple interacting factors such as the preform fibre sizing, the lubricant applied to the glass fibre stitching thread and the fabric construction. To ensure a larger, more pronounced loop could be formed, some adjustments were made to provide a more favourable needle position.

Firstly, to help increase the size of the needle loop, the needle was rotated anti-clockwise by approximately ~2 mm. This resulted in an increase in friction during the needle retraction between the thread, fabric and the needle because the thread was returning through the fabric at an angle. Secondly, the needle was lowered from its original position by approximately ~3 mm. When the needle was in the standard position, the needle loop was formed above the looper, as it reached its position to catch the loop. Lowering the needle meant that the end of the needle stroke was positioned slightly lower under the machine bed, therefore the loop formation occurred over a slightly longer distance during needle retraction. As a result, although the needle loop was smaller than usual, it formed at a more suitable position in relation to its interaction with the looper. Thus ensuring that the looper could accurately catch the loop during needle retraction. Images of the standard and optimised needle settings are presented in Figure 5.1.

5.3.2 Looper Adjustments

The optimum needle size required for stitching with glass fibre thread was larger than the standard factory recommendations, therefore, adjustment to the looper mechanism had to be made to enable successful stitch formation. As the needle size had increased significantly, during its retraction into the preform it was brushing against the looper arm and the looper was unable to travel clear of the needle during operation. Attempting to operate the machine in this set-up would have run the risk of needle fracture but more importantly, the looper was in an inadequate position to catch the needle thread, hence the inability to produce successive stitches. Adjustment of the looper elipse path was required to accommodate the larger needle size. By retracting the looper elipse back by ~0.5 mm, the looper arm was positioned correctly for catching the loop of thread at the back of the needle, without being obstructed by the needle itself (see Figure 5.1).

(a)

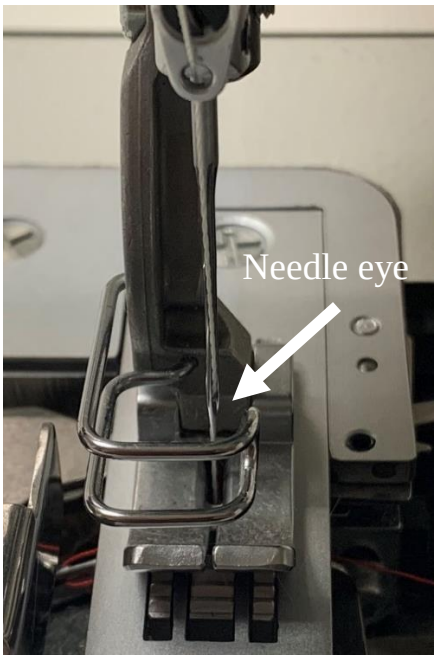

(b)

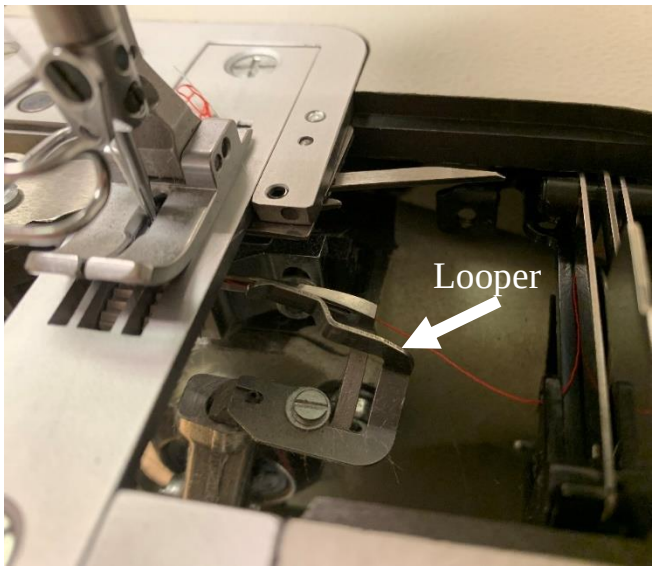

(c)

Figure 5.1 ISO-401 sewing machine settings; (a) standard needle setting with correct eye position; (b) adjusted and optimised needle settings where needle has been lowered by ~3mm and eye rotated anti-clockwise and; (c) retracted looper position by ~0.5mm.

5.4 Material Characterisation

5.4.1 Microscopy

Cross-sections of the stitched composites (2-DCS-G and 2-DCS-P) were investigated using optical microscopy to confirm the junction locations and also to identify whether resin pocket areas were present around the stitch threads. Microscopy specimens were cut from the centre of the composite plate to avoid manufacture induced non-uniformities close to the edges. For measurement of the stitch-induced resin voids, the same software and protocol was followed as detailed in Chapter 4, ensuring that calibration was performed on each new set of data.

Evidence of stitch induced defects were found when examining the cross sections of 2-DCS-G and 2-DCS-P composites. In Figure 5.2, obvious resin pockets can be observed around the stitch insertion points in both composites. Locations I and II mark the stitch thread insertion and exit points. As reported in the previous chapter and discussed in Chapter 2, this is to be expected when employing TT stitching that involves the insertion of two threads. Figure 5.3 shows a comparison of the average resin pocket dimensions for stitched composites. The large spread of data is due to the complex nature of the changes of tension that occur during stitch insertion, as discussed in the previous chapter. Stitch-induced voids measured in the composite cross sections were nearly twice as large in 2-DCS-G specimens, compared with 2-DCS-P. Therefore, using glass fibre stitching thread resulted in more extreme fibre waviness which introduced larger resin-filled pockets into the composite structure. It is proposed that this could be due to the combined effect of increased thread thickness and stiffness and high needle thread tension.

Since the glass fibre thread was significantly thicker and stiffer than the polyester thread, it is possible that it was less pliable during needle insertion into the preform. Therefore at locations I and II on Figure 5.2(b), the thread was inserted (or exited) at a larger angle in the cross-section which displaced the in-plane fibres more extremely. On the other hand, the more pliable and thinner polyester thread could form more easily around the reinforcement fibres at the insertion point, which were sufficiently stiff enough to lock it in place, resulting in a smaller angle. When stitching with glass fibre, adjustments to the thread tensions were made to ensure that the junction location was positioned correctly at the needle thread insertion point. However, this also means that between each successive stitch point, the needle thread is experiencing higher tension over the same stitch length as in 2-DCS-P. Therefore, due to increased pull from the previous stitch, the thread is inserted at location I and exits at location II at a lower angle.

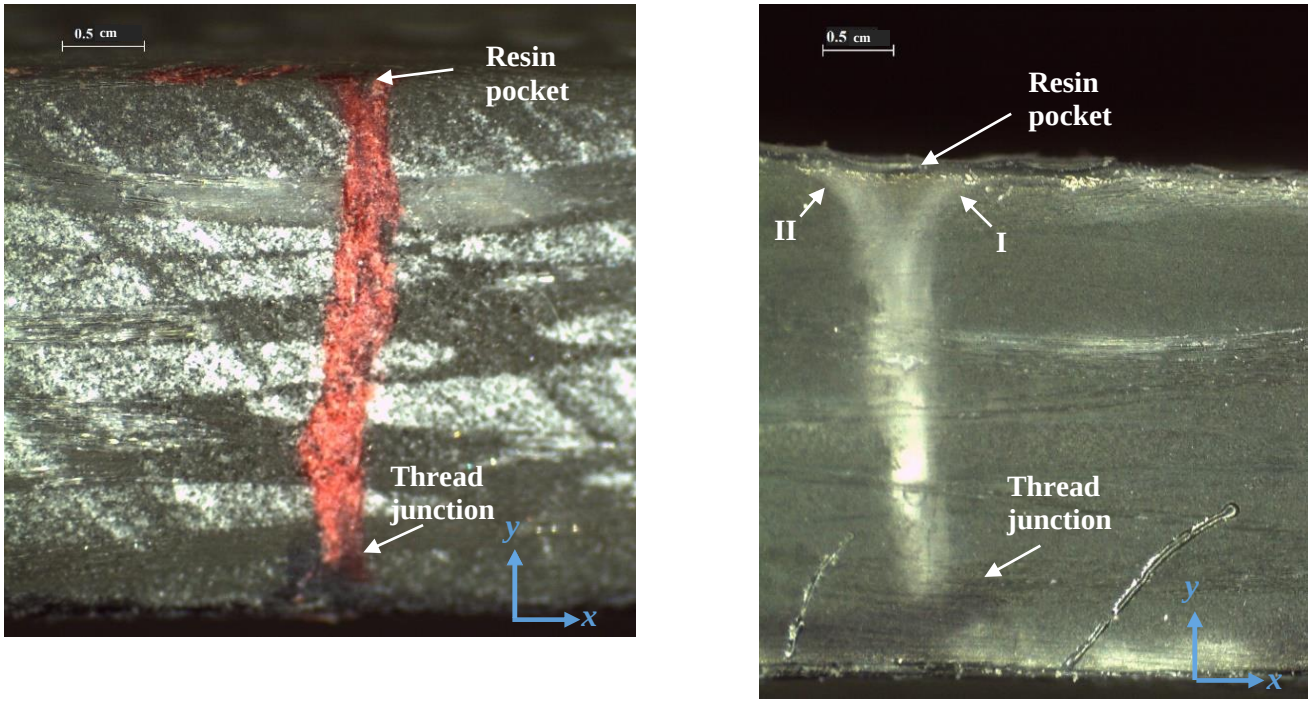

(a) (b)

Figure 5.2 (a) Micrograph of cross-sectional resin pocket for (a) 2-DCS-P; (b) 2-DCS-G composites.

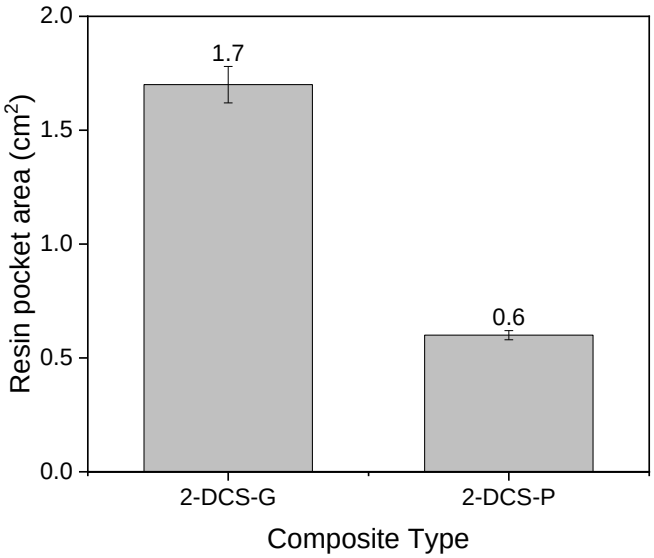

Figure 5.3 Comparison of resin pocket areas for stitched composites

5.4.2 Fibre Volume Fraction Results

To experimentally determine the fire volume fraction (FVF) of composites stitched with glass fibre (2-DCS-G), the ASTM D3171-99 standard test method for matrix burn-off was followed [166], as reported in Chapter 4. The details of the FVF method and FVF value for both 2-UNS and 2-DCS-P were reported also part of the previous Chapter 4.

In theory and based on the rule of mixtures, there is a linear relationship between in-plane composite strength and stiffness and FVF [170]. It is therefore relevant for the following discussion around tensile properties to consider the effects of stitching on the FVF because the in-plane tensile properties are dominated by the volume of reinforcing fibres. The FVF results for the stitched and unstitched composites are presented in Table 5.1. In the case of 2-DCS-P composites, the FVF was not significantly affected by the stitching, likely because of the small diameter of the polyester thread. When glass fibre stitching thread was employed (2-DCS-G), FVF was decreased by 5 % on average. The reduction in FVF of the 2-DCS-G composites can be explained by considering the composite thickness. When glass fibre stitching thread was employed, the composite thickness increased by 4.3 %, whereas there was no significant increase in the composite thickness when polyester thread was used (2-DCS-P). Therefore, since the same amount of reinforcement fibres were consolidated into all composite iterations, the increase in thickness must be attributed to an increase of volume of resin in 2-DCS-G composites, consequently leading to a reduction in FVF. To investigate this further, the fibre deviations caused by stitching must be considered. As discussed in the previous section, the fibre deviations at the stitching points for 2-DCS-G composites were larger due to the increased thickness and stiffness of the thread. It is proposed that the displaced reinforcement fibres caused more severe undulations through-the-thickness which led to the thickness of the composite plate increasing. Consequently, these areas of fibre deviation filled with resin during infusion, leading overall to larger resin pockets to form in the 2-DCS-G composites and reducing the FVF.

5.5 Tensile Properties of Stitched and Unstitched Composites

Tensile testing was conducted to investigate the mechanical properties of the stitched and unstitched composites, namely tensile strength (σ_{ULT}) tensile failure strain (ε_f) and tensile modulus (E_1). The results for these properties were subjected to an ANOVA to determine whether differences between the composite types were of statistical significance at a threshold of p<0.05. For this work, 2-DCS-G composites were tested and compared with composites from the previous chapter, 2-UNS and 2-DCS-P.

5.5.1 Protocol for Tensile Testing

The testing was carried out in-line with the industry standard ASTM D3039M [169] on a commercial INSTRON-5969 machine equipped with a 100 kN load cell in ambient conditions. The tensile test was repeated 5 times for each composite type and specimens were cut from the warp direction only due to limited specimen availability. The test parameters recommended by the standard were as follows: 2 mm/min cross-head speed, using a video extensometer with 50 mm gauge length for strain measurement and specimen dimensions of 25 mm (width) x 250 mm (length) and a gauge length of 150 mm. E was defined according to the standard as the slope between $\varepsilon = 0.1$ % and $\varepsilon = 0.3$ %. Loading was applied in the 0° direction, which was the same as the stitching direction. Tabbing was required to reduce stress concentration at the grips during testing, as described in the Chapter 4. Following tensile testing, an optical microscope was used to examine the specimen surfaces and identify the damage caused by interlaminar stitching for all stitch types.

5.5.2 Results and Discussion

The tensile properties of all stitched and unstitched composites are presented in Table 5.3 and representative stress-strain curves are presented in Figure 5.4. It is evident from that for all composite types, the loading is linear prior to sudden, brittle failure. Slight shallowing of the curve for all specimens is evident at approximately 0.2% strain. This indicates a change in modulus as a result of gradual growth of delamination and matrix cracking, before the ultimate failure point which was characterised by a loud explosive sound indicating fibre fracture and pull-out. The

shallowing occurs at the same point for both stitched and unstitched composites which suggests that stitching does not prevent the onset of damage such as ply cracking, which is in agreement with other researcher, Yoshimura and Yashiro [171].

Table 5.3 Longitudinal tensile properties of stitched and unstitched composites, standard deviation is shown in brackets.

Properties	**2-UNS**	**2-DCS-G**	**2-DCS-P**
$\sigma_{ULT}\ [MPa]$	465.4 (4.5)	466.7 (14)	449.4 (16)
$\varepsilon_f\ [\%]$	2.29 (0.06)	2.48 (0.11)	2.26 (0.05)
$E\ [GPa]$	22.9 (0.7)	20.59 (0.6)	22.4 (1.5)

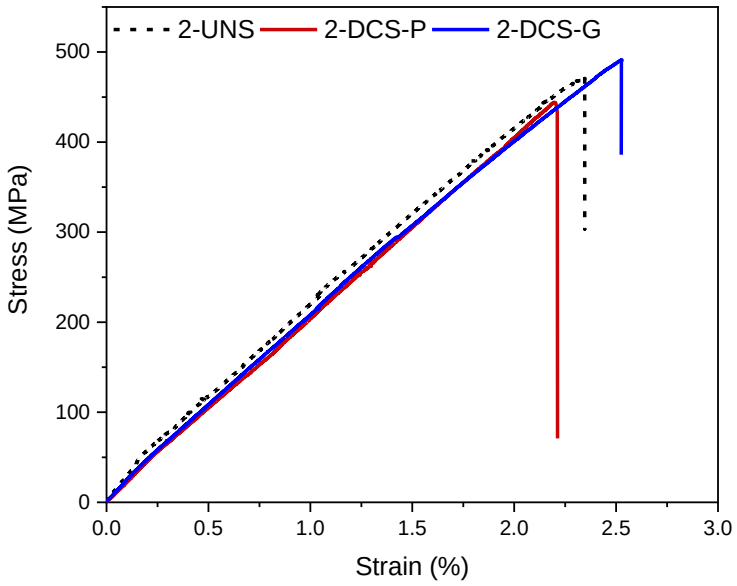

Figure 5.4 Representative stress-strain curves for stitched and unstitched composites

Photographs of the damaged cross sections and the tensile failure site of the composite specimens are presented in Figure 5.5. It is clear that 2-UNS, 2-DCS-P and 2-DCS-G composites all suffered from extensive delamination at the failure site. Similar to the case of 2-DCS-P reported in the previous chapter, post-mortem inspection of the 2-DCS-G specimens revealed that overall the tensile failure site was more confined for stitched composites. For stitched specimens the damage was more localised and the integrity of the specimens was maintained after fracture. It is also evident from Figure 5.5 that the damage was further confined by the glass fibre stitch thread (2-DCS-G), compared with the polyester stitching thread (2-DCS-P). This is likely due to the higher breaking strength of the glass fibre thread compared with the polyester thread. In 2-UNS and 2-DCS-P composites there was extensive fibre fracture and pull-out, for 2-DCS-G composites fibre pull out occurred but was highly localised and contained within the stitches. These observations indicate that while stitching does not prevent the onset of damage, ISO-401 stitching with either polyester or glass TT thread is effective in suppression of delamination and damage growth [171].

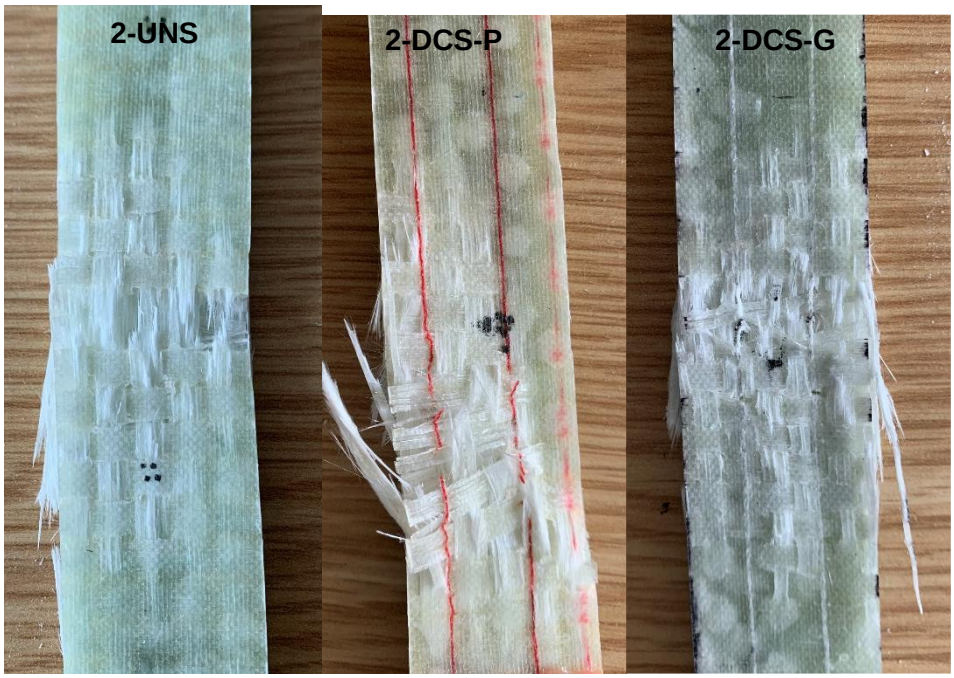

(a)

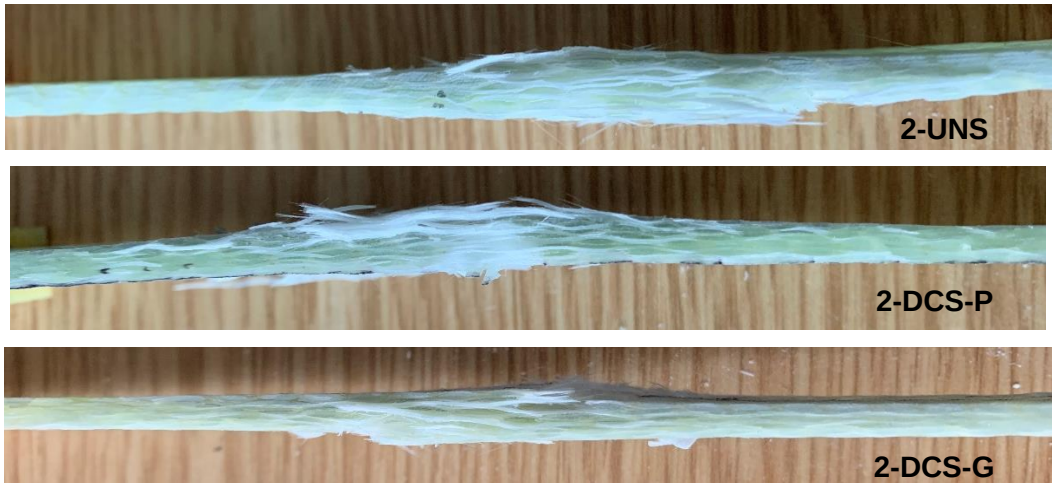

(b)

Figure 5.5 (a) Surface images of the tensile failure site; (b) cross-sectional images of the tensile failure site.

Figure 5.6 shows optical micrographs of the tensile failure site for 2-DCS-G and 2-DCS-P composites. In 2-DCS-P composites, both the needle and looper threads are fractured at the stitching junctions across the failure site. In 2-DCS-G composites, the looper threads are fractured across the failure site, whereas the needle thread is pulled out from the matrix but is not clearly fractured. Interestingly, for 2-DCS-G composites, some of the looper threads were visible at the front surface, indicating that the thread had been pulled through the thickness of the composite to the front surface by the needle thread during tensile loading. It is proposed that this is due to a combined effect of the high breaking glass fibre thread strength and the difference in thread tension. Firstly, the static needle thread tension is generally higher than the looper in ISO-401 stitching, thus there is an imbalanced pull from the needle thread on the looper thread. This is likely to be more pronounced in the junction location for stitching in this work because the needle thread tension had to be increased to place the junction at the stitch insertion site, whereas for standard ISO-401 stitching, the needle thread is secured along the bottom surface by the looper thread. Secondly, the breaking strength and stiffness of the glass fibre stitching thread is much higher than polyester thread. During loading, it is probable that the stiffer glass fibre thread debonded from the matrix and attempted to straighten in the loading direction, thus pulling the less stiff polyester thread with it, causing it to rupture. The polyester thread ruptured more easily under tension due to the imbalance of stiffness compared to the glass fibre thread. This phenomenon was not observed for 2-DCS-P composites, where both threads fractured at the corresponding surfaces because the same type of polyester thread was used for both the needle and looper threads.

Figure 5.7 shows a higher resolution micrograph of a top surface stitch point at the tensile failure site for 2-DCS-G composites, the reinforcement fibre tows have been pulled apart by the stitching threads during loading. This appears to occur locally at the fractured area, in approximately 4-6 stitch points. Referring back to Figure 5.2 which shows the consolidated composite cross section, it appears that the fractures have occurred in the specimens in regions where there is already misalignment of the tows about the stitch insertion point in an elliptical geometry. It is proposed that the observed fractures are the result of enhanced misalignment in these regions due to the pull-through of the looper thread through the composite thickness, thus parting fibres on its route.

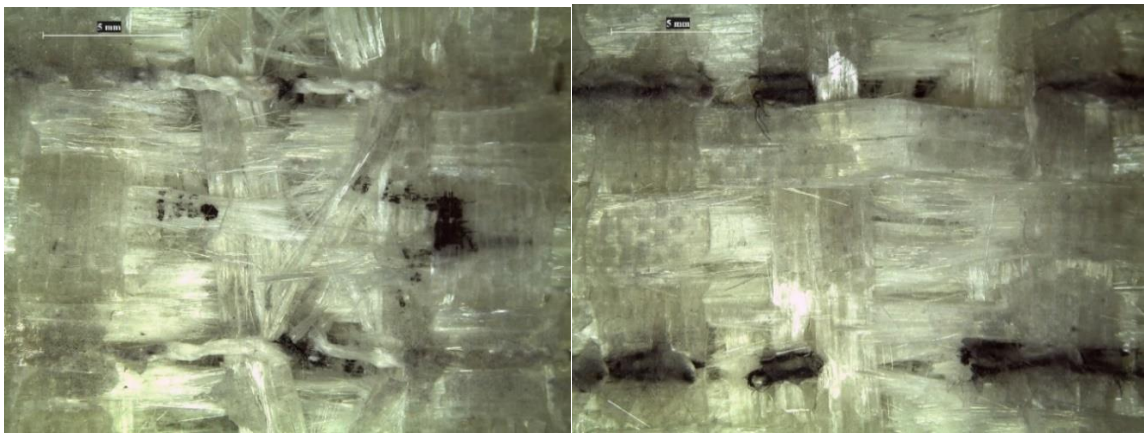

FRONT 2-DCS-G BACK

(a)

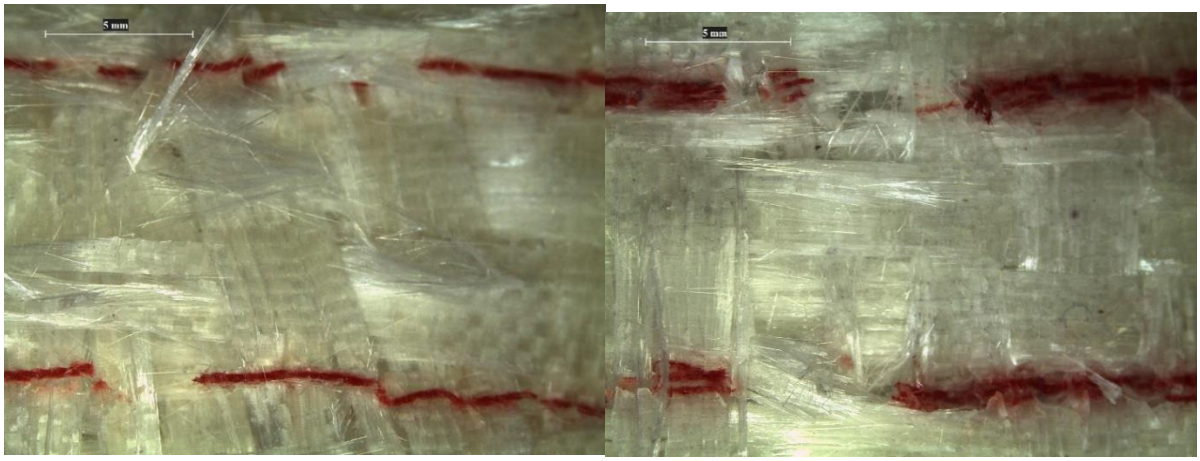

FRONT 2-DCS-P BACK

(b)

Figure 5.6 Optical micrograph of the tensile failure site (a) 2-DCS-G composites; (b) 2-DCS-P composites.

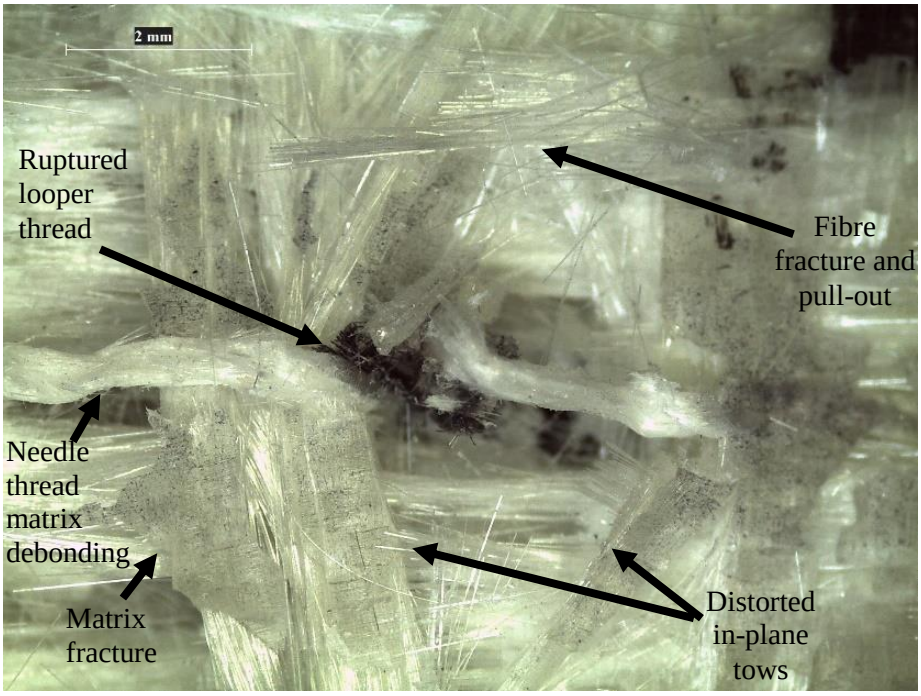

Figure 5.7 Reinforcement fibre damage around ruptured stitch threads at tensile failure point in 2-DCS-G.

The **tensile moduli** for 2-UNS, 2-DCS-G and 2-DCS-P were calculated as 22.9 GPa, 20.59 GPa and 22.4 GPa, respectively. A full comparison of the tensile moduli of all specimens is presented in Figure 5.8. Comparing the 2-UNS and 2-DCS-P composites, the tensile modulus was reduced slightly by 2.2 %, though this does not reach statistical significance, as reported in the previous chapter. However, for 2-DCS-G, the tensile modulus was reduced by 10 % which is deemed to be of statistical significance (p<0.05). Additionally, as discussed earlier, FVF was reduced significantly by 5 % for 2-DCS-G composites due to the increase in composite thickness as a result of the stitch induced resin pockets. Also, the resin pockets were measured to be larger on average compared with 2-DCS-P composites (Figure 5.3). As tensile modulus is dependent upon the volume of in-plane fibres and their orientation, the in-plane tow waviness was detrimental enough to lead to a more significant reduction in tensile modulus for 2-DCS-G [17]. Other researchers [4] have similarly found a strong positive correlation between reinforcement fibre waviness angle, induced by stitching resin pockets, and reduced tensile modulus.

In 2-DCS-P composites, the thread was much finer, causing less disturbance and deviation of the in-plane tows, which therefore did not have a significant global impact on the tensile modulus because. However, it is of note that although 2-DCS-G composites had a lower modulus,

reductions below 5% are considered modest in the literature [17,159] and indicate minimal reinforcement fibre deviations. Furthermore, the detrimental effects of stitching on the in-plane properties have been reported to be as high as 20% [17], which is much higher than found in this case. While it is a common assumption that thicker TT thread is not desirable due to the structural geometrical defects it can induce [107], it is proposed here that the glass fibre thread was still sufficiently small enough to not cause extensive damage as the modulus was only moderately reduced.

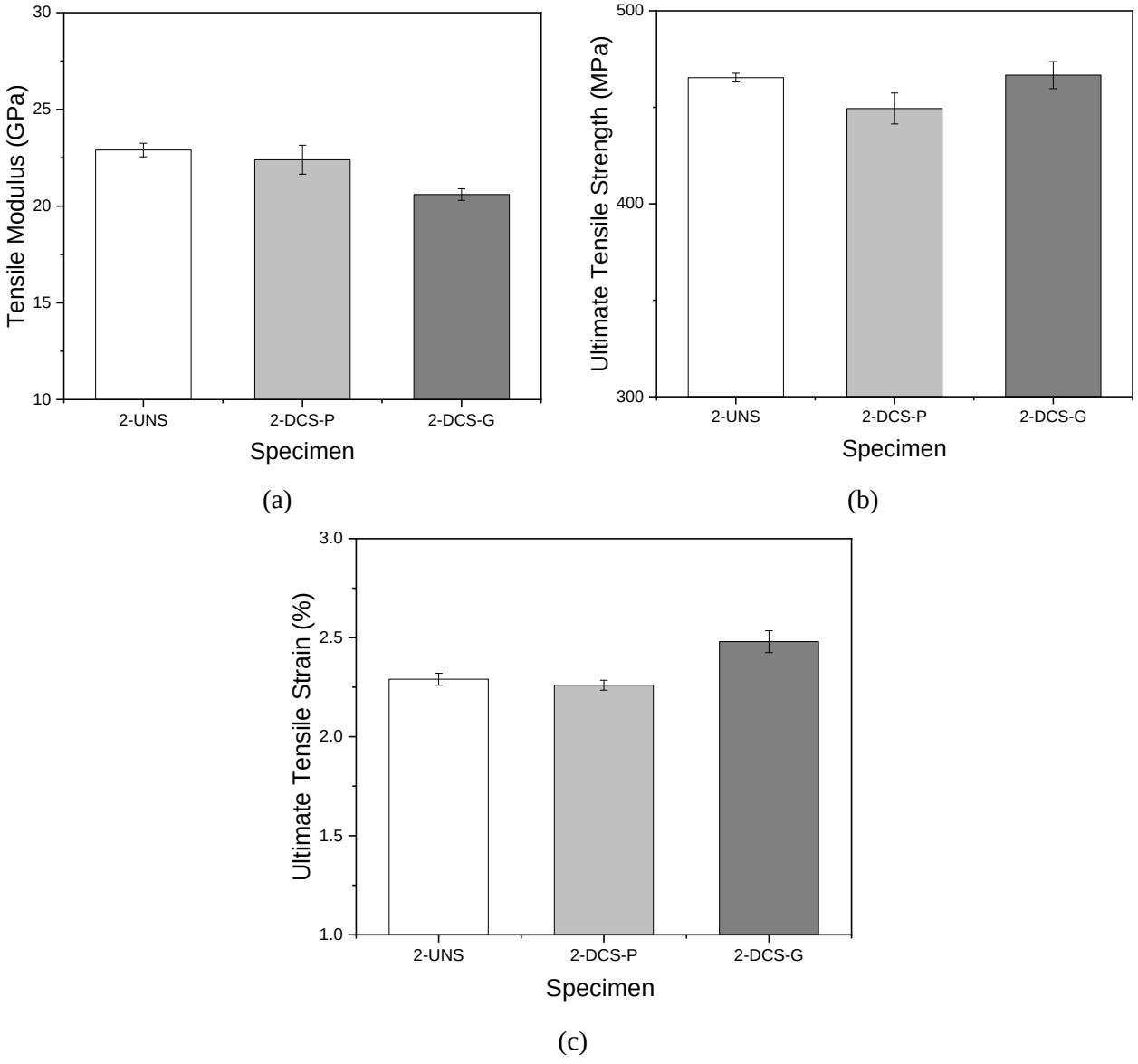

Figure 5.8 (a) Young's modulus; (b) ultimate tensile strength; (c) strain to failure.

The **tensile strengths** for 2-UNS, 2-DCS-G and 2-DCS-P were 465 MPa, 467 MPa and 449 MPa respectively. A comparison of tensile strength values is presented in Figure 5.8. The 2-UNS and 2-DCS-G composites have similar tensile strength properties but for 2-DCS-P the strength was slightly reduced, though this did not reach statistical significance. When stitching does reduce tensile strength, it can be attributed to fibre breakages caused by the stitching process [2]. Although fibre breakages are predicted to have occurred in both 2-DCS-P and 2-DCS-G composites, it is proposed that these effects were more substantial in 2-DCS-P samples due to the type of stitching thread used, thus causing a reduction in tensile strength. It is hypothesised that for 2-DCS-G composites, more energy was dissipated through stitch thread rupture, compared with 2-DCS-P, as the glass fibre stitching thread was more stiff than the fine polyester thread. Therefore, any stitch-induced geometrical damage to the 2-DCS-G composites, such as fibre breakages, were not severe enough to reduce the load bearing capacity of the in-plane tows significantly and instead the contribution of stitch thread rupture as a damage mechanism helped to preserve the tensile strength. Whereas, in 2-DCS-P composites, the stitch-induced damage was not counter-balanced by energy dissipated through fracture of the weaker polyester thread. Additionally, employing glass fibre thread caused a reduction in FVF for 2-DCS-G, yet it is demonstrated here that this did not have a significant effect on the tensile strength, despite being a fibre-dominated property. Thus, strengthening the hypothesis that the stitch thread rupture contributed significantly as a damage mechanism in 2-DCS-G composites to override the effects of stitch-induced damage.

The **tensile strains** at failure for 2-UNS, 2-DCS-G and 2-DCS-P were found to be 2.29%, 2.48% and 2.26%, respectively; a comparison of the tensile strain values for all specimens is presented in Figure 5.8. The 2-UNS and 2-DCS-P composites had similar tensile strain values whereas when glass fibre stitching thread was employed (2-DCS-G), the tensile strain was 8.3 % higher, which is statistically significant (threshold of $p<0.05$). It is suggested that the 2-DCS-G composite toughness has increased as the glass fibre stitching threads were more effective in suppressing the crack growth and extension of delamination during loading, compared with the polyester stitched composites [171]. As discussed in the paragraph above, it is considered that breakage of the stitching threads under loading absorbs some energy and can be considered a damage mechanism for stitched composites. Thus, it is proposed that the contribution of glass fibre stitch thread rupture as a damage mechanism has helped to absorb more energy during loading and improve the strain to failure of 2-DCS-G composites compared with 2-DCS-P and 2-UNS composites, due to high strength of the stitching thread.

5.6 Damage Tolerance of Stitched and Unstitched Composites

To determine the damage tolerance of both stitched and unstitched composites, specimens were subjected to impact and compression after impact (CAI) testing.

5.6.1 Impact Testing Protocol

For this work, impact testing was carried out on 2-UNS and 2-DCS-G composites. The impact response of both stitched and unstitched composites were compared to determine the effects of the stitching on the impact properties and damage response. The composites were characterised in terms of peak force, energy absorption, maximum displacement, delamination area and dent depth. The results were subjected to an ANOVA to determine whether differences between the composite types were of statistical significance at a threshold of $p<0.05$. Statistical analysis was conducted in OriginPro 2019b software.

The impact testing was conducted according to the modified ASTM D7136M standard, as proposed by Prichard and Hogg [6]. The modified test was first designed at Queen Mary University, Westfield College and is often referred to as the QMW test. The test enables miniaturised samples to be tested which is beneficial as all of the specimens can be cut from the same panel, thus reducing the scatter in data caused by variation of the FVF between composites.

The testing was carried out on an Instron CEAST 3950 drop-weight impact machine with a hemispherical impactor tup of weight 5.020 kg. The specimen dimensions were 89 mm x 55 mm. The composites were subjected to impact energy levels of 2.5 J, 5 J and 7.5 J, the impactor velocities were 1.6 m/s, 2.2 m/s and 2.7 m/s respectively. Five samples for each composite type were tested per energy level. The specimens were supported during the test by an aluminium test rig with a 40 mm central circular window to allow contact with the tup but prevent excessive bending of the composite during impact. To prevent secondary impact of the samples during testing, an automatic anti-rebound system was employed. To investigate the impact damage, non-destructive tests (NDT) were performed, prior to compression; measurement of post-impact dent depth, visual observation of the top and bottom surfaces and ultrasonic C-scan.

When composite structures are subjected to low velocity impact, the resultant damage is often characterised by being barely visible at the surface, yet more severe internal damage and backside fibre fractures may be sustained [60,172]. The post-impact dent depth measurement is used as a common method of quantifying the surface damage sustained, even though there may not be

significant visual evidence of a surface dent to the naked eye i.e. BVID (barely visible impact damage). Post-impact dent depth was measured using a depth micrometre. The dent depth measurement was taken immediately after impact to ensure any relaxation effects were negligible.

To investigate and quantify the internal impact damage, the specimens were subjected to ultrasonic C-scan. The specimens were scanned using the Midas, UK ultrasonic C-scanning system. The same scanning conditions were used as in Chapter 3, with the machine being calibrated before each use. From the C-scan images, damaged areas were measured using the measurement tool in the Midas, UK software.

5.6.2 Low Velocity Impact Results and Discussion

A summary of results from the low energy impact testing are presented in Table 5.4, Figure 5.12, Figure 5.13 and Figure 5.14. For both stitched and unstitched composites it is evident that the peak force and absorbed energy have a linear relationship with impact energy. After the initial drop in force, all composites experience an increase in force until the peak force is reached, after which, more significant damage occurs in the form of fibre fracture and shearing, along with matrix cracking and delamination. This is evidenced by the continued drop in load after the peak force has been reached [130]. The results indicate that there are some differences in the impact response of 2-DCS-G and 2-UNS composites, these are covered in detail in the below discussion.

Table 5.4 Average peak force and absorbed energy levels for ISO-401 stitched and unstitched composites, standard deviations are included in brackets.

	Impact energy (J)	**Peak force (kN)**	**Max. dent depth (mm)**	**Absorbed energy due to damage (J)**	**Damaged area (mm^2)**
2-UNS	2.5	2.77 (0.03)	1.52 (0.01)	1.04 (0.08)	177.72 (7.1)
	5	3.67 (0.03)	2.24 (0.01)	2.31 (0.09)	396..5 (18.2)
	7.5	4.67 (0.07)	2.72 (0..07)	3.72 (0.20)	523.7 (38.1)
2-DCS-G	2.5	2.88 (0.06)	1.49 (0.02)	1.17 (0.15)	104.38 (17.8)
	5	3.86 (0.08)	2.2 (0.04)	2.20 (0.05)	274.96 (36.2)
	7.5	4.74 (0.06)	2.73 (0.06)	3.47 (0.14)	445.1 (14.6)

5.6.2.1 *Physical Examination*

The impact damaged area for all impact energies did not reach the test rig boundary, therefore the damage sustained by the specimens was a result of the composite damage mechanisms and was not constrained by the test rig in any way. This is important because when damage spreads past the test boundary, it is possible that the rig has influenced the damage response. The visibility and spread of damage is of interest in stitched composites as TT stitching is widely considered to improve the impact damage response. Low-velocity impact damage modes in FRP composites are complex and can manifest through multiple mechanisms, including interlaminar delamination, intralaminar matric cracks, fibre pull-out and fibre rupture [54]. Damage modes can be identified at the specimen surface through optical microscopy techniques and visual inspection. Examination of the impacted specimens revealed that besides some expected indentation at the impacted surface, internal barely visible impact damage (BVID) was the dominant failure mode, which is typical for low-velocity impacts.

The impact damage for stitched composites was less severe and visibly more confined compared with corresponding unstitched specimens. Upon close inspection, evidence of matrix debonding, edge delamination and surface indentation was present for all composite types and additionally for stitched composites, stitch-matrix debonding. The identifiable damage was most severe at the

highest energy level, 7.5 J. Figure 5.9 presents photographs of 7.5 J impacted specimens. At each energy level, no surface damage was detected on the back surface of the composites. For both stitched and unstitched composites impacted at 2.5 J, no front surface damage was detected other than the dent from the impactor [54]. For higher impact levels of 5.0 J and 7.5 J some matrix debonding is observed on the front surface of the 2-UNS and 2-DCS-G specimens. As can be seen, matrix debonding was more extensive in the 2-UNS composites, suggesting that TT stitching has reduced the propagation of matrix damage.

For stitched composites, it was found that under all impact energies, the stitching threads were still intact post-impact and did not appear to have been ruptured at the surface. It is possible that stitches appear in-tact on the surface but have ruptured internally, in this case it is possible that the impact energy was not high enough to rupture the threads. As the stitching threads were not fractured during impact, it is proposed that some energy would have been absorbed through the additional damage mechanism of stitch-matrix debonding (identified in Figure 5.9), which is reported by other researchers [28].

Under all energy levels and for both composite types, there was a small region identifiable at the impacted point which did not suffer from delaminations or extensive cracking. This is visible in Figure 5.8 and can also clearly be seen in the c-scans in Figure 5.10 where there is a lighter area inside of the darkened border region, indicating little damage has occurred. This is known as the impact-compression zone which is considered to be free of delamination. This is an area of low shear which experiences compression during the impact event and thus delaminations do not spread from here, instead they accumulate from its boundary. The stitching does not appear to prevent the edge delaminations from forming, which is consistent with other researchers [54].

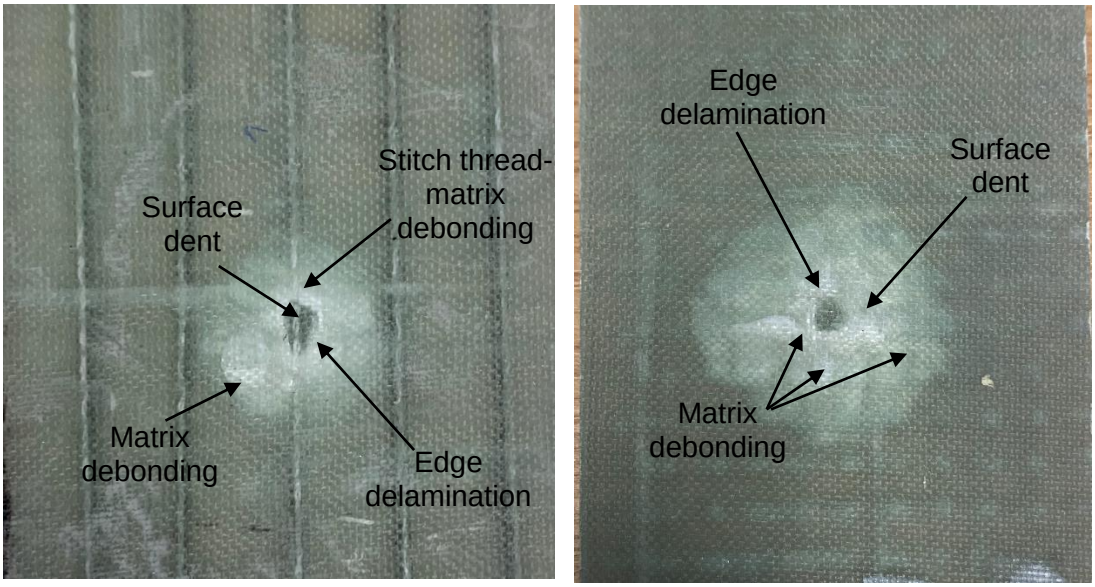

(a) (b)

Figure 5.9 Images of typical surface impact damage at 7.5J; (a) 2-DCS-G front surface; (b) 2-UNS front surface.

5.6.2.2 *C-Scan and Dent Depth Analysis*

The extent and modes of composite damage can be assessed by combining techniques such as dent depth analysis and projected damage areas measured by C-scan. As shown in Table 5.4, the dent depths for 2-UNS and 2-DCS-G are comparable, showing that TT stitching has not impeded the penetrating damage from the impactor, which has also been found by other researchers [54,84]. Stitching can increase the penetration depth [61], which is arguably an undesirable side effect of stitching as the composite is then at risk of full TT penetration which may contribute to considerable reduction in damage tolerance. This can occur as a result of high stitching density [54] or higher impact loads [84]. However, in this case stitching did not cause damage to travel completely through the thickness of the structure, which is desirable.

Despite 2-UNS and 2-DCS-G composites having similar dent depths, it can be seen in Figure 5.10, Figure 5.11 and Table 5.4, this does not correspond to overall comparable internal damage for stitched and unstitched composites. The projected damaged areas for both 2-UNS and 2-DCS-G composite increase with impact energy. For 2-DCS-G composites, the damaged areas were reduced by 41 %, 31 %, and 15 % for 2.5 J, 5.0 J and 7.5 J impact energy respectively, compared

with 2-UNS composites, these results are deemed to be statistically significant (threshold of $p<0.05$). It is proposed that the TT stitching was successfully prevented the x-y (lateral) spread of delamination due to the bridging effect of the stitches, which effectively arrested cracks as they reached the stitch lines and thus suppressed subsequent damage growth [16]. Whereas for 2-UNS composites, the lack of TT reinforcement meant there was no TT bridging effect and once formed, the delamination cracks were able to propagate unimpeded [15]. The bridging effect of the stitches was enhanced in specimens that were subjected to lower level impacts, where there was a higher reduction in 2-DCS-G damaged area compared with 2-UNS. As the impact energies increase, the reduction in damaged area due to stitching become smaller. It is possible that a higher stitching density, created by employing smaller distance between successive stitch points and adjacent stitch lines, may have more effectively suppressed damage growth by creating a more tortuous path for the crack to propagate between closely placed stitch lines.

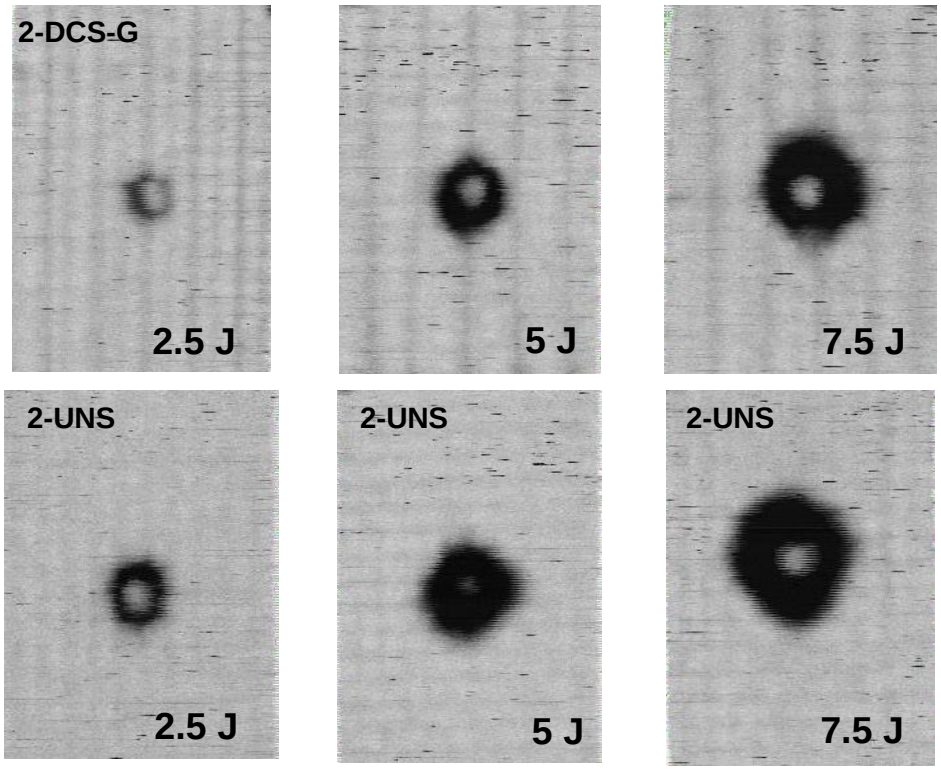

Figure 5.10 C-scan images of the projected damaged areas for stitched and unstitched composites.

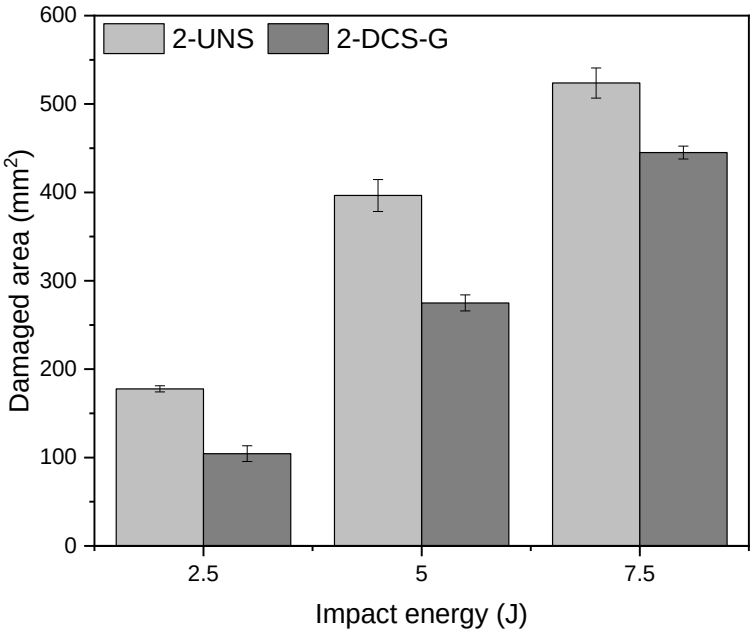

Figure 5.11 Average damaged area measured by c-scan with standard deviation.

5.6.2.3 *Low Velocity Impact Response*

Typical force-time and force-displacement curves are plotted in Figure 5.12 and Figure 5.13, both minor and major damage events can be identified from these plots. It can be seen that the 2-DCS-G composites experienced a higher average peak force at all energy levels, demonstrating overall a higher load bearing capacity compared with 2-UNS composites. The peak force increased for 2-DCS-G compared with 2-UNS composites by 4 %, 5 % and 1.5 % for 2.5 J, 5 J and 7.5 J impacts respectively. It should be noted that the 1.5 % peak force for the 7.5J was found to be statistically insignificant. The results indicate that whilst stitching has improved the damage tolerance it is less effective at higher energy levels.

A similar trend was observed when reviewing the force-displacement response in Figure 5.13. For both composite types, the maximum displacement increases with impact energy and is higher than the permanent displacement. The closed loop trace indicates partial penetration and rebounding of the impactor [128,173,174]. The loading and unloading curves are similar for both composite types indicating similar damage modes. For stitched composites subjected to 2.5 J and 5 J impacts, the permanent displacement is slightly lower than unstitched composites but for 7.5 J impacts it is comparable. As discussed earlier, the effect on stitching on reducing the delamination area was less effective as the impact energy increased. It is possible that the reason for stitching becoming less effective at higher impact energies is due to the low stitch density. It is proposed that if the density was increased, i.e. stitch space and stitch pitch closer together, the bridging effect of the stitches would have been more significant to suppress damage propagation at higher impact energy levels. The stitching density for this research was 0.025 mm^{-2}, which is considerate moderate to low compared to the literature. In [16], a high stitch density of 0.17 mm^{-2} was employed and positive correlation between peak force and stitch density was found for low velocity impact events with energy ranging between 6.7 J and 60.8 J. Stitching generally appears to have almost no effect on the maximum deformation but can withstand higher forces demonstrating the increased stiffness for stitched composites.

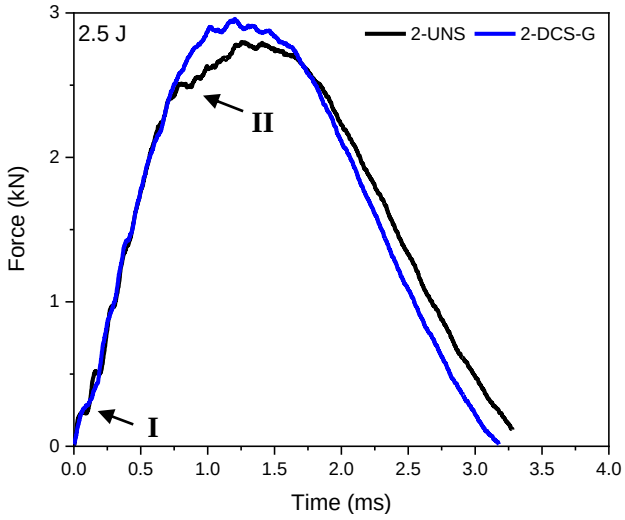

(a)

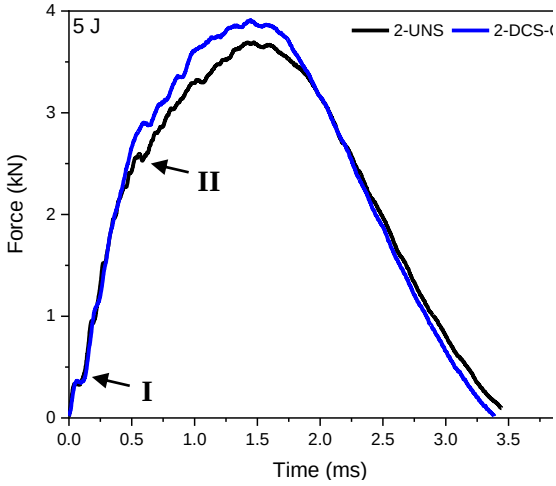

(b)

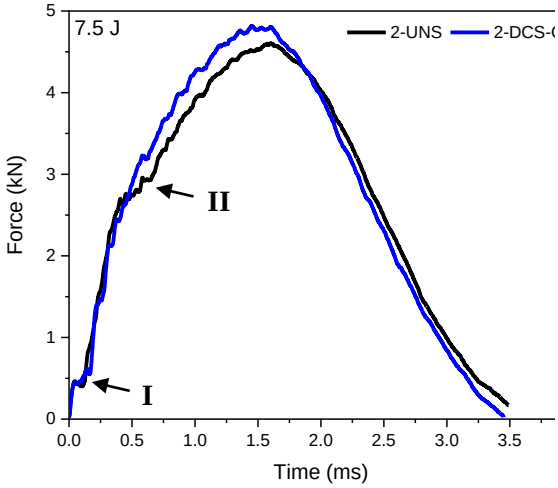

(c)

Figure 5.12 Representative force-time curves for stitched and unstitched composites arranged by impact energy level; (a) 2.5J impact; (b) 5 J impact; (c) 7.5 J impact.

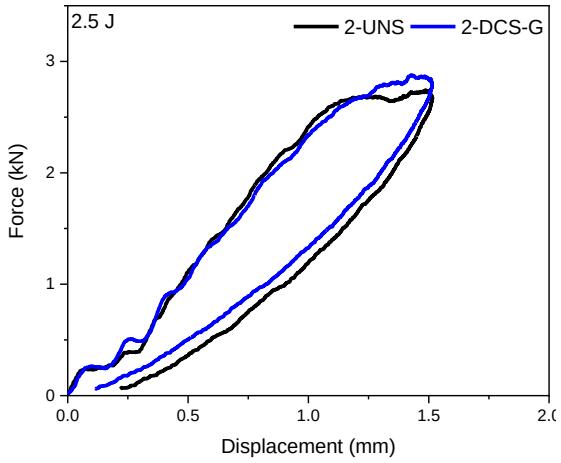

(a)

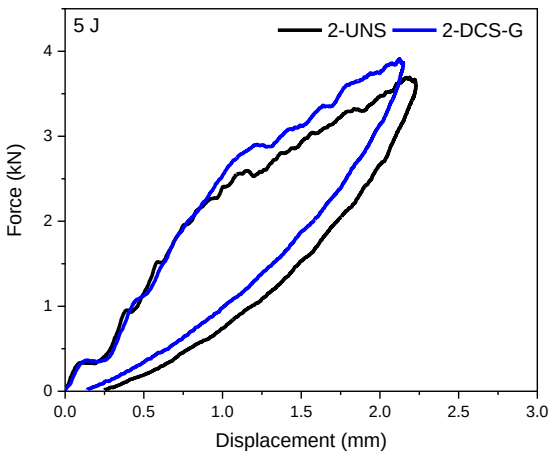

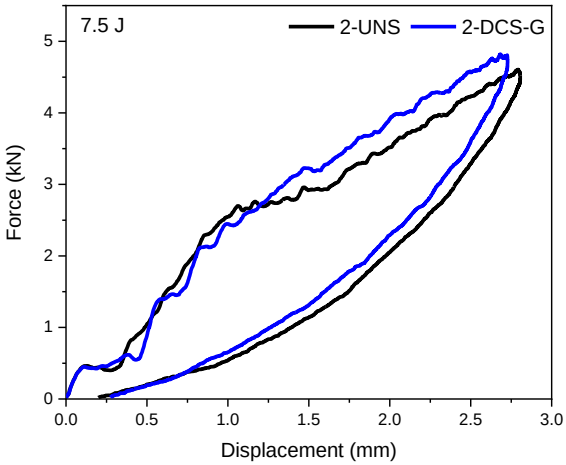

(b) (c)

Figure 5.13 Representative force-deformation curves for stitched and unstitched composites arranged by impact energy level; (a) 2.5J impact; (b) 5 J impact; (c) 7.5 J impact.

The force-time curve can be used to determine the extent of internal damage sustained by the specimens, even when the damage on the surface is found to be barely visible. It is evident from Figure 5.12 that the loading and unloading trace for 2.5 J is nearly symmetrical, indicating that significant impact damage has not been sustained [84]. In the case of 5 J and 7.5 J impact events, the unloading portion of the graph is steeper than the loading part, indicating more significant damage sustained by the material. The effect is slightly more pronounced for 2-DCS-G composites. For both composite types and at all three energy levels, there is an initial linear increase which indicates the contact between the impactor tup and the composite, where the composite briefly bends under the force of the tup [175]. Following this is a sharp drop in force which indicates the damage initiation point (location I), and inelastic behaviour, consequently resulting in a reduction in the composite stiffness due to internal delamination. This point is also known as the delamination threshold [30]. In particular, this initial damage response low low-velocity impacts is characterised by matrix damage, such as minor matrix cracking and failure at the matrix-fibre interface [28,60,176,177]. For all composite specimens, the damage initiation force has a linear relationship with the energy level. Under all impact energies (2.5 J, 5 J and 7.5 J), the damage initiation point occurs at a similar force for stitched and unstitched specimens, suggesting that the presence of TT stitching does not prevent damage from initially occurring [132]. For both composite types, small load drops can be identified at various points along the force-time trace which indicate the occurrence of matrix cracking as the dominant damage mode, as is generally expected in response to low velocity impact events. Any sharper load drops can indicate more significant damage such as fibre breakage or debonding, thus if fibre fracture did occur it is likely to have been highly localised.

At location II there is a second significant load drop which occurs at a higher impact force in 2-DCS-G composites than 2-UNS under all impact energies. All 2-DCS-G composites then experience a higher peak force compared with 2-UNS composites. Both of these observations show that stitching suppresses damage propagation during impact by creating a more torturous path for the delamination cracks to propagate via a bridging effect, despite having no effect on the damage initiation point, which is in agreement with other researchers [28,132]. In 2-UNS composites, the delamination damage can spread unimpeded as there is no TT reinforcement. This is also evident from Figure 5.13 where 2-DCS-G composites demonstrate a stiffer response, compared with 2-UNS composites.

Figure 5.14 shows the absorbed energy-time behaviour of the impacted composites. The peak force is equivalent to the prescribed impact energy. The velocity of the impactor decreases upon

contact with the composite and the impact energy is absorbed through various damage modes and elastic energy, which is stored and released through bending of the composite and rebounding of the impactor. The dominant damage modes in both composite types were mainly internal matrix cracking and delamination, which is in line with expectations for low velocity impact [16,28]. The absorbed energy of 2-DCS-G and 2-UNS composites were similar for all impact energies meaning that both composite types absorbed the same amount of energy through damage, but it is likely that the energy is absorbed through the sustenance of different damage modes of varying severity in the different composite types; for example, it is likely that for the stitched composites, additional energy would have been absorbed through the damage mode of stitch-matrix debonding, leading to less energy dissipation through more critical damage modes like delamination.

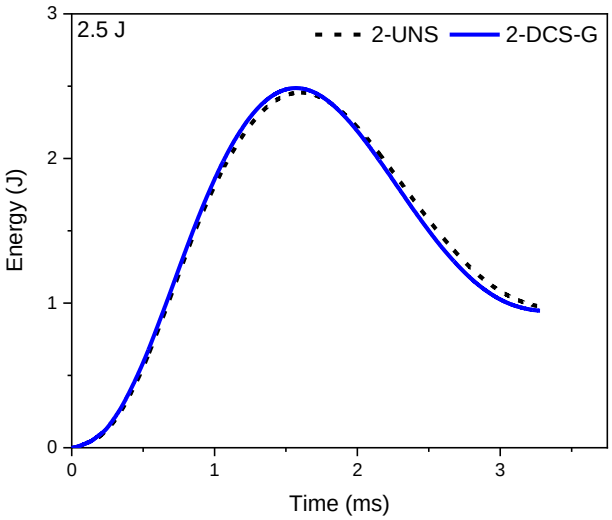

(a)

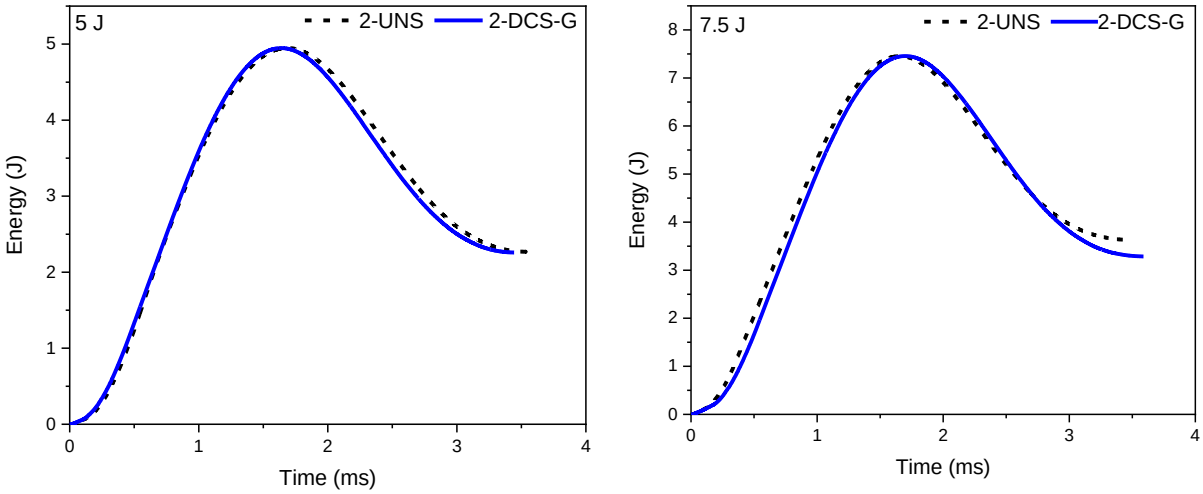

(b) (c)

Figure 5.14 Absorbed energy for stitched and unstitched composites arranged by impact energy level; (a) 2.5J impact; (b) 5 J impact; (c) 7.5 J impact.

5.6.3 Compression After Impact Response Testing Protocol

To understand the effect of ISO-401 stitching on the post-impact composite behaviour, CAI (compression after impact) testing was conducted. The impacted samples from the above discussion were compared with undamaged equivalent specimens subjected to compression loading. The results are discussed with respect to the existing impact damage, the internal fibrous structure and the known defects introduced by TT stitching.

For CAI testing, the QMW method was followed, as in [6]. An Instron 5989 test frame with fixed parallel plates was used for testing, as shown in Figure 5.15. The test parameters were as follows: 100 kN load cell, loading rate of 0.5 mm per minute until coupon failure. Composite specimens were placed in an anti-buckling test rig designed to prevent Euler buckling occurring during compression and thus lead to compressive failure that is a result of the fibrous structure, fibres properties and any defects present. The specimen is supported both at the sides, at the top and the bottom by pin guides. After the specimen was inserted into the rig, the guides were fastened gently to ensure they were pressed against the sample to prevent twisting during the test but taking care not to over-constrain the sample.

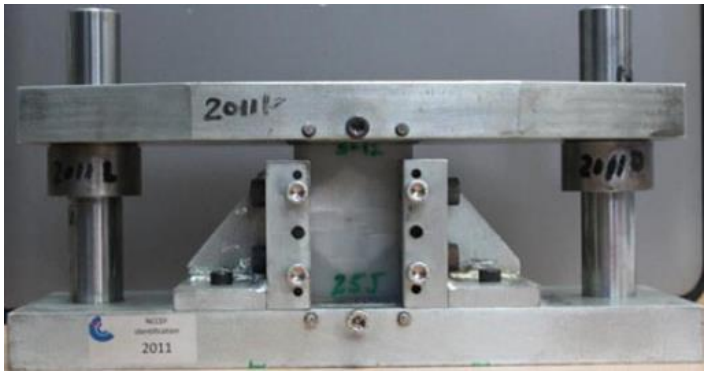

Figure 5.15 Photograph of the anti-buckling test rig developed for the CAI testing of small composites at The University of Manchester [8].

5.6.4 Results and Discussion

Typical compressive stress-displacement curves are presented in Figure 5.16 for impacted and un-impacted specimens. Any initial low gradient slope is a result of the specimen not being in full contact with the specimen fixture and should not be considered to be a characteristic of any material property. The loading curves for both stitched and unstitched are linear until the peak where catastrophic failure occurs. Throughout the test for both unstitched and stitched composites, occasional cracking was audible relating to localised matrix fractures emanating from the damaged fibres in impacted specimens, indicating gradual failure effect. Close inspection of the curves in Figure 5.16 reveals that the peak curve for undamaged 2-DCS-G, 2-DCS-G 7.5 J and 2-UNS 7.5 J is slightly softened, this indicates more extensive gradual damage occurred in these composite types. All of the specimens included in this discussion, impacted or non-impacted, failed in the centre of the specimen and not at the loading edges. Edge failure can be indicative of extensive pre-existing defects in the composites, likely caused during the manufacturing process and thus these few specimens were not included in this discussion.

The average compressive strengths of the tested composites are presented in Table 5.5 and Figure 5.16. The CAI strength for the stitched and unstitched composites decreased with increasing impact energy, this is due to the increasing amount of damage caused by the prescribed impact. After impact, the delamination damage in the composites acts as an initiation point for kink band formation and further propagation of delamination under compressive loading. Thus, damage propagates more easily in composites with pre-existing impact damage compared with undamaged specimens. The ultimate compressive failure was characterised by a loud and explosive sound which was caused by the rupturing of in-plane fibre tows and catastrophic delamination emanating from the broadening of kink bands. Inspection of the failed specimens revealed that delaminations spread horizontally across the width of the laminate, eventually causing ultimate failure [80,124]. Minimal delamination growth was observed in the loading direction [126].

The scatter of CAI strength data for stitched composites is smaller than that for unstitched composites, which is in agreement with other researchers [107] and can be attributed to the restriction in delamination growth offered by the stitches. From Figure 5.17, it is shown that the compressive strength 2-UNS undamaged composites is on average 4.7 % higher compared with 2-DCS-G undamaged composites. Though it should be noted that this difference was not statistically significant at a threshold of $p<0.05$. The compressive strength of undamaged composites is considered to be a function of the waviness of in-plane tows in the loading direction [8]. Considering that stitching was found to cause geometrical defects in the composite cross-

sections, as shown earlier in Figure 5.2, it is proposed that any reduction in compressive strength for 2-DCS-G composites is due to some stitch-induced waviness of the load bearing tows which acted as initiation sites for kink band formation [25].

Table 5.5 The impacted and non-impacted compressive strengths of stitched and unstitched composites, standard deviation shown in brackets.

		Compressive strength (MPa)		
Specimen	**Undamaged**	**2.5 J**	**5.0 J**	**7.5 J**
2-UNS	212.2 (13.5)	198.2 (10.2)	146 (7.7)	142.4 (4.4)
2-DCS-G	202.2 (12.7)	201.2 (1.6)	165.1 (5.4)	152.7 (7.6)

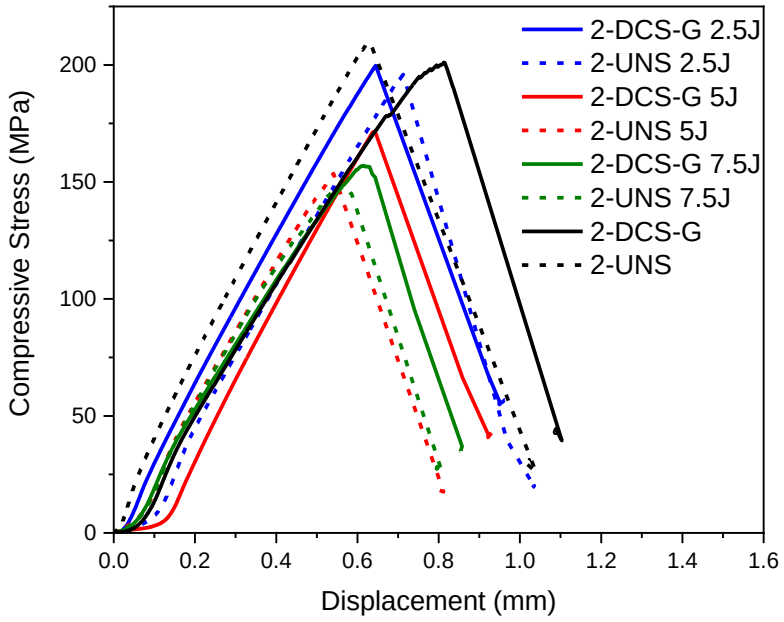

Figure 5.16 Typical compressive stress-displacement curves for stitched and unstitched composites.

It was found that the compressive strengths of 2-UNS and 2-DCS-G composites with an impact energy of 2.5 J were similar, which is an interesting finding considering that referring back to

Figure 5.11, the initial impact damage area was considerably smaller (-41 %) for 2-DCS-G composites. This suggests that although damage propagates from the weak resin rich areas around the stitch threads during compressive loading, it is somewhat counterbalanced by the bridging effect of the stitches on the damage that is propagating laterally from the original impact area. Therefore, in stitched composites with smaller damaged areas, the stitch induced defects had a more adverse impact on the compression properties. It is possible this is due to the fact that delamination travelling from the small impacted area under compressive loading is already extensive before it reaches the boundary of the stitch lines and therefore cannot be well-contained by the stitches.

Conversely, for 5.0 J and 7.5 J impacts, there was a non-significant trend of higher compressive strength for 2-DCS-G composites compared with 2-UNS composites. The increases were 13.1 % and 7.5 % higher on average for 5.0 J and 7.5 J impacts. This improvement can be attributed to the bridging effect of the stitching threads [107,127]. During compressive loading, the stitches were able to arrest and delay delaminations propagating rapidly from the damaged area more significantly compared with 2.5 J impacted 2-DCS-G composites and unstitched composites, while in 2-UNS composites, delamination spread through the structure unimpeded from the site of impact, thus reducing the compressive strength. Despite the increase of CAI strength on average for specimens with 5.0 J and 7.5 J impacts, the difference compared with 2-UNS composites was not found to be significant, it is proposed that this is due to the stitch density. It has been found that when stitching with a moderate density, such as the density used in this study, the fibre bridging is less effective because the stitches are positioned too far apart to prevent damage propagation. Instead, local buckling can occur between the stitch lines resulting in similar CAI strengths to unstitched equivalent composites [107]. Therefore, in the context of this study, increasing the stitch density has the potential to improve the damage tolerance effects of the ISO-401 TT stitching further.

The residual compressive strength was obtained from normalising the compressive strength of damaged specimens as a function of the undamaged equivalent composites, as in Figure 5.17. For 2-UNS and 2-DCS-G specimens, the residual compressive strength is shown to reduce with increasing impact energy. However, for 2-DCS-G composites, the retention of compressive strength is improved compared with 2-UNS composites. It is proposed that this is due to the combined effect of the smaller impact damaged area seen in 2-DCS-G composites, the fibre-bridging effect of the stitches during compression loading and debonding of stitches as an additional energy-absorbing damage mechanism.

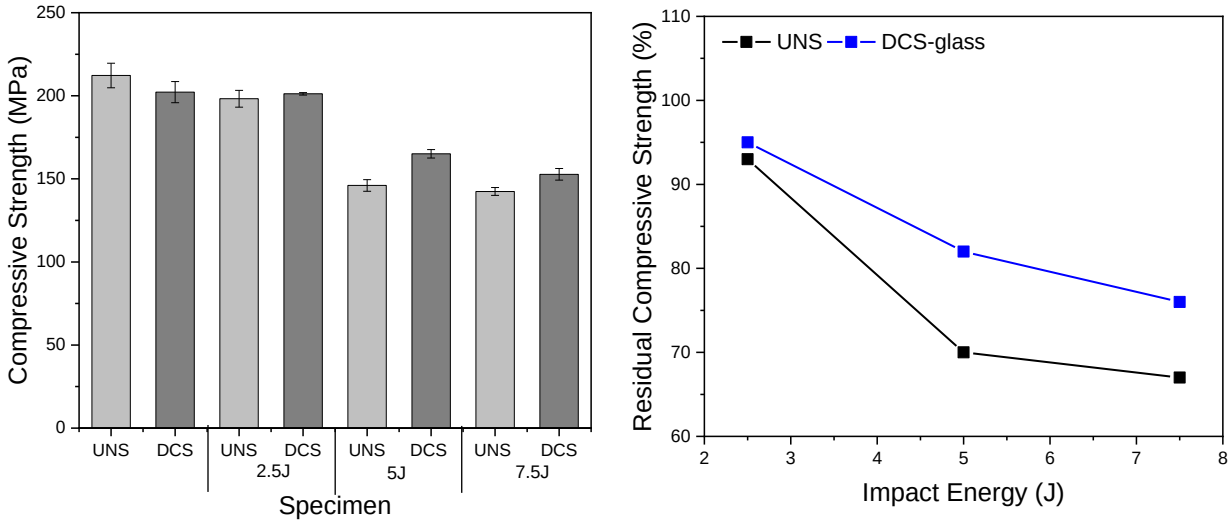

(a) (b)

Figure 5.17 (a) Comparison of compressive strength of unstitched and stitched composites; (b) residual strength of stitched and unstitched composites.

Micrographs showing the damage modes for stitched and unstitched composites, which have been subjected to 2.5 J, 5.0 J and 7.5 J impact, followed by in-plane compression until failure, are presented in Figures 5.18-20. It is evident that the compression damage modes were influenced by the impact damage as the compression failure delamination occurred on either side of the impact site, as shown in Figure 5.19. In both stitched and unstitched composites, energy dissipation has occurred through a mixture of damage modes including fibre splitting, fibre kinking, matrix cracking and delamination and additionally for stitched composites, stitch thread-matrix debonding. The compression damage was less severe in 2-DCS-G composites compared with 2-UNS at all impact energy levels.

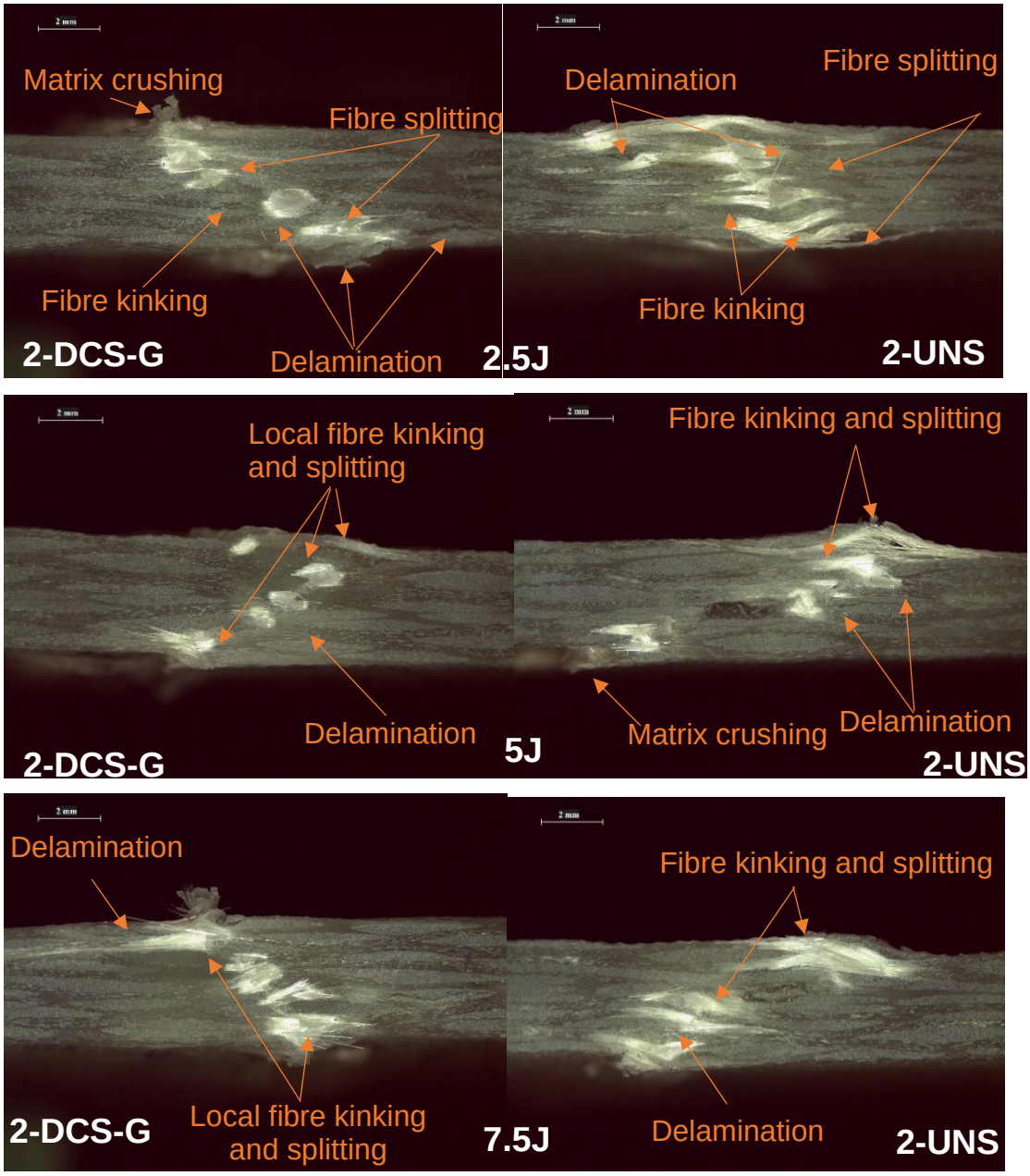

Figure 5.18 Optical micrographs of the edge cross sectional damage for stitched and unstitched specimen, arranged by impact energy level.

In 2-UNS composites, the damage was dominated by global fibre kinking and delamination, whereas in 2-DCS-G composites, fibre kinking was less severe and more localised between the stitches. In Figure 5.18, fibre kinking is less obvious in the cross-sections for 2-DCS-G composites at all energy levels and more fibre splitting is present, for 2-UNS composites global buckling of the fibres is present at every energy level. In Figure 5.19, the fracture pattern reveals kinking of the reinforcement tows and subsequent tow fracture is localised between the stitch lines. This is likely due to the fact that moderate stitch density was employed and the kink banding could spread rapidly between the stitch lines; the effect may have been less severe if the stitch lines were closer together. However, it is clear that the TT stitching in ISO-401 formation was able to offer some fibre bridging to prevent the spread of delamination and severity of fibre kinking during compression. In Figure 5.20, evidence of stitch bridging and localised kinking is observed for 2-DCS-G composites, while global kinking is seen for 2-UNS composites. At all energy levels in 2-DCS-G composites there was evidence at the specimen surface of stitching arresting the spread of damage and also of matrix cracking around the resin rich points. It is important to note that the stitch threads, from optical microscopy of the specimen top and bottom surfaces, appeared to remain intact and have not fully ruptured during compressive loading. Figure 5.20 shows intact stitching threads at the surface of 2-DCS-G 7.5 J impacted composites after compressive failure.

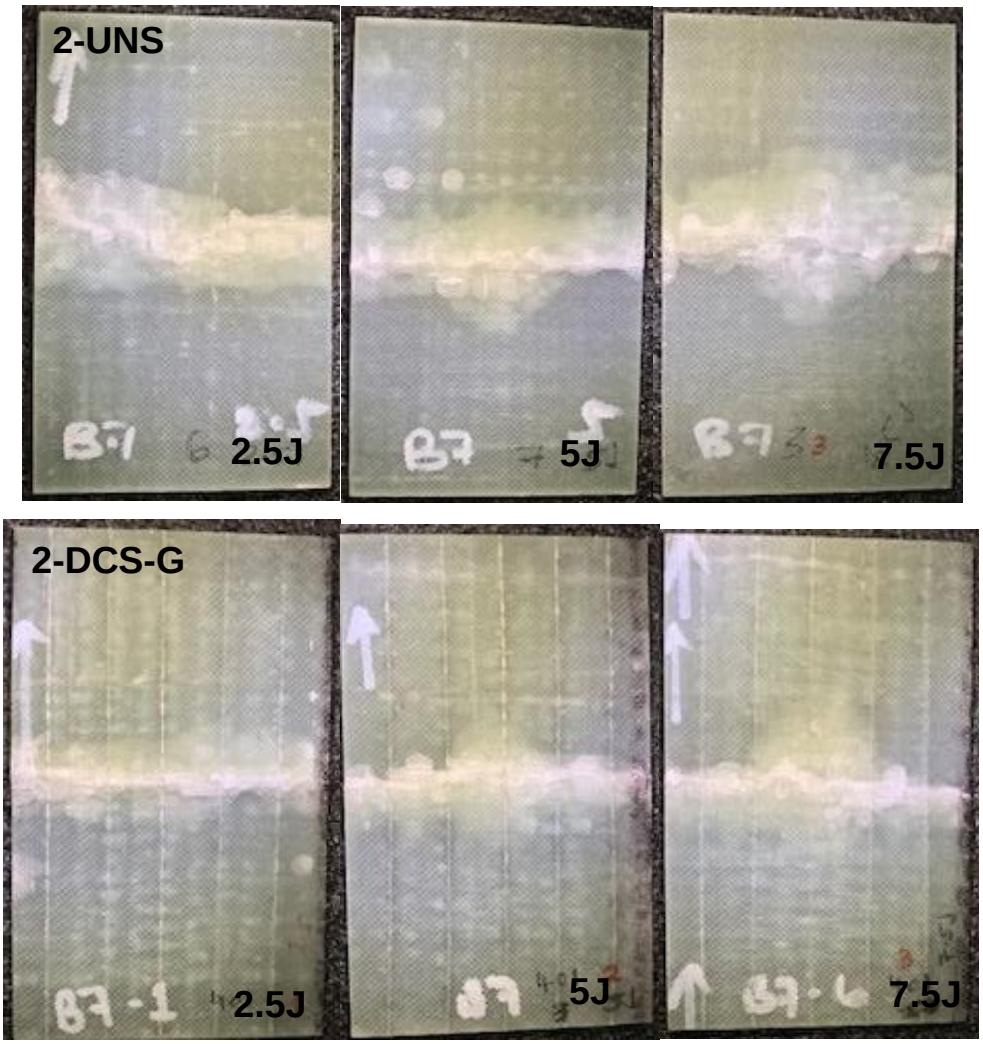

Figure 5.19 Surface images of the compression failure sites for both stitched and unstitched composites organised by impact energy.

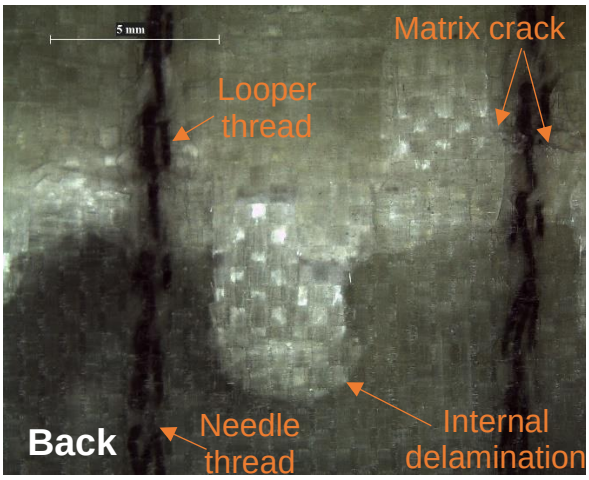

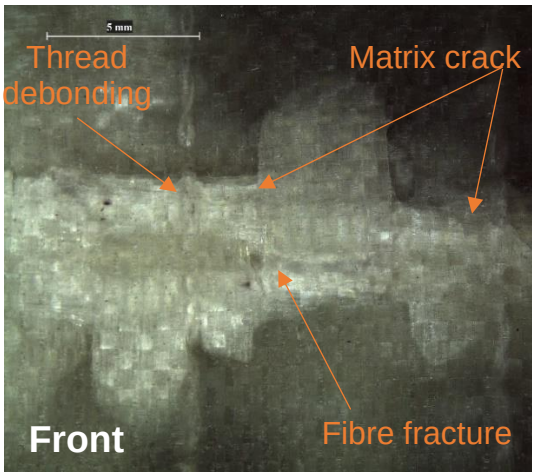

Intact stitch threads on both front and back surfaces

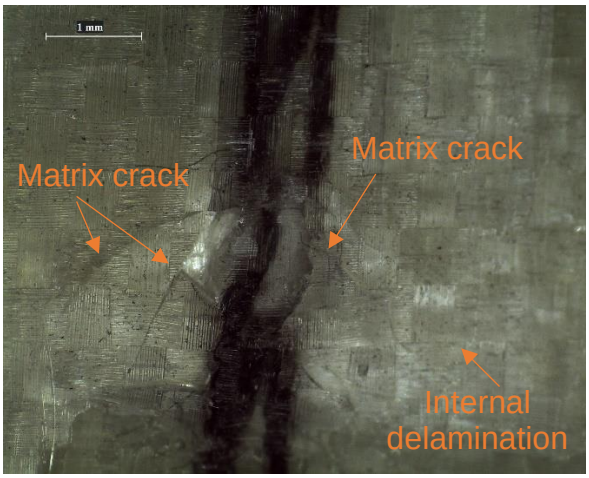

Evidence of matrix cracking around stitch point

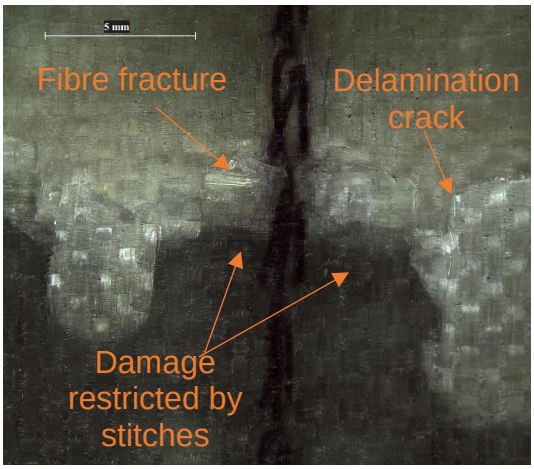

Local kinking between stitches on back surface

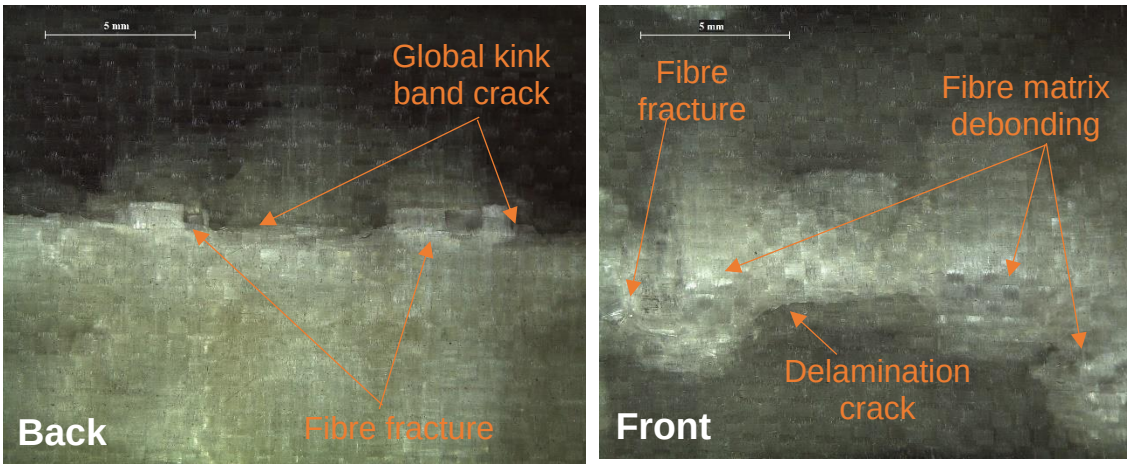

Lateral crack in 2-UNS on back and front surfaces

Figure 5.20 Optical micrographs of compression damage modes in stitched and unstitched composites after 7.5 J impact.

5.7 Concluding Remarks

By adjusting the ISO-401 machine stitch formation mechanisms for this study, it was possible to conduct TT stitching with advanced glass-fibre thread. This is significant because advanced fibres are regularly used for the stitching reinforcement of FRP composites. Thus, establishing that a commercial sewing machine has the capacity to stitch with an advanced fibre thread, without causing excessive damage to the thread, is advantageous for the use of ISO-401 geometry in the composite industry. The main issues that prevented correct stitch formation when glass fibre stitching thread was employed were the needle size and the corresponding looper positioning. Increasing the needle size helped to prevent excessive friction and fracture of the needle thread during stitching. However, the increased needle size meant that the looper was unable to travel clear of the needle during operation, which meant that successive stitching could not be achieved. By retracting the looper position slightly, the looper arm was positioned correctly for catching the thread loop at the back of the needle, without being obstructed by or coming into contact with the needle itself.

It was found that stitched composites (2-DCS-G and 2-DCS-P) had reduced tensile modulus compared with the corresponding unstitched equivalent composites. Stitching with two threads is known to cause microstructural defects in the final composite structure and since tensile modulus

is dependent on the direction and volume of the in-plane fibres, distortion caused by the stitching threads can reduce the in-plane modulus. More specifically, it was found that the tensile modulus was reduced by 10 % when advanced glass fibre was employed as the needle reinforcement thread, compared to a 2.2 % reduction when employing polyester fibre. Employing glass fibre stitching thread caused more in-plane tow fibre waviness and larger resin pockets due to its increased linear density and stiffness, compared with the polyester thread. The linear density of the polyester stitching thread was lower compared with glass fibre thread and therefore introduced less in-plane fibre waviness.

Conversely, the tensile strength and the tensile strain properties of ISO-401 stitched composites with glass fibre thread were improved when compared against unstitched and polyester stitched composites. For polyester stitched composites, the tensile strength and strain were lower than for unstitched composites. It is proposed that the role of damage suppression by the stitches and contribution of glass fibre stitch thread rupture as a damage mechanism helped to improve the tensile strength and strain to failure due to its high breaking strength. In 2-DCS-P composites, the effect of thread fracture as a contributing damage mechanism was negligible and the stitch induced defects such as resin pockets and fibre waviness were not adequately counterbalanced.

Examination of the impact and CAI properties of ISO-401 glass fibre stitched composites showed that the peak impact force was increased at all impact energy levels (2.5 J, 5 J and 7.5 J) by up to 5 %. Similarly, the damage area was reduced under all impact energy levels for stitched composites by 15-41 %. The results suggest that under impact, the stitching threads were effective in bridging and suppressing damage propagation, whereas for 2-UNS composites, the damage was able to spread unimpeded.

It was found that stitching reduced the compressive strength of un-impacted composites, due to the stitch-induced defects. Stitching improved the composites' compressive and residual strengths after 5 J and 7.5 J, whereas for 2.5 J impacts, the effect of stitching was negligible. This indicates that when the impact damaged area is larger and spread across more stitch lines as in 5 J and 7.5 J impacted specimens, the effect of fibre bridging is more pronounced and significantly delays the spread of delamination. It is suggested that increasing the stitch density could improve the fibre bridging effect. Under all impact levels, the damage caused by compression, such as fibre kink banding and delamination, was more localised due to effective suppression by the stitch threads.

Importantly, the work in this chapter demonstrates that the out-of-plane properties of FRP composites can be improved by employing ISO-401 geometry with glass fibre thread. This is

significant because whilst TT stitching is commonly applied to FRP composites to improve the out-of-plane properties, ISO-401 stitching had not been applied to composites before this work and thus the effect of this geometry on the impact and damage tolerance were unknown. This work therefore confirms that double-thread chain-stitching is suitable as a TT composite reinforcement geometry because the impact and damage tolerance can be improved with this stitch type. Another key finding from the work in this chapter is that the in-plane and out-of-plane properties of ISO-401 stitched composites can be balanced. More specifically, stitching with glass fibre thread improved the impact and damage tolerance of composites whilst having little negative effect on the tensile modulus and the tensile strength was actually increased. This is significant because a key limitation to inter-laminar stitching is that the tensile properties are commonly reduced due to the distortion of in-plane fibres.

Chapter 6

Effect of the Preform Fabric on the Stitch Junction Position and Tensile Properties

6.1 Introduction

The experimental work so far has shown that it is possible to have improved out of plane properties with little negative effect impact on the in-plane tensile properties when ISO-401 stitching is employed in FRP composites. In Chapter 4, it was demonstrated that the stitch junction position should be considered a critical stitch parameter when applying ISO-401 to composite laminates as it can affect the tensile properties. Building on this concept, the work in this chapter is dedicated to understanding the effect of the preform fabric properties on the formation of the ISO-401 stitch geometry. In an effort to optimise the ISO-401 for composites, the following study was designed to better understand the relationship between the preform fabric and the formation of the ISO-401 stitch geometry for advanced composites.

During the stitch formation process, manipulation of the preform fabric and tows is required and it is acknowledged in the textile industry that the properties of the fabric being sewn can often dictates the machine type and settings used [178]. For example, reducing sewing faults and seam pucker can be achieved by balancing the fabric properties (surface friction, tensile, compression and thickness) with sewing machine speed and foot pressure [179]. A fabric's mechanical properties such as bending, compression, shear and surface friction are known to influence the process of stitch formation. As the fabric moves through the machine and passes the needle plate, significant compression of the plies is required between the feed dog and presser foot and during the needle descent, the fabric is required to bend and shear around the needle movement [178]. Fabrics with low shear can be easily distorted during the stitching process [180], therefore in the context of composites, the warp and weft yarns can become misaligned during handing. Similarly, fabrics with low bending rigidity have been found to cause seam puckering, whereas higher

rigidity can be more favourable for a flat seam [180–182]. However, handling and stitch formation problems can occur if the shear and bending rigidity is too high due to greater resistance to manipulation [180]. Thus, the interactions between the fabric properties and stitching process are complex.

In the context of FRP composites, the effect of the fabric parameters on the stitch formation and stitching process have not been well investigated to date. To support the industrial adoption of the ISO-401 stitch type for composites, it is likely that an optimised stitch geometry would be required to be replicated in various types of composite. Thus, it is desirable to be able to make machine adjustments to accommodate differences in fabric parameters and replicate the desirable stitch geometry. In the textile industry, understanding the interaction between fabric parameters and sewing process is important so that the machinery can be adjusted to reduce the potential of seam puckering, a faulty seam and to create a neat seam appearance. To achieve this for composites, a deeper understanding of the relationship between fabric properties and stitching parameters is required.

In the experimental work for this chapter, ISO-401 interlaminar stitching is conducted on two similar types of E-glass reinforcement fabric, the fabrics are of the same weight and construction but have different fabric properties. It is important to characterise the fabric properties to better understand the relationship between the preform fabric and its effect on the stitch formation. Therefore, the bending rigidity, compression rigidity, surface friction and shear properties of the fabrics are experimentally investigated and the relationship between these properties and the final junction position is examined. Finally, the resultant composites are evaluated and compared to unstitched equivalents under tensile loading.

6.2 Composite Manufacturing Process

Some basic fabric properties for both of the fabric types investigated for this chapter are displayed in Table 6.1. Fabric type 2 is the same fabric as was used in Chapter 5, therefore the resultant composites 2-UNS and 2-DCS are also the same. Fabric and composites group type 2 were used as a benchmark to compare a different type of fabric, fabric type 3. Fabric 3 has some similar characteristics to type 2; it is made from the same fibre type, the same weaving geometry and is the same weight.

Preforms for each fabric type were manufactured from 8-plies of fabric with dimensions 300 mm x 300 mm. For each fabric, two types of composite were manufactured, unstitched and ISO-401 machine stitched: 2-UNS (unstitched, fabric 2), 3-UNS (unstitched, fabric 3), 2-DCS (stitched, fabric 2) and 3-DCS (stitched, fabric 3). Specification of the composite properties are provided in Table 6.2. The preforms were consolidated with a Bisphenol-A type epoxy (Araldite LY1564) resin and an amine type (Aradur 2954 cycloaliphatic polyamine) hardener (supplied by Huntsman UK Ltd). Stitching was performed prior to the VARIM process, details of the full VARIM process are presented in Chapter 4.

Double-thread chain-stitching was performed on the preforms using the Durkopp Adler 195-17 1120-01 machine, as described in Chapter 4. In the previous chapter, the adjustments made to the sewing machine to enable ISO-401 stitching with glass fibre thread were documented. Since the same E-glass stitching thread was employed here, the adjustments remained in place for the process of preform stitching for this chapter. Two sewing thread types were employed, polyester core-spun and E-glass fibre 2-ply twisted. For both machine stitched composite subtypes (2-DCS and 3-DCS), glass fibre thread was employed as the needle thread and polyester as the looper thread. For all stitched composites, stitching was conducted in the 0° direction. Both the stitch pitch and stitch pace were kept constant as 4 mm and 10 mm respectively.

Table 6.1 Basic preform fabric properties, standard deviation is shown in brackets

	Fabric Type 2	**Fabric Type 3**
Fibre type	E-glass	E-glass
Tow diameter [mm]	4.4	3
Filament diameter [µm]	15	15
Yarn linear density [Tex]	1200	1200
Ply thickness [mm]	0.67 (0.01)	0.72 (0.02)
Construction	Plain weave 1/1	Plain weave 1/1
Weight [gsm]	600	600
Warp and weft density [1/cm]	2	1.5
Crimp factor [%]	1.7	2.2

Table 6.2 Basic composite properties, standard deviation is shown in brackets

	2-UNS	**2-DCS**	**3-UNS**	**3-DCS**
Needle thread fibre	-	E-Glass	-	Polyester
Looper thread fibre	-	Polyester	-	Polyester
Needle thread diameter [mm]	-	0.34 (0.03)	-	0.34 (0.03)
Looper thread diameter [mm]	-	0.24 (0.03)	-	0.24 (0.03)
Composite thickness [mm]	3.5	3.65	3.78	3.52
Stitch density (1/cm^2)	-	0.025	-	0.025
FVF [%]	58 (1.34)	55 (0.35)	51.7 (0.2)	54.9 (0.2)
Composite density [g/cm^3]	1.99 (0.003)	1.93 (0.002)	1.91 (0.002)	1.94 (0.004)

6.3 Material Characterisation

6.3.1 Fibre Volume Fraction Method

To experimentally determine the fibre volume fraction (FVF) of the composites, the ASTM D3171-99 standard test method for matrix burn-off was followed [166], as reported in Chapter 5. The FVF values for each composite type are reported in Table 6.2. For 2-DCS composites, the FVF was reduced compared to unstitched equivalent composites but for 3-DCS composites it was slightly higher, likely due to the different properties of the two fabrics, which is discussed in more detail along with the tensile properties in section 6.6.

6.3.2 Microscopy

Optical microscopy was used to determine the stitch junction location, the resin pocket sizes and to investigate the damaged areas of tensile specimens. For measurement of the stitch-induced resin voids, the same software and protocol was followed as detailed in Chapter 5, ensuring that calibration was conducted on each new set of data.

6.3.2.1 *Stitch Junction Position*

Once the preforms had been stitched, prior to resin infusion, the thread junction measurement was performed. Since the stitch length is pre-determined by the machine settings (4 mm in this case), the junction position was characterised by measuring the exposed needle thread loop length and width at the underside perform surface, example images of the stitch junctions at the composite underside are presented in Figure 6.1. An optical microscope was used to image the surface of each preform and from these micrographs, measurement of the exposed needle thread length and width were taken using ImageJ software. Approximately 30 junction measurements were taken for each preform type and a one-way ANOVA was then performed to compare the differences.

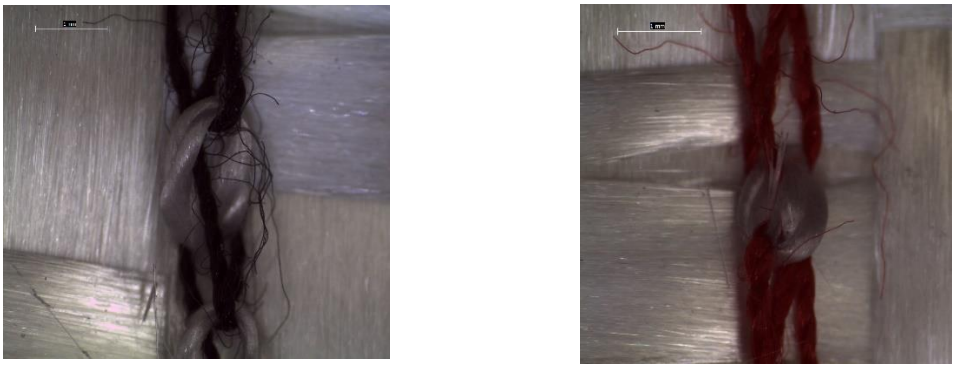

(a) (b)

Figure 6.1 Optical micrographs of the junction positions for stitched preforms; (a) fabric type 2; (b) fabric type 3.

6.3.2.2 *Resin Voids*

As reported in the earlier chapters, resin voids are common geometrical defects that occur in stitched composites. Figure 6.2 presents examples of resin pockets around the stitch points for 2-DCS-G (also presented in Chapter 5) and 3-DCS-G composites. Figure 6.3 presents a comparison of the measured resin pocket areas in the stitched composites. Resin voids in 2-DCS-G composites were 47% smaller than the voids measured in 3-DCS-G composites. It is proposed that the difference in size was caused by the fabric properties during the stitching process; this is discussed further in section 6.5.

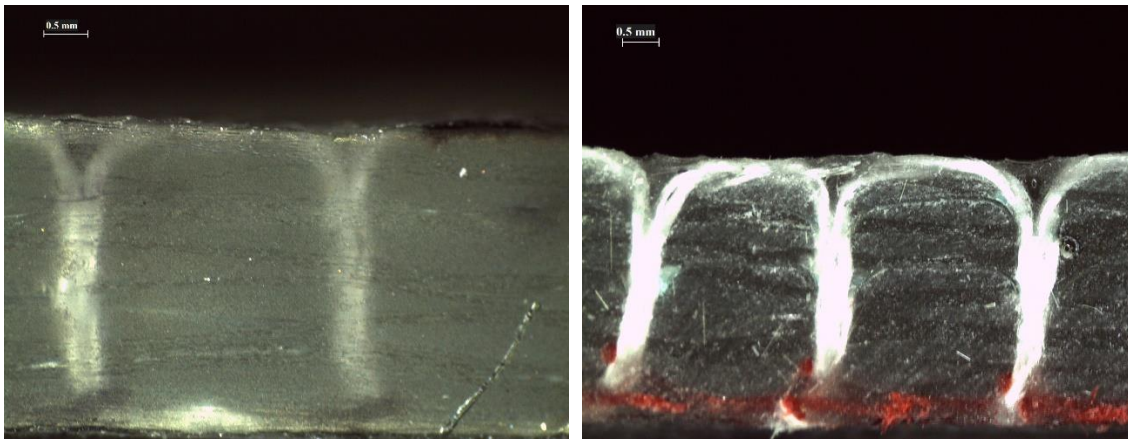

(a) (b)

Figure 6.2 Cross-sectional micrographs of stitched composites with visible resin pockets; (a) 2-DCS-G; (b) 3-DCS-G.

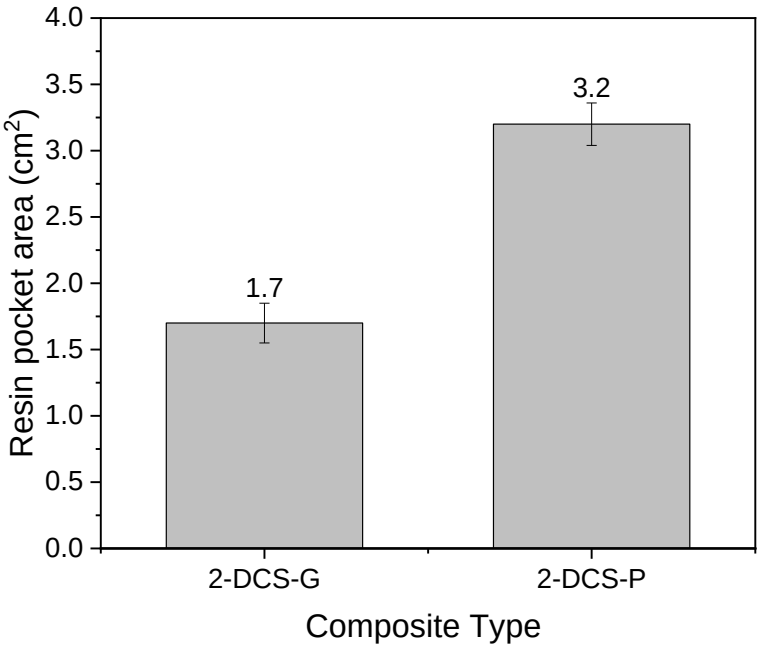

Figure 6.3 Bar graph comparing the resin pocket sizes measured in the stitched composite cross-sections.

6.4 Fabric Analysis

6.4.1 Fabric Touch Tester Protocol

The Fabric Touch Tester (FTT) by SDL Atlas (shown in Figure 6.4) is a device used in the textile industry to determine the fundamental physical properties of fabrics and to predict the fabric comfort properties [183]. The instrument is able to measure the following fabric properties: thickness, compression, bending, surface friction and thermal properties. To do this it uses five types of sensors: displacement, heatflux, temperature, pressure and friction. In total, the FTT software generates 13 indices, however for this study only three were of relevance; surface friction coefficient (SFC), compression average rigidity (CAR) and bending average rigidity (BAR). A description of the relevant measurements can be viewed in Table 6.3. A total of five specimens per fabric type were tested. The fabric specimens were cut into an 'L' shape, as presented in Figure 6.5, of dimensions 310 x 310 x 110 cm as per the manufacturer guidelines.

The FTT testing area consists of an upper and a lower plate and the specimen shape ensures both warp and weft directions are tested. During the test, the upper plate moves downwards to compress the specimen and load cells beneath the bottom plate measure the pressure. CAR and fabric thickness is determined from this process. Whilst the upper plate is compressing the fabric, the lower plate is forced downwards, thus pulling the warp and weft legs of the 'L' shaped specimen across the surface friction module, which enables the determination of the SFC. Simultaneously as the lower testing plate moves downwards, the fabric is bent, this activates the bending evaluation module which is used to calculate the bending angles to determine BAR for both warp and weft [184].

Table 6.3 FTT fabric property indices

Fabric Property	**Abbreviation**	**Unit**	**Description**
Surface friction coefficient	SFC	-	Friction coefficient on the fabric surface with a ribbed plate.
Compression average rigidity	CAR	Kgf/mm^{-3}	Forces needed to compress the fabric per mm.
Bending average rigidity	BAR	Kgf/rad^{-1}	Forces needed to bend the fabric per radian.

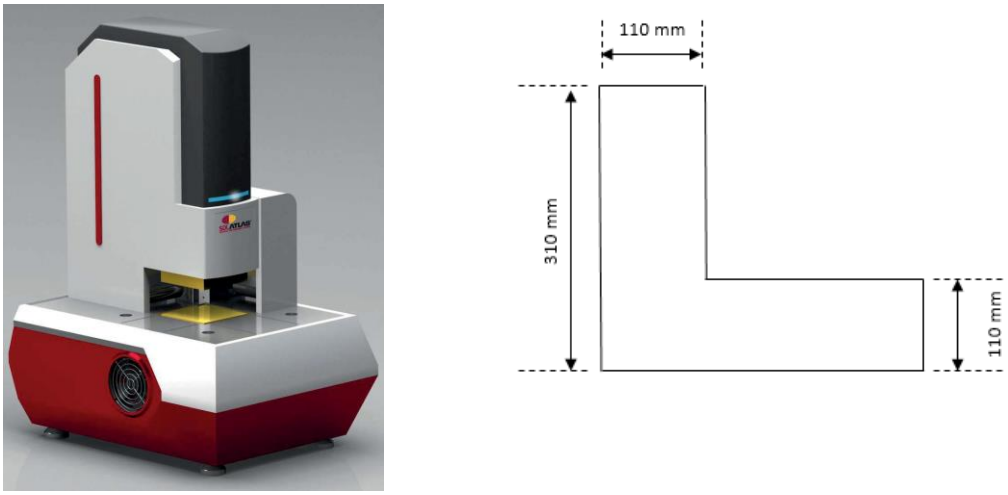

(a) (b)

Figure 6.4 (a) Image of the FTT instrument by SDL Atlas [184]; (b) schematic showing the FTT fabric sample dimensions [183].

6.4.2 Bias Extension Test Protocol

To test the shear properties of the fabrics, a bias extension test was adapted from the industry standard ASTM D5035. The testing was carried out on a commercial INSTRON-5569 machine equipped with a 10 N load cell in ambient conditions, the test was repeated five times for each fabric type. The test parameters were as follows, cross-head speed 10mm/second and specimen dimensions of 200mm (length) x 50mm (width) and a gauge length of 100mm. Specimens were cut along the bias so that the direction of the warp and weft tows were orientated at 45° to the loading direction. Specimen cutting was performed using a rotary blade to minimise mishandling and slippage of the cut tows. Specimens were then left to relax in ambient conditions for 24 hours prior to testing. An image of the test set-up is presented in Figure 6.5.

To prevent slippage of the fabric strip during testing, the jaws were modified using jaw padding. The test was terminated when the samples began to visually suffer from tow slip and pull-out. The full test was recorded using a high resolution camera LaVision 3D VZ16-0250 and the stills from various points in the test were imported into ImageJ software in order to calculate the shear angle. During the test, different areas of the test specimen experience different types of shear and it is therefore important that the angle measurements are taken from the pure shear region in the central zone. To ensure that the yarns in the central zone have free edges, the original length of the specimen must be more than twice that of the specimen width. Assuming that the warp and weft yarns are inextensible and there is no slip occurring, the deformation in zone C is therefore in pure shear, as in Figure 6.6. Area B is in half in-plane shear and A does not deform [185].

Measurement of the shear angle was performed at five displacement intervals, 4 mm, 8 mm, 12 mm, 16 mm, and 20 mm. From early experiments, it was found that obvious fibre pull out occurred for both fabrics at a displacement of ~24 mm, therefore testing was terminated at this point. For each specimen at each displacement interval, three measurements were taken in the constant shear region to ensure repeatability of the results. In total, five specimens of each fabric were tested.

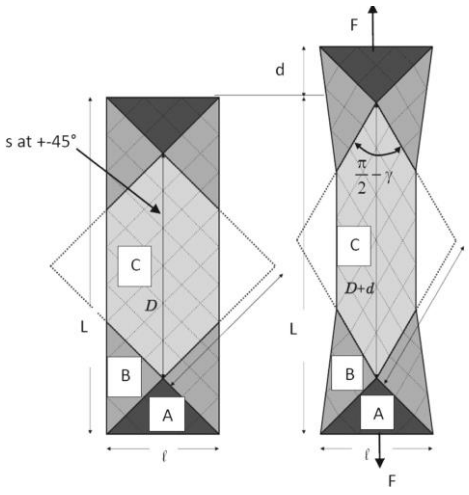

(a) (b)

Figure 6.5 (a) Bias extension test set-up; (b) bias extension test specimen shear regions adapted from [185].

6.4.3 Results and Discussion

The surface friction, bending, compression and shear properties of both preform fabrics are presented in Table 6.4 and Figure 6.6. The surface friction coefficient of fabric 3 was on average of 43% higher in the warp and 23% higher in the weft direction for fabric type 3, compared with fabric 2, which was statistically significant at a threshold of $p<0.05$. From visual inspection of the fabrics it was found that fabric 3 has more severe undulations of the tows in the fabric structure, therefore having a less smooth surface compared with fabric 2. For example, is evident from Figure 6.7 that the yarns in the warp and weft tows are more raised and clustered together in fabric 3, measuring on average ~ 3mm across, compared with fabric 2, where the tows are more flat and dispersed, measuring on average ~4.4mm across. These characteristics result in fabric 2 presenting as a more open structure with visible gaps between the tows compared with fabric 3 where gaps between tows are smaller and not always visible. Thus for fabric 2, the undulations of the warp and weft tow fibres are less pronounced, therefore presenting less surface roughness compared

with fabric 3. Additionally, the ply thickness of fabric 3 was approximately 16% higher than fabric 2.

From Figure 6.6, it is evident that Fabric 2 had significantly higher bending rigidity, compression rigidity and shear resistance compared with fabric 3. All of the results reached statistical significance at a threshold of $p<0.05$. The CAR of fabric 2 was 49% higher than fabric 3 and the BAR of fabric 2 in the warp and weft directions were 43% and 68% higher compared with fabric 3. It can be seen in Figure 6.7, at each displacement measurement point, the shear angles between fabric 3 tows were higher than fabric 2. Demonstrating that fabric 2 has higher resistance to shearing action compared with fabric 3.

Overall, the results indicate that the fabric properties and behaviour of fabric 2 and fabric 3 are significantly different. The structure of fabric 2 is shown to be more resistant to manipulation, compared with fabric 3 where the warp and weft tows can be moved and manipulated (sheared) more easily. This is significant because during stitching, a certain amount of manipulation of the fabric is required in order to form and set the stitch correctly [178,180,182]. Since the fabric parameters are directly related to the handling of the fabric during stitching, it is proposed that both fabrics will handle and behave differently during the stitching process, thus potentially giving rise to different stitch junction positions.

Table 6.4 Fabric mechanical property results, standard deviation is shown in brackets

	Fabric Type 2		**Fabric Type 3**	
	Warp	**Weft**	**Warp**	**Weft**
SFC	0.14 (0.05)	0.13 (0.01)	0.20 (0.03)	0.16 (0.05)
BAR [Kgf/rad^{-1}]	7.46 (0.39)	8.83 (1.4)	4.27 (0.22)	2.83 (0.53)
CAR [Kgf/mm^{-3}]	1.03 (0.18)		0.53 (0.09)	

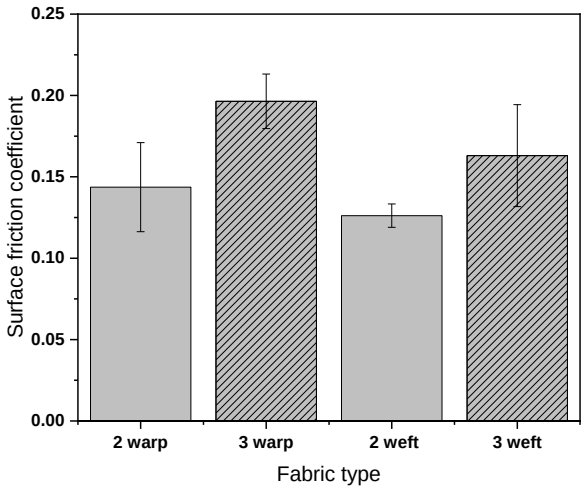

(a)

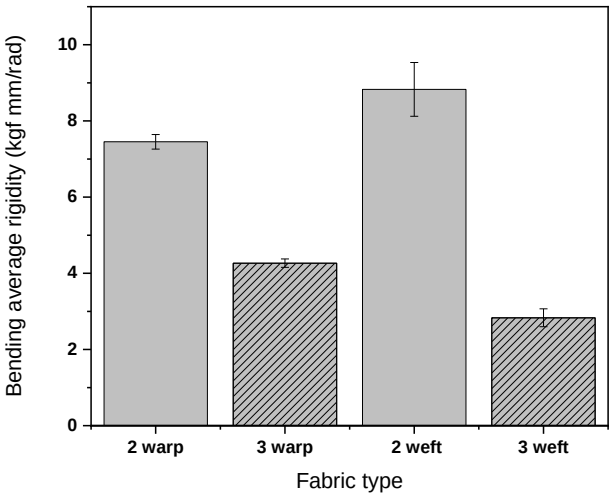

(b)

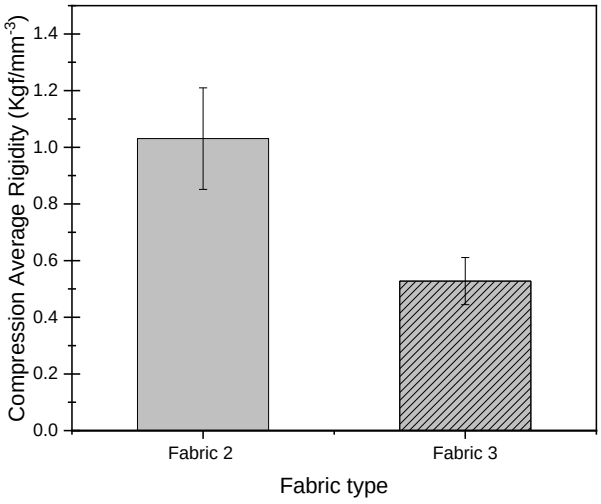

(c)

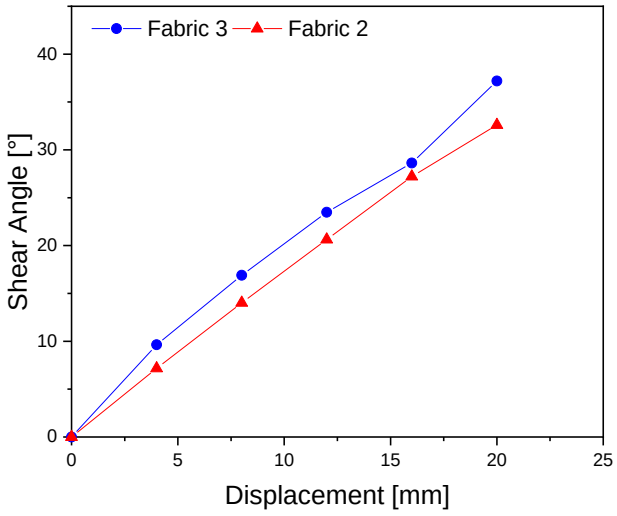

(d)

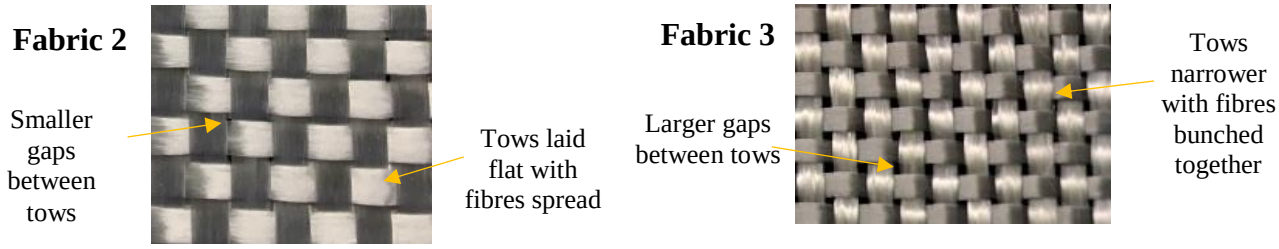

(e)

Figure 6.6 Comparison of fabric parameters; (a) surface friction coefficient; (b) bending average rigidity; (c) compression average rigidity; (d) shear angle as function of displacement; (e) surface images of fabrics 2 and 3.

6.5 Discussion of Stitch Formation and Junction Position

A comparison of the measured length and width of the exposed needle thread loop are presented in Table 6.5 and Figure 6.7. The exposed thread length is of particular importance as it dictates where the junction between the needle and looper thread occurs. Each sewing cycle involves dynamic fluctuation of tension exerted on the needle and stitching threads, until the stitch is set where it remains compressed under static tension [186]. The static pre-tension acting on the threads is the main influence of the correct thread junction [187], yet despite the machine settings, handling and processing of the preforms remaining the same, the measured junction position for each of the fabrics was found to be significantly different at a threshold of $p < 0.05$. The junction position of fabric 2 occurred closer to the middle of two respective stitch points, compared with fabric 3 where it was positioned closer to the needle hole. For fabric 2, the exposed needle thread loop length was on average 16% longer compared with fabric 3.

Since other factors were kept constant throughout the stitching process, the difference in junction location is most likely due to the interaction between the forces exerted on the threads during the stitching process and the response of the fabric to this manipulation. The extent and nature of the fabric manipulation by the stitching process directly relates to the fabric shear, bending, compression and surface friction properties. Thus, fabric 2 and fabric 3 present different junction locations as a result of their differing properties. For fabric 2, the earlier discussion confirmed that the structure was more tightly woven and presented a higher resistance under bending, shear and compression. This suggests that fabric 2 would have had more resistance to manipulation during the stitching process compared with fabric 3. Conversely, fabric 3 tows would have been easier to manipulate and adjust during the process. Reviewing key points of the stitch formation process in Figure 6.9 can reveal how the fabric parameters have influenced the final junction setting.

Table 6.5 Stitch junction position results, standard deviation is shown in brackets

	Needle thread loop	
	Length [mm]	**Width [mm]**
Fabric 2	1.42 (0.37)	1.02 (0.27)
Fabric 3	1.22 (0.15)	1.10 (0.14)

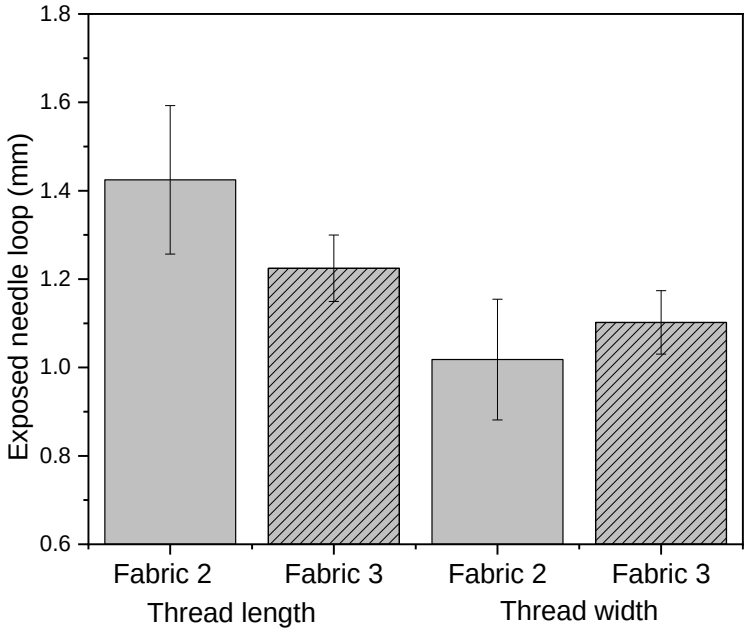

Figure 6.7 Comparison of the exposed surface needle loop measurements for stitched composites.

As the needle is reaching the bottom of its stroke, as in Figure 6.8 (a), the looper is retracting, releasing the interlooping threads onto the needle. The needle thread that was originally inserted in a relatively orthogonal position through the preform, normal to the z-plane, is now being pulled at the underside in the direction of the needle and looper mechanism position. This creates tension at two locations for the new stitch; the insertion point where the thread is being pulled at a smaller angle through the fabric and at the bottom surface where the needle thread is exiting the preform at a larger angle. Manipulating the thread in this way requires the in-plane tow fibres to adjust around the needle thread. During this cycle, it is proposed that fabric 3 tows would have been easier to manipulate compared with 2, due to its lower shear and bending resistance.

The needle thread is then tensioned as it retracts to pull the new junction into place, as in Figure 6.8 (b); meanwhile the fabric is still compressed under the presser foot. Due to the easier movement and compression of the fabric 3 tows, the needle thread tension is not transferred to compressing the fabric and instead can effectively pull the junction into place, with the threads then interlacing close to the needle hole. This is because the in-plane tows offer more flexibility and movement around the needle cycle and the inserted thread. However, in the case of fabric 2, the in-plane tows have more resistance to manipulation which restricts the needle thread

movement, thus it cannot fully retract to pull the looper thread into the same position as fabric 3. Instead, the junction for fabric 2 becomes locked further from the needle hole and fabric 2 has a longer length of the needle thread loop exposed at the bottom surface compared with fabric 3.

As it was found that the stitch junction position was placed slightly differently for the two preform types due to the fabric properties, the composite cross-sections were examined after infusion to review any differences in size of the stitch-induced resin pockets. Referring back to Figure 6.3, on average, the resin pockets in 2-DCS-G composites were nearly half of those found in 3-DCS composites. This is interesting because the stitch thread junction was placed just outside of the needle hole, which was to generally cause larger resin pockets (Chapter 4). The junction placement for 3-DCS-G composites was placed at the stitch insertion point, which usually produces smaller resin pockets, but in this case the resin pockets were larger. It is proposed that this must be due to the difference in fabric properties, since the stitching threads and conditions remained consistent. As the tows in fabric 3 could be more easily manipulated at the needle thread insertion and exit points during the sewing process, the high tensioned thread was able to deviate the fabric at a larger angle. For fabric 2 however, which was less pliable, the angle at these points was smaller because the in-plane tows could not be as easily displaced by the thread, therefore resulting in smaller resin pockets.

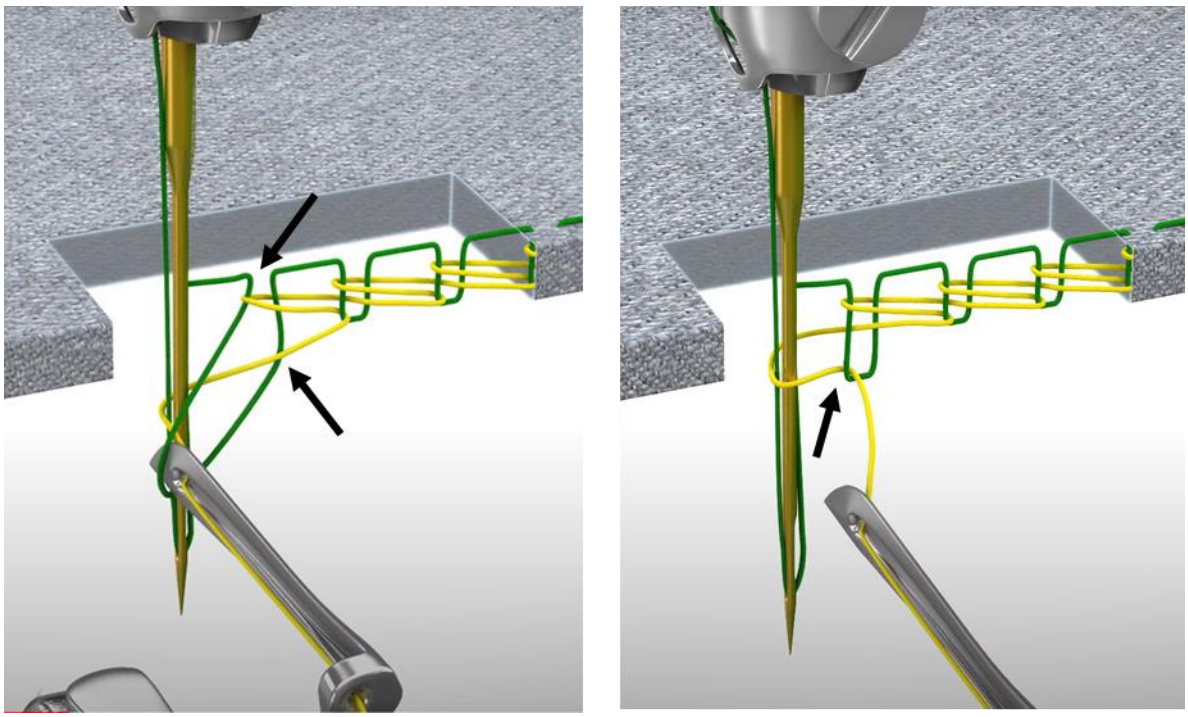

(a) (b)

Figure 6.8 Key stages of the stitch formation process showing areas of dynamic manipulation of the stitching threads, still taken from animation from [122].

6.6 Tensile Properties

6.6.1 Protocol for Tensile Testing

Tensile testing was conducted to investigate the mechanical properties of the stitched and unstitched composites, namely tensile strength (σ_{ULT}) tensile failure strain (ε_f) and tensile modulus (E_1). The results for these properties were subjected to an ANOVA to determine whether differences between the composite types were of statistical significance at a threshold of p<0.05. For this work, 3-DCS-G and 3-UNS composites were tested and compared with composites from the previous chapter, 2-UNS and 2-DCS-G. The same testing protocol was followed as in Chapter 5.

6.6.2 Results and Discussion

It has been confirmed that the properties of the fabric affected the formation of the ISO-401 stitch geometry and therefore the influenced the position of the thread interlooping junction. It is

relevant to consider the effects of ISO-401 stitching on the tensile properties of composites developed from fabric 2 and 3 preforms. The tensile properties and stress-strain behaviour of all stitched and unstitched composites are presented in Table 5.6 and Figure 6.9 respectively.

Table 6.6 Longitudinal tensile properties of stitched and unstitched composites, standard deviation is shown in brackets

Properties	**2-UNS**	**2-DCS**	**3-UNS**	**3-DCS**
$\sigma_{ULT}\,[MPa]$	465.4 (4.5)	466.7 (14)	422 (4.2)	452.3 (15)
$\varepsilon_f\,[\%]$	2.29 (0.06)	2.48 (0.11)	2.19 (0.12)	2.42 (0.06)
$E\,[GPa]$	22.9 (0.7)	20.59 (0.6)	23.41 (0.86)	23.83 (0.26)

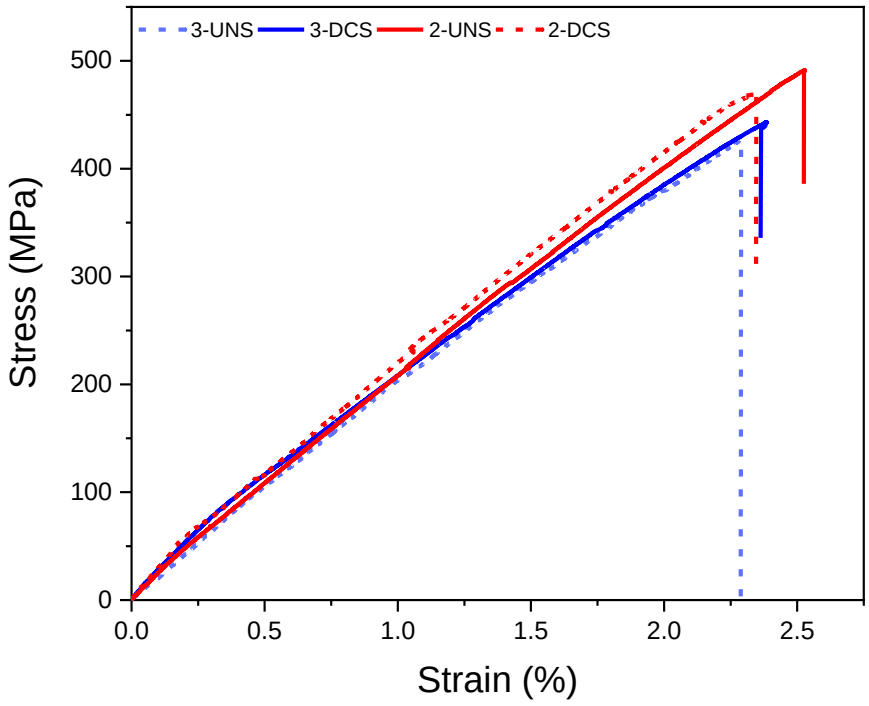

Figure 6.9 Representative stress-strain curves for stitched and unstitched composites.

As Figure 6.10 shows, the loading behaviour of all unstitched and stitched composite specimens is generally linear and then followed by sudden and brittle failure. It can be seen from the graph that the toughness is higher for 2-DCS-G and 3-DCS-G composites compared with the unstitched equivalents. A slight softening of the stress-strain curve for all specimens occurs around 0.15%, indicating the plastic straightening of crimped in-plane fibres. During the test there were audible cracking sounds from each specimen from around 15-20 kN, there was no significant difference of the onset of audible cracking between stitched and unstitched composites. Since there are no sudden drops along the stress-strain curves before the failure point which would indicate fibre failure, the audible cracking sounds can be attributed to matrix cracking and local delaminations which are evidence of gradual failure. The failure modes were similar to those discussed in the previous chapter consisted mostly of matrix cracking, delamination, and fibre fracture, and additionally for stitched composites, stitch thread matrix debonding and stitch thread rupture. The final failure is characterised by an explosive sound resulting from the rupture of in-plane tows and fibres. Figures 6.10 and 6.11 show the typical tensile failure sites for stitched and unstitched composites. Post mortem examination of the failure site revealed stitched specimens, due to the TT reinforcement, had more localised delamination, whereas for unstitched specimens the damage was more extensive. Section 6.6.3 covers the damage modes in more detail.

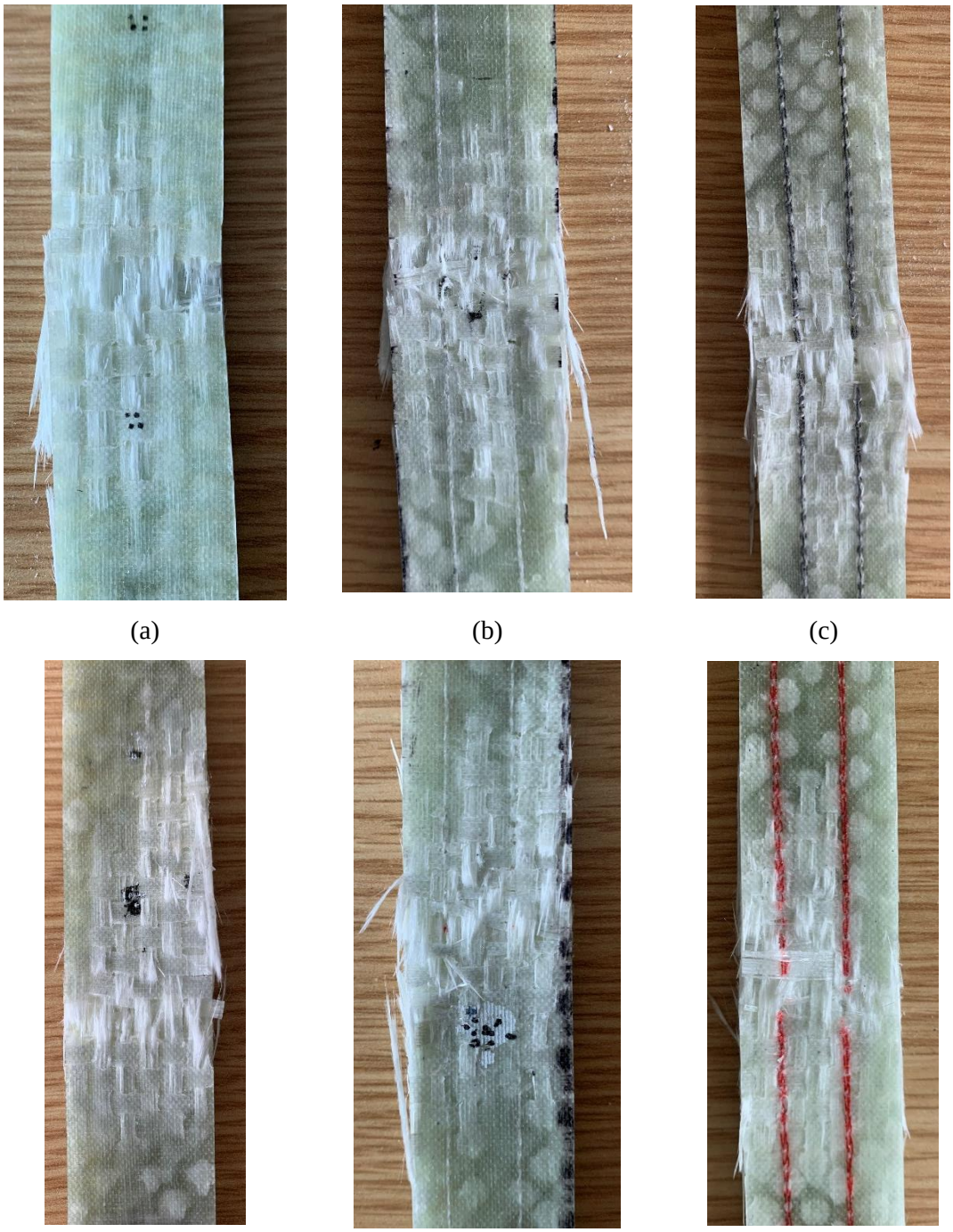

(a) (b) (c)

(d) (e) (f)

Figure 6.10 Images of the tensile failure site; (a) 2-UNS front; (b) 2-DCS-G front; (c) 2-DCS-G back (d) 3-UNS; (e) 3-DCS-G front; (f) 3-DCS-G back.

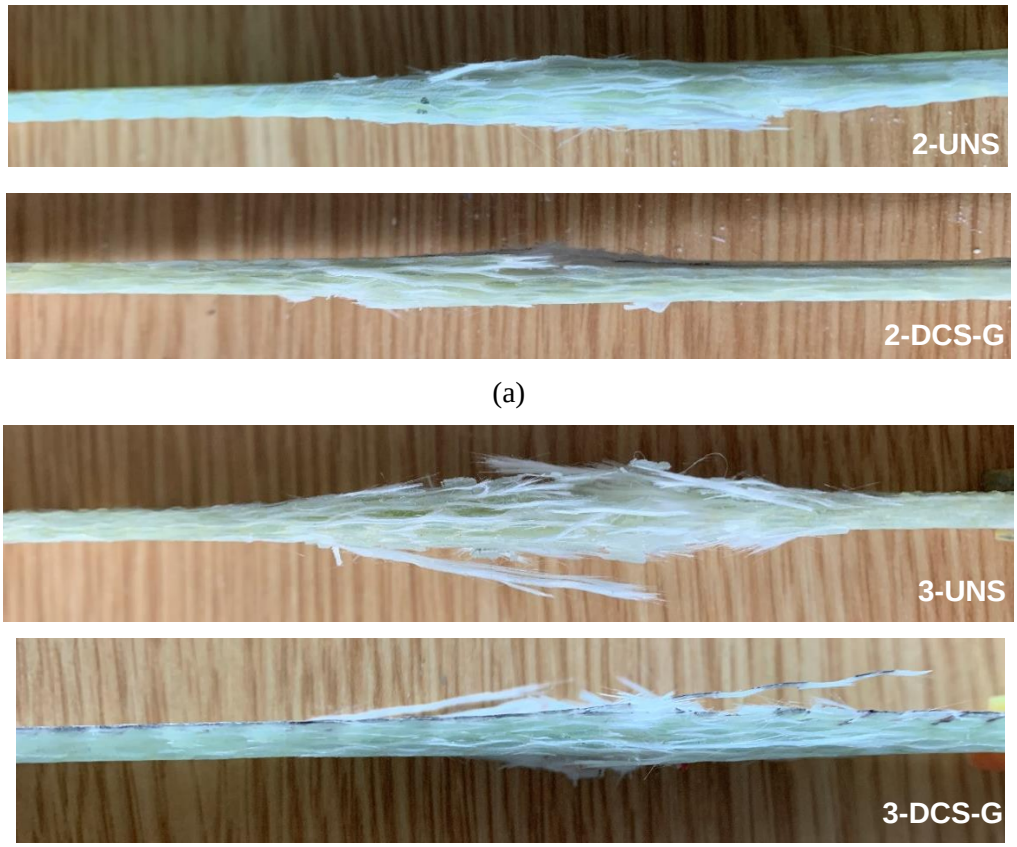

Figure 6.11 Cross-sectional images of the tensile failure site arranged by composite type.

The average **tensile modulus** values for all stitched and unstitched composites are presented in Table 6.6 and Figure 6.12. The modulus of plain woven composites is influenced by the load-distribution of the warp and weft yarns. [188]. Therefore, it is highly dependent on the in-plane volume fraction and orientation of the reinforcing fibres [4,159]. Composites with a higher proportion of in-plane fibres usually have a higher tensile modulus. This also means that fibre distortions due to stitching are associated with reduction of in-plane tensile modulus. Since the tensile modulus is dominated by the axial stiffness of in-plane fibres, any misalignment of these or reduction in volume fraction can be detrimental to the modulus. On the other hand, stitching can improve the tensile modulus by a combination of increasing the volume fraction of fibres and keeping fibres in a well-aligned orientation [17]. In the context of this study, variations in the FVF must be taken into consideration as stitching has been demonstrated to affect the FVF value.

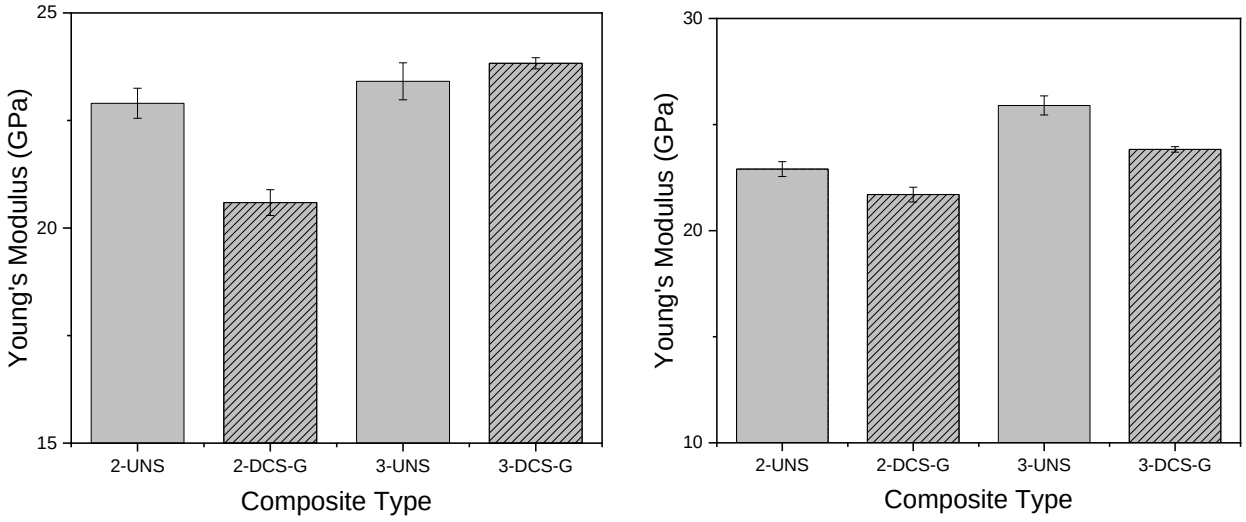

(a) (b)

Figure 6.12 (a) Average Young's modulus for stitched and unstitched composites with standard deviation; (b) normalised Young's modulus where FVF of 2-DCS has been normalised to match 2-UNS and FVF of 3-UNS has been normalised to match 3-DCS.

For type 2 composites, it can be seen in Figure 6.12 that stitching (2-DCS) caused a 10% reduction in tensile modulus, which was found to be significant at a threshold of $p<0.05$. Stitching also caused a small but statistically significant reduction in FVF value by 5%. In contrast, for composites type 3-DCS-G, tensile modulus was slightly increased by 1.8%, though this did not reach statistical significance. It was also found that stitching caused an increase in FVF by 6.2% compared with 3-UNS, which was statistically significant at a threshold of $p<0.05$ It is proposed that the contrasting effect of stitching on the FVF of the composite types was influenced by the individual fabric properties.

During the composite manufacturing process, the preforms are subjected to compression due to the tension of the stitching threads [186] and the presser foot force, and under the vacuum conditions necessary for resin infusion process. Referring back to the fabric analysis, section 6.4.3, it was revealed that the compressive behaviours of both fabrics were very different. It was found that fabric 3 was less rigid than fabric 2, requiring an average 49 % less force during compression testing, compared with fabric 2. Therefore, it is proposed that for composite type 3-DCS-G, the preform fabric plies were compacted more tightly, particularly during the stitching process, which resulted in a higher FVF value compared with the unstitched equivalent composites. Despite the stitching process causing larger resin pockets in 3-DCS-G composites, it is proposed that the compacting forces of the stitching and resultant increase in FVF were more dominant over the

resin voids, leading to an increase in modulus. The induced fibre waviness was severe enough to counteract the positive effect of increased FVF on the modulus. Whereas for type 2-DCS-G composites, stitching caused a reduction in FVF, suggesting that the rigid nature of the fabric meant that the preform was not compressed sufficiently due to the stitching. Therefore the lack of preform compression and stitching induced defects such as in-plane fibre waviness and resin pockets, though smaller than in 2-DCS-G composites, were contributed to a reduction in the FVF value.

Since stitching caused a change in FVF for both composite types, it is relevant to normalise the modulus values for comparison. For 3-UNS, the FVF value was normalised to the average value for 3-DCS-G (54.9 %). For 2-DCS-G, the modulus value was normalised to the 2-UNS FVF value (57.9 %). The resulting values are plotted in Figure 6.13. When the modulus for 2-DCS was normalised, the reduction in modulus compared with 2-UNS was less severe at 5.2 % and the difference was not highlighted as statistically significant. When the modulus value for 3-UNS was normalised, it was evident that 3-DCS actually caused a small reduction of 7.7 % in tensile modulus. The results suggest that when the FVF is normalised for both composite types 2 and 3, stitching caused a slight reduction in tensile modulus due to stitch induced damage of the in-plane tows.

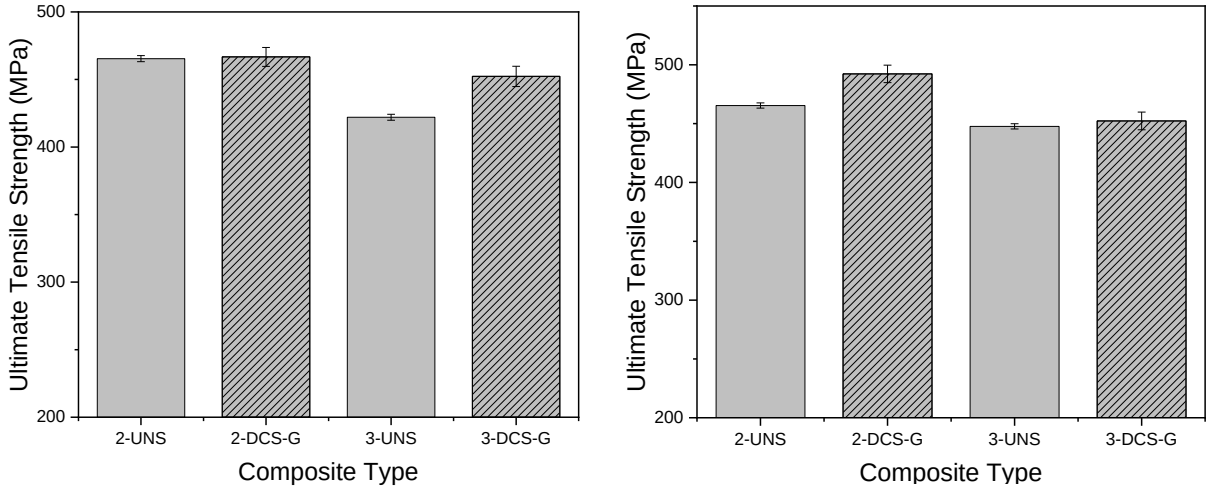

Figure 6.13 (a) Average tensile strength for stitched and unstitched composites with standard deviation; (b) normalised tensile strength where FVF of 2-DCS has been normalised to match 2-UNS and FVF of 3-UNS has been normalised to match 3-DCS.

Overall, ISO-401 stitching did not severely reduce the tensile modulus for both composite types. When the modulus reduction is around 5 %, which is considered a moderate reduction and it is suggested the extent of the fibre waviness can be considered small [159]. It is understood that the stitching process induces some in-plane fibre waviness into the final composite structure and the extent of the misalignment is dependent upon the stitching parameters [17]. From the cross-sectional images in Figure 6.3, it is evident that the TT stitching has introduced a degree of in-plane fibre misalignment which resulted in a reduction in tensile modulus. It can clearly be seen that some of the in-plane tows are misaligned around the stitch points, contributing to reduced load bearing capacity and therefore reduced tensile modulus.

Figure 6.14 and Table 6.6 presents the values of **tensile strength** for 2-UNS, 2-DCS, 3-UNS and 3-DCS composites. The tensile strength of 2-DCS is comparable to the unstitched equivalent (2-UNS), with no significant difference found despite the reduction of FVF due to stitching. Importantly, the presence of the stitching thread did not reduce the tensile strength, which is commonly the case [17]. For 3-DCS, the tensile strength was moderately increased by 7.2 % compared with 3-UNS, which reached significance at a threshold of $p<0.05$. This increase can mainly be attributed to the increased FVF value as a result of the TT stitching. Other researchers have similarly found that stitching can have a positive or no effect on the tensile strength [42]. This has been attributed to the stitching process causing localised in-plane fibre damage that does

not catastrophically damage the whole fibre and to the ability of the stitching threads to redistribute stress evenly between the reinforcing fibres [17,42].

Comparing the normalised tensile strength of 2-DCS to 2-UNS, there was a small but significant increase of 5.5 % on average. This is expected as the tensile strength was comparable to 2-UNS yet the FVF value was lower, thus increasing the FVF through normalisation increased the tensile strength of 2-DCS composites. Comparing the normalised tensile strength of 3-UNS to 3-DCS, a smaller increase of 1.2 % was found and was no longer of statistical significance. For both stitched composite types, the results suggest that whilst the tow waviness induced by the stitching process is present, it can be considered relatively localised and it does not reach such an extent to where the load bearing capacity of the tows is significantly affected. Moreover, it is also possible that any increase in tensile strength, such as for 3-DCS composites, could be a result of the TT stitching balancing the in-plane tow fibre distribution, thus leading to redistribution of stress along the in-plane fibres which contributed to the increased tensile strength [42].

The **tensile strain** at failure of stitched and unstitched composites are presented in Table 6.6 and Figure 6.15. It is clear that both 2-DCS and 3-DCS experienced higher failure strains than unstitched equivalent composites. For 2-DCS the failure strain was increased by an average of 8.3 % compared with 2-UNS and for 3-DCS the increase was 10.5 %. Comparing the normalised strain values in Figure 6.15, the increase seen for 3-DCS composites becomes smaller and is no longer considered statistically significant. Conversely for 2-DCS composites, the increase becomes bigger. The results suggest that, despite the introduction of in-plane fibre waviness, the TT stitches actually act as crack inhibitors, helping to arrest cracks as they occurs and suppress the damage, thus failure of stitched composites is more gradual. This is in-line with a study by Yudhanto et. al, [159], where a correlation was found between increased tensile failure strain and impediment of delamination growth by the stitching threads.

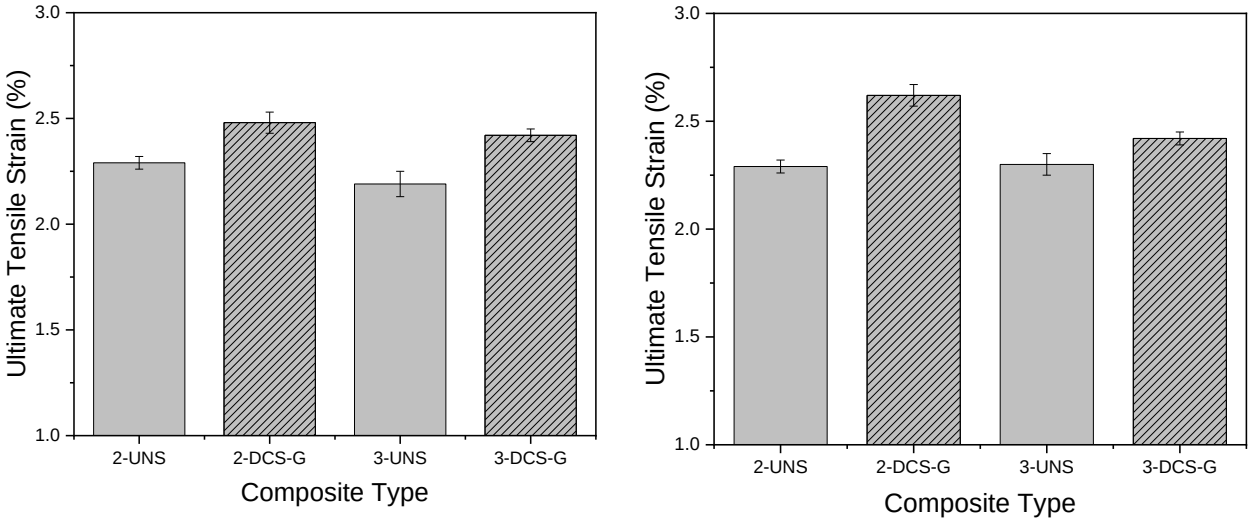

(a) (b)

Figure 6.14 .(a) Average failure strain for stitched and unstitched composites with standard deviation; (b) normalised failure strain where FVF of 2-DCS has been normalised to match 2-UNS and FVF of 3-UNS has been normalised to match 3-DCS.

6.6.3 Physical Examination

Close examination of the 3-DCS-G tensile failure sites, as in Figure 6.15, revealed that only the polyester looper thread had ruptured, the needle thread stitching had suffered from pull out and debonding from the matrix but had not fully ruptured. This was similarly found in 2-DCS-G composites, as discussed in the previous chapter. Also, in both 2-DCS-G and 3-DCS-G composites, the looper thread is visible at the top surface across the tensile failure site, meaning that it has been fractured and pulled through the thickness by the needle thread under loading conditions. It is proposed that the same mechanisms are occurring here in 3-DCS-G composites as were described in the previous chapter for 2-DCS-G composites. That is, since the looper thread is weaker than the glass fibre needle thread, the imbalance caused the polyester thread to fracture and be pulled through by the needle thread.

It has been reported in the literature that the stitch junctions act as damage initiation sites under loading. This is mainly attributed to the fact that at these points, the in-plane tows are pushed apart by the stitching threads and the voids are filled with matrix resin only in the final composite, thus leading areas of structural weakness [17]. Without inspecting the growth of damage during tensile testing, it is near impossible to find proof that damage has been initiated at these points. However

for this study, inspection of the post-mortem of the whole specimen surfaces, not just directly at the failure site, revealed evidence of damage growth at the stitches. Figure 6.16 presents an example of evidence of reinforcement fibre debonding and splitting at the stitch points in 3-DCS-G composites. The image was taken from an area of the test piece between the ruptured site and the tabbing, where mainly internal delaminations occurred and there was no evidence of catastrophic failure. Whilst this does not prove damage such as cracking has been initiated at these points, it does suggest that delamination and fibre damage has formed around and potentially grown from these areas during loading.

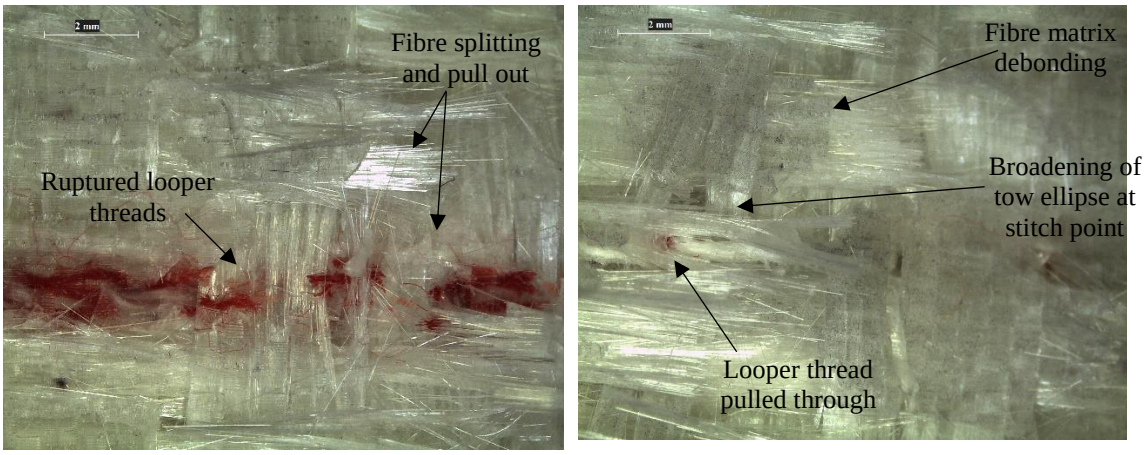

(a) (b)

Figure 6.15 . Optical micrographs of 3-DCS-G composites after tensile testing; (a) ruptured looper threads on back surface; (b) intact needle thread on front surface with evidence of looper threads pull through and broadening of the tows around stitch points.

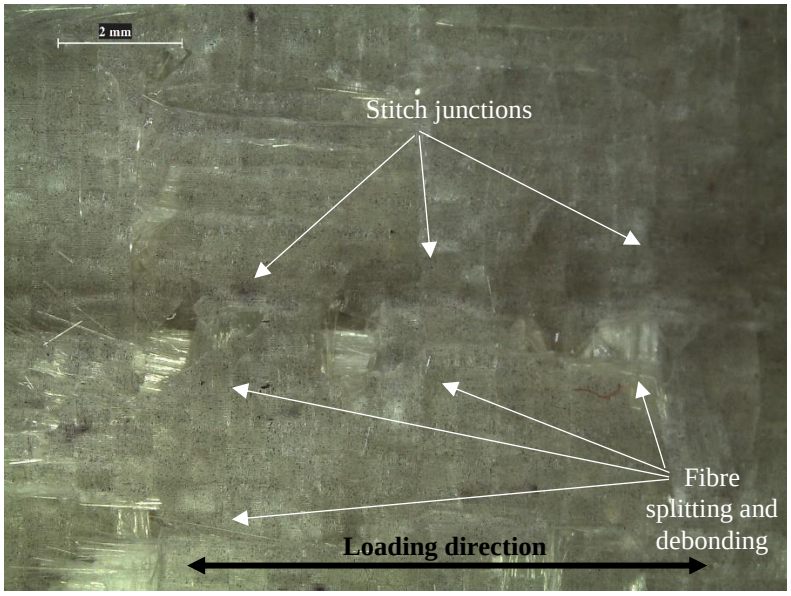

Figure 6.16 Example of damage visible around stitch points after tensile failure in stitched composites (3-DCS-G specimen).

6.7 Concluding Remarks

It has been found that the measured fabric characteristics, such as: shear, compression, bending and surface friction, affected the ISO-401 stitch geometry, specifically the position of the interlooping stitch junction. Though both fabrics were of the same weight and weave type, their characteristics were found to be significantly different. Fabric type 2 was found to be more stiff and resistant to bending, shear and compression loads, whereas fabric 3 was less resistant to these loads and therefore more pliable and easily manipulated during the stitching and stitch formation process. As a result, the stitch junction position was placed closer to the needle insertion point for fabric 3 and for fabric 2, it was further from the needle hole.

When the preform fabric was more susceptible to manipulation, as in fabric 3, the stitching process was found to have a less detrimental impact and that the tensile properties can be enhanced. For 3-DCS composites, the tensile modulus was slightly increased compared with 3-UNS, whilst the tensile strength is increased significantly. The improvement in properties can be attributed mainly to the FVF increase. The FVF of 3-DCS was increased due to the fabric behaviour during the stitching process. The in-plane tows of fabric 3 were easily manipulated during stitch formation and so the preform plies were adequately compacted by the stitching process and remained compacted post-stitching due to the static tension of the threads compressing the preform. When the FVF value of 3-UNS was normalised to match that of 3-DCS, the improvement in failure strength became less significant and a small drop in modulus was observed, suggesting that stitching caused some significant waviness to the in-plane tows which impacted the stiffness of the in-plane tows.

For fabric type 2, the effects of stitching were more severe due to more resistance to manipulation and compaction during sewing. For 2-DCS composites, the tensile strength was comparable to 2-UNS but tensile modulus was reduced. In this case the FVF was reduced suggesting that the fabric plies were not adequately compressed by the stitching process and static thread tensions. After normalisation, tensile strength of 2-DCS was improved and the reduction in modulus was less severe. Considering this, it is proposed that a combination of the stitch induced defects, such as fibre waviness, and lack of preform compression by the stitches caused the FVF to be reduced.

Strain to failure was found to be improved for both type of stitched composites. This suggests that the stitch threads are able to restrict delamination, thus spreading less rapidly in stitched composites. Also, in stitched composites additional damage modes such as stitch thread

debonding and fracture would have required more energy during damage propagation. As a result, the failure of stitched composites was more gradual.

The results presented in this chapter indicate that the design and development stages of stitched composites for structural elements should account for the preform fabric properties and the effect these properties can have on the TT stitch geometry and the resultant FVF and tensile properties. In line with this, it was demonstrated here that reduction in the volume fraction of fibres in the final composite caused by the stitching process can be avoided by careful selection of the preform fabric. It was found that by selecting a reinforcement fabric which can be adequately manipulated and compressed during the sewing process and by the static thread tension once the stitches have been inserted, fabric 3 in this case, the FVF is actually slightly increased along with Young's modulus. This is significant because a major drawback to TT stitching is that it is commonly the case that interlaminar stitching can cause a reduction in FVF.

Chapter 7 Conclusions and Further Work

7.1 Conclusions

The aim of this research was to find a form of through-thickness (TT) stitch-type reinforcement for fibre reinforced polymer (FRP) composites which effectively improves their damage tolerance without causing excessive damage to the in-plane reinforcement fibres and resultant tensile properties. This was achieved by applying a novel stitch type to FRP composites, the ISO-401 double-thread chain-stitch. Despite being a common stitch type used in the textile industry, prior to this work it had not been applied to composites before. Whilst it was clear from the subject literature that there has been a dedicated effort towards adapting stitching for composite reinforcement, much of the knowledge of the available geometries and understanding of the stitch formation process remains in the textile industry. This work has investigated both the in-plane tensile and out-of-plane damage tolerance of ISO-401 stitched composites, with varying stitch densities, reinforcement fabrics types and stitch thread types. The main achievements and contributions to knowledge are detailed below.

7.1.1 Optimising the ISO-401 stitch geometry for FRP composites

(a) The ISO-401 stitch junction position can be optimised for FRP composites

It was found that the ISO-401 stitch junction position could be optimised to maintain the in-plane composite tensile properties. By adjusting the stitch thread junction location to occur at the needle thread insertion point, as in type 1C composites produced for this research, even when the stitch density was increased, the tensile properties were comparable to unstitched equivalent composites. This is significant because high stitching density is often favoured as it improves the out-of-plane properties, yet it frequently reduces the in-plane tensile properties. It was found that in 1C composites, the resin pocket observed around the stitching point was between 60-65% smaller than in cases where the junction was placed external to the stitch insertion hole, as in types 1A and 1B composites. Restricting the needle thread path so that the inter-looping junction occurred

close to the needle hole resulted in a smaller distance between the insertion thread and returning thread. Therefore, fewer in-plane fibres were pushed apart by the static thread tension and thus resin pockets in the composite structure were significantly smaller in these composites. The internally placed 1C-type stitch junction was optimal as the stitch induced defects had minimal effect on the tensile properties.

(b) ISO-401 stitched composites have similar tensile properties to ISO-301 stitched composites

As ISO-401 stitching had not been considered for composite reinforcement before this work, it was an important element of this study to benchmark the tensile properties of ISO-401 stitching against composites stitched with the most common stitch reinforcement used in the composite industry, ISO-301 lock-stitch. The stitched composites had lower Young's modulus values than unstitched, the reduction in modulus was similar for both ISO-401and ISO-301 at 2.2 % and 2.6 % respectively. This confirms that whilst stitching can reduce composite stiffness, ISO-401 stitching does not cause significantly more severe reductions compared with the commonly used ISO-301 stitch type. The tensile strength of ISO-301 stitched composites was reduced slightly more so than in ISO-401 stitched composites. On inspection of the composite cross-sections, this was attributed to the 15 % larger resin pockets that occurred in ISO-301 stitched composites, compared with ISO-401 stitched composites. These findings are significant because there are manufacturing advantages associated with ISO-401 stitching that can address some of the limitations associated with ISO-301 stitching. For example, higher productivity can be achieved when employing ISO-401 due to the use of a looper mechanism as opposed to a rotary hook and for ISO-301. Also, in ISO-401, both the looper and needle threads are supplied on industrial sized creels, therefore thread replacement occurs more infrequently compared with ISO-301 where the limited capacity of the bobbin restricts the seam length.

(c) ISO-401 Sewing machinery from the textile industry can be modified for the stitching of FRP composite preforms with glass fibre thread

The Durkopp Adler 173-141621 single needle machine acquired for ISO-401 stitching for this project was primarily developed for the textile industry. It was found in this study that when the sewing thread was changed from polyester to glass fibre, stitches could not be formed properly

due to insufficient friction between the glass fibre stitching thread and glass fibre preform fabric, and the increased needle size and its relationship to the looper mechanism. Therefore, some adjustments to the sewing machine were made to overcome these issues. Firstly, the needle was rotated anti-clockwise by approximately ~2 mm and lowered from its original position by approximately ~3 mm, which resulted in increased friction between the thread, fabric and the needle because the thread was returning at an angle and over a longer distance. Secondly, the looper elipse was retracted back by ~0.5 mm to accommodate the larger needle size. This is significant because the use of existing machinery makes interlaminar stitching an attractive reinforcement technique and this work demonstrates that small modifications can be made to a standard sewing machine to facilitate the production of ISO-401 stitched composites.

(d) ISO-401 stitching improves the damage tolerance of FRP composites

As ISO-401 stitching had not been considered for composite reinforcement before this work, it was important to this thesis to characterise the damage tolerance of ISO-401 stitched composites. Stitching was found to reduce the impact area by up to 41 % and increase the peak impact force at each energy level. Thus, the ISO-401 stitching geometry has worked to suppress damage propagation during impact, creating a more torturous path for the delamination cracks to propagate by asserting a bridging effect. For the impacted composites, stitching improved the compressive strength by up to ~13 %. This can mainly be attributed to the fact that the initial impact damaged area was smaller in stitched specimens and the stitch threads helped to contain the propagation of delamination under loading conditions. Interestingly, stitching slightly reduced the compressive strength of undamaged composites. This indicates that the geometrical defects around the stitch points acted as crack initiation sites.

7.1.2 The effect of the preform fabric properties on ISO-401 stitched composites

(a) The preform fabric properties influence the ISO-401 stitch formation process

When ISO-401 stitching was performed under the same conditions on two similar glass fibre preform fabrics, for example they were the same weight and construction but had different mechanical properties, the stitch junction position was different. When the preform fabric was more stiff and resistant to bending, shear and compression loads the thread junction position was placed further from the needle hole (fabric 2). This is because the preform fabric tows were less

able to be displaced around the stitch threads during stitch formation. It was found that this restricted the thread movement meaning it could not fully retract to pull the looper thread into the needle hole. Whereas when the fabric was less resistant to bending, shear and compression loads (fabric 3), therefore more pliable and easily manipulated during the stitch formation process, the junction was positioned at the optimum position at the needle insertion point. This indicates that more pliable preform fabrics are better suited to achieving the optimum ISO-401 stitch junction position.

(b) The preform fabric characteristics affect the resultant composite fibre volume fraction and Young's modulus

Composites developed from fabric 3 had an increased FVF by 6.2 % because they were compressed and compacted more tightly by the stitching process, compared with composites developed from fabric 2 preforms which had reduced FVF by 5 % because the preforms were more resistant to compression. In line with this, since the tensile properties are a fibre-dominated property, when the FVF was increased (composites type 3) the tensile properties were also improved and similarly when FVF was reduced, as in type 2 composites, the tensile properties were reduced. This is significant because interlaminar stitching can commonly cause a reduction in FVF, thus this work demonstrates that during the composite design process, the preform fabric selection can be made to ensure stitching does not negatively affect the volume fraction of fibres after infusion.

7.2 Concluding Remarks

Interlaminar stitching is a proven technique for the TT reinforcement of composites, however for it to be worthwhile, the out-of-plane properties need to be significantly increased while the in-plane properties should ideally be at least maintained. In reality, it is commonly the case that TT reduces the in-plane properties due to distortions of the reinforcement fibres caused by the stitching process and insertion of z-direction threads. The optimisation of stitching in this thesis has demonstrated that stitching can be adapted for the composite structure to cause less detrimental damage to the in-plane fibres. The novelty of the research has been shown in the employment of a new stitch geometry for the composite industry, ISO-401 double-thread chain-stitch. Overall, the findings from this thesis support that ISO-401 should be considered a suitable reinforcement

type for composites. Moreover, the mechanical properties of composites reinforced with ISO-401 were found to be similar to that of those stitched with a commonly used composite stitch type, modified lock-stitch.

7.3 Recommendations for Further Work

This work has focused on investigating the potential of a new stitch type, ISO-401, for composite reinforcement. Resulting from this study, a number of recommendations for future work are detailed below.

- In this research, the mechanical properties of ISO-401 stitched composites were determined by undertaking tensile, impact and damage tolerance testing. However, other mechanical tests such as interlaminar fracture toughness (Mode I and Mode II) and flexural tests were not carried out as it was beyond the scope of this work. Conducting further mechanical tests and assessing the impact of the different junction positions on these properties would contribute towards achieving a deeper understanding of the properties of stitch-reinforced composites.

- Stitching is not only used as a TT technique for composite panels but also as a joining technique to replace bolts or metal fasteners. A future project could consider the effects of the ISO-401 on the joint properties, compared with ISO-301. This would inform on optimising the ISO-401 stitch junction position specifically for the joining of composite panels.

- For this work, when comparing both ISO-401 and ISO-301 stitching methods, the ISO-401 thread paths were predicted to be less damaging to the sewing threads. This is particularly important when using advanced fibre threads such as glass or carbon due to their brittle nature. Further work could investigate this assumption by using advanced imaging methods such as scanning electron microscopy (SEM) to inspect stitch threads for damage after preform stitching and making comparisons between ISO-401 and ISO-301.

- The composites developed this work were manufactured from biaxial preforms, where the tows were oriented in the 0/90° directions and stitching was always performed in the

0° direction. Future work could consider the effect of ISO-401 stitching on the mechanical properties of multiaxial preforms and stitching in multiple directions.

- In this research, tensile and compression damaged specimens were analysed after ultimate failure using optical microscopy for evidence of damage modes. A future study could utilise a combination of advanced imaging techniques such as SEM and x-ray tomography to gain better understand how damage is formed and propagates in ISO-401 stitched composites under loading conditions. To achieve this, specimens could be loaded to set intervals and removed from the test fixture for imaging investigation.

Reference List

1. Tong, L., 3D fibre reinforced polymer composites , 1st ed., Elsevier, Boston, 2002.

2. Mouritz, A.P.; Cox, B.N., "A mechanistic interpretation of the comparative in-plane mechanical properties of 3D woven, stitched and pinned composites", *Compos. Part A Appl. Sci. Manuf.* **2010**, 41, 709–728. doi:10.1016/j.compositesa.2010.02.001.

3. Reeder, J.R., "Stitching vs. a Toughened Matrix: Compression Strength Effects", *J. Compos. Mater.* **1995**, 29, 2464–2487. doi:10.1177/002199839502901805.

4. Yudhanto, A.; Lubineau, G.; Ventura, I.A.; Watanabe, N.; Iwahori, Y.; Hoshi, H., "Damage characteristics in 3D stitched composites with various stitch parameters under in-plane tension", *Compos. Part A Appl. Sci. Manuf.* **2015**,. doi:10.1016/j.compositesa.2014.12.012.

5. Verma, K.K.; Viswamurthy, S..; Gaddikeri, K.M.; Ramesh, S.; Kumar, S.; Bose, S., "Tufting thread and density controls the mode-I fracture toughness in carbon/epoxy composite", *Compos. Struct.* **2021**, 261, 113272. doi:10.1016/j.compstruct.2020.113272.

6. Prichard, J.C.; Hogg, P.J., "The role of impact damage in post-impact compression testing", *Composites.* **1990**, 21, 503–511. doi:10.1016/0010-4361(90)90423-T.

7. Hassan, M.H.; Othman, A.R.; Kamaruddin, S., "A review on the manufacturing defects of complex-shaped laminate in aircraft composite structures", *Int. J. Adv. Manuf. Technol.* **2017**, 91, 4081–4094. doi:10.1007/s00170-017-0096-5.

8. Potluri, P.; Hogg, P.; Arshad, M.; Jetavat, D.; Jamshidi, P., Influence of fibre architecture on impact damage tolerance in 3D woven composites, in: Appl. Compos. Mater., Springer Netherlands, Dordrecht, 2012: pp. 799–812. doi:10.1007/s10443-012-9256-9.

9. Giurgiutiu, V., Structural health monitoring of aerospace composites, Elsevier Science & Technology, San Diego, 2015. doi:10.1016/C2012-0-07213-4.

10. Mouritz, A.P.; Gallagher, J.; Goodwin, A.A., "Flexural strength and interlaminar shear strength of stitched GRP laminates following repeated impacts", *Compos. Sci. Technol.* **1997**, 57, 509–522. doi:10.1016/S0266-3538(96)00164-9.

11. Dransfield, K.A.; Jain, L.K.; Mai, Y.-W., "On the effects of stitching in CFRPs—I. mode

I delamination toughness", *Compos. Sci. Technol.* **1998**, 58, 815–827. doi:10.1016/S0266-3538(97)00229-7.

12. Trabelsi, W.; Michel, L.; Othomene, R., "Effects of stitching on delamination of satin weave carbon-epoxy laminates under mode I, mode II and mixed-mode I/II loadings", *Appl. Compos. Mater.* **2010**,. doi:10.1007/s10443-010-9128-0.

13. Mouritz, A.P.; Leong, K.H.; Herszberg, I., "A review of the effect of stitching on the in-plane mechanical properties of fibre-reinforced polymer composites", *Compos. Part A Appl. Sci. Manuf.* **1997**,. doi:10.1016/S1359-835X(97)00057-2.

14. Mouritz, A.P.; Bannister, M.K.; Falzon, P.J.; Leong, K.H., "Review of applications for advanced three-dimensional fibre textile composites", *Compos. Part A Appl. Sci. Manuf.* **1999**, 30, 1445–1461. doi:10.1016/S1359-835X(99)00034-2.

15. Zhao, N.; Rödel, H.; Herzberg, C.; Gao, S.L.; Krzywinski, S., "Stitched glass/PP composite. Part I: Tensile and impact properties", *Compos. Part A Appl. Sci. Manuf.* **2009**, 40, 635–643. doi:10.1016/j.compositesa.2009.02.019.

16. Tan, K.T.; Watanabe, N.; Iwahori, Y., "Effect of stitch density and stitch thread thickness on low-velocity impact damage of stitched composites", *Compos. Part A Appl. Sci. Manuf.* **2010**, 41, 1857–1868. doi:10.1016/j.compositesa.2010.09.007.

17. Mouritz, A.P.; Cox, B.N., "A mechanistic approach to the properties of stitched laminates", *Compos. Part A.* **2000**, 31, 1–27.

18. Xuan, J.-Q.; Li, D.-S.; Jiang, L., "Fabrication, properties and failure of 3D stitched carbon/epoxy composites with no stitching fibers damage", *Compos. Struct.* **n.d.**, 220, 602–607. doi:10.1016/j.compstruct.2019.03.080.

19. Karahan, M.; Ulcay, Y.; Eren, R.; Karahan, N.; Kaynak, G., "Investigation into the Tensile Properties of Stitched and Unstitched Woven Aramid/Vinyl Ester Composites", *Text. Res. J.* **2010**, 80, 880–891. doi:10.1177/0040517509346441.

20. Karahan, M.; Ulcay, Y.; Karahan, N.; Kuş, A., "Influence of stitching parameters on tensile strength of aramid/vinyl ester composites", *Medziagotyra*. **2013**, 19, 67–72. doi:10.5755/j01.ms.19.1.3829.

21. Göktaş, D.; Kennon, W.R.; Potluri, P., "Improvement of Mode I Interlaminar Fracture Toughness of Stitched Glass/Epoxy Composites", *Appl. Compos. Mater.* **2017**,.

doi:10.1007/s10443-016-9560-x.

22. Kaya, G.; Soutis, C.; Potluri, P., "Tensile Properties of a Novel Graphene Pattern Stitched Carbon/Epoxy 3D Composite", *IOP Conf. Ser. Mater. Sci. Eng.* **2018**, 460, 012015. doi:10.1088/1757-899X/460/1/012015.

23. Paul, D.; Kelly, L.; Venkayya, V.; Hess, T., "Evolution of U.S. military aircraft structures technology", *J. Aircr.* **2002**, 39, 18–29. doi:10.2514/2.2920.

24. Ogale, A.; Mitschang, P., "Tailoring of textile preforms for fibre-reinforced polymer composites", *J. Ind. Text.* **2004**, 34, 77–96. doi:10.1177/1528083704046949.

25. Yudhanto, A.; Watanabe, N.; Iwahori, Y.; Hoshi, H., "Compression properties and damage mechanisms of stitched carbon/epoxy composites", *Compos. Sci. Technol.* **2013**, 86, 52–60. doi:10.1016/j.compscitech.2013.07.002.

26. Kirmasha, Y.K.; Sharba, M.J.; Leman, Z.; Sultan, M.T.H., "Mechanical performance of unstitched and silk fiber-stitched woven kenaf fiber-reinforced Epoxy composites", *Materials (Basel).* **2020**, 13, 1–16. doi:10.3390/ma13214801.

27. Mitschang, P.; Ogale, A., "Effect of sewing threads on interlaminar shear strength and flexural bending strength of stitched non-crimp carbon fabric laminates", *Adv. Compos. Lett.* **2006**, 15, 199–206. doi:10.1177/096369350601500602.

28. Aymerich, F.; Pani, C.; Priolo, P., "Effect of stitching on the low-velocity impact response of [03/903]s graphite/epoxy laminates", *Compos. Part A Appl. Sci. Manuf.* **2007**, 38, 1174–1182. doi:10.1016/J.COMPOSITESA.2006.06.005.

29. Francesconi, L.; Aymerich, F., "Impact damage resistance of thin stitched carbon/epoxy laminates", *J. Phys. Conf. Ser.* **2015**, 628, 12099. doi:10.1088/1742-6596/628/1/012099.

30. Tan, K.T.; Watanabe, N.; Iwahori, Y., "Impact Damage Resistance, Response, and Mechanisms of Laminated Composites Reinforced by Through-Thickness Stitching", *Int. J. Damage Mech.* **2012**, 21, 51–80. doi:10.1177/1056789510397070.

31. Bilisik, K.; Yolacan, G., "Warp and weft directional tensile properties of multistitched biaxial woven E-glass/polyester composites", *J. Text. Inst.* **2014**, 105, 1014–1028. doi:10.1080/00405000.2013.869433.

32. Deconinck, P.; Capelle, J.; Bouchart, V.; Chevrier, P.; Ravailler, F., "Delamination

propagation analysis in tufted carbon fibre-reinforced plastic composites subjected to high-velocity impact", *J. Reinf. Plast. Compos.* **2014**, 33, 1353–1363. doi:10.1177/0731684414533017.

33. Dell'anno, G.; Cartié, D.D.; Partridge, I.K.; Rezai, A., "Exploring mechanical property balance in tufted carbon fabric/epoxy composites", *Compos. Part A.* **2007**, 38, 2366–2373. doi:10.1016/j.compositesa.2007.06.004.

34. Liu, L.S.; Zhang, T.; Wang, P.; Legrand, X.; Soulat, D., "Influence of the tufting yarns on formability of tufted 3-Dimensional composite reinforcement", *Compos. Part A Appl. Sci. Manuf.* **2015**, 78, 403–411. doi:10.1016/j.compositesa.2015.07.014.

35. Cui, H.; Melro, A.R.; Yasaee, M., "Inter-fibre failure of through-thickness reinforced laminates in combined transverse compression and shear load", *Compos. Sci. Technol.* **2018**,. doi:10.1016/j.compscitech.2018.06.011.

36. Mouritz, A.P., "Review of z-pinned composite laminates", *Compos. Part A Appl. Sci. Manuf.* **2007**, 38, 2383–2397. doi:10.1016/j.compositesa.2007.08.016.

37. Francesconi, L.; Aymerich, F., "Effect of Z-pinning on the impact resistance of composite laminates with different layups", *Compos. Part A Appl. Sci. Manuf.* **2018**, 114, 136–148. doi:10.1016/j.compositesa.2018.08.013.

38. Hamouda, T.; Seyam, A.-F.; Peters, K., "Evaluation of the Integrity of 3D Orthogonal Woven Composites with Embedded Polymer Optical Fibers", *Compos. Part B.* **2015**, 78, 79–85. doi:10.1016/j.compositesb.2015.03.092.

39. Ahmed, S.; Zheng, X.; Zhang, D.; Yan, L., "Impact Response of Carbon/Kevlar Hybrid 3D Woven Composite Under High Velocity Impact: Experimental and Numerical Study", *Appl. Compos. Mater.* **2020**, 27, 285–305. doi:10.1007/s10443-020-09809-3.

40. Dau, F.; Dano, M.L.; Duplessis-Kergomard, Y., "Experimental investigations and variability considerations on 3D interlock textile composites used in low velocity soft impact loading", *Compos. Struct.* **2016**, 153, 369–379. doi:10.1016/j.compstruct.2016.06.034.

41. Hu, Q.; Memon, H.; Qiu, Y.; Liu, W.; Wei, Y., "A comprehensive study on the mechanical properties of different 3d woven carbon fiber-epoxy composites", *Materials (Basel).* **2020**, 13, 1–13. doi:10.3390/ma13122765.

42. Rong, M.Z.; Zhang, M.Q.; Liu, Y.; Zhang, Z.W.; Yang, G.C.; Zeng, H.M., "Effect of Stitching on In-Plane and Interlaminar Properties of Sisal/Epoxy Laminates", *J. Compos. Mater.* **2002**, 36, 1505–1526. doi:10.1177/0021998302036012163.

43. Wood, M.D.K.; Sun, X.; Tong, L.; Katzos, A.; Rispler, A.R.; Mai, Y.W., "The effect of stitch distribution on Mode I delamination toughness of stitched laminated composites - experimental results and FEA simulation", *Compos. Sci. Technol.* **2007**, 67, 1058–1072. doi:10.1016/j.compscitech.2006.06.002.

44. Bilisik, K.; Yolacan, G., "Off-axis tensile properties of multistitched plain woven E-glass/polyester composites", *Fibers Polym.* **2014**, 15, 589–598. doi:10.1007/s12221-014-0589-x.

45. Yudhanto, A.; Watanabe, N.; Iwahori, Y.; Hoshi, H., "Effect of stitch density on fatigue characteristics and damage mechanisms of stitched carbon/epoxy composites", *Compos. Part A Appl. Sci. Manuf.* **2014**,. doi:10.1016/j.compositesa.2014.01.013.

46. Bilisik, K.; Kaya, G., "Tensile/Shear Behaviour of Multi-stitched/Nano Composites", *J. Electron. Mater.* **2017**, 46, 3987–3994. doi:10.1007/s11664-017-5365-4.

47. Kang, T.J.; Lee, S.H., "Effect of Stitching on the Mechanical and Impact Properties of Woven Laminate Composite", *J. Compos. Mater.* **1994**, 28, 1574–1587. doi:10.1177/002199839402801604.

48. Mahato, K.K.; Dutta, K.; Ray, B.C., "Static and Dynamic Behavior of Fibrous Polymeric Composite Materials at Different Environmental Conditions", *J. Polym. Environ.* **2018**, 26, 1024–1050. doi:10.1007/s10924-017-1001-x.

49. Mahato, K.K.; Biswal, M.; Rathore, D.K.; Prusty, R.K.; Dutta, K.; Ray, B.C., Effect of loading rate on tensile properties and failure behavior of glass fibre/epoxy composite, in: IOP Conf. Ser. Mater. Sci. Eng., 2016: p. 12017. doi:10.1088/1757-899X/115/1/012017.

50. Goktas, Devrim, Potluri, Prasad & Kennon, R., Orthogonal Stitching of 2D Fabrics for Improved Delamination Resistance., in: ICCM19. Can. Assoc. Compos. Struct. Mater., Montreal, 2013: pp. 7984–7991.

51. Weimer, C.; Mitschang, P., "Aspects of the stitch formation process on the quality of sewn multi-textile-preforms", *Compos. - Part A Appl. Sci. Manuf.* **2001**, 32, 1477–1484. doi:10.1016/S1359-835X(01)00046-X.

52. Tan, K.T.; Watanabe, N.; Iwahori, Y., "X-ray radiography and micro-computed tomography examination of damage characteristics in stitched composites subjected to impact loading", *Compos. Part B.* **2011**, 42, 874–884. doi:10.1016/j.compositesb.2011.01.011.

53. Tan, K.T.; Watanabe, N.; Sano, M.; Iwahori, Y.; Hoshi, H., "Interlaminar Fracture Toughness of Vectran-stitched Composites - Experimental and Computational Analysis", *J. Compos. Mater.* **2010**, 44, 3203–3229. doi:10.1177/0021998310369581.

54. Tan, K.T.; Watanabe, N.; Iwahori, Y., "X-ray radiography and micro-computed tomography examination of damage characteristics in stitched composites subjected to impact loading", *Compos. Part B Eng.* **2011**,. doi:10.1016/j.compositesb.2011.01.011.

55. Tao, A.; Wang, R.; Wang, Z.; Zhao, P.; Yan, X., "The influence of surface treatment of stitch threads and stitching on interlaminar properties of unidirectional laminates", *Compos. Interfaces*. **2016**, 23, 373–382. doi:10.1080/09276440.2016.1141591.

56. Rana, S.; Fangueiro, R., Advanced Composite Materials for Aerospace Engineering, Elsevier Science & Technology, Cambridge, 2016. doi:10.1016/c2014-0-00846-5.

57. Vasiliev, V. V.; Morozov, E. V., Advanced Mechanics of Composite Materials, 2nd ed., Elsevier, Amsterdam ;, 2007. doi:10.1016/B978-0-08-045372-9.X5000-3.

58. Elkazaz, E.; Crosby, W.A.; Ollick, A.M.; Elhadary, M., "Effect of fiber volume fraction on the mechanical properties of randomly oriented glass fiber reinforced polyurethane elastomer with crosshead speeds", *Alexandria Eng. J.* **2020**, 59, 209–216. doi:10.1016/j.aej.2019.12.024.

59. Jones, I.A.; Pickett, A.K., Mechanical properties of textile composites, in: Des. Manuf. Text. Compos., 2005: pp. 292–329. doi:10.1533/9781845690823.292.

60. Richardson, M.O.W.; Wisheart, M.J., "Review of low-velocity impact properties of composite materials", *Compos. Part A Appl. Sci. Manuf.* **1996**, 27, 1123–1131. doi:10.1016/1359-835X(96)00074-7.

61. Muraganandhan; Murali, V., Mode-I fracture and impact analysis on stitched and unstitched glass/epoxy composite laminate, in: Procedia Eng., 2012. doi:10.1016/j.proeng.2012.06.265.

62. Kadir, B.; Huseyin, O.; Gaye, K., "Development Of Multistitched Three-Dimensional (3D)

Nanocomposite And Evaluation Of Its Mechanical And Impact Properties", *Autex Res. J.* **2017**, 17, 238–249. doi:10.1515/aut-2016-0008.

63. Stig, F.; Hallström, S., "Effects of crimp and textile architecture on the stiffness and strength of composites with 3D reinforcement", *Adv. Mater. Sci. Eng.* **2019**, 2019, 1–8. doi:10.1155/2019/8439530.

64. Huang, T.; Wang, Y.; Wang, G., "Review of the Mechanical Properties of a 3D Woven Composite and Its Applications", *Polym. - Plast. Technol. Eng.* **2018**, 57, 740–756. doi:10.1080/03602559.2017.1344857.

65. Rudov-Clark, S.; Mouritz, A..; Lee, L.; Bannister, M.., "Fibre damage in the manufacture of advanced three-dimensional woven composites", *Compos. Part A. Appl. Sci. Manuf.* **2003**, 34, 963–970. doi:10.1016/S1359-835X(03)00213-6.

66. Needels, J.T.; Gage, P.J.; Ellerby, D.T.; Venkatapathy, E.; Peterson, K.H.; Vander Kam, J.C., Application of Risk Informed Decision Making to a Highly Reliable Three Dimensionally Woven Thermal Protection System for Mars Sample Return, American Institute of Aeronautics and Astronautics, 2020. doi:doi:10.2514/6.2020-0709.

67. Feldman, Jay; Ellerby, Don; Stackpoole, Mairead; Peterson, Keith; Venkatapathy, E., Development of 3D Woven Ablative Thermal Protection Systems (TPS) for NASA Spacecraft, 2015. doi:doi:10.2514/6.2020-0709.

68. Knaupp, M.; Baudach, F.; Franck, J.; Scharr, G., "Impact and post-impact properties of cfrp laminates reinforced with rectangular z-pins", *Compos. Sci. Technol.* **2013**, 87, 218–223. doi:10.1016/j.compscitech.2013.08.018.

69. Partridge, I.K.; Cartié, D.D.., "Delamination resistant laminates by Z-Fiber® pinning: Part I manufacture and fracture performance", *Compos. Part A Appl. Sci. Manuf.* **2005**, 36, 55–64. doi:10.1016/j.compositesa.2004.06.029.

70. Pingkarawat, K.; Mouritz, A.P., "Improving the mode I delamination fatigue resistance of composites using z-pins", *Compos. Sci. Technol.* **2014**, 92, 70–76. doi:10.1016/j.compscitech.2013.12.009.

71. Hoffmann, J.; Scharr, G., "Mode I delamination fatigue resistance of unidirectional and quasi-isotropic composite laminates reinforced with rectangular z-pins", *Compos. Part A. Appl. Sci. Manuf.* **2018**, 115, 228–235. doi:10.1016/j.compositesa.2018.10.013.

72. Pegorin, F.; Pingkarawat, K.; Mouritz, A.., "Mixed-mode I/II delamination fatigue strengthening of polymer composites using z-pins", *Compos. Part B, Eng.* **2017**, 123, 219–226. doi:10.1016/j.compositesb.2017.05.016.

73. Dell'Anno, G.; Treiber, J.W.G.; Partridge, I.K., "Manufacturing of composite parts reinforced through-thickness by tufting", *Robot. Comput. Integr. Manuf.* **2016**, 37, 262–272. doi:10.1016/j.rcim.2015.04.004.

74. Gnaba, I.; Legrand, X.; Wang, P.; Soulat, D., "Through-the-thickness reinforcement for composite structures: A review", *J. Ind. Text.* **2018**, <xocs:firstpage xmlns:xocs=""/>. doi:10.1177/1528083718772299.

75. Colin de Verdiere, M.; Skordos, A.A.; May, M.; Walton, A.C., "Influence of loading rate on the delamination response of untufted and tufted carbon epoxy non crimp fabric composites: Mode I", *Eng. Fract. Mech.* **2012**, 96, 11–25. doi:10.1016/j.engfracmech.2012.05.015.

76. Park, B.Y.; Kim, S.C.; Jung, B., "Interlaminar fracture toughness of carbon fiber/epoxy composites using short Kevlar fiber and/or Nylon-6 powder reinforcement", *Polym. Adv. Technol.* **1997**, 8, 371–377. doi:10.1002/(SICI)1099-1581(199706)8:6<371::AID-PAT658>3.0.CO;2-I.

77. Colin de Verdiere, M.; Skordos, A.A.; Walton, A.C.; May, M., "Influence of loading rate on the delamination response of untufted and tufted carbon epoxy non-crimp fabric composites/Mode II", *Eng. Fract. Mech.* **2012**, 96, 1–10. doi:10.1016/j.engfracmech.2011.12.011.

78. Martins, A..; Aboura, Z.; Harizi, W.; Laksimi, A.; Khellil, K., "Analysis of the impact and compression after impact behavior of tufted laminated composites", *Compos. Struct.* **2018**, 184, 352–361. doi:10.1016/j.compstruct.2017.09.096.

79. Carvelli, V.; Koissin, V.; Kustermans, J.; Lomov, S. V.; Tomaselli, V.N.; Van Den Broucke, B.; Verpoest, I.; Witzel, V., Progressive damage in stitched composites: Static tensile tests and tension-tension fatigue, in: ICCM Int. Conf. Compos. Mater., 2009.

80. Farley, G.L.; Dickinson, L.C., "Removal of Surface Loop from Stitched Composites Can Improve Compression and Compression-after-Impact Strengths", *J. Reinf. Plast. Compos.* **1992**, 11, 633–642. doi:10.1177/073168449201100604.

81. Hayes, S.; Mcloughlin, J., 3 – The sewing of textiles, in: Join. Text., 2013: pp. 62–122. doi:10.1533/9780857093967.1.62.

82. British Standards Online, "Stitches and seams. Classification and terminology of seam types BS 3870-2:1991, ISO 4916:1991", *BSI Online*. **1991**,.

83. Tyler, D.J., Carr and Latham's Technology of Clothing Manufacture, 4th ed., Wiley, Hoboken, 2009.

84. Hosur, M. V; Karim, M.R.; Jeelani, S., "Studies on Stitched Woven S2 Glass/Epoxy Laminates under Low Velocity and Ballistic Impact Loading", *J. Reinf. Plast. Compos.* **2004**, 23, 1313–1323. doi:10.1177/0731684404037048.

85. Colovic, G., Sewing, stitches and seams, in: Garment Manuf. Technol., Elsevier, 2015: pp. 247–273. doi:10.1016/B978-1-78242-232-7.00010-2.

86. Stylios, G.K., The mechanics of stitching, in: Join. Text. Princ. Appl., 2013: pp. 47–61. doi:10.1533/9780857093967.1.47.

87. Carvalho, M.; Carvalho, H.; Silva, L.F., Problems relating to sewing, in: Join. Text. Princ. Appl., 2013: pp. 149–174. doi:10.1533/9780857093967.1.149.

88. Jones, I.; Stylios, G.K., Introduction, in: Join. Text., 2013: pp. xxvii–xxix. doi:10.1016/B978-1-84569-627-6.50025-1.

89. Jana, P., Sewing equipment and work aids, in: Garment Manuf. Technol., Elsevier, 2015: pp. 275–315. doi:10.1016/B978-1-78242-232-7.00011-4.

90. Chen, A.; Zou, H.-J.; Du, R., "Modeling of Industrial Sewing Machines and the Balancing of Thread Requirement and Thread Supply", *J. Text. Inst. Issue 3, Parts 1 3*. **2001**, 92, 256–268. doi:10.1080/00405000108659575.

91. Dransfield, K.; Baillie, C.; Mai, Y.W., "Improving the delamination resistance of CFRP by stitching-a review", *Compos. Sci. Technol.* **1994**, 50, 305–317. doi:10.1016/0266-3538(94)90019-1.

92. Koissin, V.; Kustermans, J.; Lomov, S. V.; Verpoest, I.; Van Den Broucke, B.; Witzel, V., "Structurally stitched NCF preforms: Quasi-static response", *Compos. Sci. Technol.* **2009**, 69, 2701–2710. doi:10.1016/j.compscitech.2009.08.015.

93. Zajaczkowski, J., "Effect of belt extensibility on variation of the relative position of a

needle and a hook in a sewing machine", *Int. J. Cloth. Sci. Technol.* **2000**, 12, 303–310. doi:10.1108/09556220010377841.

94. Dal, V.; Yargıcı, M.E.; Salman, S., "Analyzing The Effects Of Sewing Machine Needle Coating Materials On The Needle's Heating During Sewing", *Ege Univ. J. Text. Appar.* **2014**, 24,.

95. Stjepanovič, Z.; Strah, H., "Selection of suitable sewing needle using machine learning techniques", *Int. J. Cloth. Sci. Technol.* **1998**, 10, 209–218. doi:10.1108/09556229810693582.

96. Carvalho, M.; Rocha, A.M.; Carvalho, H., "Comparative Study of Needle Penetration Forces in Sewing Hems on Toweling Terry Fabrics: Influence of Needle Type and Size", *Autex Res. J.* **2020**, 20, 194–202. doi:10.2478/aut-2019-0047.

97. Manziuk, E., "Influence of geometric parameters of the rotary hook on interaction of its elements in high-speed modes sewing machine", *Int. J. Cloth. Sci. Technol.* **2018**, 30, 828–838. doi:10.1108/IJCST-04-2018-0053.

98. Kennon, W.R.; Hayes, S.G., "The Effects of Feed Retardation on Lockstitch Sewing", *J. Text. Inst.* **2000**, 91, 509–522. doi:10.1080/00405000008659124.

99. Žunič-Lojen, D.; Geršak, J., "Thread Loadings in Different Measuring Positions on the Sewing Machine", *Text. Res. J.* **2005**, 75, 498–506. doi:10.1177/0040517505053870.

100. Carvalho, H.; Silva, L.F.; Rocha, A.; Monteiro, J., "Automatic presser-foot force control for industrial sewing machines", *Int. J. Cloth. Sci. Technol.* **2012**, 24, 36–55. doi:10.1108/09556221211194336.

101. Clapp, T.G.; Little, T.J.; Thiel, T.M.; Vass, D.J., "Sewing dynamics: objective measurement of fabric/machine interaction", *Int. J. Cloth. Sci. Technol.* **1992**, 4, 45–53. doi:10.1108/eb002993.

102. Tan, K.T.; Yoshimura, A.; Watanabe, N.; Iwahori, Y.; Ishikawa, T., "Effect of stitch density and stitch thread thickness on damage progression and failure characteristics of stitched composites under out-of-plane loading", *Compos. Sci. Technol.* **2013**, 74, 194–204. doi:10.1016/j.compscitech.2012.11.001.

103. Lomov, S. V.; Belov, E.B.; Bischoff, T.; Ghosh, S.B.; Truong Chi, T.; Verpoest, I., "Carbon composites based on multiaxial multiply stitched preforms. Part 1. Geometry of

the preform", *Compos. Part A Appl. Sci. Manuf.* **2002**, 33, 1171–1183. doi:10.1016/S1359-835X(02)00090-8.

104. Beier, U.; Fischer, F.; Sandler, J.K.W.; Altstädt, V.; Weimer, C.; Buchs, W., "Mechanical performance of carbon fibre-reinforced composites based on stitched preforms", *Compos. Part A Appl. Sci. Manuf.* **2007**,. doi:10.1016/j.compositesa.2007.02.007.

105. Mohsin, M.A..; Iannucci, L.; Greenhalgh, E.., "Fibre-volume-fraction measurement of carbon fibre reinforced thermoplastic composites using thermogravimetric analysis", *Heliyon*. **2019**, 5, e01132–e01132. doi:10.1016/j.heliyon.2019.e01132.

106. Tan, K.T.; Watanabe, N.; Iwahori, Y.; Ishikawa, T., "Understanding effectiveness of stitching in suppression of impact damage: An empirical delamination reduction trend for stitched composites", *Compos. Part A.* **2012**, 43, 823–832. doi:10.1016/j.compositesa.2011.12.022.

107. Tan, K.T.; Watanabe, N.; Iwahori, Y.; Ishikawa, T., "Effect of stitch density and stitch thread thickness on compression after impact strength and response of stitched composites", *Compos. Sci. Technol.* **2012**, 72, 587–598. doi:10.1016/j.compscitech.2012.01.003.

108. Aktas, A.; Potluri, P.; Porat, I., "Development of through-thickness reinforcement in advanced composites incorporating rigid cellular foams", *Appl. Compos. Mater.* **2013**,. doi:10.1007/s10443-012-9285-4.

109. Lee, J.S.; Hong, S.J.; Yu, W.R.; Kang, T.J., "The effect of blank holder force on the stamp forming behavior of non-crimp fabric with a chain stitch", *Compos. Sci. Technol.* **2007**, 67, 357–366. doi:10.1016/j.compscitech.2006.09.009.

110. Chen, S.; McGregor, O.P.L.; Harper, L.T.; Endruweit, A.; Warrior, N.A., "Defect formation during preforming of a bi-axial non-crimp fabric with a pillar stitch pattern", *Compos. Part A Appl. Sci. Manuf.* **2016**, 91, 156–167. doi:10.1016/j.compositesa.2016.09.016.

111. Ahmed, U.; Tariq, A.; Nawab, Y.; Shaker, K.; Khaliq, Z.; Umair, M., "Comparison of Mechanical Behavior of Biaxial, Unidirectional and Standard Woven Fabric Reinforced Composites", *Fibers Polym.* **2020**, 21, 1308–1315. doi:10.1007/s12221-020-9915-7.

112. Hayes, S.G., "THE EFFECTS OF CHECK-SPRING TRAVEL ON LOCKSTITCH

SEWING", *Res. J. Text. Appar.* **2001**, 5, 54–64. doi:10.1108/RJTA-05-02-2001-B006.

113. Corporation, U.S., Union Special Lockstitch Formation Type 301, 1980.

114. Goktas, D., "INTERLAMINAR PROPERTIES OF 3D TEXTILE COMPOSITES", **2016**,.

115. Waddington, B., "Influence of 3D Preform Construction on Composite Damage Tolerance: Stitching and 3D Weaving", **2019**,.

116. Stylios, G., Prognosis of sewability problems in garment manufacture using computer-based technology, in: 1990 IEEE Int. Conf. Syst. Eng., 1990: pp. 371–373. doi:10.1109/ICSYSE.1990.203174.

117. Behera, B..; Chand, S.; Singh, T..; Rathee, P., "Sewability of denim", *Int. J. Cloth. Sci. Technol.* **1997**, 9, 128–140. doi:10.1108/09556229710168261.

118. Raj, D.V.K.; Devi, M.R., "Performance analysis of the mechanical behaviour of seams with various sewing parameters for nylon canopy fabrics", *Int. J. Cloth. Sci. Technol.* **2017**, 29, 470–482. doi:10.1108/IJCST-05-2016-0054.

119. Jankoska, M. and Demboski, G., "THE INFLUENCE OF THE SEWING SPEED AND FABRIC THICKNESS ON SEWING MACHINE STITCH FORMATION PARAMETERS", *Adv. Technol.* **2017**, 6, 72–77.

120. Alagha, M.J.; Amirbayat, J.; Porat, I., "A Study of Positive Needle Thread Feed during Chainstitch Sewing", *J. Text. Inst. Issue 2, Parts 1 2*. **1996**, 87, 389–395. doi:10.1080/00405009608659090.

121. Jaouachi, B.; Khedher, F.; Adolphe, D., "Compared basic stitch's consumptions using image analysis, geometrical modelling and statistical techniques", *J. Text. Inst.* **2019**, 110, 1280–1292. doi:10.1080/00405000.2018.1559016.

122. Groz-Beckert, Stitch Type 401: Double Chainstitch, GroZ-Beckert, 2020. https://www.youtube.com/watch?v=MfkKF28get0.

123. Brad, R.; Barac, L.; Brad, R., "Defect Detection Techniques for Airbag Production Sewing Stages", *J. Text.* **2014**, 2014, 1–7. doi:10.1155/2014/738504.

124. Hogg, P.J.; Bibo, G.A., 10 - Impact and damage tolerance, in: J.M.B.T.-M.T. of A.F.C. Hodgkinson (Ed.), Woodhead Publ. Ser. Compos. Sci. Eng., Woodhead Publishing, 2000: pp. 211–247. doi:https://doi.org/10.1533/9781855738911.211.

125. Hull, D.; Shi, Y.B., "Damage mechanism characterization in composite damage tolerance investigations", *Compos. Struct.* **1993**, 23, 99–120. doi:10.1016/0263-8223(93)90015-I.

126. Abir, M.R.; Tay, T.E.; Ridha, M.; Lee, H.P., "Modelling damage growth in composites subjected to impact and compression after impact", *Compos. Struct.* **2017**, 168, 13–25. doi:10.1016/j.compstruct.2017.02.018.

127. Erdogan, G.; Bilisik, K., "Compression after low-velocity impact (CAI) properties of multistitched composites", *Mech. Adv. Mater. Struct.* **2018**, 25, 623–636. doi:10.1080/15376494.2017.1308601.

128. Aktaş, A.; Aktaş, M.; Turan, F., "Impact and post impact (CAI) behavior of stitched woven-knit hybrid composites", *Compos. Struct.* **2014**, 116, 243–253. doi:10.1016/j.compstruct.2014.05.024.

129. Hodgkinson, J.M., Mechanical testing of advanced fibre composites, Elsevier Science & Technology, Cambridge, 2000. doi:10.1533/9781855738911.

130. Francesconi, L.; Aymerich, F., Impact damage resistance of thin stitched carbon/epoxy laminates, in: J. Phys. Conf. Ser., 2015: p. 12099. doi:10.1088/1742-6596/628/1/012099.

131. Verma, L.; Jefferson Andrew, J.; Sivakumar, S.M.; Balaganesan, G.; Vedantam, S.; Dhakal, H.N., "Compression after high-velocity impact behavior of pseudo-elastic shape memory alloy embedded glass/epoxy composite laminates", *Compos. Struct.* **2021**, 259, 113519. doi:10.1016/j.compstruct.2020.113519.

132. Tan, K.T.; Yoshimura, A.; Watanabe, N.; Iwahori, Y.; Ishikawa, T., "Effect of stitch density and stitch thread thickness on damage progression and failure characteristics of stitched composites under out-of-plane loading", *Compos. Sci. Technol.* **2013**,. doi:10.1016/j.compscitech.2012.11.001.

133. Bilisik, K.; Yolacan, G., "Experimental characterization of multistitched two-dimensional (2D) woven E-glass/polyester composites under low-velocity impact load", *J. Compos. Mater.* **2014**, 48, 2145–2162. doi:10.1177/0021998313494918.

134. Wu, E.; Wang, J., "Behavior of Stitched Laminates under In-Plane Tensile and Transverse Impact Loading", *J. Compos. Mater.* **1995**, 29, 2254–2279. doi:10.1177/002199839502901702.

135. Cartié, D.D.R.; Irving, P.E., "Effect of resin and fibre properties on impact and

compression after impact performance of CFRP", *Compos. - Part A Appl. Sci. Manuf.* **2002**, 33, 483–493. doi:10.1016/S1359-835X(01)00141-5.

136. Soutis, C., "Measurement of the static compressive strength of carbon-fibre/epoxy laminates", *Compos. Sci. Technol.* **1991**, 42, 373–392. doi:10.1016/0266-3538(91)90064-V.

137. Liu, X.H.; Moran, P.M.; Shih, C.F., "The mechanics of compressive kinking in unidirectional fiber reinforced ductile matrix composites", *Compos. Part B Eng.* **1996**, 27, 553–560. doi:10.1016/S1359-8368(96)00008-X.

138. Moran, P.M.; Liu, X.H.; Shih, C.F., "Kink band formation and band broadening in fiber composites under compressive loading", *Acta Metall. Mater.* **1995**, 43, 2943–2958. doi:10.1016/0956-7151(95)00001-C.

139. Wang, Y.; Emerson, M.J.; Conradsen, K.; Dahl, A.B.; Dahl, V.A.; Maire, E.; Withers, P., "Evolution of Fibre Deflection Leading to Kink-band Formation in Unidirectional Glass Fibre/Epoxy Composite Under Axial Compression", **2021**,.

140. Wang, Y.; Chai, Y.; Soutis, C.; Withers, P.J., "Evolution of kink bands in a notched unidirectional carbon fibre-epoxy composite under four-point bending", *Compos. Sci. Technol.* **2019**, 172, 143–152. doi:10.1016/j.compscitech.2019.01.014.

141. Wang, Y.; Burnett, T.L.; Chai, Y.; Soutis, C.; Hogg, P.J.; Withers, P.J., "X-ray computed tomography study of kink bands in unidirectional composites", *Compos. Struct.* **2017**, 160, 917–924. doi:10.1016/j.compstruct.2016.10.124.

142. Pimenta, S.; Gutkin, R.; Pinho, S.T.; Robinson, P., "A micromechanical model for kink-band formation: Part I - Experimental study and numerical modelling", *Compos. Sci. Technol.* **2009**, 69, 948–955. doi:10.1016/j.compscitech.2009.02.010.

143. Leopold, C.; Harder, S.; Philipkowski, T.; Liebig, W. V; Fiedler, B., "Comparison of analytical approaches predicting the compressive strength of fibre reinforced polymers", *Materials (Basel).* **2018**, 10, 2517. doi:10.3390/ma11122517.

144. Wang, Ying; Garcea, Serafina; Lowe, Tristan; Maire, Eric; Soutis, Constantinos; Withers, P., Ultra-fast time-lapse synchrotron radiographic imaging of compressive failure in CFRP., in: 17th Eur. Conf. Compos. Mater., 2016.

145. Erdogan, G.; Bilisik, K., "Compression after low-velocity impact (CAI) properties of

multistitched composites", *Mech. Adv. Mater. Struct.* **2018**, 25, 623–636. doi:10.1080/15376494.2017.1308601.

146. Tan, K.T.; Watanabe, N.; Iwahori, Y., "Finite element model for compression after impact behaviour of stitched composites", *Compos. Part B Eng.* **2015**,. doi:10.1016/j.compositesb.2015.04.022.

147. Tan, Y.; Wu, G.; Suh, S.S.; Yang, J.M.; Hahn, H.T., "Damage tolerance and durability of selectively stitched stiffened composite structures", *Int. J. Fatigue*. **2008**, 30, 483–492. doi:10.1016/j.ijfatigue.2007.04.008.

148. Aymerich, F.; Priolo, P., "Characterization of fracture modes in stitched and unstitched cross-ply laminates subjected to low-velocity impact and compression after impact loading", *Int. J. Impact Eng.* **2008**, 35, 591–608. doi:10.1016/j.ijimpeng.2007.02.009.

149. Aymerich, F.; Onnis, R.; Priolo, P., "Analysis of the effect of stitching on the fatigue strength of single-lap composite joints", *Compos. Sci. Technol.* **2006**, 66, 166–175. doi:10.1016/j.compscitech.2005.04.023.

150. Godwin, E.W., 4 - Tension, in: J.M.B.T.-M.T. of A.F.C. Hodgkinson (Ed.), Woodhead Publ. Ser. Compos. Sci. Eng., Woodhead Publishing, 2000: pp. 43–74. doi:https://doi.org/10.1533/9781855738911.43.

151. Adrian P. Mouritz, 15 - Fibre–polymer composites for aerospace structures and engines, in: Introd. to Aerosp. Mater., Elsevier Ltd, 2012: pp. 338–393. doi:10.1533/9780857095152.338.

152. Tan, K.T.; Watanabe, N.; Iwahori, Y.; Ishikawa, T., "Understanding effectiveness of stitching in suppression of impact damage: An empirical delamination reduction trend for stitched composites", *Compos. Part A Appl. Sci. Manuf.* **2012**,. doi:10.1016/j.compositesa.2011.12.022.

153. Yudhanto, A.; Watanabe, N.; Iwahori, Y.; Hoshi, H., "The effects of stitch orientation on the tensile and open hole tension properties of carbon/epoxy plain weave laminates", *Mater. Des.* **2012**, 35, 563–571. doi:10.1016/j.matdes.2011.09.013.

154. Hu, H.; Zhang, M.; Fangueiro, R.; De Araujo, M., "Mechanical Properties of Composite Materials Made of 3D Stitched Woven-knitted Preforms", *J. Compos. Mater.* **2010**, 44, 1753–1767. doi:10.1177/0021998309359211.

155. Joshi, P.; Kondo, A.; Watanabe, N., "Progressive failure analysis of carbon-fibre/epoxy composites laminates to study the effect of stitch densities under in-plane tensile loading", *Plast. Rubber Compos.* **2017**, 1–8. doi:10.1080/14658011.2017.1300124.

156. Velmurugan, R.; Solaimurugan, S., "Improvements in Mode I interlaminar fracture toughness and in-plane mechanical properties of stitched glass/polyester composites", *Compos. Sci. Technol.* **2007**, 67, 61–69. doi:10.1016/j.compscitech.2006.03.032.

157. Beier, U.; Sandler, J.K.W.; Altstädt, V.; Spanner, H.; Weimer, C., "Mechanical performance of carbon fibre-reinforced composites based on stitched and bindered preforms", *Compos. Part A Appl. Sci. Manuf.* **2009**,. doi:10.1016/j.compositesa.2009.08.012.

158. Beier, U.; Fischer, F.; Sandler, J.K.W.; Altstädt, V.; Weimer, C.; Buchs, W., "Mechanical performance of carbon fibre-reinforced composites based on stitched preforms", *Compos. Part A Appl. Sci. Manuf.* **2007**, 38, 1655–1663. doi:10.1016/j.compositesa.2007.02.007.

159. Yudhanto, A.; Watanabe, N.; Iwahori, Y.; Hoshi, H., "Effect of stitch density on tensile properties and damage mechanisms of stitched carbon/epoxy composites", *Compos. Part B Eng.* **2013**, 46, 151–165. doi:10.1016/j.compositesb.2012.10.003.

160. Jana, P.; Khan, N.A., "The sewability of lightweight fabrics using X-feed mechanism", *Int. J. Fash. Des. Technol. Educ.* **2014**, 7, 133–142. doi:10.1080/17543266.2014.906661.

161. Goren, A.; Atas, C., "Manufacturing of polymer matrix composites using vacuum assisted resin infusion molding", *Arch. Mater. Sci. Eng.* **2008**, 34, 117–120.

162. Liu, D., "Delamination Resistance in Stitched and Unstitched Composite Plates Subjected to Impact", *J. Reinf. Plast. Compos.* **1990**, 9, 59–69. doi:10.1177/073168449000900104.

163. Prince Jeya Lal, L.; Ramesh, S.; Parasuraman, S.; Natarajan, E.; Elamvazuthi, I., "Compression after impact behaviour and failure analysis of nanosilica-toughened thin epoxy/gfrp composite laminates", *Materials (Basel).* **2019**, 12, 3057. doi:10.3390/ma12193057.

164. Dani, M.S.H.; Venkateshwaran, N., "Role of Surface Functionalized Crystalline Nano-silica on Mechanical, Fatigue and Drop Load Impact Damage Behaviour of Effective Stacking Sequenced E-glass Fibre-reinforced Epoxy Resin Composite", *Silicon.* **2021**, 13, 757–766. doi:10.1007/s12633-020-00486-2.

165. McDonnell, C.; Hayes, S.; Potluri, P., "Investigation into the tensile properties of ISO-401 double-thread chain-stitched glass-fibre composites", *Int. J. Light. Mater. Manuf.* **2021**, 4, 203–209. doi:https://doi.org/10.1016/j.ijlmm.2020.11.001.

166. International, A., "ASTM D3171-99 Standard test methods for constituent content of composite materials", *Annu. B. ASTM Stand.* **1999**, 1–10.

167. Abeysooriya, R.; Wickramasinghe, G., "Regression model to predict thread consumption incorporating thread-tension constraint: study on lock-stitch 301 and chain-stitch 401", *Fash. Text.* **2014**, 1, 1–8. doi:10.1186/s40691-014-0014-5.

168. Jaouadi, M.; Msahli, S.; Babay, A.; Zitouni, B., "Analysis of the modeling methodologies for predicting the sewing thread consumption", *Int. J. Cloth. Sci. Technol.* **2006**, 18, 7–18. doi:10.1108/09556220610637477.

169. ASTM, "Astm D3039M-17 Test Method for Tensile Properties of Polymer Matrix Composite Materials", *Annu. B. ASTM Stand.* **2014**, 1–13. doi:10.1520/D3039.

170. Measurement, N.O.T., Polymer Matrix Composites Guidelines for Characterization of structural materials, SAE International on behalf of CMH-17, a division of Wichita State University, Warrendale, Pa, 2002.

171. Yoshimura, A.; Yashiro, S.; Okabe, T.; Takeda, N., "Characterization of tensile damage progress in stitched CFRP laminates", *Adv. Compos. Mater.* **2007**, 16, 223–244. doi:10.1163/156855107781393740.

172. Delaney, M.P.; Fung, S.Y.; Kim, H., "Dent depth visibility versus delamination damage for impact of composite panels by tips of varying radius", *J. Compos. Mater.* **2018**, 52, 2691–2705. doi:10.1177/0021998317752502.

173. Icten, B.M.; Atas, C.; Aktas, M.; Karakuzu, R., "Low temperature effect on impact response of quasi-isotropic glass/epoxy laminated plates", *Compos. Struct.* **2009**, 91, 318–323. doi:10.1016/j.compstruct.2009.05.010.

174. Dalfi, H.; Babu-Katnum, K.; Potluri, P.; Selver, E., "The role of hybridisation and fibre architecture on the post-impact flexural behaviour of composite laminates", *J. Compos. Mater.* **2021**, 55, 1499–1515. doi:10.1177/0021998320972462.

175. Ma, J.; Yan, Y.; Liu, Y.J.; Yang, L., "Compression strength of stitched foam-core sandwich composites with impact induced damage", *J. Reinf. Plast. Compos.* **2012**, 31,

1236–1246. doi:10.1177/0731684412455956.

176. Kim, J.-K.; Sham, M.-L., "Impact and delamination failure of woven-fabric composites", *Compos. Sci. Technol.* **2000**, 60, 745–761. doi:10.1016/S0266-3538(99)00166-9.

177. Katnam, K.B.; Dalfi, H.; Potluri, P., "Towards balancing in-plane mechanical properties and impact damage tolerance of composite laminates using quasi-UD woven fabrics with hybrid warp yarns", *Compos. Struct.* **2019**, 225,. doi:10.1016/j.compstruct.2019.111083.

178. Ionescu, I.; Loghin, M.C.; Hanganu, L.C.; Grigoras, S.; Stirbu, C., "Experimental stand for determing fabric compresability during sewing processes", *Ann. DAAAM Proc.* **2009**, 437.

179. Jones, I. (Ian); Stylios, G., Joining textiles : principles and applications, n.d. http://www.sciencedirect.com/science/book/9781845696276 (accessed October 16, 2017).

180. Hui, P.C..; Chan, K.C..; Yeung, K..; Ng, F.S.., "Application of artificial neural networks to the prediction of sewing performance of fabrics", *Int. J. Cloth. Sci. Technol.* **2007**, 19, 291–318. doi:10.1108/09556220710819500.

181. Giorgio Minazio, P., "FAST - Fabric Assurance by Simple Testing", *Int. J. Cloth. Sci. Technol.* **1995**, 7, 43–48. doi:10.1108/09556229510087146.

182. Gürarda, A., "The Effects Of Seam Parameters On The Stiffness Of Woven Fabrics", *Ege Univ. J. Text. Appar.* **2009**, 19, 242–247.

183. Musa, A.B.H.; Malengier, B.; Vasile, S.; Van Langenhove, L.; De Raeve, A., "Analysis and Comparison of Thickness and Bending Measurements from Fabric Touch Tester (FTT) and Standard Methods", *AUTEX Res. J.* **2018**, 18, 51–60. doi:10.1515/aut-2017-0011.

184. SDLATLAS, Fabric Touch Tester, 2003. https://sdlatlas.com/products/ftt-fabric-touch-tester.

185. Barbagallo, G.; Madeo, A.; Azehaf, I.; Giorgio, I.; Morestin, F.; Boisse, P., "Bias extension test on an unbalanced woven composite reinforcement: Experiments and modeling via a second-gradient continuum approach", *J. Compos. Mater.* **2017**, 51, 153–170. doi:10.1177/0021998316643577.

186. Mousazadegan, F.; Latifi, M., "Investigating the relation of fabric's buckling behaviour and tension seam pucker formation", *J. Text. Inst.* **2019**, 110, 562–574. doi:10.1080/00405000.2018.1496601.

187. Žunič-Lojen, D.; Geršak, J., "Study of the tensile force of thread in relation to its pre-tension", *Int. J. Cloth. Sci. Technol.* **2001**, 13, 240–250. doi:10.1108/09556220110396812.

188. Aisyah, H.A.; Paridah, M.T.; Khalina, A.; Sapuan, S.M.; Wahab, M.S.; Berkalp, O.B.; Lee, C.H.; Lee, S.H., "Effects of fabric counts and weave designs on the properties of LaminatedWoven Kenaf/Carbon fibre reinforced epoxy hybrid composites", *Polymers (Basel).* **2018**, 10, 1320. doi:10.3390/polym10121320.